EFFECT OF SLATOR BLADE ORIENTATION ON THE PERFORMANCE OF AN AXIAL FLOW COMPRESSOR

BRUCE CAMERON MARSHALL

EFFECT OF STATOR BLADE ORIENTATION
ON THE PERFORMANCE OF AN AXIAL FLOW COMPRESSOR

by

Bruce Cameron Marshall
Lieutenant, United States Navy
B. Ch. E., Cornell University, 1959

Submitted in partial fulfillment of the
requirements for the degree of

AERONAUTICAL ENGINEER

from the

NAVAL POSTGRADUATE SCHOOL
September 1967

ABSTRACT

A mean streamline analysis of the effect of stator blade orientation on the performance of an axial flow compressor was performed by means of a computer program. Measurements were made on a 3-stage axial flow compressor at the Naval Postgraduate School at six stator stagger angles between 23.8° and 44.3° for a fixed orientation of the rotor blades. Maximum efficiency and pressure ratio were measured at a stator stagger angle of 31.8°. Results at other blade settings showed that by varying stator stagger angle with flow rate optimum efficiencies and pressure ratios can be achieved over a wide range of operating conditions.

The results of the analysis were compared with the measured results. Suggestions are made for improving the manner of adapting cascade test data to performance predictions.

By applying a non-dimensional deflection coefficient it could be shown that minimum work input corresponded to maximum efficiency.

The test compressor has a tip diameter of 36 in. and a hub/tip ratio of 0.6. The blading tested is of the free-vortex type with a design degree of reaction of 0.5. Tip speed was about 185 ft/sec.

Thesis by Bruce C. Marshall entitled: "Effect of Stator Blade Orientation on the Performance of an Axial Flow Compressor"

ERRATA SHEET

Page	Line	Change	To
17	3	g/cm^3	dimensionless
17	5	temperatve	temperature
28	6	assessories	accessories
28	17/18	dia-meter	diam-eter
45	20/21	analy-tically	analyt-ically
59	9	delete "(g/cm^3)"	
78	Fig.15	Note 2: "DEMENSIONS"	DIMENSIONS
100	Fig.37	Maximum 3-Stage Effiency	Maximum 3-Stage Efficiency

TABLE OF CONTENTS

LIST OF TABLES

LIST OF ILLUSTRATIONS

LIST OF ILLUSTRATIONS (Cont.)

LIST OF ILLUSTRATIONS (Cont.)

LIST OF ILLUSTRATIONS (Cont.)

LIST OF SYMBOLS

Symbol	Meaning	Fortran	Units
ALE	air flow angle after the inlet guide vanes	ALE	deg
b	number of blades in rotor or stator row	BLDR BLDS	-
c	blade chord length of rotor or stator	CHR CHS	in.
CCC	volume flow rate calibration constant	CCC	ft^3/sec per ft/sec
C_D	profile drag coefficient of blading	-	-
C_{Dmin}	minimum profile drag coefficient for rotor or stator blade	CDR CDS	-
c_f	conversion factor for barometric pressure	-	psfa/in. of Hg
c_p	specific heat at constant pressure	CP	Btu/lbm, ^oR
d	mean diameter of blading	DD	in.
DW	referred flow rate increment, $\dot{w}\sqrt{T_{to}}/P_A$	DW	lbm$\sqrt{^oR}$/sec psia
h	height of part of annulus area ΔA	-	in.
L	diffuser length proposed in Appendix E	-	in.
LMAX	number of stages for program AXCO3	LMAX	-

Symbol	Meaning	Fortran	Units
m	slope factor which modifies $(i_o)_{10}$ for the camber of the blade section	SLOPM	-
n	slope factor which modifies δ_o for the camber of the blade section	SLOPM	-
N	compressor speed measured by electronic counter	TACH	rpm
NCASE	run number of programs ONRFLO and ONRETA	NCASE	-
NRUN	number of data points per run of program ONRETA	NRUN	-
NUM	case number of program AXCO3	NUM	-
P_A	atmospheric pressure	PA	psfa
P_{Bar}	barometric pressure	PBAR	in. of Hg
P_i	static pressure in inlet duct	PI	psfa
P_{r3-s}	ratio of total pressure behind third stator to total pressure ahead of first rotor	PRATS3	-
P_o	static pressure at permanent Pitot-static tube	PO	psfa
P_{sd}	static pressure with reference to atmospheric after the third stator	-	counts
P_{sda}	static pressure after the third stator	-	psfa
P_{si}	static pressure with reference to atmospheric in inlet duct	PSI	counts

Symbol	Meaning	Fortran	Units
P_{so}	static pressure with reference to atmospheric at permanent Pitot-static tube	PSO	counts
P_{td}	total pressure with reference to atmospheric after the third stator	-	counts
P_{tda}	total pressure after the third stator	-	psfa
$\overline{P_{tda}}$	average total pressure after the third stator, integrated radially	-	psfa
P_{tig}	total pressure with reference to atmospheric between the inlet guide vanes and the first rotor	PTIG	counts
P_{tiga}	total pressure ahead of the first stage or after the inlet guide vanes	PTIGA	psf
P_{Wa}	actual horsepower of compressor	-	(ft-lbf)/sec
P_{Wth}	theoretical horsepower of compressor	-	(ft-lbf)/sec
q_d	velocity head after the third stator	-	counts
q_{d1}	velocity head after the third stator	-	psf

Symbol	Meaning	Fortran	Units
q_i	dynamic head in inlet duct, below atmospheric	QI	counts
q_{i1}	dynamic head in inlet duct	QI1	psf
q_o	dynamic head of permanent Pitot-static tube, below atmospheric	QO	counts
q_{o1}	dynamic head of permanent Pitot-static tube	QO1	psf
r	radius in program ONRFLO	R	in.
RN	referred speed of program AXCO3 $N/\sqrt{T_{to}}$	RN	rpm/$\sqrt{^oR}$
r_o	outside radius	-	in.
RSTAG	rotor stagger angle measured from the blade chord at the mid-radius to a line parallel to the axis	STAGR	deg
s	spacing of blades $\pi d/b$	-	in.
SMAX	maximum limit $(i - i_{10})/\epsilon_{10}$ determined from Fig. 29	SMAX	-
SMI	minimum limit $(i - i_{10})/\epsilon_{10}$ determined from Fig. 29	SMI	-
SSTAG	stator stagger angle measured from the blade chord at the mid-radius to a line parallel to the axis	STAGS	deg

Symbol	Meaning	Fortran	Units
sy	specific gravity of mercury	-	g/cm^3
T_{Bar}	temperature at barometer	TBAR	^oF
T_o	static temperatue at inlet screen	TO	^oF
T_r	reading of torque meter	TRAW	lb
T_{rq}	actual torque	TRQ	ft-lb
T_{td}	total temperature after the third stator	-	^oR
T'_{td}	total temperature at the discharge of an isentropic compression from P_{tiga} to P_{td}	-	^oR
T_{tiga}	total temperature ahead of the first stage or after the inlet guide vanes	-	^oR
T_{to}	total temperature at inlet screen	TTO	^oR
U_{av}	peripheral speed at mean radius	UAV	ft/sec
V_a	axial or through flow velocity in compressor annulus	-	ft/sec
V_d	velocity after the third stator	-	ft/sec
V_D	difference in inlet velocity at 16.0 in. radius and that measured in boundary layer	VD	ft/sec
V_i	velocity in the inlet duct	VI	ft/sec

Symbol	Meaning	Fortran	Units
V_{iad}	velocity in inlet duct adjusted for slight compressor speed variations	VIAD	ft/sec
V_{iav}	average of four values of V_{iad} at each radius	VA	ft/sec
V_o	velocity at the permanent Pitot-static probe	VO	ft/sec
V_{oav}	average velocity at the permanent Pitot-static probe	VOAV	ft/sec
V_u	peripheral component of velocity	VU	ft/sec
$\mathcal{V}_c$	actual volume flow rate	VFC	ft^3/sec
$\mathcal{V}_D$	volume flow deficiency due to losses in inlet duct boundary layer	VFD	ft^3/sec
$\mathcal{V}_t$	volume flow rate neglecting losses in inlet duct boundary layer	VFT	ft^3/sec
W	air velocity realtive to the rotating blade row	W	ft/sec
W_u	peripheral component of relative velocity	WU	ft/sec
$\dot{w}$	weight flow rate	WDOT	lbm/sec
$\dot{w}_r$	referred weight flow rate $\dot{w}\sqrt{T_{to}}/P_A$	WREM	lbm $\sqrt{^oR}$/sec psia

Symbol	Meaning	Fortran	Units
α_1	inlet angle of absolute flow	A	deg
β_1	inlet angle of relative flow	A	deg
γ	ratio of specific heat at constant pressure and specific heat at constant volume	GAM	-
δ	deviation angle of blade row	SD	deg
ΔA	part of the annulus area in the center of which V_{iav} is measured	A	ft^2
Δh_{is}	isentropic specific enthalpy difference for frictionless compression	-	Btu/lbm^{o}R
ΔP_{3-S}	total pressure difference across the three stages	DELP	counts
ΔP_{3-SA}	actual total pressure difference	DELTAP	psf
ΔP_{3-Sth}	theoretical total pressure difference across the three stages	-	psf
ΔS	entropy difference	-	Btu/lbm^{o}R
$\Delta T_{t3-S}'$	isentropic temperature difference from T_{tiga} to T_{td}'	-	^{o}R
ϵ	actual deflection for blade row	DFACT	deg
ϵ_{10}	nominal deflection for blade row at incidence for minimum profile drag loss	DFSTAR	deg
η_{3-S}	three stage total-to-total efficiency	ETAST3	-

Symbol	Meaning	Fortran	Unit
i	actual incidence angle of blade row	SI	deg
i_{10}	nominal incidence of blade row for minimum profile drag loss	STARI	deg
π	geometrical constant 3.14159	-	-
ρ_d	air density after the third stator	-	lb sec^2/ft^4
ρ_i	air density at the inlet	RHOI	lb sec^2/ft^4
ρ_o	air density at the permanent Pitot-static probe	-	lb sec^2/ft^4
σ	blading solidity	SO	-
τ_{av}	average dimensionless deflection coefficient	TAUAV	-
ϕ_{av}	flow coefficient, ratio of through flow velocity to peripheral speed	PHIVA	-
ψ_{av}	average dimensionless pressure coefficient	PSIAV	-
ω	angular velocity	OMEG	rad/sec

SECTION 1

INTRODUCTION

Axial flow compressors have a wide range of application. They are usually matched to a turbine in a set. Both open-cycle sets, such as aircraft turbo-jet engines, and closed-cycle sets for power generation are in service. In every application compressor efficiency is the critical factor in set performance. Accurate predictions of off-design compressor performance must be made during the design stage to be able to make corrections prior to manufacturing.

Theoretical analysis of the flow in an axial compressor involves three-dimensional partial differential equations of a complex nature (1). In these equations it is difficult to account for real gas effects such as boundary layer growth on machine walls and blade surfaces. The resulting wakes behind blade rows create non-uniform conditions; hence, it becomes necessary to base prediction methods on experimental data.

These data would be obtained best on an actual compressor. However, most compressors have relatively short blades and small flow annuli. Even if only small pressure probes were inserted between the rows of blades, the flow in these machines would be substantially altered. Test rigs must therefore be used that have large dimensions.

A first approximation of the flow in axial turbomachines can be obtained in rectilinear cascade test rigs. The intersections of a co-axial cylinder with the blades of a row produce a series of identical and identically oriented profiles which are unwrapped into a plane to establish the corresponding rectilinear cascade. A finite number of straight blades with profiles similar to, but larger than those obtained,is then arranged in a rectangular duct through which air is blown at the appropriate inflow angle. Flow surveys taken ahead of and behind the blade row give experimental data of air turning angle and total pressure loss for various blade geometries. Such a rectilinear cascade is in use at the Naval Postgraduate School. The results of extensive testing of compressor airfoil shapes at NASA have been summarized by Lieblein (2).

The usual problem in compressor design consists in selecting flow areas, blade shapes and blade layout to satisfy design specifications. Additional studies are frequently necessary if the design performance is not reached. An example is the study of Vavra which was made when the so-called Clark CSN-1 compressor of the ML-1 nuclear gas turbine of Aerojet-General Nucleonics failed to perform as required. Vavra analyzed the design changes proposed by the manufacturers and made further recommendations (3). However the ML-1 project was cancelled before the improved compressor could be built so that it was not possible to verify the suggested changes by experiments.

The so-called inverse problem consists in predicting the performance of an existing machine with a known blading by means of rectilinear cascade data and other experience factors. Such an approach was carried out by Gibbons and Bartels (4) for the 12-stage Allis-Chalmers axial flow compressor which supplies air to the turbine test facilities at the Naval Postgraduate School. Because of the unorthodox performance of the first stages, and also due to small flow annuli and short blade heights, it was not possible to predict the performance of the machine accurately. However, the analysis gave important indications for design changes to improve the performance of the compressor.

This thesis makes another attempt to solve the inverse problem for a 3-stage axial flow compressor built by the California Institute of Technology with the support of the Office of Naval Research. The compressor is sufficiently large so that the insertion of pressure probes causes relatively small flow perturbations. The machine was designed to permit variations in blade shapes, blade angles, tip clearances, and staging. The installation at the California Institute of Technology is described by Bowen, et al. (5) This report also describes a theory of perfect fluid flow in axial flow turbomachines. The results of this theory are compared with the measured data of the first stage of a so-called "free-vortex" type blading. Part 2 of the report by Bowen, et al. (6), gave a detailed investigation of multi-stage flow for both "free-vortex" blading and a more complex "solid body rotation" blading. Measurements of blade skin friction losses were greater than expected from cascade tests. The growth of boundary layer along the inner and the outer annulus walls of the flow was less than expected. Alsworth and Iura (7) conducted extensive and detailed measurements of flow patterns in a single stage of "free-vortex" blading. They carried out accurate measurements of the blade skin friction losses and the radial distribution of work input. The final report from the California Institute of Technology was a hot-wire anemometer study of compressor stall by Iura and Rannie (8). They observed that stalled flow regions rotate in the direction of blade rotation without changing shape but with a speed that is not proportional to rotor speed.

After the Turbo-Propulsion Laboratory of the Naval Postgraduate School was built, the compressor was relocated there. Since then it has been used for laboratory courses to supplement instruction in basic theories of turbomachines.

The present study was conducted for this compressor because of the possibility of changing its blade angles. For fixed stator and rotor blade angles a highly peaked curve of efficiency versus flow rate is usually obtained with axial flow compressors. At a slightly changed stator blade angle the peak will be displaced somewhat. A family of efficiency curves for various stator stagger angles is expected to yield a flatter efficiency curve over a wider range of flow rates for fixed rotor blade angles. The wide variation in flow rates required of the engines for the supersonic transport has led to design proposals by General Electric for compressors where the stator blade angles can be changed during operation of the jet engine. Hence, the thesis topic is of current interest.

For the tests it was necessary to obtain extremely accurate pressure measurements. An extremely sensitive bourdon tube pressure indicator was added to the instrumentation. A permanent Pitot-static tube was installed, and accurate flow rate calibrations were carried out. A parallel theoretical effort produced predictions of compressor performance by an existing computer program which was modified and adapted for use on the I. B. M. Model 360 computer system installed at the Naval Postgraduate School.

The author wishes to express a debt of gratitude to the faculty of the Department of Aeronautics of the Naval Postgraduate School for his engineering education. Particular thanks are due to Professor M. H. Vavra for his enthusiasm and guidance in showing what can be done with that education.

SECTION 2

O. N. R. 3-STAGE AXIAL FLOW COMPRESSOR

The compressor installation is shown in Fig. 1. The compressor inlet is in the background of the picture. The exit section is equipped with a throttle valve. A torque meter is installed on the shaft between the drive motor and the compressor. The overall dimensions of the equipment are given in Fig. 2.

A basic criterion of the design of the compressor was flexibility of operation. Each blade row may be removed. The angle setting of each blade is adjustable in 0.5° increments. In order to minimize flow disturbances by pressure probes the outside diameter of the blading is 36 in. For the same reason, the compressor has a hub/tip ratio of 0.6, giving an inside diameter of 21.6 in. and a blade height of 7.2 in. To permit simulation of conditions in a multistage unit, the machine has three stages. One row of inlet guide vanes simulates the effects of previous stages. Two rows of exit guide vanes remove the whirl component after the third stage. To insure that general alignment and tip clearances are maintained the compressor casing is very rigid.

The outer casing consists of two cast iron half-cylindrical shells bolted together along the horizontal plane through the axis. The rows of inlet guide vanes, stator blades, and exit guide vanes are held by bolts extending through the casing (Fig. 3). Inside the casing a hollow steel shaft carries three cast iron drums for each of the rows of rotor blades. The shaft is supported by two roller bearings whose outer races are pressed into the supporting strut assemblies (Fig. 4). These assemblies rest in close fitting channels in the casing (Fig. 5). The six assembly struts have symmetrical airfoil sections. Figure 6 shows the nine blade rows after assembly.

The casing was designed to give maximum accessibility for measuring instruments. Six rectangular instrument ports are located in the upper half at 30° from either side of the vertical (Fig. 3). They are placed in the second and third rotor planes, the first, second and third stator planes, and behind the third stator. The ports hold a special instrument carriage permitting detailed flow surveys in any axial plane. The casing has numerous radial survey holes whose locations are specified in Fig. 7.

The blades are made of ALCOA 356 aluminum alloy without heat treatment. There are thirty rotor blades and thirty-two stator blades per row. The details of construction of the blades are illustrated in Figs. 8 and 9. The blading is designed to have a degree of reaction of 0.5 at the mean radius. The rotor blades are twisted by 49° from hub to tip, and the stator blades by 13°. At the mean radius, the important blade parameters are:

Parameter	Rotor	Stator
Camber angle	20.32°	29.98°
Design stagger angle	43.80°	28.80°
Thickness-to-chord ratio	0.1	0.1
Chord length	2.60 in.	2.60 in.

The values of the blade parameters at other radii, and the method used for calculating the thickness distribution, are specified in Ref. 5.

The point of maximum thickness was set at 0.35 of the chord length from the leading edge. The thickness was modified over the rear 15 per cent of the section to provide a trailing edge thickness 0.02 in. The thickness distribution is applied about a parabolic mean camber line. Figure 10 is a picture of a "free-vortex" stator blade. Tip clearances of 0.020 in. for stator, and 0.037 in. for rotor, are maintained by the use of shims at the point of attachment.

The attaching device permits variation of rotor and stator blade stagger angle. Figure 11 shows how these changes are made. The blade shaft extends through the rotor drum at the hub. An adjusting plate is secured to the blade shaft by a tapered pin. The plate has a series of eleven taps on a circle about the shaft axis which are spaced at intervals of 4.5^{o}. Between the adjusting plate and the rotor drum is a fixed sector which is attached to the drum by a pin which guarantees its alignment. The fixed sector has eleven holes which are spaced at intervals of 4.0^{o} of arc about the blade shaft axis. Blade alignment is maintained by a set screw through both holes in the adjusting plate and the fixed sector. If the center holes of the plate and the sector are lined up, the blade is at the design stagger angle of 43.8^{o} for the "free-vortex" rotor. An angle change of 4.0^{o} can be accomplished by keeping the set screw in the center hole of the adjusting plate and moving the blade so the screw is inserted into the next hole of the fixed sector. Small angle changes of 0.5^{o} are accomplished by moving the blade slightly so that the two holes immediately adjacent to the center holes are lined up since blade angle is changed only by the difference in arc between the two holes. A similar arrangement is used for the stator blade settings (Fig. 10). Figure 12 illustrates stator blade settings which are one degree smaller than the design stagger angle. The two blades on the right-hand side of the figure belong to the first stator row. The set screw is two holes away from the center or reference holes. The blades on the left-hand side of Fig. 12 belong to the row of inlet guide vanes. They are set at an angle which is by 0.5^{o} smaller than the design stagger angle.

The assessories to the basic compressor will be described by following a path from the inlet to the exit and to the power source. The instrumentation of the compressor will be described in its appropriate place in the same sequence. Details of instrument calibrations are contained in Appendix A.

The inlet duct is seen in the background of Fig. 1. It consists of a screen, an entrance bellmouth, and a length of straight pipe. Figure 13 shows the large mesh screen which prevents the ingestion of foreign matter from the compressor bay apron. Mounted on the screen is a mercury thermometer used to determine ambient temperature. It has provisions for psychrometric analysis of the incoming air. Immediately behind the screen is the bellmouth. It changes the diameter rather abruptly from almost two diameters at the flare, to 36 in. in the axial distance of about 15 in. A cylindrical inlet duct two diameters long connects the bellmouth to the compressor proper. The inner surface of the duct is enameled to give smooth flow surfaces.

The flow rate through the compressor was determined by surveys in the inlet duct. Details of the calibration are given in Appendix B. The survey plane is about midway between the bellmouth and the compressor. The surveys were made with a Prandtl-type Pitot tube. In Fig. 14 the probe is installed for taking a vertical traverse. It is possible to disassemble the probe while the compressor is running (Fig. 15).

It may then be remounted for a horizontal traverse. Traverses at 30° and 60° from the vertical direction are possible. These traverses can be made by unbolting the entire inlet duct from the compressor and rotating it on its cradle. The design of the probe prevents measurements closer than 0.25 in. to the inlet duct wall.

A honeycomb straightener is installed behind the inlet Pitot tube to equalize the flow entering the compressor (Fig. 14). Attached to the forward strut assembly is an ogival wooden fairing (Fig. 5) to provide a smooth transition of the flow from the inlet duct to the compressor annulus.

Pressure measurements may be taken at any one of the radial survey ports described. Figure 16 shows the probe used for these measurements. It is a United Sensor three-hole probe, model YC-120. A central hole measures stagnation or total pressure. A static port is located on each of two faces of a wedge at an angle of 45° from the total pressure hole. The static pressures are balanced on a water manometer to insure alignment of the probe in flow direction. The probe is mounted on a probe holder which has vernier scales permitting radius adjustments to 0.01 in. and angle adjustments to 0.1°.

The accurate determination of flow rate is essential to compressor analysis. For this purpose a modified Prandtl type Pitot-static probe was installed. Figure 17 shows the installation details. The probe is inserted in a radial survey hole located ahead of the inlet guide vane row. It protrudes forward into a channel between two adjacent struts of the supporting assembly which is shown in Fig. 5. The probe is approximately at the center of the channel between struts. The probe is positioned in the radial survey hole by a brass plug, and secured to the casing by a simple locking device. Figure 18 shows the probe and its locking device in the background. In the middle of the figure are seen the three-hole probe and its holder located between the inlet guide vanes and the first rotor. In the foreground, a plug, originally located at the same axial position as the probe, has been removed to show a hole through which the probe can be inserted.

Pressures obtained by the probes were measured by a Texas Instruments Fused Quartz Precision Pressure Gauge which is shown in Fig. 19. The velocity head in the inlet is about 0.6 in. of water. A low-pressure bourdon tube was obtained for the gauge which measures from 0 to 166 in. of water with the instrument reading from 0 to 200,000 counts. The calibration constant of the low pressure bourdon tube was determined to be 240.423 counts/psf of the pressure gauge (See Appendix A.). The pressure gauge operates both in manual and servo modes, the latter providing automatic nulling of the unit.

Since flexibility of pressure selection was desirable, two Giannini Sp-101A pressure scanners were connected to the pressure and reference ports of the bourdon tube. One of the scanners is seen in the foreground of Fig. 19. The arrangement of pressures to the 12-channel switches is shown in Fig. 20. Later in the study a simpler system of five valves and two manifolds was constructed (Fig. 21) to eliminate leakage flows that seem to have occurred in the scanners. At this time the original 3-hole probe was placed permanently behind the third stator (Fig. 22). Another 3-hole probe was placed ahead of the first stage rotor. This arrangement permitted direct measurement of the pressure increase across the three stages, ΔP_{3-S}.

Figure 22 also shows the instrument traverse carriage mentioned before. It was used for a survey of total pressure in peripheral direction behind the third stator at two different radii (See Appendix C.). It is possible to vary the radial locations of the probe with an accuracy of 0.01 in. The probe may be rotated through 360° about its axis. The carriage can move the probe 15° in peripheral direction, which covers a whole blade spacing since a stator blade channel covers 11.25°, and a rotor blade channel 12.0° in peripheral direction. The locations of the radial survey holes with reference to the indicated meridional angle of the carriage are shown in Fig. 23. The represented stator profiles are at the design stagger angle at the mean radius. The actual stagger angle measured with respect to a plane through the axis is the complement of the indicated angle.

A short cylindrical duct connects the compressor to the exit elbow, which is equipped with sheet metal turning vanes to minimize losses. A transition piece connects the elbow to the throttle valve which is seen in Fig. 1. The valve consists of two rectangular metal doors which move in slides. The position of the doors is controlled by a right- and left-hand threaded lead screw which is rotated by a Graham variable-speed transmission. A revolution counter indicates the approximate valve opening.

The compressor is driven by a 50 HP Fairbanks Morse induction motor. It requires a three-phase, sixty-cycle, 440 volt power supply, and can operate at two fixed speeds; namely, at about 900 rpm or 1200 rpm.

Attached to the motor shaft is a Baldwin-Lima-Hamilton SR-4 torque meter type A. It is shown in Fig. 24 during calibration with known weights attached to a lever. In the background may be seen a Brown Instruments strain gauge readout which is of the standard Wheatstone bridge type. A conversion constant of 4.1565 ft-lb/lb of torque meter readout was determined (See Appendix A.). Under the protective cover next to the torque meter in Fig. 24 is installed a six lobe flux cutter to measure the motors speed by means of an electronic counter.

SECTION 3

FLOW RATE CALIBRATION

The permanent Pitot-static tube was installed to provide rapid and accurate measurements of volume flow rate. At a given throttle valve setting this probe was calibrated against the result of two traverses of the cylindrical inlet duct. Through-flow velocities in the flow annulus ahead of the inlet guide vanes were varied from 110 ft/sec to 70 ft/sec, so that compressibility effects could be ignored. The objective of the calibration was to determine a calibration constant which gave the volume flow rate when multiplied by the velocity measured at the permanent probe.

An initial survey of the inlet duct was made at the highest possible flow rate of 512 ft^3/sec. Figure 25 shows a plot of the measured velocities of both horizontal and vertical traverses. The smooth velocity profile in the duct is evident. Figure 26 is a graph of the measured velocities in the inlet duct at the lower flow rate of 310 ft^3/sec, which shows a higher degree of scatter. For these tests the pressure indicator was operated in the servo mode. Even in the meter mode the indicated pressure oscillated considerably. Pressure fluctuations seemed to have been initiated by the vibration of the brass rod on which the traversing Pitot-static tube was mounted in the inlet duct. The pressure indicator corrects a disparity between the angular position of a mirror of the bourdon tube and the indicator dial at the rate of the full scale reading of 200,000 counts in 120 seconds. With the oscillating pressure applied to the sensitive instrument, oscillations of 50 counts were observed for a pressure corresponding to a reading of 600 counts. To reduce these oscillations, variable length capillary tube damping devices were installed both in the total and static pressure lines of the traverse Pitot-static tube. Details of the arrangement and the results of tests are shown in Appendix B-1.

A special survey was made to determine the thickness of the boundary layer on the walls of the cylindrical inlet duct. However, construction of the traverse probe prevented taking readings closer than 0.25 in. from the wall. Figure 27 is a plot of the readings at high and low flow rates. In each case it is evident that large losses occur near the walls. With the velocity distributions of Fig. 27 the flow rate is about 2.5 per cent smaller than the value obtained without considering the changes near the walls.

Data were taken in the boundary layer at intervals of 0.25 in. from 17.75 in. to 16.00 in. In the main stream, data were taken at 4.0 in. intervals from 16.00 in. to the centerline. With horizontal and vertical traverses, four points were obtained at each radius and two at the axis for a total of 46 locations. At each station the following measurements were taken:

q_i - velocity head in the inlet duct (counts)

q_o - velocity head of the permanent Pitot-static probe (counts)

P_{si} - static pressure with reference to atmosphere in inlet duct (counts)

P_{so} - static pressure with reference to atmosphere at permanent Pitot-static probe (counts)

T_o - temperature at the inlet screen (^oF)

P_{Bar} - barometric pressure (in. of Hg)

T_{Bar} - temperature of column of mercury (^oF)

The barometric pressure P_{Bar} (in. Hg) was converted into pounds per square foot to obtain the atmospheric pressure P_A by

$$P_A = P_{Bar} \; (71.467) \qquad \text{(psfa)} \qquad (1)$$

where the constant was obtained by correcting the height of the column of mercury for temperature variations in specific gravity of the liquid. The inlet temperature was converted to absolute temperature,and was considered to be the total temperature T_{to} because of the low velocities, or

$$T_{to} = T_o + 459.7 \qquad (^oR) \qquad (2)$$

The static pressure P_i at the inlet was converted from the meter reading to an absolute pressure by

$$P_i = P_A - \frac{P_{si}}{240.423} \qquad \text{(psfa)} \qquad (3)$$

where the constant was obtained by the calibration procedure described in Appendix A. The pressure P_o measured at the permanent probe was obtained in a similar manner. The local air density ρ_i at the inlet was computed from

$$\rho_i = \frac{0.002378 \, P_i}{(14.696)(144)} \, \frac{518.7}{T_{to}} = \frac{P_i}{T_{to}} \left(5.82 \times 10^{-4}\right) \quad (\text{lb sec}^2/\text{ft}^4) \qquad (4)$$

and similarly ρ_o at the permanent probe. The velocity head in the inlet q_{i1} was converted from the meter reading,

$$q_{i1} = \frac{q_i}{240.423} \qquad \text{(psf)} \qquad (5)$$

The dynamic head at the permanent probe q_{o1} was obtained similarly. The velocity V_i in the inlet is then

$$V_i = \sqrt{\frac{2 \, q_{i1}}{\rho_i}} \qquad \text{(ft/sec)} \qquad (6)$$

A similar procedure gave the velocity V_o at the permanent probe. The arithmetic average of the 46 values of V_o obtained during the carrying out of the traverses gives the average value V_{oav} of

$$V_{oav} = \frac{1}{46} \sum_{j=1}^{46} V_{oj} \qquad \text{(ft/sec)}$$

The measured values of V_i were adjusted to account for variations in flow rate due to slight compressor speed variations

$$V_{iad} = V_i \frac{V_{oav}}{V_o} \qquad \text{(ft/sec)}$$

The four values of V_{iad} obtained at each radius were averaged by

$$V_{iav} = \frac{1}{4} \sum_{j=1}^{4} V_{iadj} \qquad \text{(ft/sec)}$$

The volume flow rate was first calculated by neglecting the losses in the boundary layer to give $\dot{V}_t$. In general the volume flow rate is obtained by

$$\dot{V} = 2\pi \int_0^{r_o} V \, r \, dr \qquad (\text{ft}^3/\text{sec})$$

If the above equation were integrated directly, the velocity at the axis would not be included in the volume flow rate calculation because the zero radius is a member of the product under the integral. Therefore the integral was replaced by a summation.

$$\dot{V}_t = \sum V_{iav} \, \Delta A \qquad (\text{ft}^3/\text{sec})$$

The quantity $\Delta A = 2 \pi r h/144$ represented that part of the annulus area in the center of which V_{iav} was measured, where h is the height of the area. This method assumed that the velocity measured at the radius of 16.0 in. exists also at the wall. A volume flow rate deficiency was then calculated to account for the difference in velocities at 16.0 in. radius and those measured in the boundary layer, or

$$V_D = V_{iav\ 16''} - V_{iav\ B.L.} \qquad \text{(ft/sec)}$$

By a trapezoidal integration the volume flow deficiency $\mathcal{V}F_D$ becomes

$$\mathcal{V}F_D = 2\pi \int_{16.0}^{18.0} V_D \ r \ dr \qquad (\text{ft}^3/\text{sec})$$

Then the actual volume flow rate is

$$\mathcal{V}F_c = \mathcal{V}F_t - \mathcal{V}F_D \qquad (\text{ft}^3/\text{sec})$$

A calibration constant CCC for each run was obtained from

$$CCC = \frac{\mathcal{V}F_c}{V_{oav}} \qquad (\text{ft}^3/\text{sec per ft/sec})$$

A first series of calibration runs was invalidated when a leakage hole was discovered in the traversing Pitot-static tube. After repairs, the calibration constants CCC were obtained with a maximum relative error of 0.1 per cent. The final calibration constant was 4.4050 ft^3/sec per ft/sec velocity obtained from the readings of the permanently installed Pitot-static probe.

A data reduction computer program, ONRFLO, for these calibration procedures, was generated for the I. B. M. Model 360 computer. A listing of the program is included as Appendix B-2. Sample output data from the final run is given in Appendix B-3.

SECTION 4

MEASUREMENT OF COMPRESSOR PERFORMANCE

The objective of the study was to determine the effect of changes of the stator blade orientation on compressor performance. It was decided to restrict performance investigation to the three stages only; namely, from a station ahead of the first rotor to a station after the last stator, or between locations SP-2 and SP-8 of Fig. 7. The effects of the inlet, the inlet guide vanes, the exit guide vanes, and the diffuser were not considered.

For tests at a particular stator stagger angle the barometric pressure P_{Bar} was determined first. For various settings of the throttle valve the following measurements were taken:

T_o - ambient temperature (^oF)

P_{so} - static pressure with reference to atmosphere at the permanent Pitot-static probe (counts)

q_o - velocity head at the permanent Pitot-static probe (counts)

P_{tig} - total pressure with reference to atmospheric between the inlet guide vanes and the first rotor (counts)

ΔP_{3-S} - total pressure difference across the three stages (counts)

T_r - reading of torque meter (lb)

N - compressor speed measured by electronic counter (rpm)

With the relations listed on p. 35 these measuring data establish the following quantities:

$$P_A = P_{Bar}\,(71.467) \qquad \text{(psfa)} \qquad (1)$$

$$T_{to} = T_o + 459.7 \qquad (^oR) \qquad (2)$$

$$P_o = \frac{P_{so}}{240.423} \qquad \text{(psfa)} \qquad (3)$$

$$\rho_o = \frac{0.002378\ P_o\ 518.7}{(14.696)(144)\ T_{to}} = \frac{P_o}{T_{to}}(5.82 \times 10^{-4})\ (\text{lb sec}^2/\text{ft}^4) \qquad (4)$$

$$q_{o1} = \frac{q_o}{240.423} \qquad (\text{psf}) \qquad (5)$$

$$V_o = \sqrt{\frac{2\ q_{o1}}{\rho_o}} \qquad (\text{ft/sec}) \qquad (6)$$

The absolute total pressure ahead of the first stage, or after the inlet guide vane, P_{tiga}, is

$$P_{tiga} = P_A - \frac{P_{tig}}{240.423} \qquad (\text{psf}) \qquad (7)$$

The pressure difference across the three stages ΔP_{3-SA} is obtained from

$$\Delta P_{3-SA} = \frac{\Delta P_{3-S}}{240.423} \qquad (\text{psfa})$$

From the torque meter reading T_r the actual torque T_{rq} is

$$T_{rq} = T_r\ (4.1565) \qquad (\text{ft-lbf})$$

where the constant was obtained by the calibration procedure described in Appendix A. The angular velocity ω is with the measured speed, N

$$\omega = \frac{2\pi N}{60} \qquad (\text{rad/sec})$$

Both volume and weight flow rates were calculated. The volume flow rate VF_c is then

$$VF_c = V_o\ (4.4050) \qquad (\text{ft}^3/\text{sec}) \qquad (8)$$

where the constant was obtained by the calibration procedure described in the preceding section and Appendix B. The weight flow rate $\dot{w}$ is

$$\dot{w} = \sqrt{F_c}\,\frac{32.174\ P_A\ 518.7}{(14.696)(144)\ T_{to}} = \sqrt{F_c}\,\frac{P_A}{T_{to}}\,(7.886) \quad \text{(lbm/sec)} \tag{9}$$

For comparison with the prediction program a referred flow rate $\dot{w}_r$ is defined by

$$\dot{w}_r = \frac{\dot{w}\sqrt{T_{to}}}{P_A/144} \quad (\text{lbm}\sqrt{{}^oR}/\text{sec psia}) \tag{10}$$

Two basic indices of performance were computed; namely, the 3-stage pressure ratio P_{r3-s}, where

$$P_{r\,3-s} = \frac{P_{tiga} + \Delta P_{3-sA}}{P_{tiga}} \tag{11}$$

and the 3-stage total-to-total efficiency η_{3-s} obtained from

$$\eta_{3-s} = \frac{P_{Wth}}{P_{WA}} \tag{12}$$

where P_{Wth} and P_{Wa} are the theoretical and actual horsepower, respectively. The theoretical power is P_{Wth}, given by

$$P_{Wth} = \dot{w}\ \Delta h_{is}(778.3) \quad \text{(ft-lbf/sec)}$$

where Δh_{is} is the isentropic specific enthalpy difference for a frictionless compression from P_{tiga} to P_{td} after the third stator. Assuming a perfect gas there is

$$\Delta h_{is} = c_p\ \Delta T'_{t\,3-s} \quad (\text{Btu/lbm, }{}^oR)$$

where $\Delta T'_{t3-s}$ is the isentropic temperature difference from the total temperature T_{tiga} ahead of the first stage, to T'_{td} after the third stator (See Fig. 28.). Since T_{tiga} very nearly equals the ambient temperature T_{to}, there is

$$\Delta h_{is} = c_p T_{to} \left(\frac{T_{td}'}{T_{tiga}} - 1 \right) \qquad \text{(Btu/lbm, } ^oR)$$

With the isentropic relation

$$\frac{T_{td}'}{T_{tiga}} = \left(\frac{P_{td}}{P_{tiga}} \right)^{\frac{\gamma-1}{\gamma}}$$

the final expression for the determination of the theoretical power is

$$P_{Wth} = \dot{w}\, c_p T_{to} \left[(P_{r3-S})^{\frac{\gamma-1}{\gamma}} - 1 \right] 778.3 \qquad \text{(ft-lbf/sec)} \tag{13}$$

The actual power is obtained from

$$P_{WA} = T_{rq}\, \omega \qquad \text{(ft-lbf/sec)}$$

The total-to-total efficiency at the three stages is then

$$\eta_{3-S} = \frac{\dot{w}\, c_p T_{to}}{T_{rq}\, \omega} \left[\left(P_{r3-S} \right)^{\frac{\gamma-1}{\gamma}} - 1 \right] 778.3 \tag{14}$$

For comparison with other compressor data certain non-dimensional parameters are introduced. The average flow function ϕ_{av} is the ratio of through flow velocity V_a and peripheral speed at the mean diameter U_{av}, or with

$$V_a = \frac{VF_c}{651.4/144} = VF_c\,(0.221) \qquad \text{(ft/sec)}$$

and, for the mean diameter of 14.4 in.

$$U_{av} = \omega \frac{14.4}{12} \qquad \text{(ft/sec)}$$

there is

$$\phi_{av} = \frac{VF_c}{\omega} \frac{(12)(144)}{(14.4)(651.4)} = \frac{VF_c}{\omega}(0.1842) \tag{15}$$

An average dimensionless stage pressure coefficient ψ_{av} is defined by

$$\frac{\Delta P_{3-SA}}{3} = \psi_{av} \rho_o U_{av}^2 \qquad \text{(psf)}$$

or

$$\psi_{av} = \frac{\Delta P_{3-SA}}{3 \rho_o U_{av}^2} \tag{16}$$

The so-called dimensionless deflection coefficient τ_{av} is defined by

$$\frac{\Delta P_{3-Sth}}{3} = \frac{\Delta P_{3-SA}}{3 \eta_{3-S}} = \frac{\psi_{av}}{\eta_{3-S}} \rho_o U_{av}^2 \qquad \text{(psf)}$$

$$= \tau_{av} \rho_o U_{av}^2 \qquad \text{(psf)}$$

Hence,

$$\tau_{av} = \frac{\psi_{av}}{\eta_{3-S}} \tag{17}$$

The performance calculations were made for the conditions along the mean radius of the stage, 14.4 in., by assuming that these conditions are representative of the performance of the 3-stage compressor. Detailed investigations which support this simplification are given in Appendix C. The data reduction was accomplished by the computer program ONRETA, which is listed also in Appendix C.

Data were taken on 11 occasions for the following settings of stator stagger angle:

Run	Stator Stagger Angle
1, 2, 3	27.8^o
4, 5	23.8^o
6, 7	31.8^o
8, 9	35.8^o
10	39.8^o
11	44.3^o

SECTION 5

PERFORMANCE PREDICTION PROGRAM

The program used to predict the performance of multi-stage compressors is called AXCO3. It is listed in Appendix D and represents an adaptation of a program by Vavra (3), modified by Gibbons and Bartels (4).

The method assumes that the flow is axisymmetric. Computations are made for the streamlines at the mean radius of a stage. A stage by stage analysis of the machine is performed. The output of one stage is used as input for the next stage. The computation is started at a flow rate less than that anticipated for surge, and the flow rate is then increased by small increments to cover the whole operating range of the machine.

Program AXCO3 uses two principal subroutines; namely, one called ROTOR and the other called STATOR. They establish the velocity triangles of a rotor or a stator row of blades, respectively, from the known geometry of the bladings, flow rate, and discharge conditions of the preceding row of blades. Both subroutines make use of three additional subroutines.

Subroutine THEORY calcualates the flow conditions for minimum profile losses. Cascade data by Lieblein are used for this purpose (2). These data are presented as curves for zero-camber incidence angle $(i_0)_{10}$, slope factor n, zero camber deviation angle $(\epsilon_0)_{10}$, and slope factor m, all given as functions of the inlet air angles β_1 or α_1, with the blading solidity σ as a parameter. The solidity σ is defined as the ratio of blade chord c and blade spacing s.

The curves described above have been expressed by polynomials in powers of solidity and inlet air angle which are used in subroutine THEORY. The accuracy of the polynomials has been verified, and the errors are listed in Appendix D. The incidence angle for minimum loss is determined by an iteration procedure which changes the inlet air angle until agreement is reached within a tolerance of 0.02°. The deflection which occurs at the minimum profile loss can then be calculated with the established polynomials also.

The subordinate subroutine CASCAD calculates the performance of the blading at the actual incidence or inlet flow angle of the blade row by using a graph of Lieblein that establishes the change of the deviation angle with incidence angle ($d\delta/di$) as a function of inlet flow angle and solidity.

In the earlier computer programs the curves of this graph were expressed by a polynomial that covered the range of solidities from 0.0 to 1.8. Since the curves have nearly exponential character, which cannot be expressed with ease by polynomial functions, it was found that an error of the order of 10 per cent was possible. Therefore, a new polynomial was established for solidities between 0.6 and 1.4 which limits the error to less than 1.9 per cent.

Subroutine CASCAD further utilizes experimental limits on blading performance by Howell (9) which are illustrated in Fig. 29. Howell found that for most cascades the ratio of the profile drag coefficient C_D at an arbitrary incidence angle i and C_{Cmin} at the minimum loss incidence i_{10} is a unique function of the quantity $(i - i_{10})/\epsilon_{10}$, where ϵ_{10} is the optimum flow deflection for the incidence angle i_{10}. Since the applicability of the data presented in Ref. 2 is limited to design point calculations, where the incidence angles are close to the nominal incidence i_{10}, the curves cannot be used for off-design analyses without restrictions. Without such limits the flow deflections ϵ could be increased simply by increasing the incidence angle i, since the data of Ref. 2 do not establish criteria for flow separations which are associated with a radical increase in profile losses. Experimental results of Howell show that the flow deflection ϵ at incidence i should not exceed the optimum deflection ϵ_{10} by more than 25 per cent to avoid excessive losses. He states that this limit occurs if the profile loss coefficient C_D is about twice the minimum loss coefficient C_{Dmin}. The solid curve in Fig. 29, labeled ϵ/ϵ_{10}, is supposed to be the relation between ϵ/ϵ_{10} and $(i-i_{10})/\epsilon_{10}$ as obtained from subroutine CASCAD with the data from Ref. 2. It will be assumed that this curve holds for negative values of $(i-i_{10})/\epsilon_{10}$ only. For positive values of this parameter the dashed curve will be applied to satisfy the limitations of Howell. This curve is somewhat arbitrary but represents the best estimate for the actual operating condition of compressor cascades. Figure 29 further shows a curve relating the ratio C_D/C_{Dmin} to $(i-i_{10})/\epsilon_{10}$, which is adapted from Ref. 9. Both this curve and the dashed curve for the deflection ratio have been expressed analytically in subroutine CASCAD. If the ratio C_D/C_{Dmin} exceeds a value of 2.0 for positive quantities $(i-i_{10})/\epsilon_{10}$, the program prints out "surge in blade row xx" and proceeds with calculations at an increased flow rate. The positive value of $(i-i_{10})/\epsilon_{10}$ at which this occurs is the input quantity SMAX. If C_D/C_{Dmin} exceeds a value of 2.0 at incidence angles i smaller than i_{10}, the program prints out "minimum pressure in blade row xx" and halts computation. The negative value of

$(i - i_{10})/\epsilon_{10}$ at which this occurs is the input quantity SMI. In both instances the symbol xx refers to the number of the blade row, and indications are given also whether the row is a stator or a rotor. For any incidence angle within the useful operating range, the values of the deflection ratio and of the ratio C_D/C_{Dmin} are computed by subroutine CASCAD and control returned to the blade row subroutines ROTOR or STATOR.

The efficiency of a blade row is determined by subroutine ETACAL. Losses due to tip clearances, secondary flows, and wall friction are taken into account with the relations proposed by Vavra (1).

If conditions of surge exist, the flow rate is increased by about 1.0 per cent and the entire computation is repeated. If the incidence angles are in the so-called useful operating region of Fig. 29, the output of subroutine ROTOR or STATOR becomes the input for the subroutine that calculates the next row of blades. Interstage data are printed out as the program progresses from one stage to the next. If all blade rows of a machine have been processed, the overall compressor efficiency and pressure ratio are computed for the particular flow rate. This flow rate is then increased by a specified amount, and the calculating process is repeated. If the so-called minimum pressure is reached, the computation stops and a summary of the overall performance parameters is printed out.

The details of the calculation of the flow through the inlet duct, the inlet guide vanes, the exit guide vanes, the diffuser and the discharge passages are not described in this thesis since it is concerned only with the performance prediction of the three stages of the compressor from a station ahead of the first rotor to the discharge at the third stator. The methods applied for the flow analysis in these passages may be found in Vavra (3) and Gibbons and Bartels (4).

According to Howell there occur additional effects that influence the off-design calculations. The growth of boundary layers on the walls of the annular flow channel will change the velocity profiles and can reduce significantly the effective flow area. The program takes account of this effect by a blockage factor that can vary from stage to stage. This boundary layer growth is responsible also for increasing peaks in the radial distribution of the axial velocity components in succesive stages. These higher velocities outside of the wall boundary layers produce smaller incidence angles for the main portion of the flow, thereby decreasing the actual flow deflection and reducing the work absorbed by the fluid in the stage. Hence in a compressor that consists of stages with identical bladings, the last stages will produce smaller pressure ratios than the stages at the compressor inlet. Experience shows the efficiency in successive stages is not reduced by the peaking of the velocity profiles, and their effects are usually taken into account by a so-called work-done factor that is about unity for the first stage and gradually decreases for the successive stages. Such work-done factors can be introduced in program AXCO3, but for the present compressor they will be taken as unity because of the small number of stages and the large blade heights. For the same reasons the blockage factor is assumed to be equal to unity also.

The geometry of the blades could be obtained from the information of Ref. 5. Values at the mean radius were used for the analysis. Bowen (5) determined that the average flow angle at the mean radius after the inlet guide vanes ALE was 20.0^o for the design inlet guide vane stagger angle of 11.4^o, independent of flow rate. From Fig. 12 it can be recognized that the inlet guide vanes were set at a stagger angle of 10.9^o for the tests. Therefore a value of 19.5^o was used in the analysis program for the average flow angle leaving the inlet guide vanes. Reference 5 does not give values of C_{Dmin} for the blading. It is possible to introduce in the program various values of C_{Dmin} both for rotor and stator blading. Hence it was possible to estimate an average apparent value of C_{Dmin} for blading by comparing measured results to predictions of the analysis program for several assumed values of C_{Dmin}.

A prediction of the 3-stage efficiency for different stator stagger angles is shown in Fig. 30 for an assumed value of C_{Dmin} of 0.020. The light line connecting the individual peak efficiencies represents the calculated operating envelope which could be obtained if continuous control of stator stagger angle for maximum efficiency were possible.

For comparison with measured performance a series of calculations were made for stator stagger angles of 23.8^o, 27.8^o, 31.8^o, 35.8^o, 39.8^o, and 44.3^o. For each stagger angle, values of C_{Dmin} of 0.000, 0.006, and 0.008 were assumed. To avoid confusion with the computations of actual performance based on measured quantities, which have been called runs, each calculation of the analytical prediction program has been assigned a two-digit case number. The first digit identifies the stator stagger angle of the case as follows:

First Digit	Stator Stagger Angle
1	23.8^{o}
2	27.8^{o}
3	31.8^{o}
4	35.8^{o}
5	39.8^{o}
6	44.3^{o}

The second digit identifies the assumed value of C_{Dmin} of the case as follows:

Second Digit	Assumed Value of C_{Dmin}
1	0.000
2	0.006
3	0.008

For example, case 42 is the predicted performance at a stator stagger angle of 35.8^{o} with a value of C_{Dmin} of 0.006. The summary output of each case is presented in Appendix D.

SECTION 6

DISCUSSION OF RESULTS

Experimental data for performance measurements were taken during 55 hours of running time. Another 81 hours of operation were used for miscellaneous calibration and testing, including 44 hours for flow rate calibrations.

The rotor stagger angle was set at 43.8^{o} for all runs. The design stator stagger angle is 28.8^{o}. For the performance tests, the stator stagger angle was set at 23.8^{o}, 27.8^{o}, 31.8^{o}, 35.8^{o}, 39.8^{o}, and 44.3^{o}. Measured performance is presented in comparison with the predicted results of AXCO3,and also by establishing dimensionless performance parameters. Figures 31 through 36 are graphs of measured performance in comparison with the prediction by AXCO3 for each stator blade angle setting. Figures 37 and 38 are summary plots of maximum efficiency and pressure ratio for all stator blade angle settings. Figures 39 through 44 are graphs of the non-dimensional parameters at each stator stagger angle. Figure 45 is a summary plot of maximum efficiencies and associated deflection coefficients for all stator blade angle settings. Figure 46 is a summary plot of maximum pressure coefficients for all stator blade angle settings.

On each of Fig. 31 through Fig. 36 the 3-stage efficiency reaches a peak value for each stator stagger angle. The referred flow rate at which this peak occurs decreases as the stator stagger angle increases.

Also plotted on each of Fig. 31 through Fig. 34 are the results predicted by AXCO3 for the three estimated values of C_{Dmin} of 0.000, 0.006 and 0.008. The predicted 3-stage efficiency reaches a peak for each C_{Dmin}. The referred flow rate associated with predicted peak efficiency decreases with increase in stator stagger angle. The referred flow rate at which the predicted peak efficiency occurs decreases with increase in C_{Dmin} at a given stator stagger angle.

AXC03 predicts the condition of surge for each case according to the criteria of Howell shown in Fig. 29. The surge condition is assumed to exist whenever the parameter $(i-i_{10})/\epsilon_{10}$ exceeds the maximum positive value SMAX which has been inserted in the program. The incidence angle for the rotor blade rows becomes larger as the through-flow velocity decreases until a surge condition is indicated. AXC03 predicts surge at the same referred flow rate for each setting of stator stagger angle. This is due to the fixed angle of the inlet guide vanes. The assumption has been made that the air flow angle leaving a blade row does not change with variations in flow rate in the incompressible flow regime. This result was verified by Bowen (5). The inlet guide vanes were not rotated as the stator stagger angle was varied. At all stator stagger angle settings the first stage rotor had the same incidence angle at particular flow rates. In the stage-by-stage analysis, "surge in rotor 1" was indicated at the same flow rate in each run, regardless of the stator stagger angle setting of subsequent stators. The region of referred flow rates smaller than that at which surge is indicated by the program is marked with a dashed line on Figs. 31 through 34, and is less than 41.5 lbm$\sqrt{^{o}R}$/sec psia for every case.

When the value of the parameter $(i-i_{10})/\epsilon_{10}$ is determined to be less than SMI, the negative value of the parameter which has been inserted in AXC03, the program stops the computation and prints "minimum pressure in blade row xx." The referred flow rate at which computation is stopped decreases as stator stagger angle is increased. At stator stagger angles of 31.8^o and lower (Figs. 31 through 33) the referred flow rate at which computation is stopped is larger than the maximum flow rate of the graph. At a stator stagger angle of 35.8^o (Fig. 34), the computation stops at a referred flow rate of 45.5 lbm $\sqrt{^oR}$/sec psia. At stator stagger angles of 39.8^o and 44.3^o (Figs. 35 and 36), the program did not establish useful data. At the high stator angles the referred flow rate at which computation was stopped was lower than the referred flow rate for surge in the first stage rotor. The latter flow rate remained unchanged at a fixed inlet guide vane angle.

This difficulty illustrates some of the limitations of program AXCO3 when applied to an actual machine. The program assumes that the compressor is designed properly. Changes from stage to stage must be gradual. For example the annulus area may change gradually from stage to stage with no adverse effects. The checks for minimum pressure and surge limits are applied in each blade row. Surge in any blade row is interpreted as surge in the machine, and similar limitations are imposed for minimum pressure. The program cannot cope with discontinuities similar to those that occur by leaving the angle of the inlet guide vanes unchanged. It is possible to imagine a situation where the angle setting of the inlet guide vanes might have to remain unchanged; for instance, if the inlet guide vanes must support the front bearing of the rotor shaft. In such a design the first rotor would have higher blade efficiencies than succeeding blade rows at large flow rates, while at lower flow rates the blade efficiencies of the first rotor would be smaller than for succeeding blade rows. The 3-stage efficiency of an actual machine is an overall parameter which includes the effect of the different blading efficiencies for different blade rows. In an actual machine the flow will adjust itself to these conditions, whereas program AXC03 cannot cope with these peculiar circumstances. For these reasons the program did not produce performance data for the higher stator stagger angles of 39.8^{o} and 44.3^{o}.

The detection of the actual surge point during the tests is difficult with the available instrumentation and must be based on acoustic phenomena. Incipient surge, probably due to rotating stall, was associated with an unmistakable oscillating change in sound level produced by the compressor. This effect appeared suddenly even when flow rate was decreased slowly. To eliminate the sound due to this surge condition it was necessary to increase the flow rate by about 5 to 10 per cent. A flow rate slightly above the surge point could then be reached by gradual throttling. For each run one test point was taken in the surge region and one test point as close as possible to the surge point. Efficiency at test points in the surge region was below 0.90 for all stator stagger angles. The efficiency at the data point close to stall rose from 0.89 to 0.94 as the stator stagger angle was increased from 23.8^{o} to 31.8^{o}, and efficiency decreased to 0.89 with further increase in stator stagger angle to 44.3^{o}. As the surge condition is approached the rate of decrease of efficiency is set by the relative location on the efficiency versus referred flow rate graph of the two data points in the surge region and close to surge. At a stator stagger angle of 31.8^{o} which produced the maximum

3-stage efficiency and at 35.8^{o}, efficiency decreased most rapidly as the surge condition was approached. For other stator stagger angles the efficiency decreased less rapidly. It is not possible to make a meaningful comparison between measured surge point data and the surge condition calculated by AXC03 because surge was predicted to occur at the same referred flow rate for each case.

It is possible to compare measured values of maximum 3-stage efficiency with the maxima calculated by program AXC03. For all four stagger angles at which computations were made, the maximum 3-stage efficiencies were predicted to occur at flow rates about 5 per cent greater than the flow rates at which the measured maxima occurred. According to Howell the point of maximum efficiency occurs for a value of the parameter $(i-i_{10})/\epsilon_{10}$ about equal to +0.19 (Fig. 29). At greater positive values of the parameter the losses are believed to increase rapidly. Since the measured maximum efficiency occurred at a flow rate which was about 5 per cent less than was predicted, an analysis of off-design performance of a compressor stage was made. The method of Vavra (Ref. 1) assumes that the air flow angles leaving a blade row do not change with flow rate in incompressible flow. The velocity triangle changes caused by a reduction from design flow rate are shown in Fig. 47. The subscript d refers to the design condition, and the primed quantities refer to off-design. The analysis was conducted at the maximum efficiency point for a stator stagger angle of 27.8^{o}. The following quantities were measured:

Design flow coefficient ϕ_d = 0.517

Inlet flow angle α_1 (fixed) = 20.0^{o}

The off-design flow rate was fixed at 5 per cent less than the design flow rate, to correspond to the flow rate at which the measured maximum efficiencies occurred. The off-design flow coefficient is

$$\phi' = (0.95)\ (0.517)$$

The peripheral components of velocity are:

$$\frac{V_{u1d}}{U} = \phi_d \tan \alpha_1$$

$$\frac{V_{u1}'}{U} = 0.95\ \phi_d \tan \alpha_1$$

$$\frac{W_{u1d}}{U} = \frac{U - V_{u1d}}{U} = 1 - \phi_d \tan \alpha_1$$

$$\frac{W_{u1}'}{U} = \frac{U - V_{u1}'}{U} = 1 - 0.95\ \phi_d \tan \alpha_1$$

The relative inlet flow angles for both conditions are:

$$\beta_{1d} = \arctan \frac{W_{u1d}/U}{\phi_d} = \arctan\left[\frac{1}{\phi_d} - \tan \alpha_1\right]$$

$$\beta_1' = \arctan \frac{W_{u1}'/U}{0.95\ \phi_d} = \arctan\left[\frac{1}{0.95\ \phi_d} - \tan \alpha_1\right]$$

With the same rotor stagger angle, the difference in incidence angle i between design flow rate and off-design flow rate is the difference in β_1

$$i' - i_d = \beta_1' - \beta_{1d} = 59.2^\circ - 57.5^\circ = +1.7^\circ$$

The difference between the parameter $(i - i_{10})/\epsilon_{10}$ at the design flow rate and the parameter at a flow rate 5 per cent less than design is

$$\Delta \frac{(i - i_{10})}{\epsilon_{10}} = \frac{+1.7}{+11.2} = +0.15$$

where ϵ_{10} was calculated by AXCO3. The measured maximum efficiencies occurred at a value of the parameter $(i - i_{10})/\epsilon_{10}$ which was greater by 0.15 than the value of the parameter for which the program AXCO3 predicted maximum efficiencies.

Lieblein's data were obtained from compilations and reductions of cascade test data primarily for blade profiles which were NACA

65 (A_{10}) - series airfoils built up on equivalent circular arc camber lines. The free-vortex blades installed in the compressor have a thickness distribution which was derived from the theory of Ref. 1 applied to a parabolic mean camber line. If the actual incidence for minimum profile loss for the installed blades were smaller by 1.7^o than calculated by subroutine THEORY, all values of the parameter $(i-i_{10})/\epsilon_{10}$ calculated in subroutine CASCAD would be larger by 0.15 than they actually are. The flow rate at which the maximum efficiency is calculated would be 5 per cent greater than the flow rate at which maximum efficiency was actually measured.

Howell presented results of cascade tests of British C-1 and C-2 airfoil shapes for several values of solidity. The C_D/C_{Dmin} curve of Fig. 29 was obtained by interpolation for a solidity of 0.8. If the upper limit of the parameter $(i-i_{10})/\epsilon_{10}$ for minimum loss were extended by 0.15 from 0.19 to 0.34, the flow rate at which maximum efficiency was calculated analytically would coincide with the flow rate for measured maximum efficiency.

The measured efficiency curves are more peaked than the curve computed by AXCO3. If the C_D/C_{Dmin} curve of Fig. 29 had a greater slope in regions where C_D/C_{Dmin} approaches a value of 2.0, the predicted efficiency curves would be less flat and would more nearly approximate the curves of measured performance.

It was one object of this thesis to attempt to determine the value of C_{Dmin} for the installed blade profile. Vavra (1), p. 377, indicates that these values usually do not exceed 0.008. For each stator stagger angle, analytical calculations were made for estimated C_{Dmin} of 0.000, 0.006 and 0.008. The results for the smaller stator stagger angles are plotted on Fig. 31 through Fig. 34. The value of C_{Dmin} was estimated for each stator stagger angle:

Stator Stagger Angle	Estimated C_{Dmin}
23.8	0.008
27.8	0.004
31.8	0.003
35.8	0.007

The arithmetic average of the estimated values is 0.0055, but there is is obviously considerable scatter in the experimental data.

A summary plot of maximum peak efficiencies is presented in Fig. 37. If continuous control of stator stagger angle were possible, as in the proposed SST engine, Fig. 37 would be an operating curve for maximizing efficiency at any flow rate. The peak maximum 3-stage efficiency was 0.956, measured at a stator stagger angle of 31.8. Also shown is a flatter curve of predicted peak 3-stage efficiencies using C_{Dmin} of 0.006 for the four lower stator stagger angles. The maximum predicted value is 0.942 at a stator stagger angle of 30^{o}. The predicted values occur at flow rates 5 per cent higher than corresponding measured values. The measured values decline more steeply at stagger angles other than the angles for maximum efficiency than do the analytically calculated values. The curve relating stator stagger angle to performance shows that, in the region near the maximum efficiency, relatively small changes in angle are required for large variations in flow rate. Between stator stagger angle settings of 27.8^{o} and 35.8^{o}, a 10 per cent variation in flow rate requires only an 8^{o} angle change. In the regions more distant from the maximum efficiency point, large angle changes are required to handle small flow rate changes.

Figures 31 through 36 also contain plots of 3-stage pressure ratio versus referred flow rate for each stator stagger angle.

As expected, the measured maximum pressure ratio occurred at a referred flow rate between that for maximum efficiency and for surge. It was not possible to determine maxima for the calculated data of AXCO3 because for each case the largest pressure ratio occurred at the flow rate tagged "surge." The program does not compute performance at lower flow rates. The check for surge occurs in subroutine CASCAD. Based on cascade data, Howell stated that unacceptable losses occur at values of ϵ / ϵ_{10} greater than 1.25. This conservative criterion is particularly applicable in a design where a wide range of flow rates is not required. However for the purpose of evaluating pressure ratio for an existing machine, the criterion appears to be too restrictive. It would be more advantageous if AXCO3 used the criterion to predict surge but then proceeded to complete the calculations at that flow rate rather than stopping computation.

The measured pressure ratio was in general by 0.25 per cent greater than predicted by AXCO3, and the measured ΔP_{3-SA} was about 11 per cent greater. Total pressure is relatively simple to measure. The yaw and pitch errors of the 3-hole probe are very small. Any error in total pressure measurement is expected to produce a total pressure lower than expected. Since the predictions are lower at every flow rate, it is possible that the difference in blading between the installed blade profiles and the NACA airfoils, which are represented by Liebleins's data, may be the cause of the difference as was suggested in the discussion of 3-stage efficiency. A summary plot of maximum 3-stage pressure ratio on an expanded scale is presented in Fig. 38. The peak value of maximum pressure ratio occurred at a stator stagger angle of 31.8°

While writing the thesis, an error was discovered in Eq. 1, which converts the reading of the mercury barometer P_{Bar} in in. of mercury to P_A in psfa and corrects for the temperature variation of the specific gravity of the liquid. The incorrect equation

$$P_A = P_{Bar}\,(0.4928 + T_{Bar}\;\; 0.5/10{,}000)\,144 \qquad \text{(psfa)}$$

was used. At 70.0°F the constant by which P_{Bar} was multiplied was 71.457 psfa/in. of Hg. Reference 10 lists the specific gravity of mercury "sy" for the temperature range 0°F to 150°F as

$$sy = 13.638 - 1.354 \times 10^{-3}(T_{Bar}) \qquad (\text{g/cm}^3)$$

The conversion factor is

$$c_f = 69.892\;\frac{sy}{13.59} \qquad \text{(psfa/in. of Hg)}$$

At 70°F the correct conversion factor is 69.55, or the atmospheric pressure on which all calculations were based was 3 per cent higher than the actual atmospheric pressure. By Eqs. 3, 4 and 7 the calculated static pressure P_o and air density ρ_o at the permanent Pitot-static tube,and the total pressure after the inlet guide vanes P_{tiga},were 3 per cent higher than actual also. By Eqs. 6, 8 and 10 the calculated velocity V_o, volume flow rate VF_c, and referred flow rate $\dot{w}_r$ were 0.983 of the actual values. The calculated pressure ratio P_{r3-s} was 0.998 of the actual value by Eq. 11. By Eqs. 9 and 14 the values of weight flow rate $\dot{w}$ and 3-stage efficiency were calculated to be 1.2 per cent higher than the actual values.

The test results are presented in non-dimensional form in Figs. 39 through 44. Plotted against the flow coefficient ϕ_{av}, the efficiencies follow the same pattern as when plotted against referred flow rate,since Eqs. 10 and 13 differ only by a constant. Figure 45 is a summary plot of the maximum 3-stage efficiciency for each stator stagger angle versus flow coefficient and is similar to Fig. 37 for the same reason. Figure 46 is a summary plot of maximum pressure rise coefficient for each stator stagger angle. The pressure rise reaches a maximum at a blade angle of 33^{o} and a flow coefficient of 0.475. The curve of corresponding stator stagger angles has an almost constant slope.

Theoretically, the deflection coefficient τ_{av} represents the change in peripheral flow components in a blade row divided by the peripheral speed. Figure 47 is a stage velocity triangle showing design and off-design conditions in a compressor stage. At the design condition

$$\tau_d = \frac{\Delta W_{ud}}{U} = \frac{\Delta V_{ud}}{U}$$

An assumption in this analysis is that the air leaving angle from a blade row does not vary with incidence. Hence the angles α_1 and β_1 remain constant. The relation between the off-design deflection coefficient τ' and the off-design flow coefficient ϕ' is fixed by similar triangles

$$\frac{1 - \tau'}{1 - \tau_d} = \frac{\phi'}{\phi_d}$$

and

$$\tau' = 1 - (1 - \tau_d)\frac{\phi'}{\phi_d}$$

or τ' is expected to vary linearly with ϕ'.

At flow coefficients greater than that for maximum 3-stage efficiency, calculated deflection coefficients τ_{av} varied linearly with flow coefficient in Figs. 39 through 44. For most runs the graph of τ_{av} broke sharply from the linear segment at the maximum efficiency point. For each case the curve continued at a reduced slope in the region between the break and prior to surge. Experience seems to indicate this identifies a region of incipient stall. As the blades become fully stalled, the nature of the flow changes drastically. It has been suggested that this change is reflected in a sharp increase in the slope of the deflection curve. The author was reluctant to operate the compressor in the region of stall for extended periods of time because of related vibration and noise problems. However a slight upturn of the deflection coefficient curve was apparent at stator stagger angles of 23.8° and 27.8° (Figs. 39 and 40).

The deflection coefficient τ is a measure of work input. It will be necessary to make an approximation for the theoretical power P_{Wth}. Equation 11 can be rewritten

$$P_{r\,3\text{-}S} = 1 + \frac{\Delta P_{3\text{-}S}}{P_{tiga}} \qquad \text{(psfa)}$$

Making a first order expansion, Eq. 13 can be rewritten

$$P_{Wth} = \dot{w} R_G \frac{\gamma}{\gamma - 1} T_{to} \left[1 + \frac{\gamma - 1}{\gamma} \frac{\Delta P_{3\text{-}S}}{P_{tiga}} - 1 \right] \qquad \text{(ft-lbf)/sec}$$

$$= \frac{\dot{w} R_G T_{to}}{P_{tiga}} \Delta P_{3\text{-}S} = V\!F_c \, \Delta P_{3\text{-}S} \qquad \text{(ft-lbf)/sec}$$

Substituting P_{Wth} in Eq. 12, the efficiency becomes

$$\eta_{3\text{-}S} = \frac{V\!F_c \, \Delta P_{3\text{-}S}}{T_{rq} \, \omega}$$

Rewriting Eq. 15

$$V\!F_c = A \, \phi_{av} \, U_{av} \qquad (\text{ft}^3/\text{sec})$$

and introducing Eq. 16 into Eq. 17, there is

$$\tau_{av} = \frac{T_{rq}}{3 \rho_o U_{av}^2 A R \phi_{av}}$$

or the deflection coefficient is a direct function of the torque T_{rq} or work input.

Figure 45 is a graph of the τ_{av} which was calculated at maximum 3-stage efficiency for each stator stagger angle. The minimum of these deflection coefficients occurs at the maximum efficiency. At maximum efficiency the minimum work input was required.

SECTION 7

CONCLUSIONS AND RECOMMENDATIONS

It has been shown that maximum efficiency can be achieved for each flow rate. The computer program AXCO3 can be used to predict efficiency within 2 per cent, with an error of 5 per cent in flow rate. Pressure ratio may be predicted within 0.25 per cent.

It is recommended that further measurements be made at increased rotor stagger angles. Inlet guide vane angles should be varied to simulate the effects of preceding blade rows. Blade shapes with higher blade loadings should be tested.

Scatter in the data may be caused by variations in inlet flow and accentuated by oscillations of the pressure gauge. A proposed improved inlet duct is described in Appendix E.

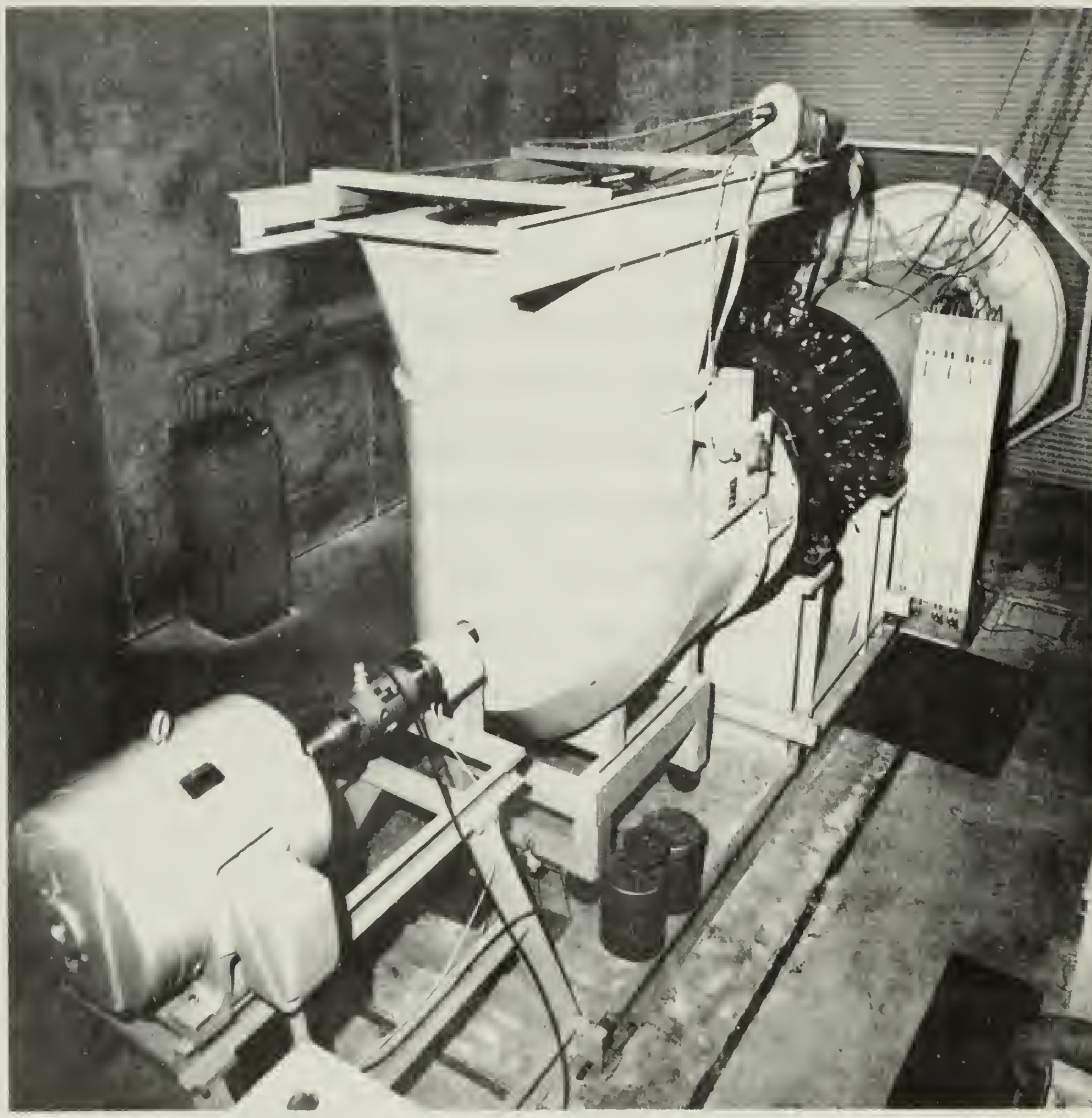

FIGURE I COMPRESSOR INSTALLATION

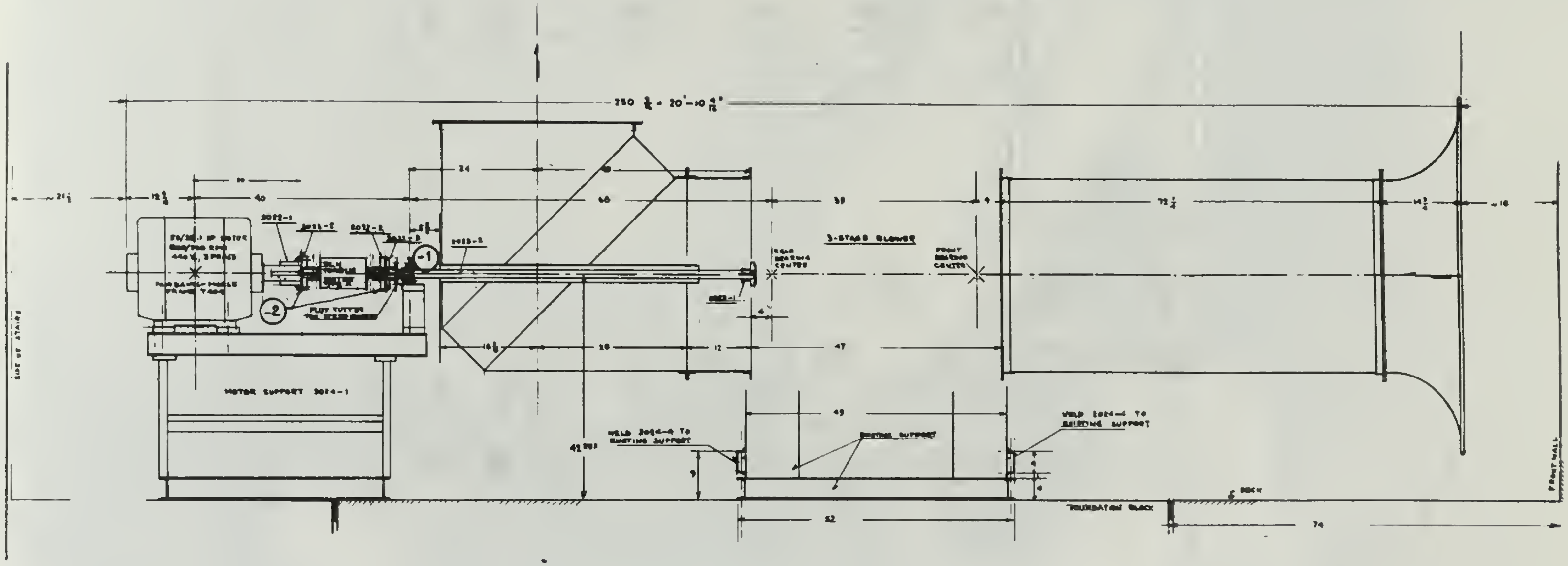

FIGURE 2 ACCESSORIES TO COMPRESSOR

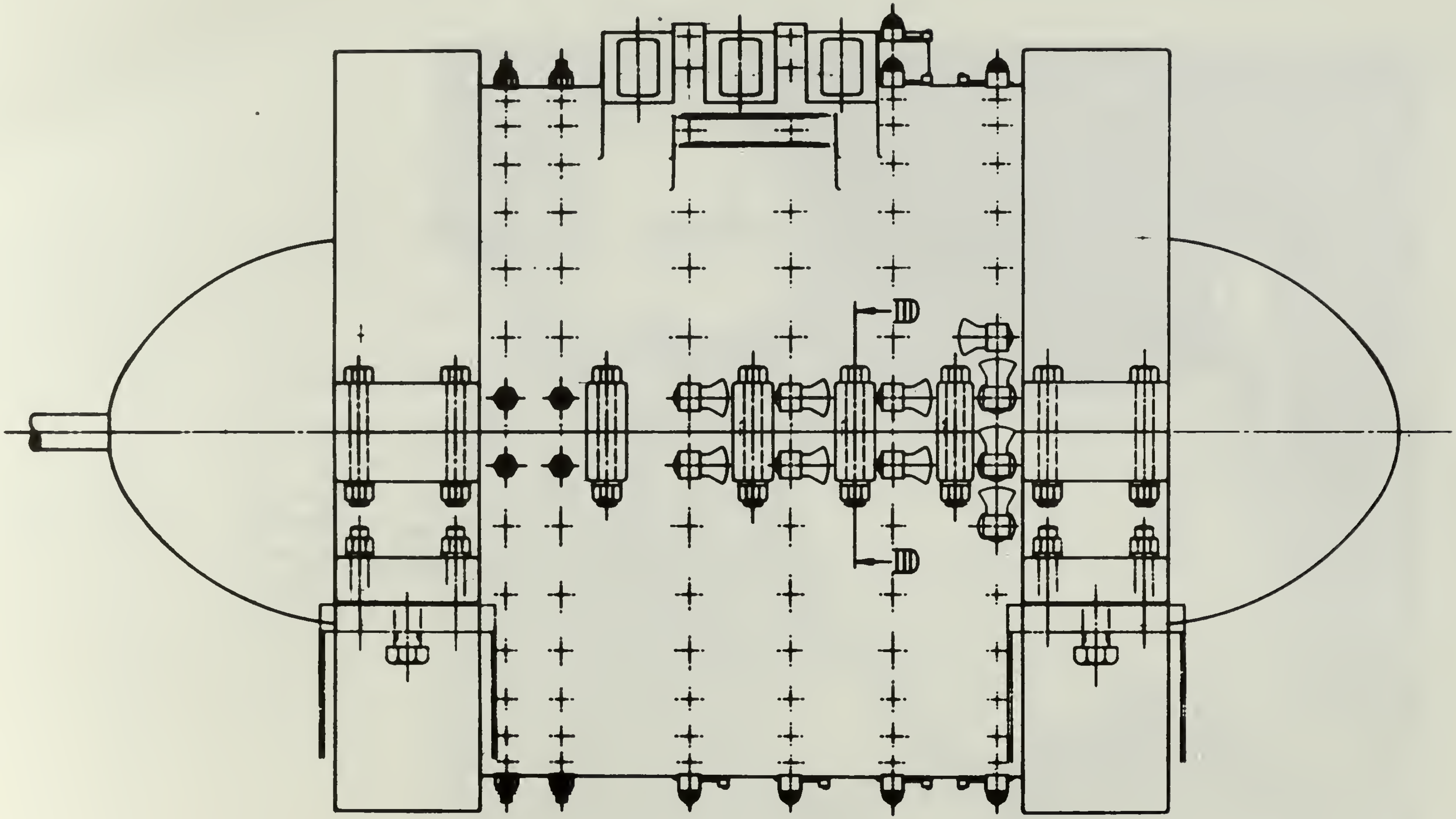

FIGURE 3 COMPRESSOR CASING

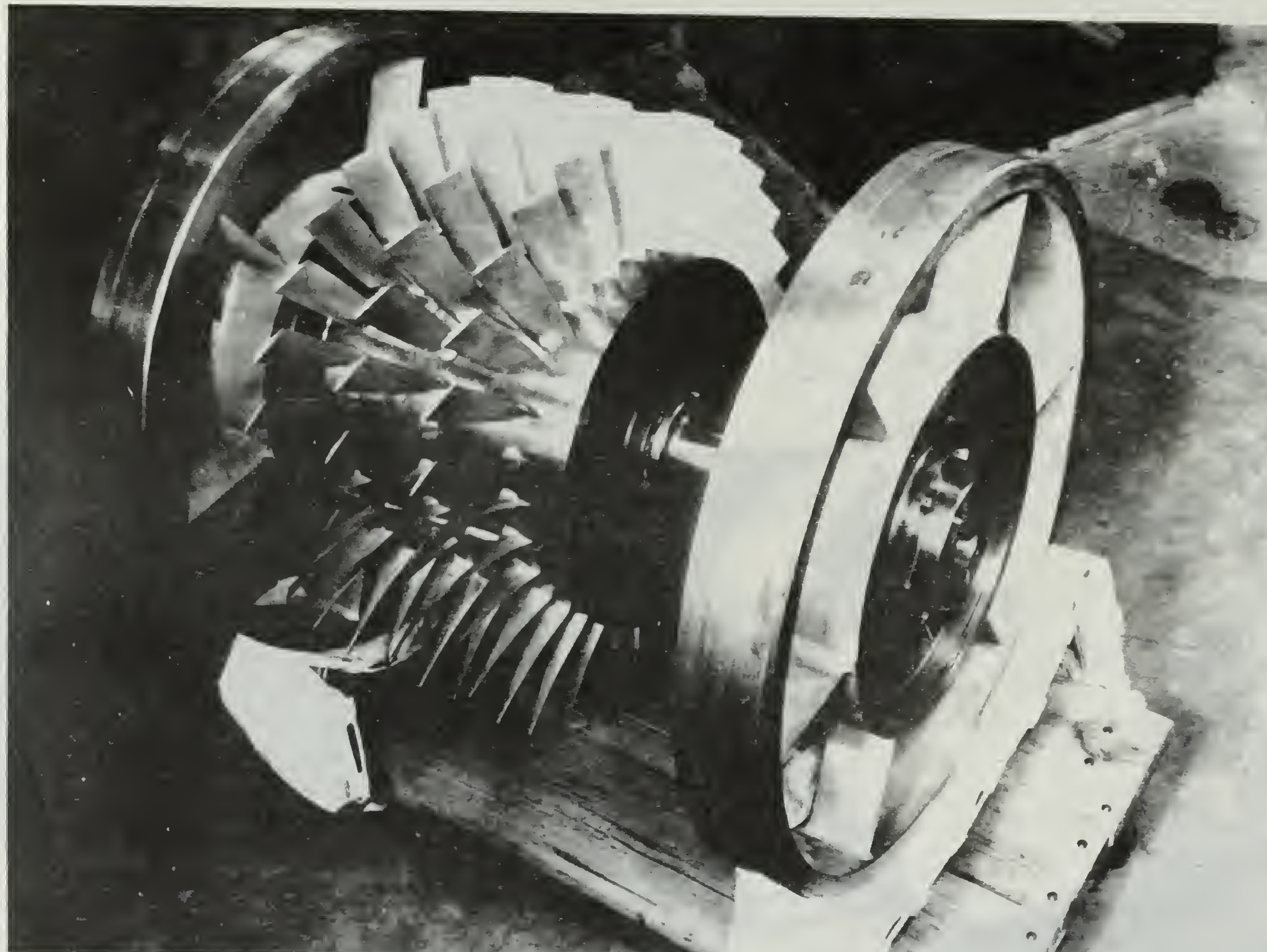

FIGURE 4 ROTOR BLADES, DRUM AND SHAFT MOUNTED IN SUPPORTING STRUT ASSMBLIES

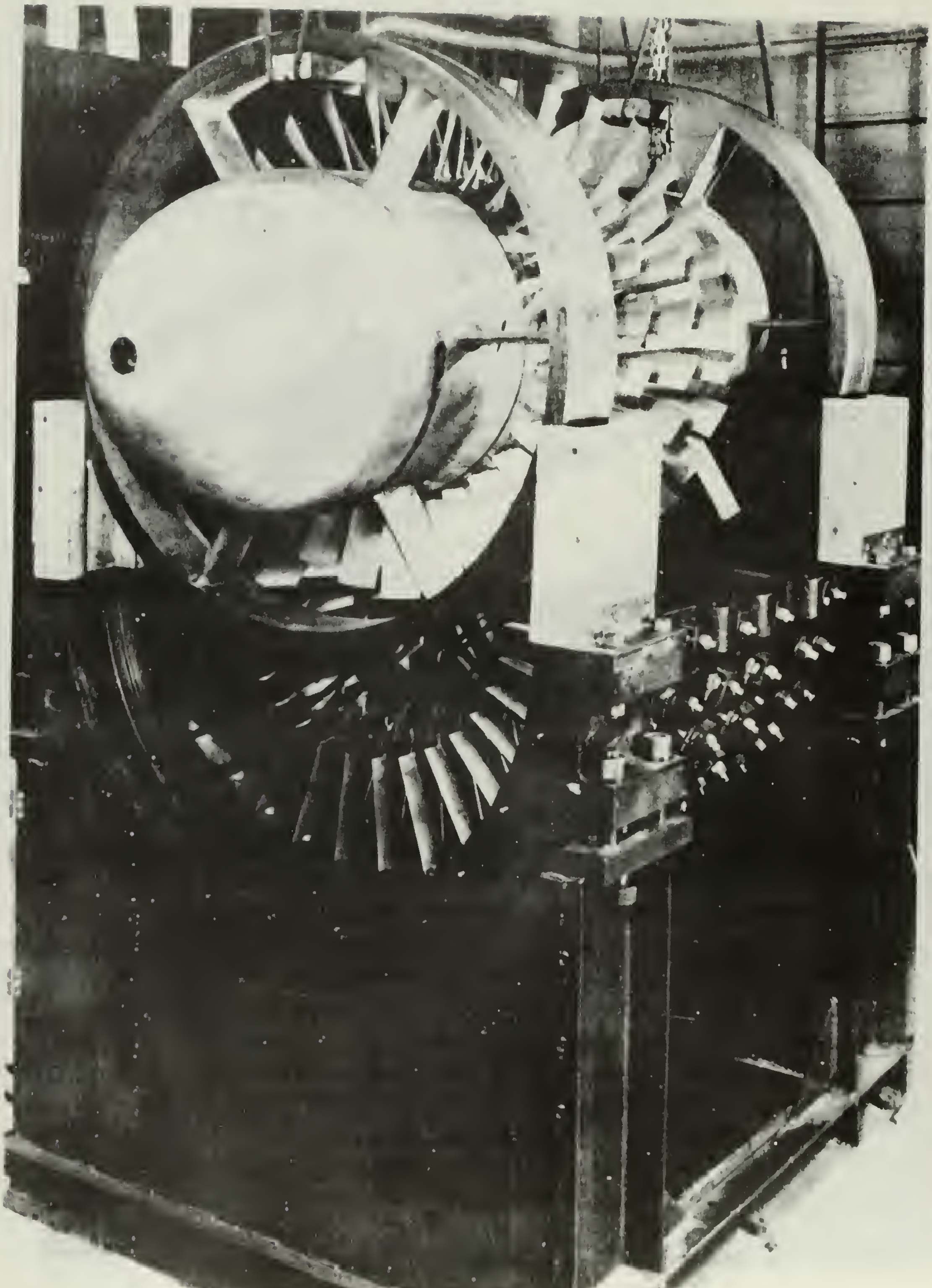

FIGURE 5 ASSEMBLY OF ROTOR IN LOWER CASING

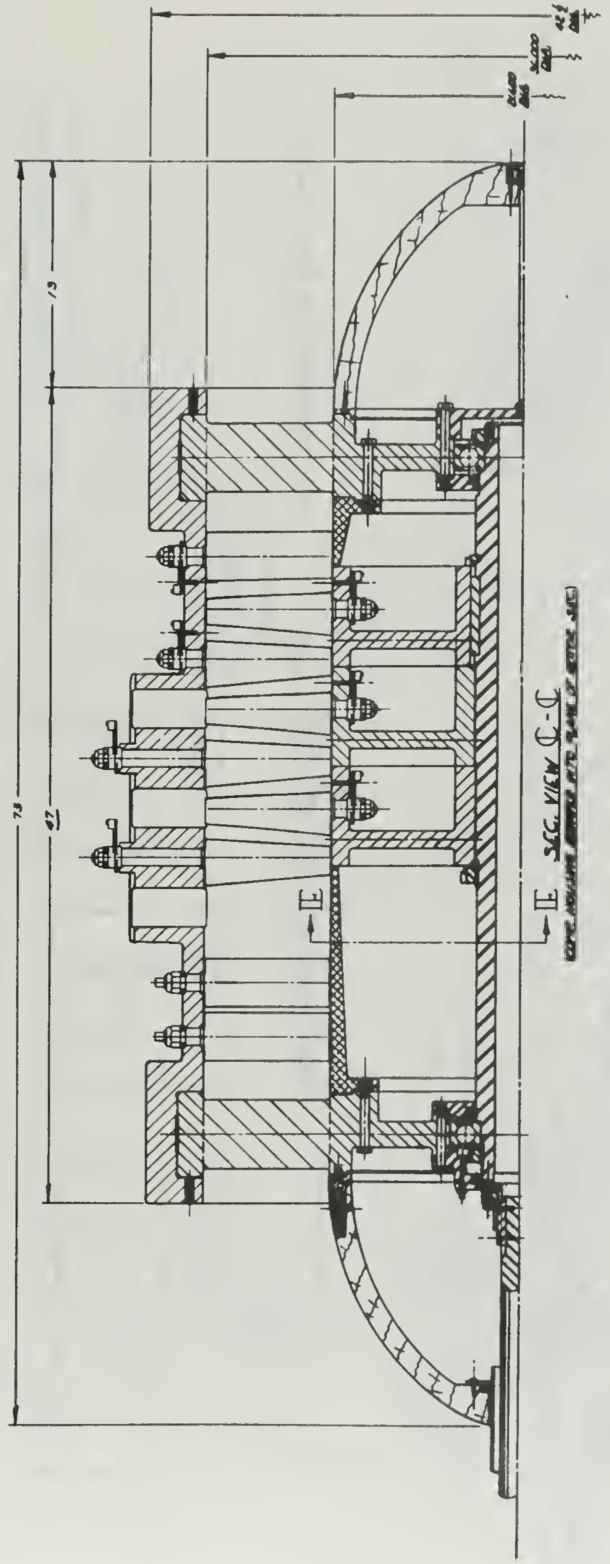

FIGURE 6 COMPRESSOR SECTIONAL VIEW

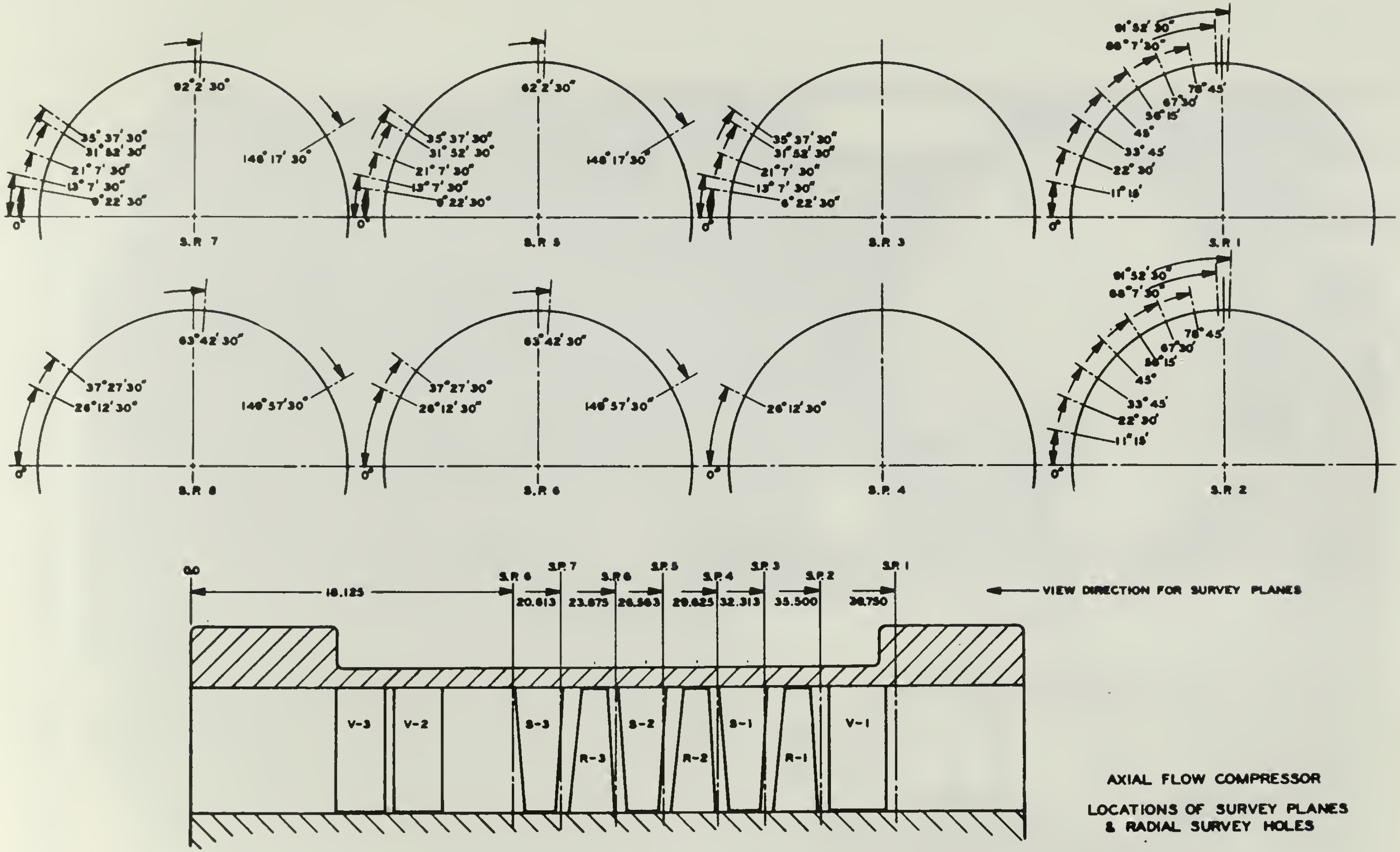

FIGURE 7 LOCATION OF RADIAL SURVEY HOLES

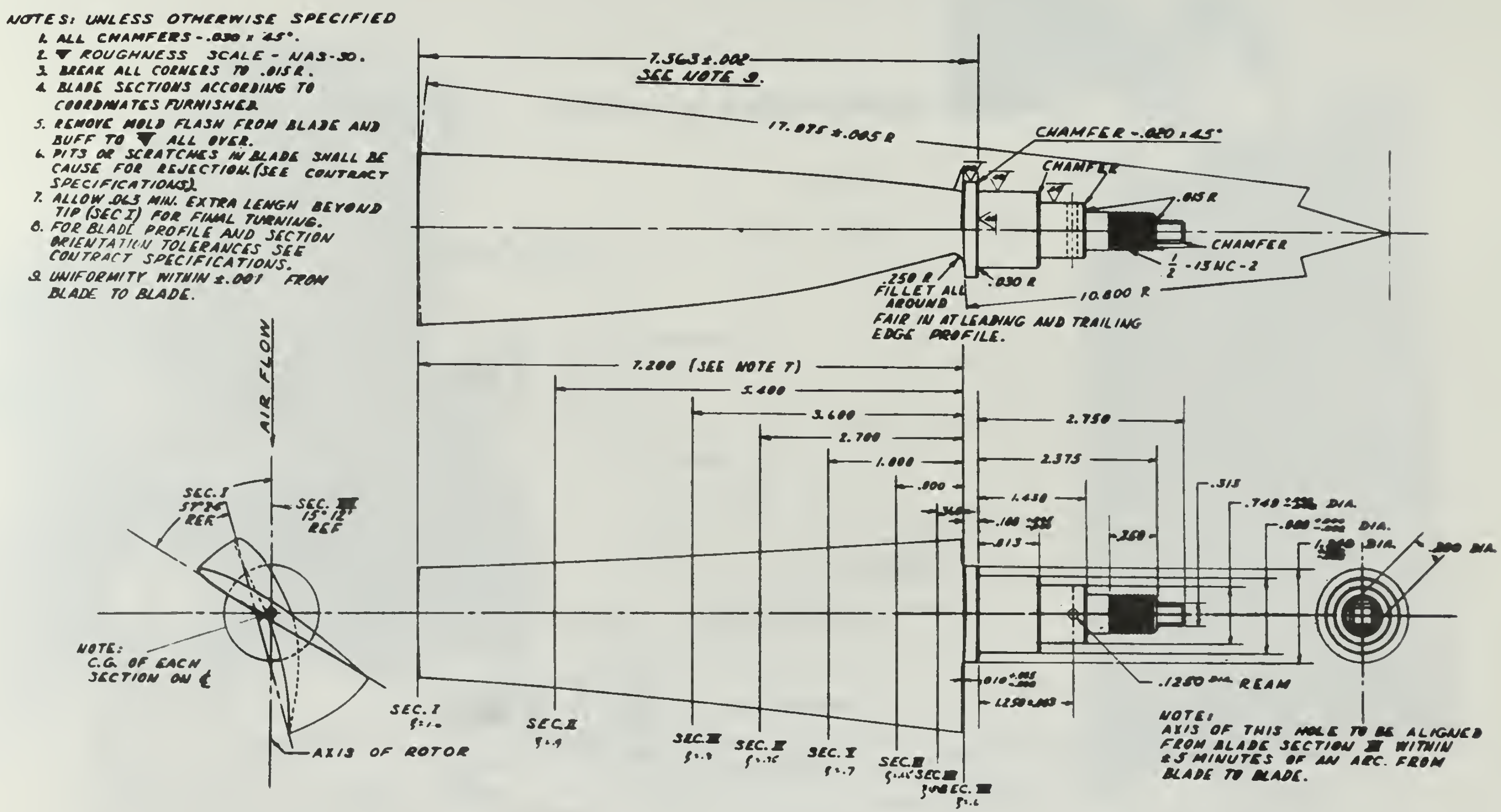

FIGURE 8 DETAIL OF FREE - VORTEX ROTOR

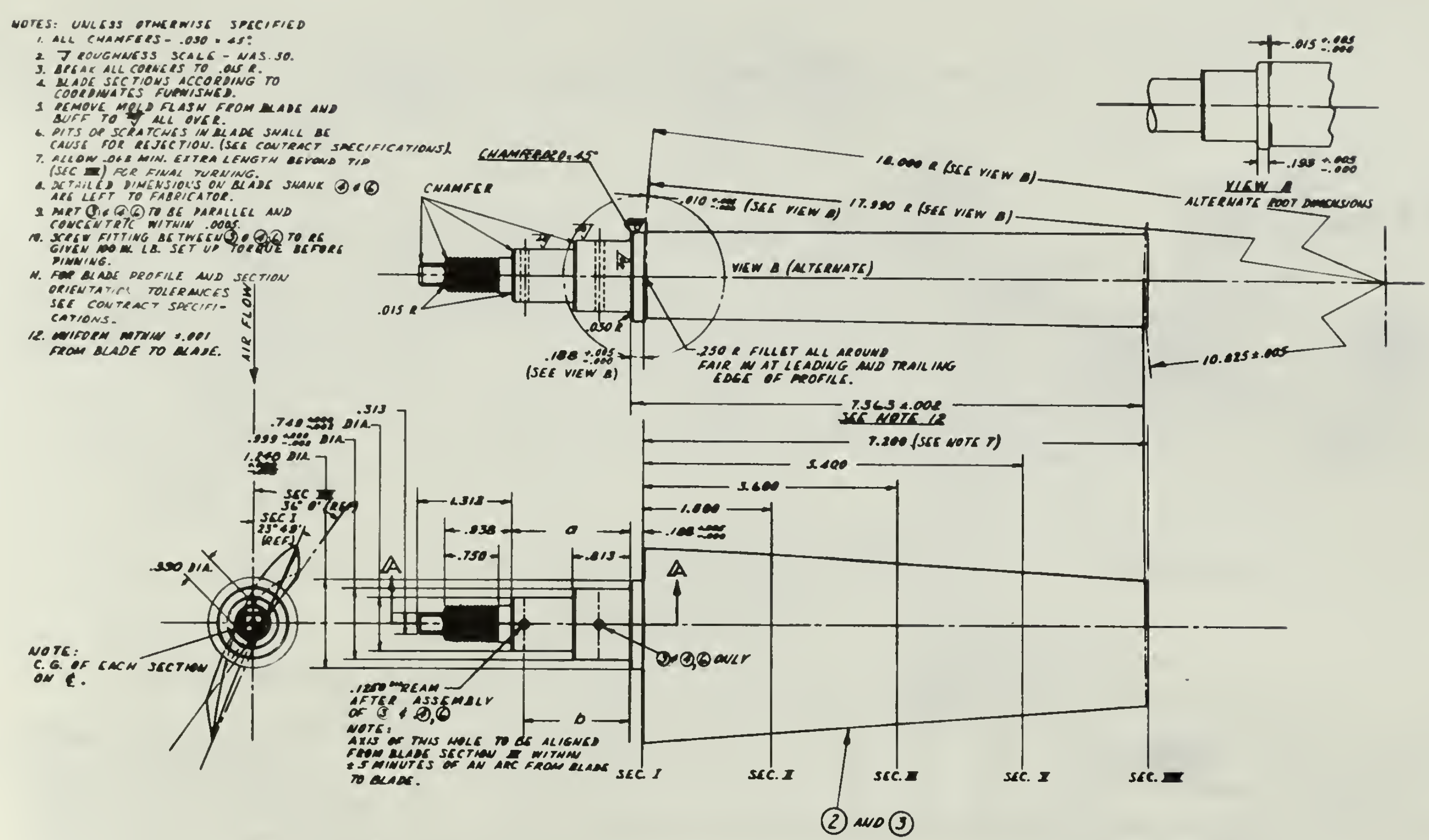

FIGURE [illegible] DETAIL OF FREE-VORTEX STATOR

FIGURE 10 FREE-VORTEX STATOR BLADE

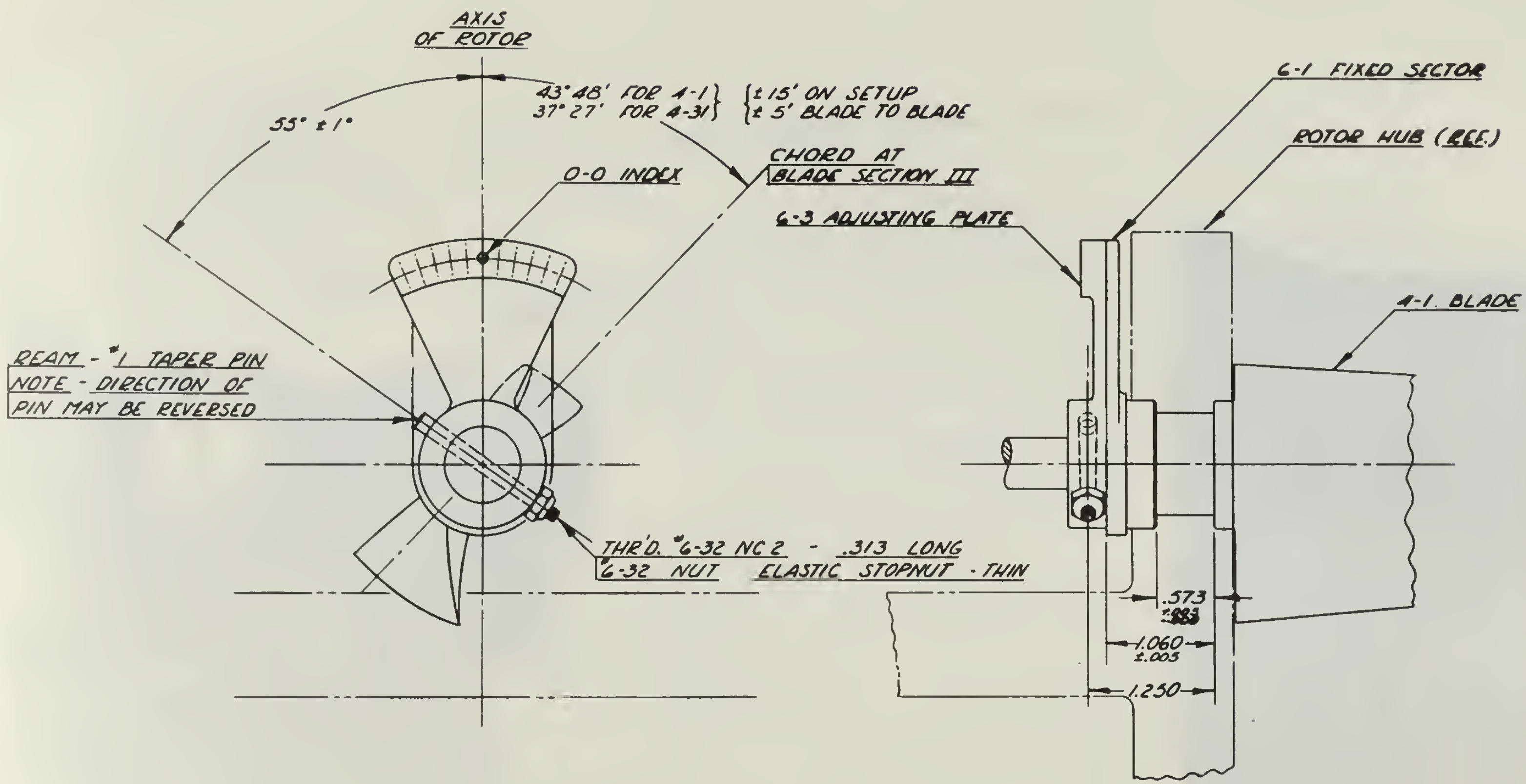

FIGURE 11 ROTOR STAGGER ANGLE ADJUSTMENT

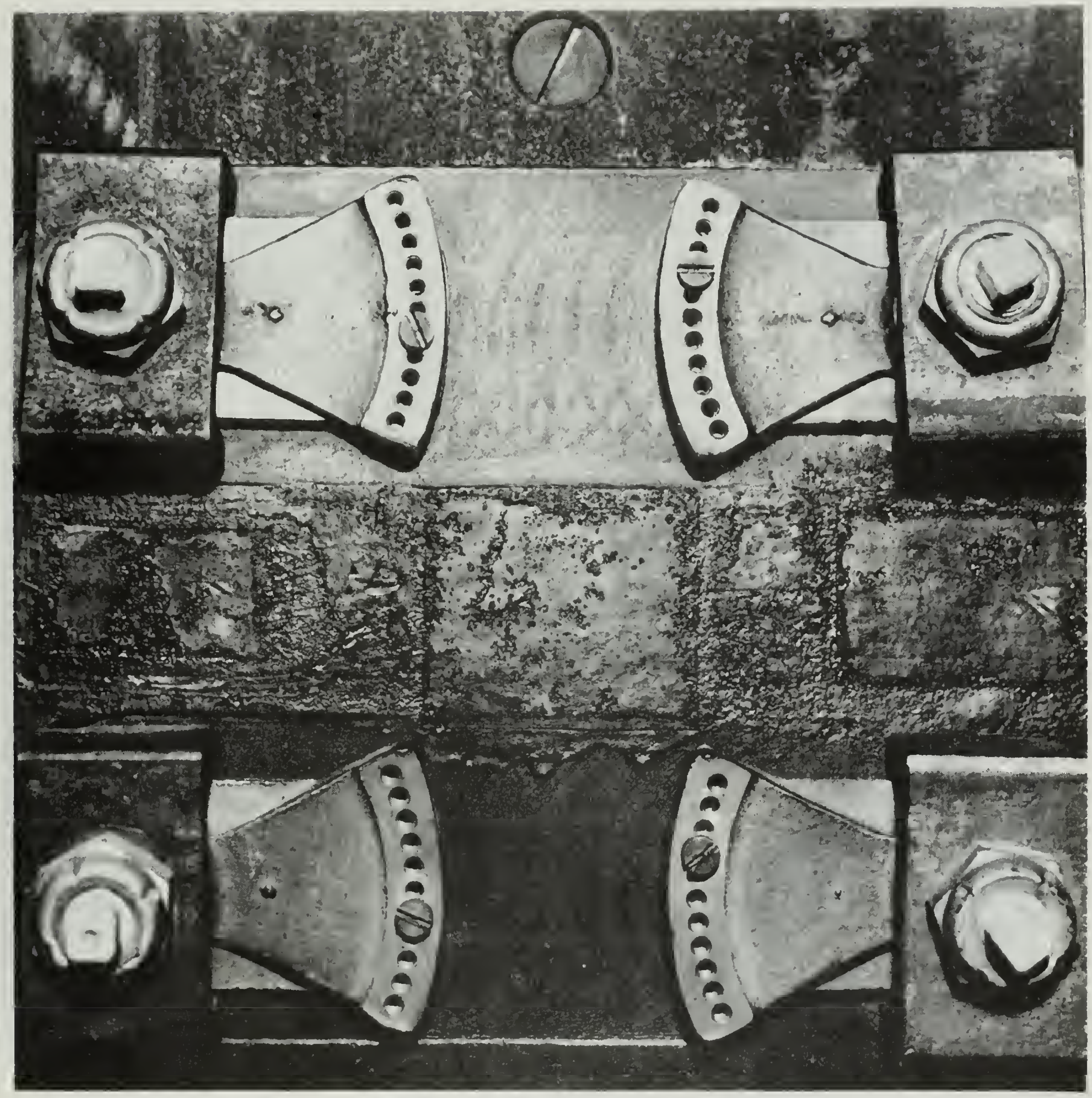

FIGURE 12 EXTERNAL STAGGER ANGLE ADJUSTMENT

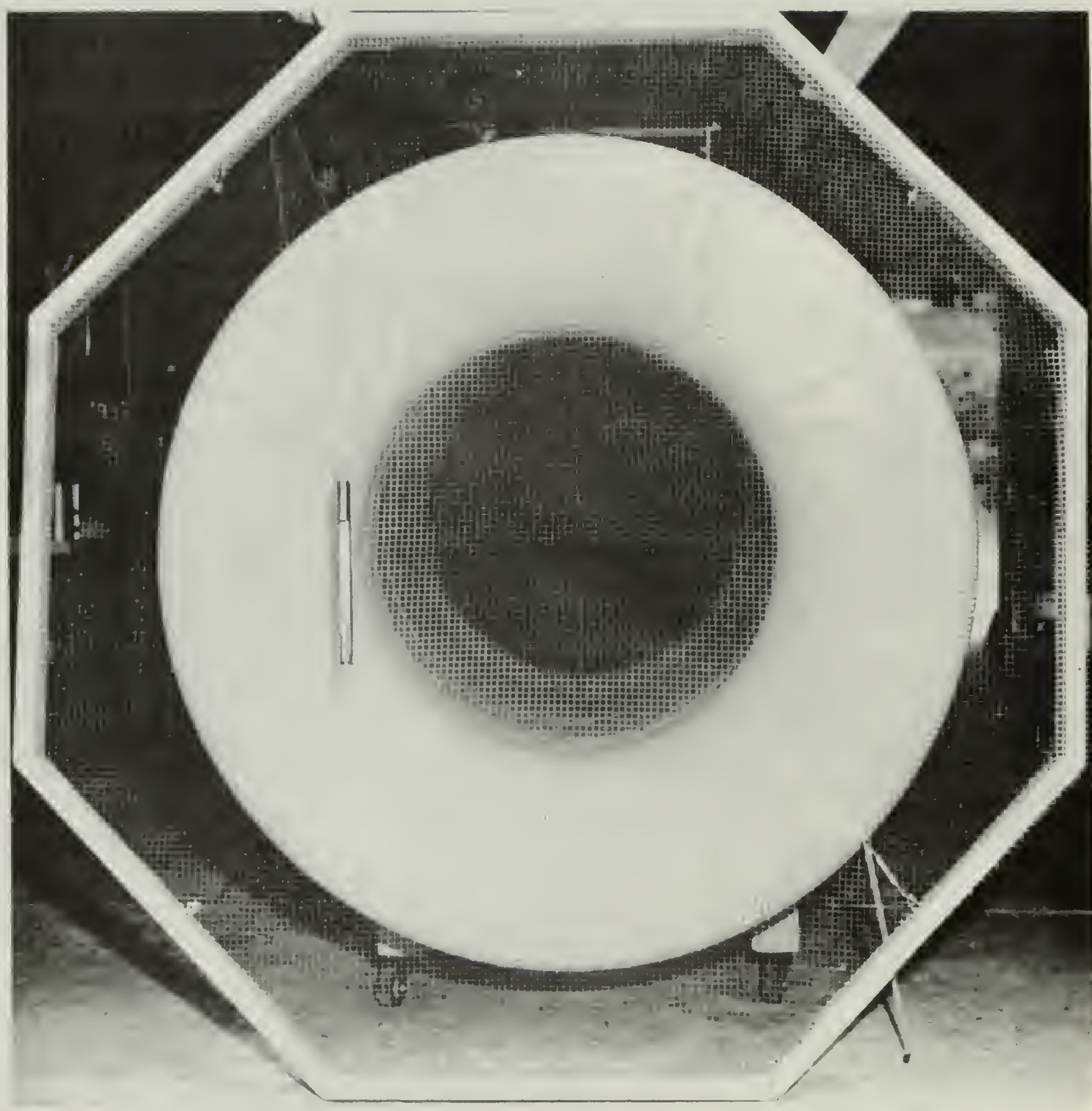

FIGURE 13 INLET BELLMOUTH

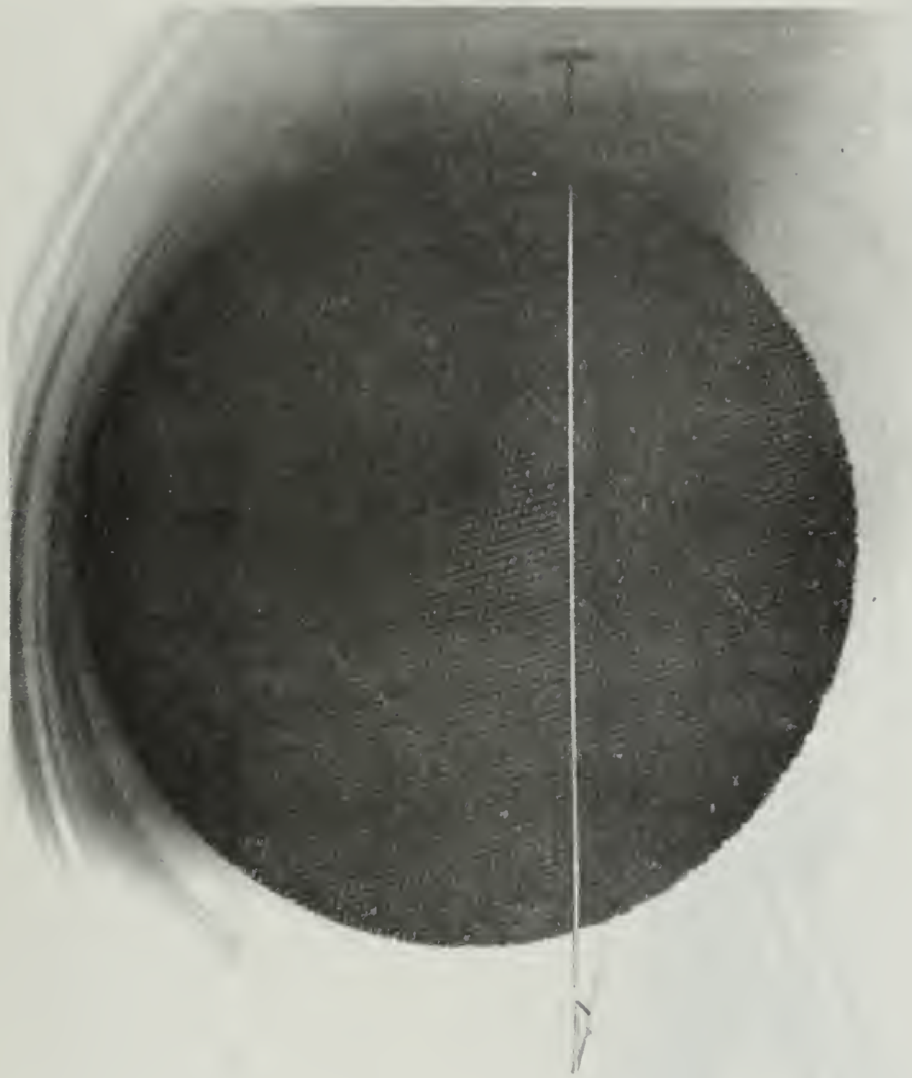

FIGURE 14 INLET PITOT-STATIC TRAVERSE

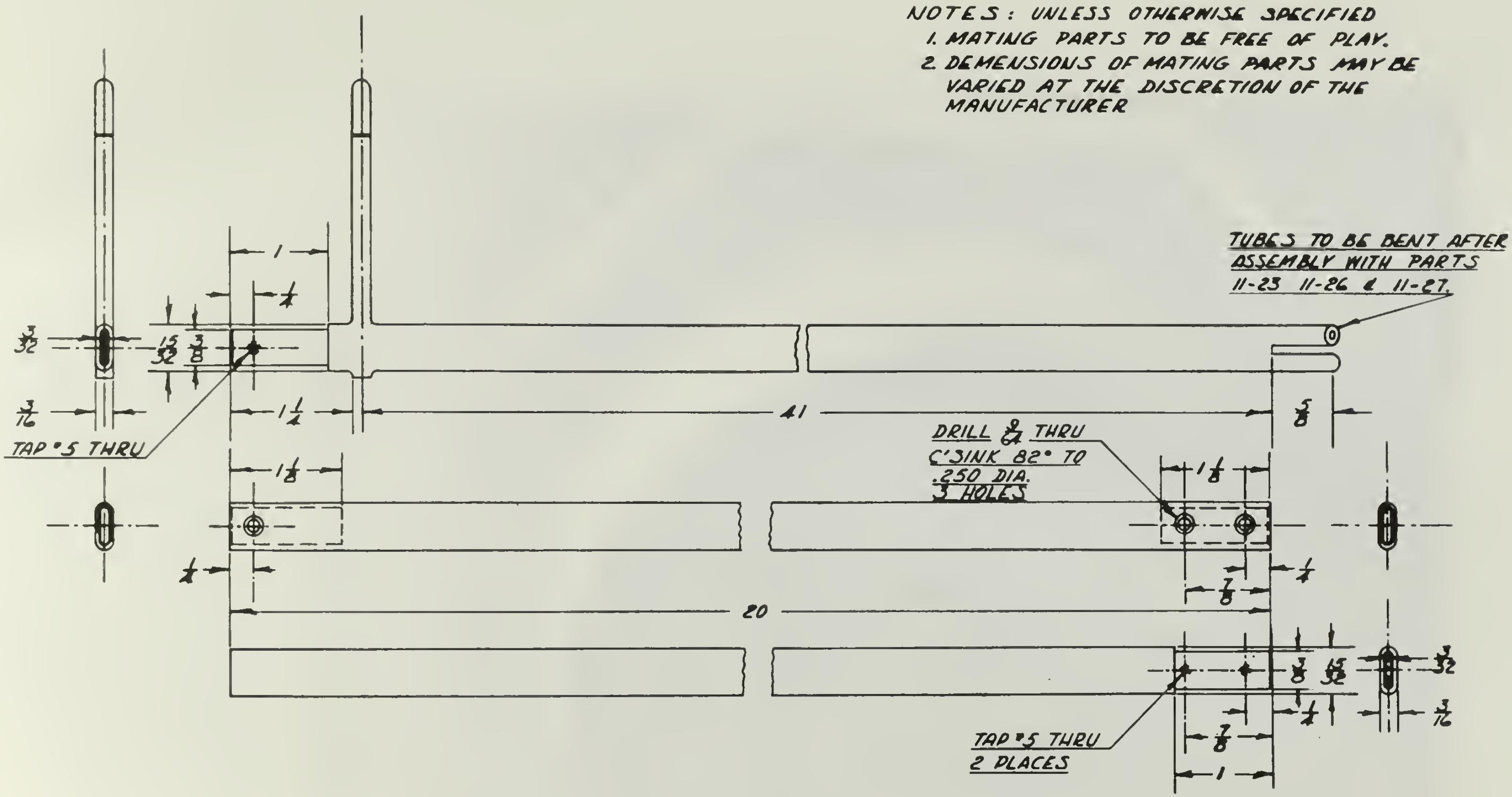

FIGURE 15 DETAIL OF INLET PITOT-STATIC TRAVERSE

FIGURE 16 THREE-HOLE PROBE DETAIL

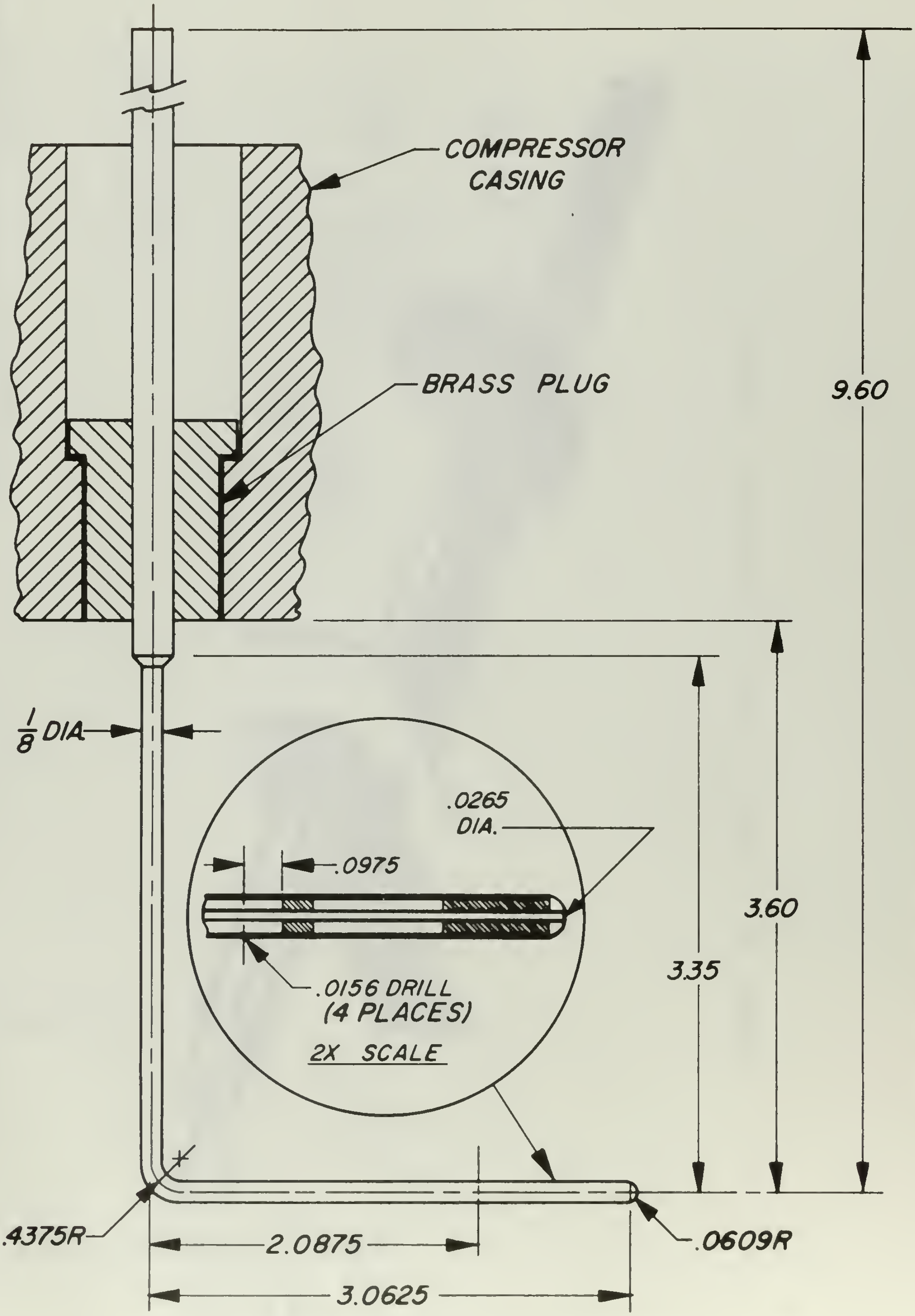

FIG. 17 PERMANENT PITOT—STATIC TUBE

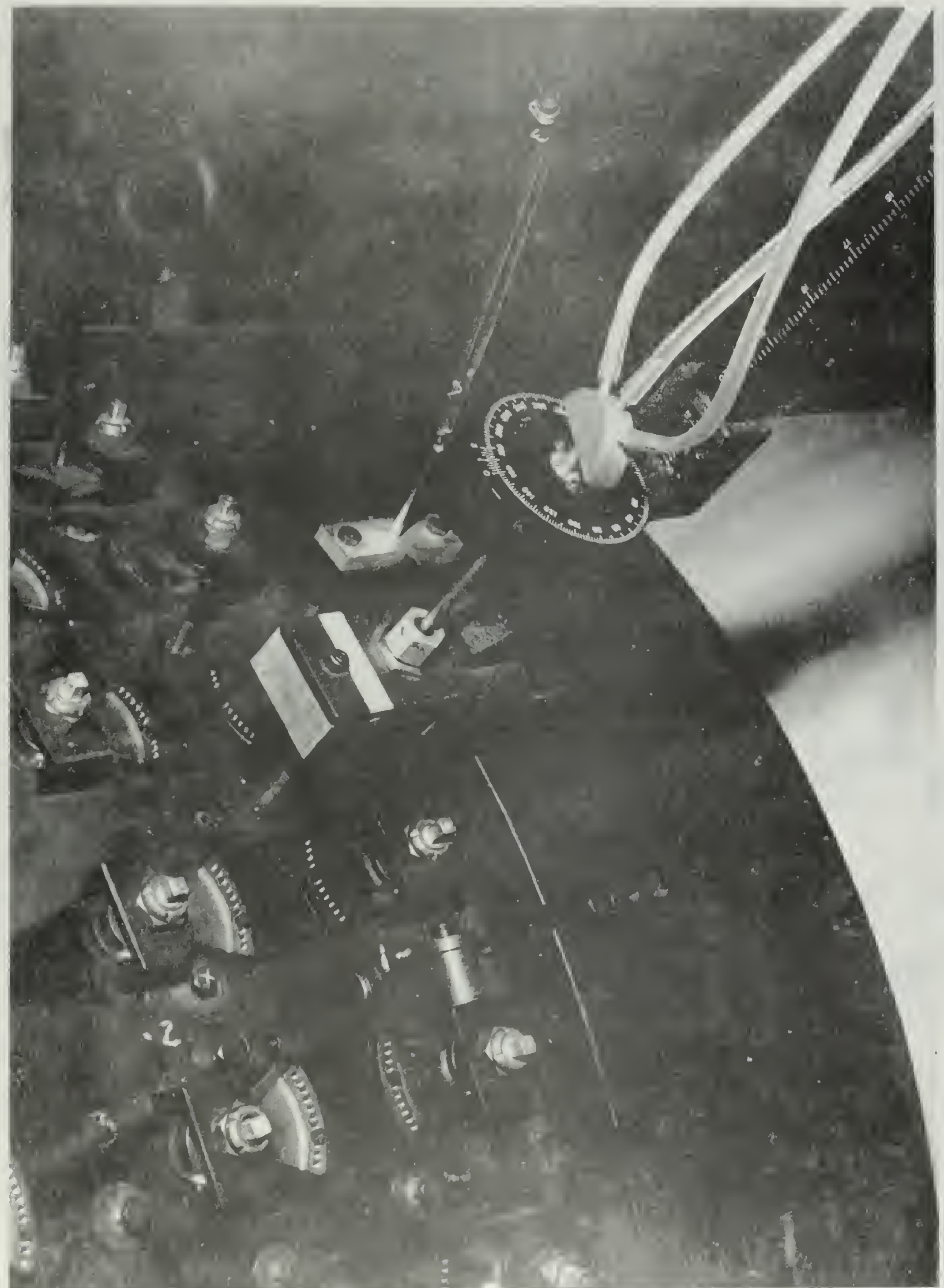

FIGURE 18 PERMANENT PITOT – TUBE AND THREE – HOLE PROBE AHEAD OF FIRST ROTOR

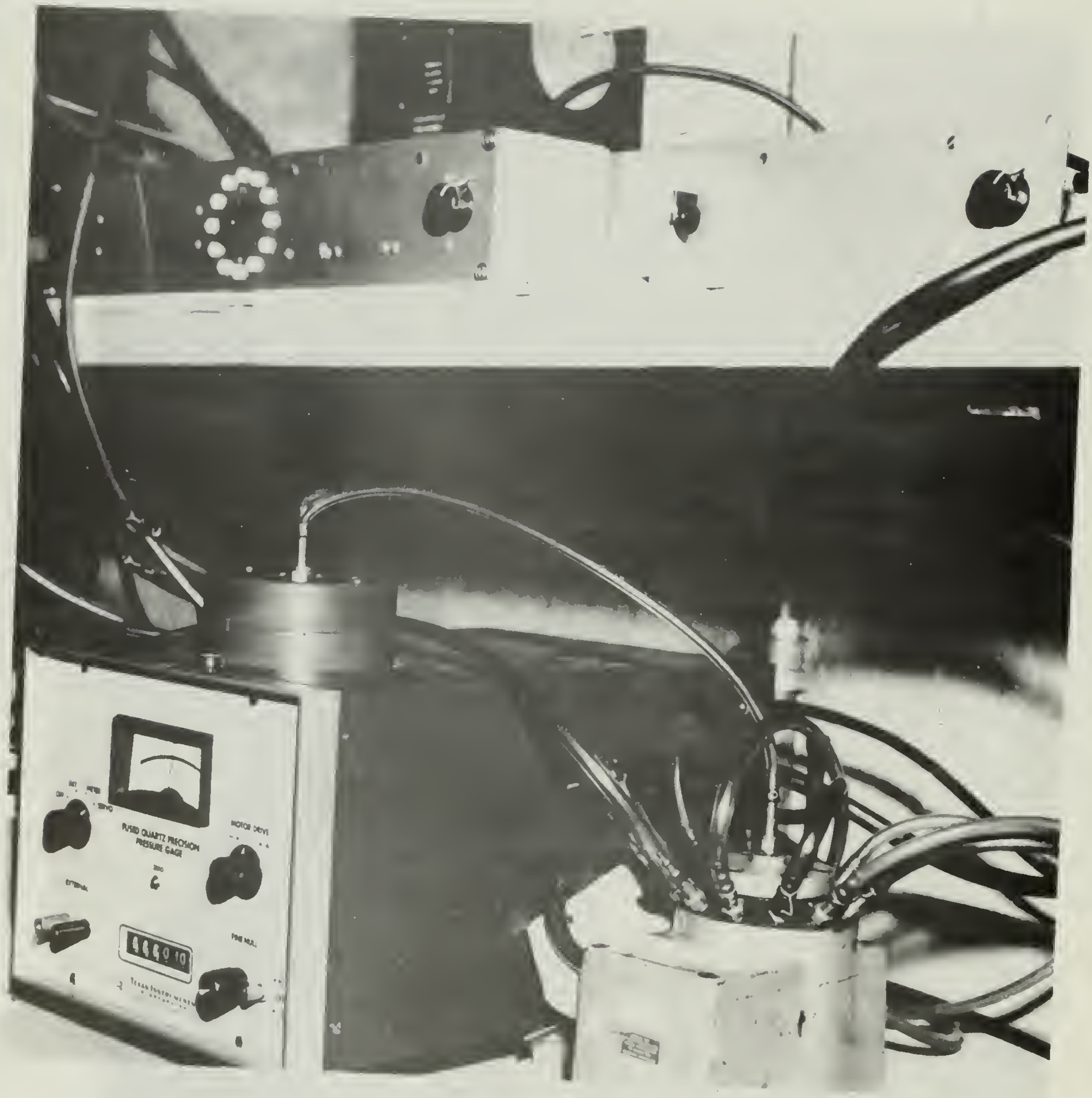

FIGURE 19 PRESSURE READOUT INSTRUMENTATION

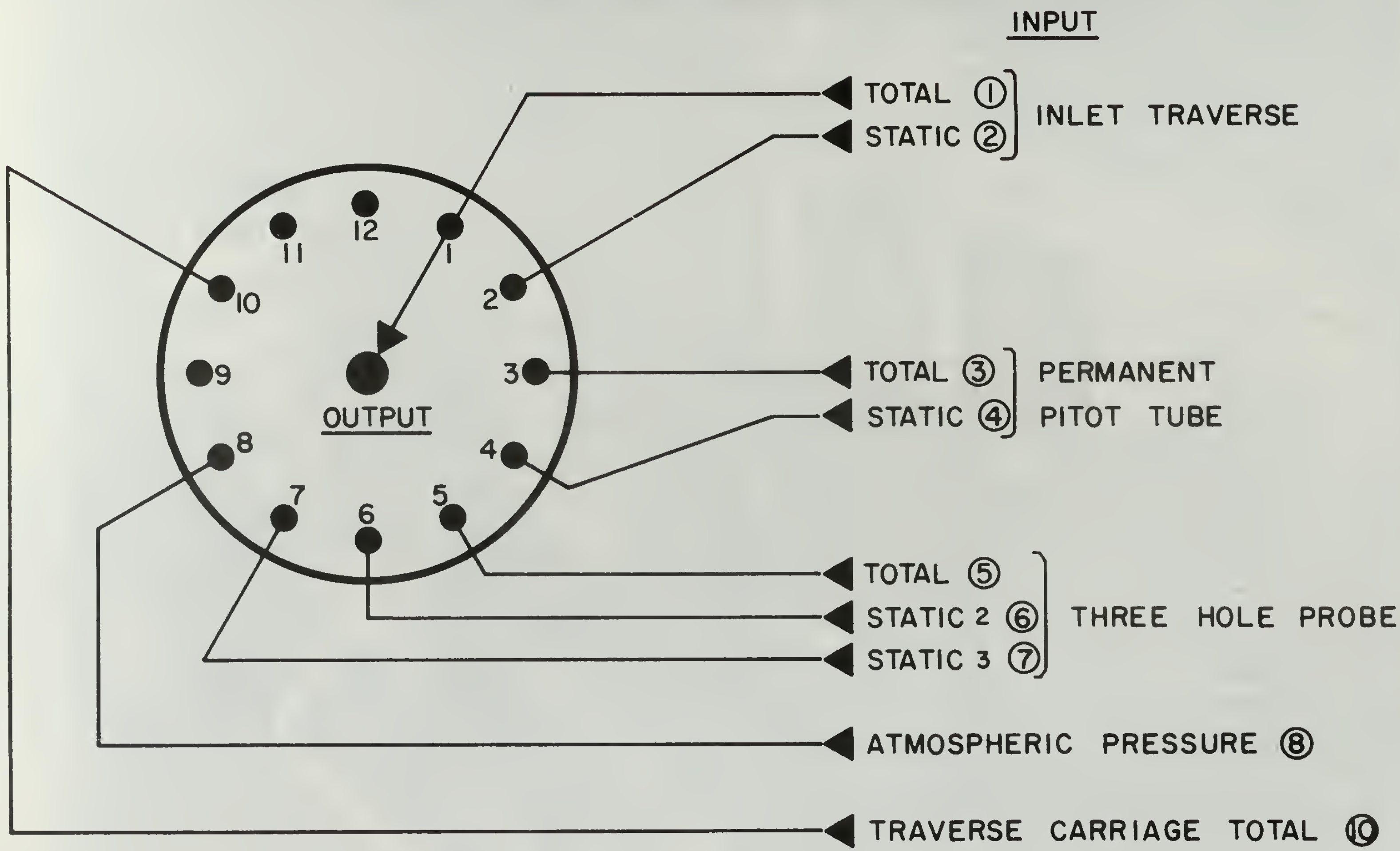

FIG. 20 PRESSURE SELECTION BY SCANNER VALVE

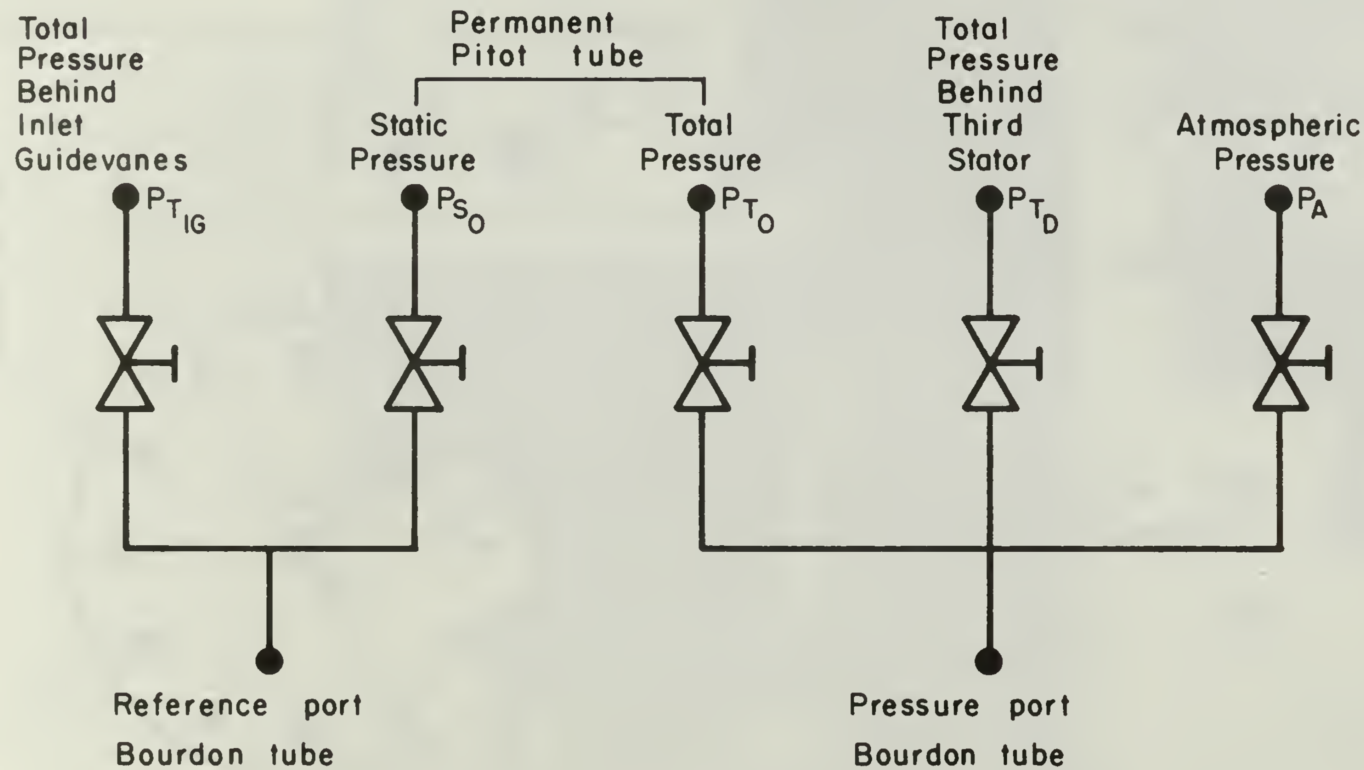

FIG. 21 SIMPLIFIED PRESSURE SELECTION SYSTEM.

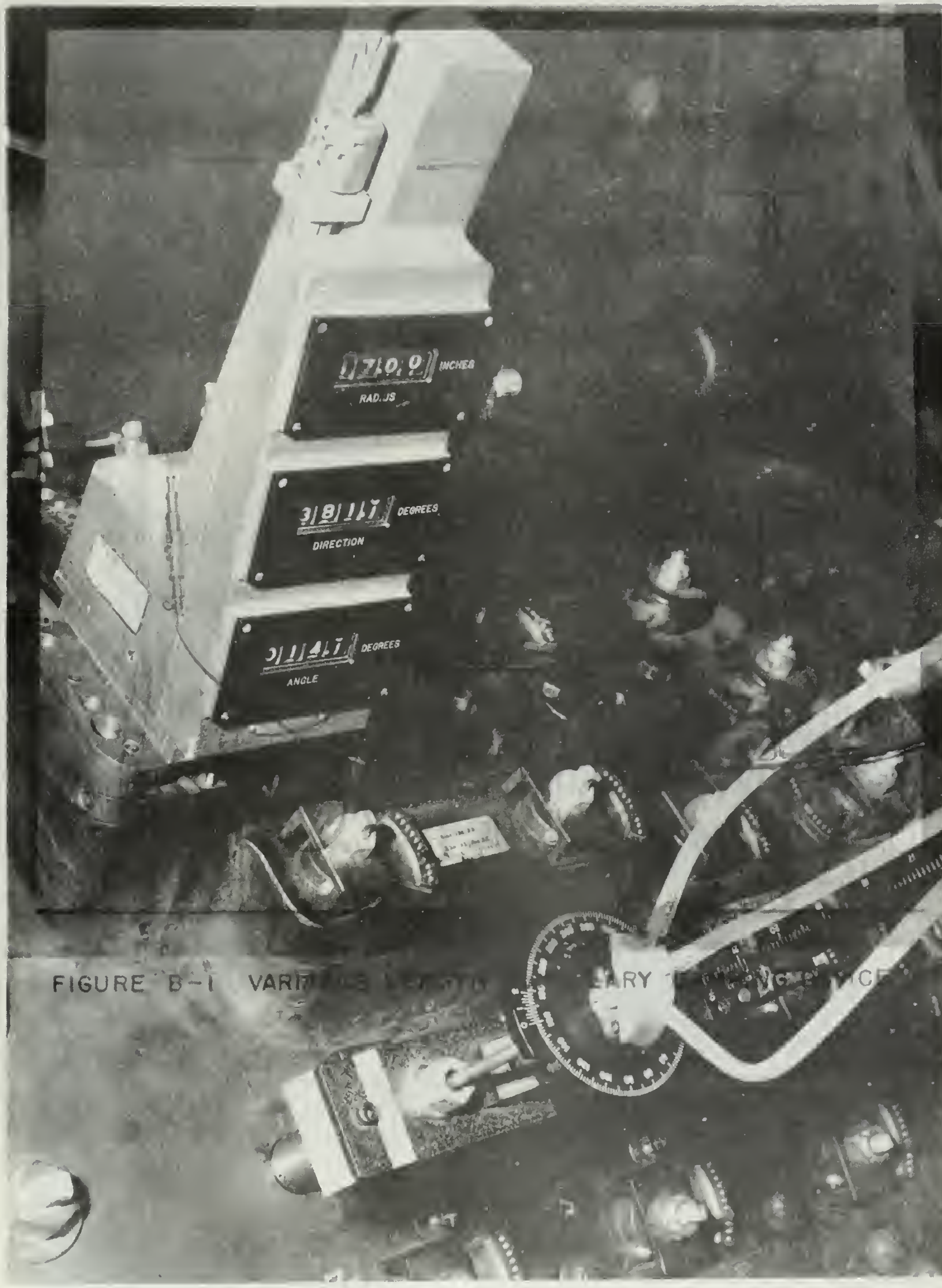

FIGURE 22 TRAVERSE CARRIAGE AND THREE — HOLE PROBE BEHIND THIRD STATOR

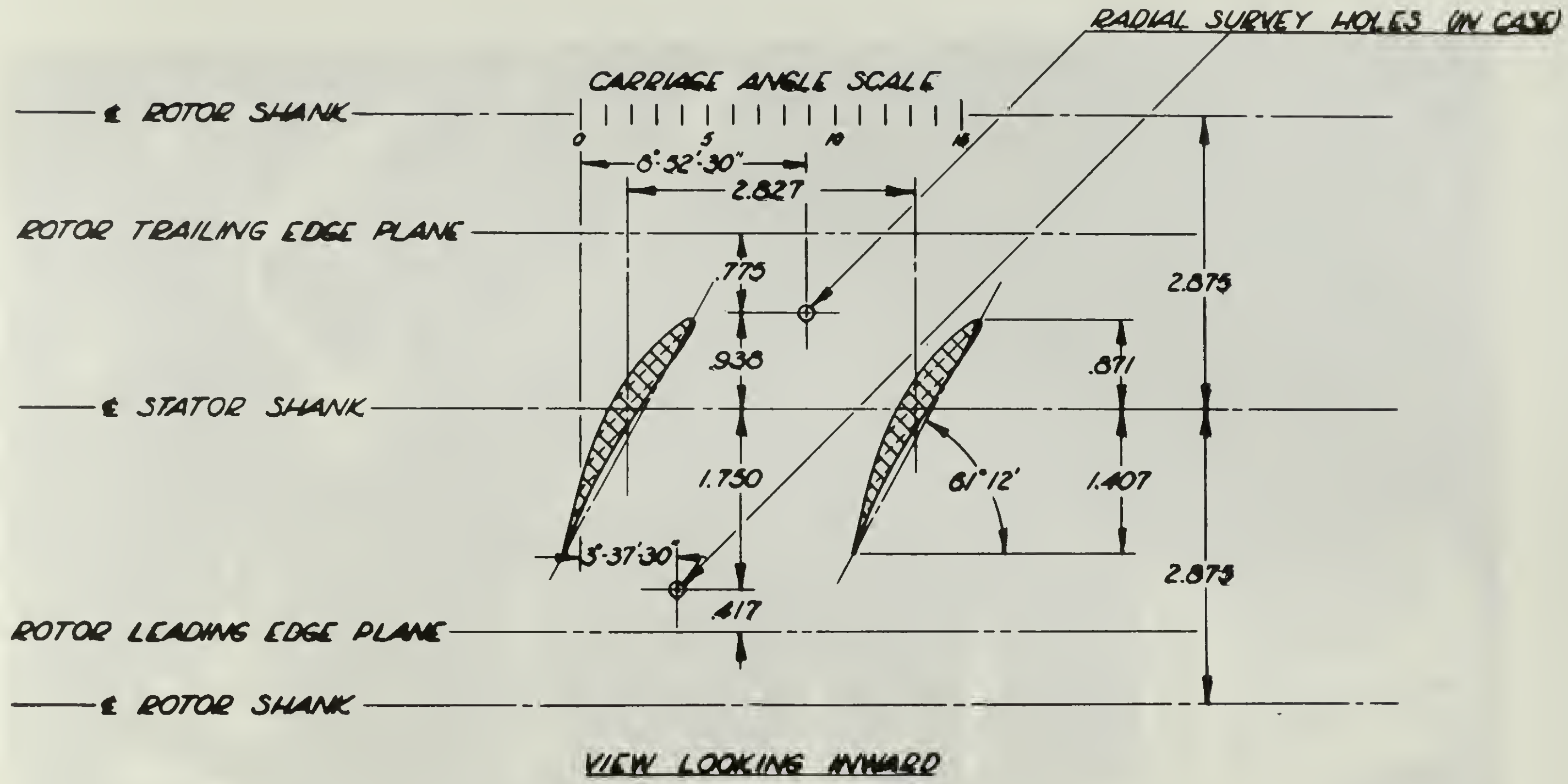

FIGURE 23 RELATION OF TRAVERSE CARRIAGE TO SURVEY HOLES

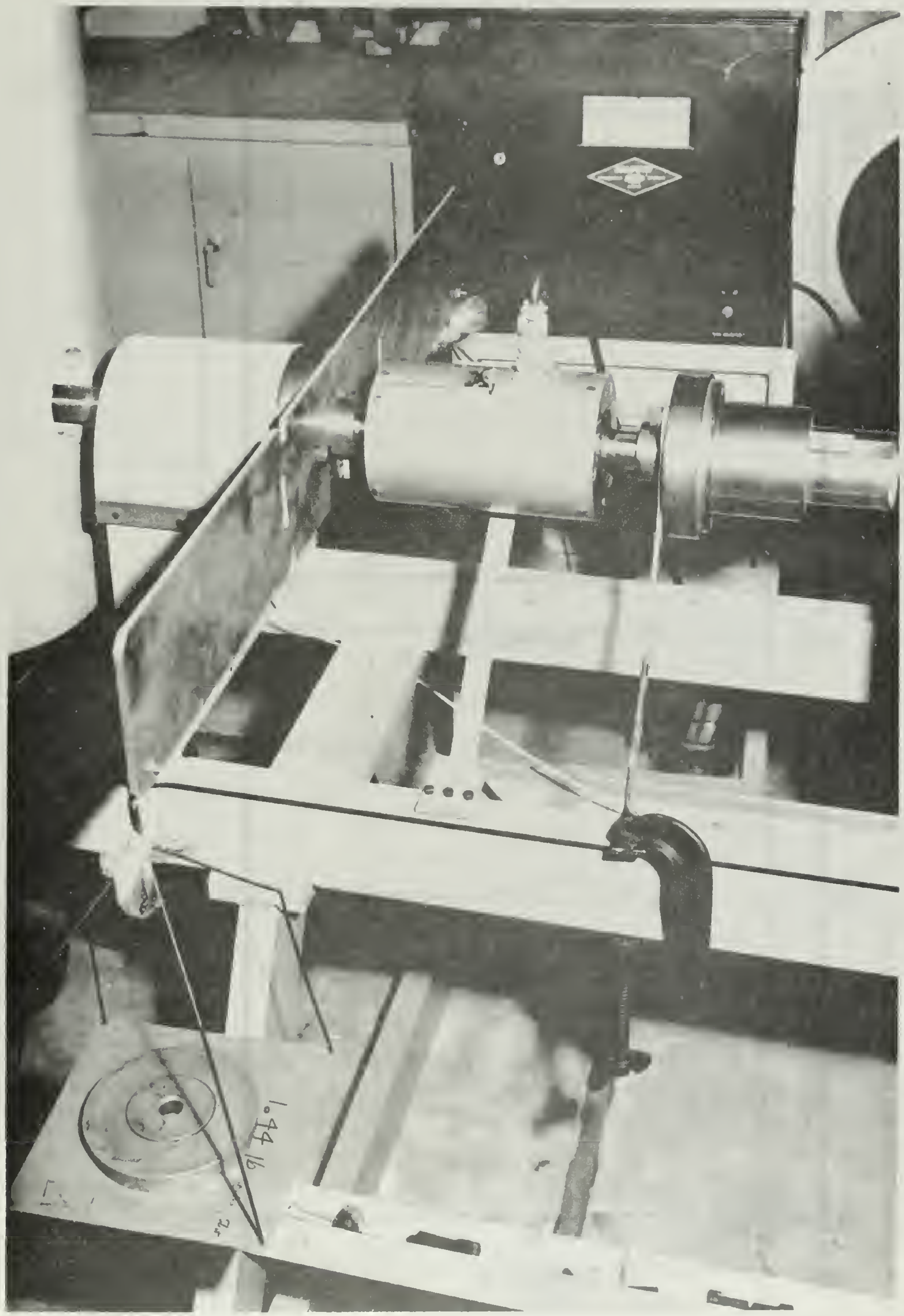

FIGURE 24 TORQUE METER DURING CALIBRATION

FIGURE 25 TRAVERSE OF INLET DUCT RUN D-1
VOLUME FLOW RATE 512 FT^3/SEC

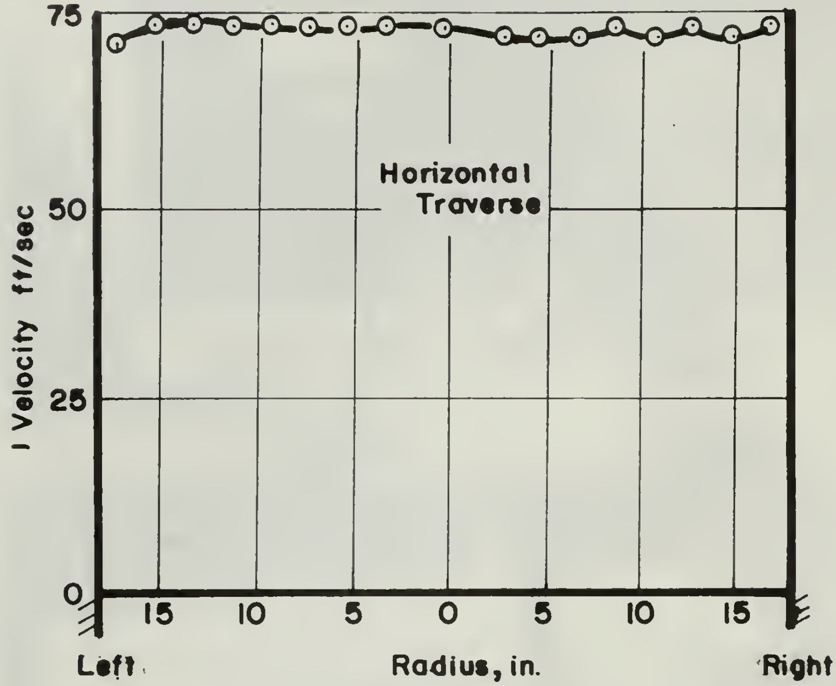

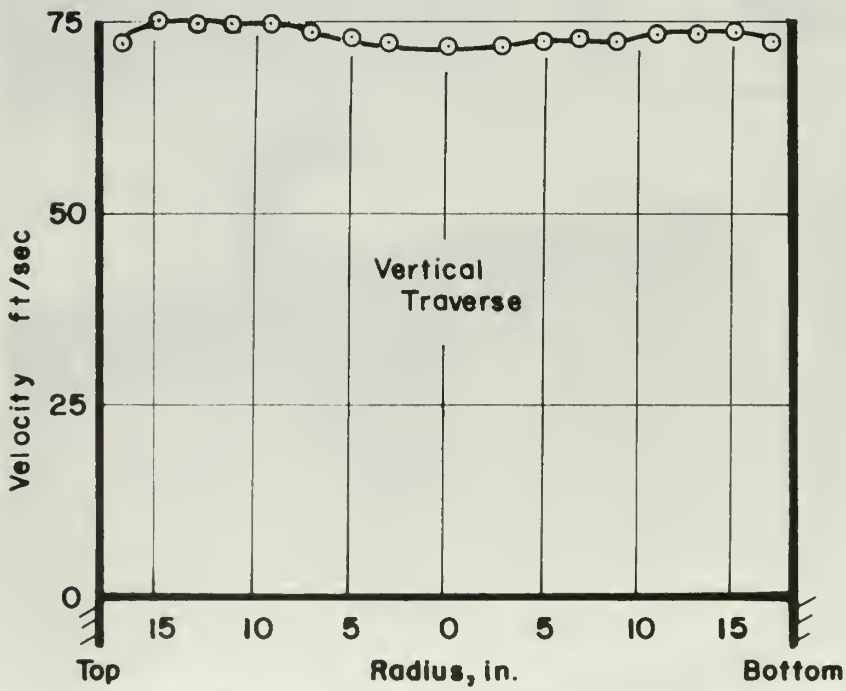

FIGURE 26 TRAVERSE OF INLET DUCT RUN D-7
VOLUME FLOW RATE 310 FT^3/SEC.

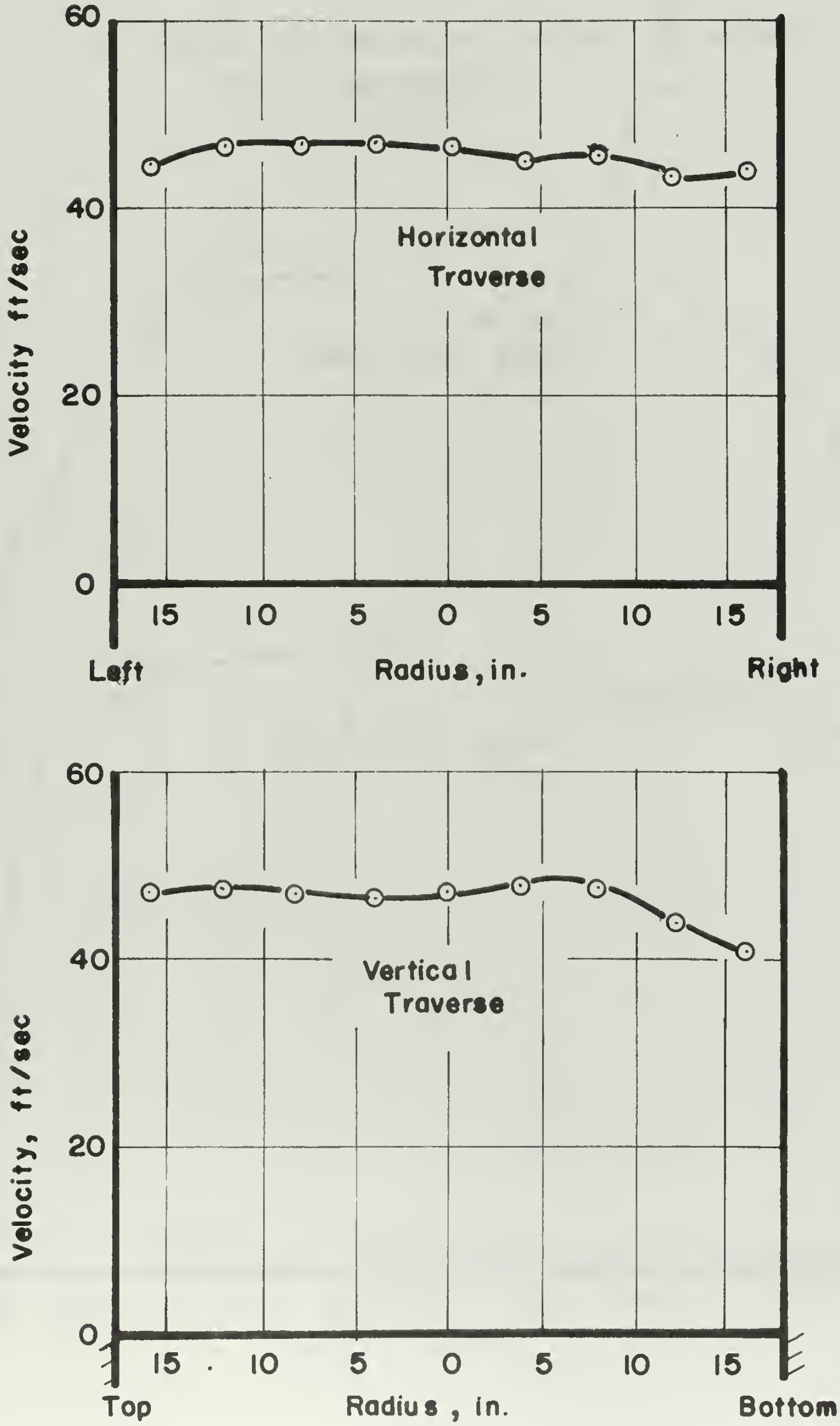

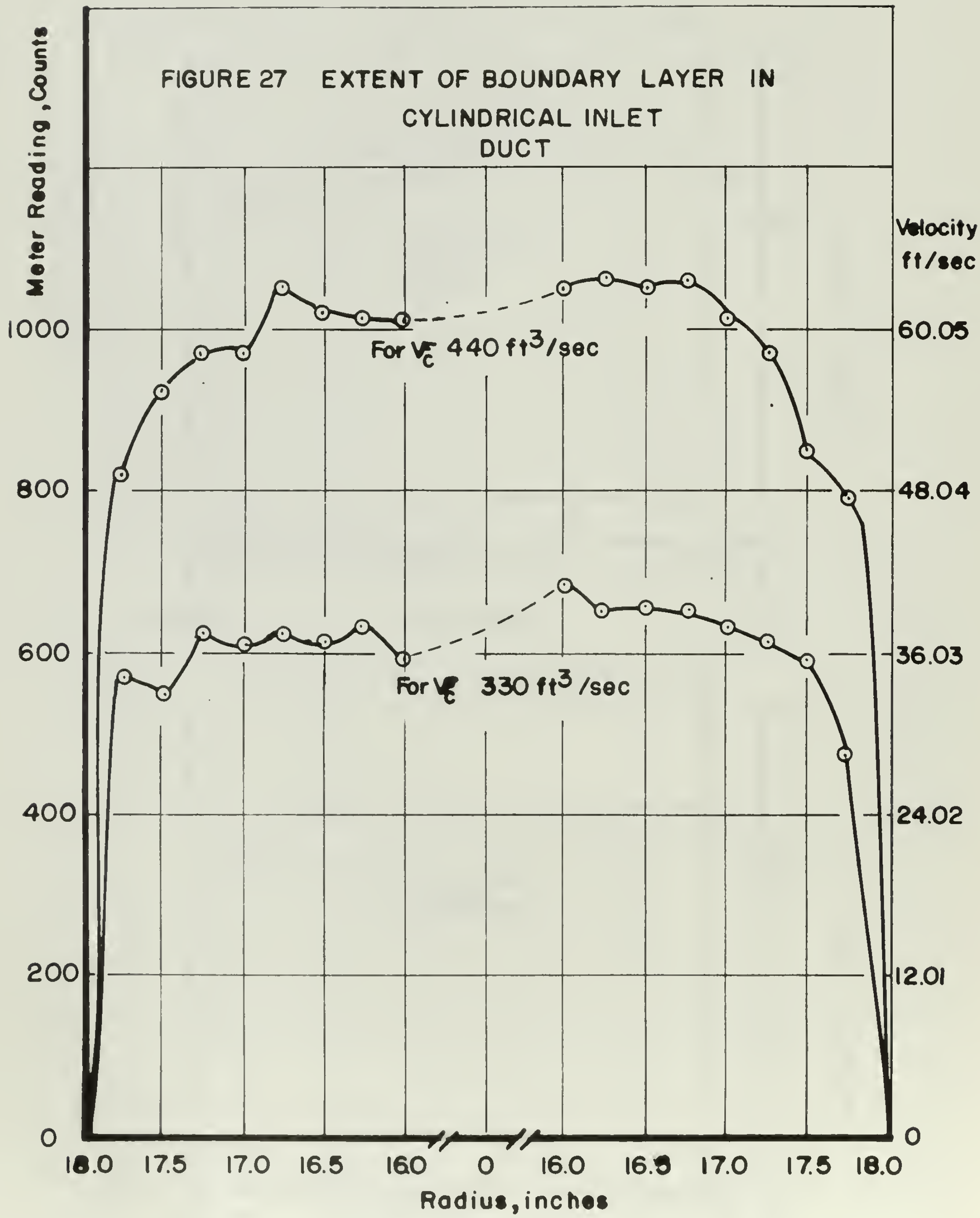
FIGURE 27 EXTENT OF BOUNDARY LAYER IN CYLINDRICAL INLET DUCT
Meter Reading, Counts
Velocity ft/sec
For V_c 440 ft^3/sec
For V_c 330 ft^3/sec
1000
800
600
400
200
0
60.05
48.04
36.03
24.02
12.01
0
18.0 17.5 17.0 16.5 16.0 0 16.0 16.5 17.0 17.5 18.0
Radius, inches

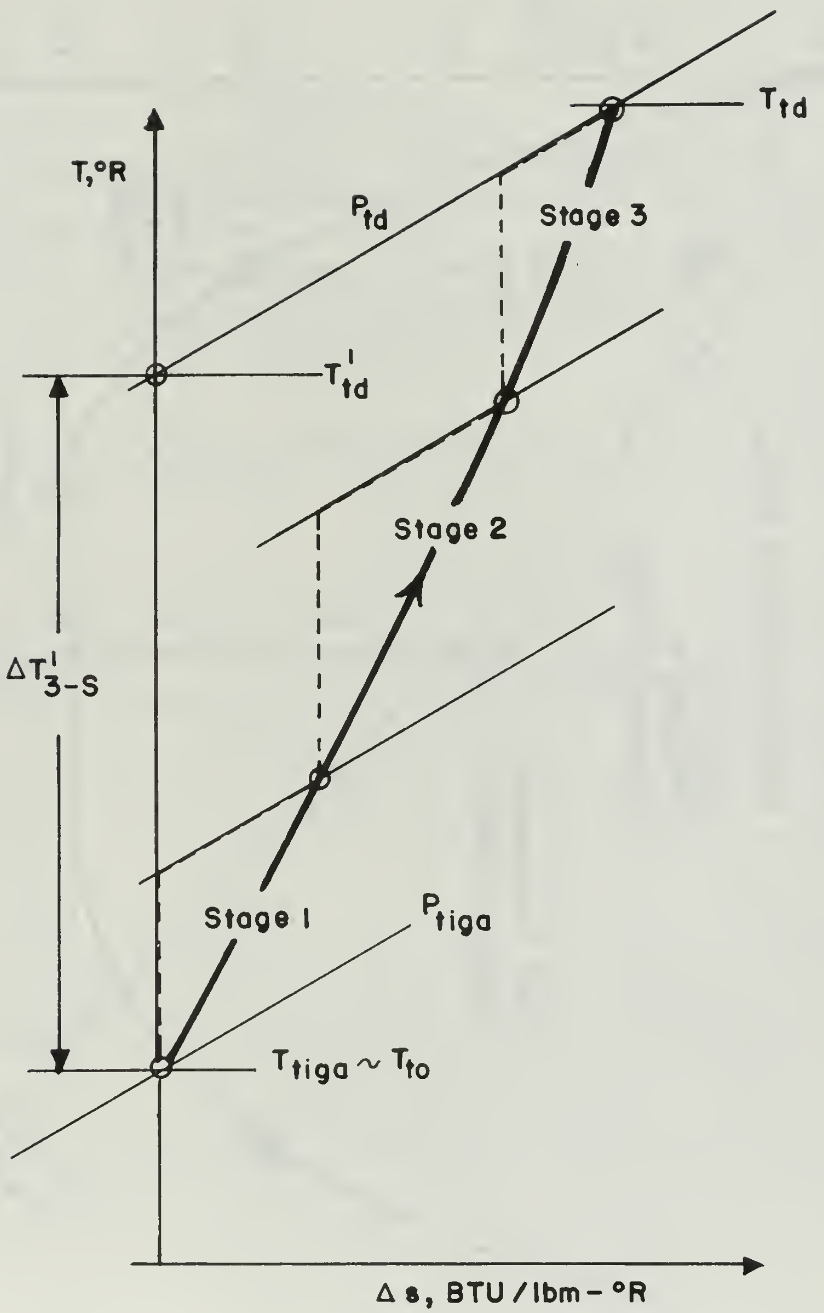

FIGURE 28 TEMPERATURE—ENTROPY DIAGRAM OF COMPRESSION PROCESS IN 3-STAGE MACHINE

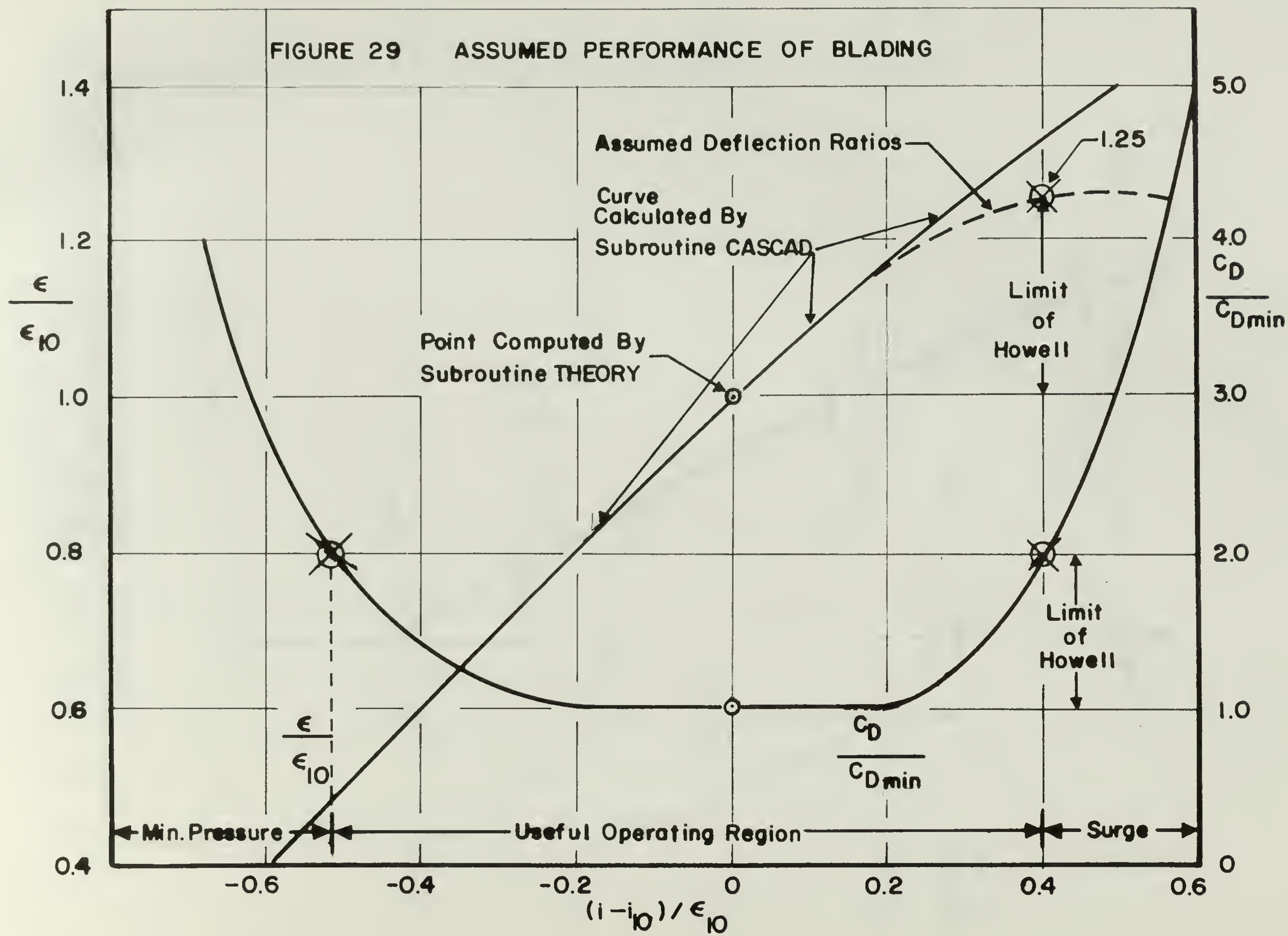

FIGURE 29 ASSUMED PERFORMANCE OF BLADING

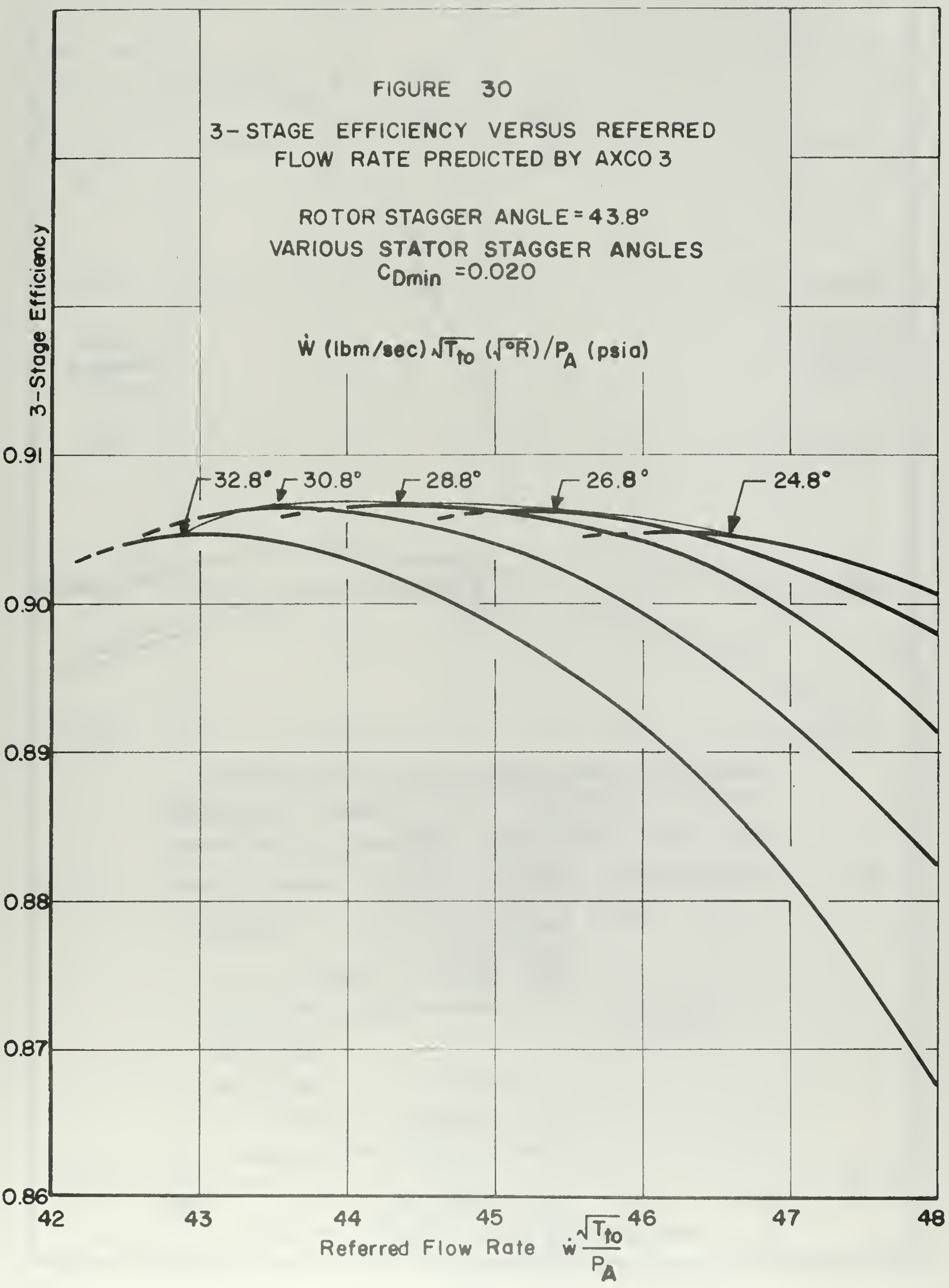
FIGURE 30
3-STAGE EFFICIENCY VERSUS REFERRED FLOW RATE PREDICTED BY AXCO 3
ROTOR STAGGER ANGLE = 43.8°
VARIOUS STATOR STAGGER ANGLES
C_{Dmin} = 0.020
$\dot{W}$ (lbm/sec) $\sqrt{T_{t0}}$ ($\sqrt{°R}$)/P_A (psia)
32.8°
30.8°
28.8°
26.8°
24.8°
3-Stage Efficiency
0.91
0.90
0.89
0.88
0.87
0.86
42
43
44
45
46
47
48
Referred Flow Rate $\dot{w}\frac{\sqrt{T_{t0}}}{P_A}$

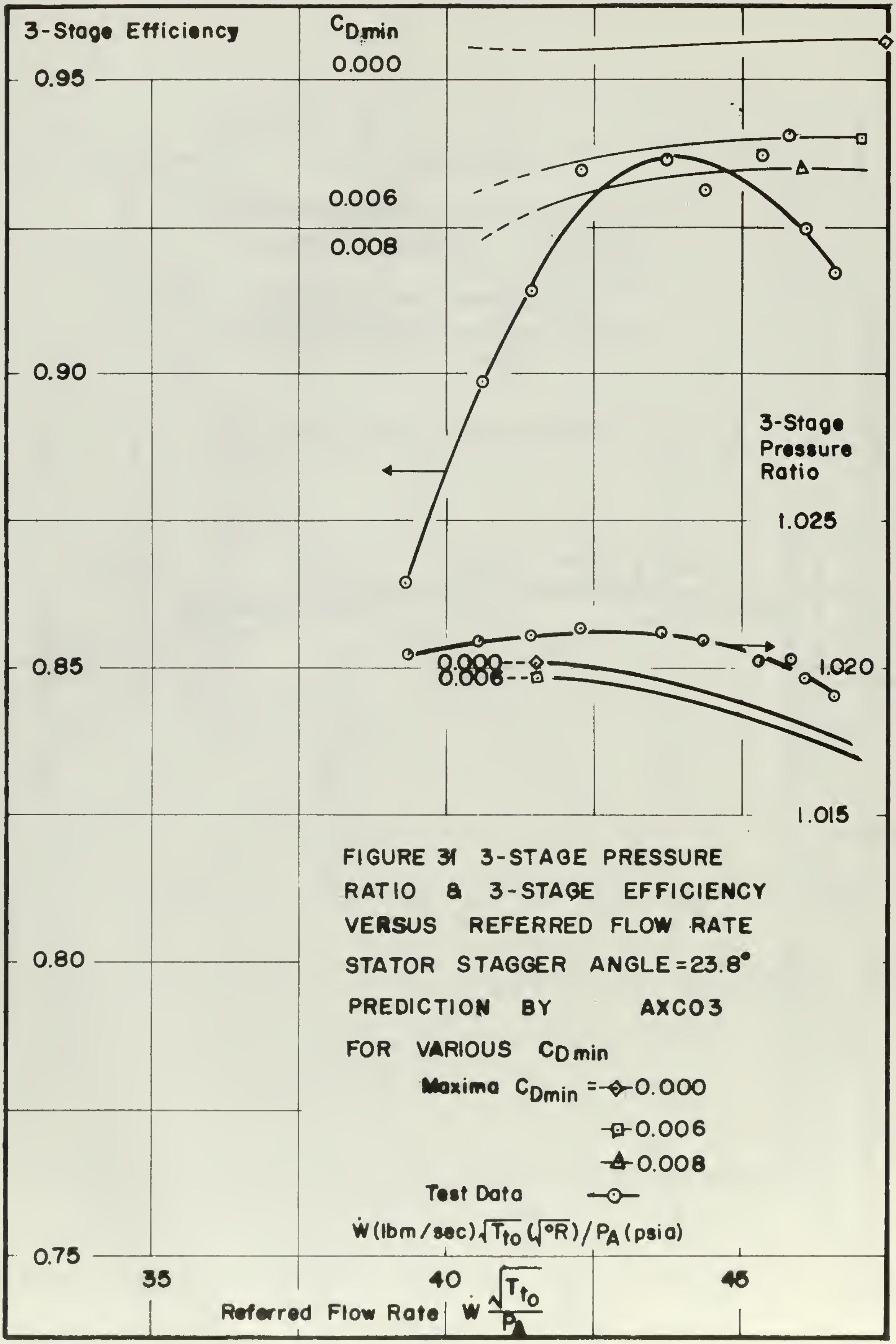

FIGURE 31 3-STAGE PRESSURE RATIO & 3-STAGE EFFICIENCY VERSUS REFERRED FLOW RATE STATOR STAGGER ANGLE = 23.8° PREDICTION BY AXCO3 FOR VARIOUS $C_{D min}$

Maxima C_{Dmin} = ◇ 0.000, □ 0.006, △ 0.008

Test Data ⊙

$\dot{W}$ (lbm/sec) $\sqrt{T_{t0}}$ ($\sqrt{°R}$) / P_A (psia)

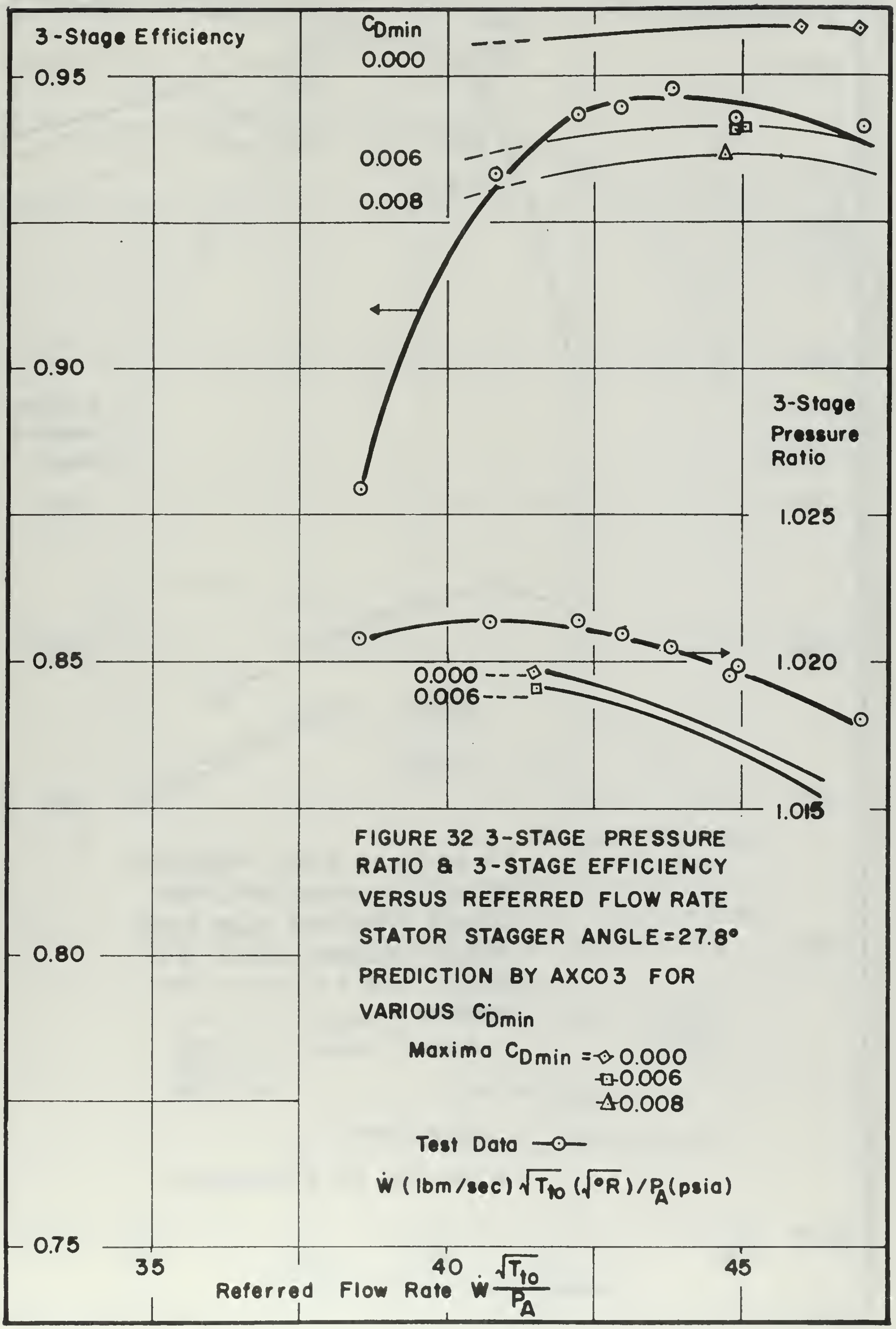

FIGURE 32 3-STAGE PRESSURE RATIO & 3-STAGE EFFICIENCY VERSUS REFERRED FLOW RATE STATOR STAGGER ANGLE = 27.8° PREDICTION BY AXCO3 FOR VARIOUS C_{Dmin}

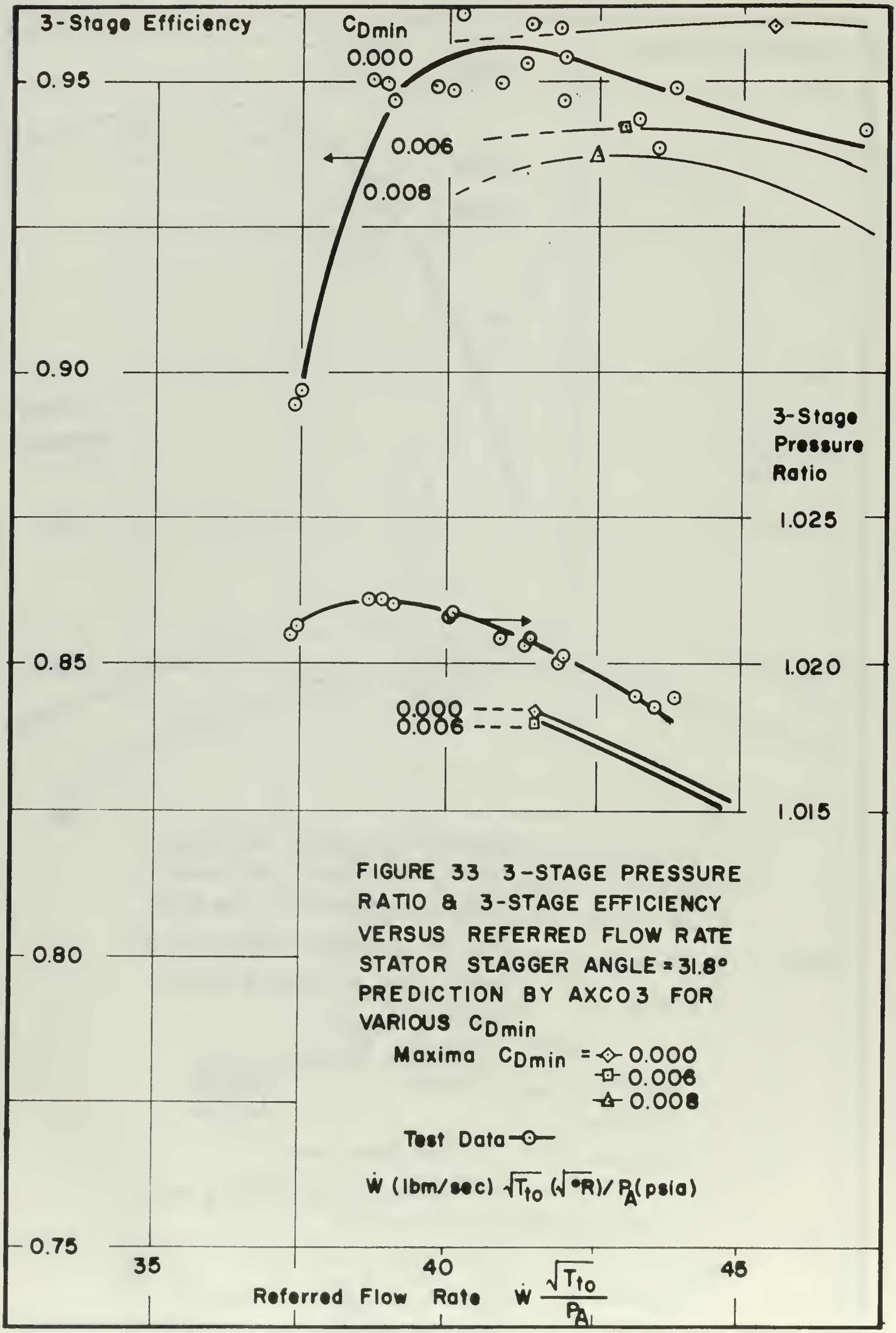
3-Stage Efficiency
CDmin
0.000
0.006
0.008
0.95
0.90
0.85
0.80
0.75
3-Stage Pressure Ratio
1.025
1.020
1.015
0.000
0.006
35
40
45
Referred Flow Rate $\dot{W}\frac{\sqrt{T_{to}}}{P_A}$
FIGURE 33 3-STAGE PRESSURE RATIO & 3-STAGE EFFICIENCY VERSUS REFERRED FLOW RATE STATOR STAGGER ANGLE = 31.8° PREDICTION BY AXCO3 FOR VARIOUS C_{Dmin}
Maxima C_{Dmin} = 0.000
0.006
0.008
Test Data
$\dot{W}$ (lbm/sec) $\sqrt{T_{to}}$ ($\sqrt{°R}$)/ P_A(psia)

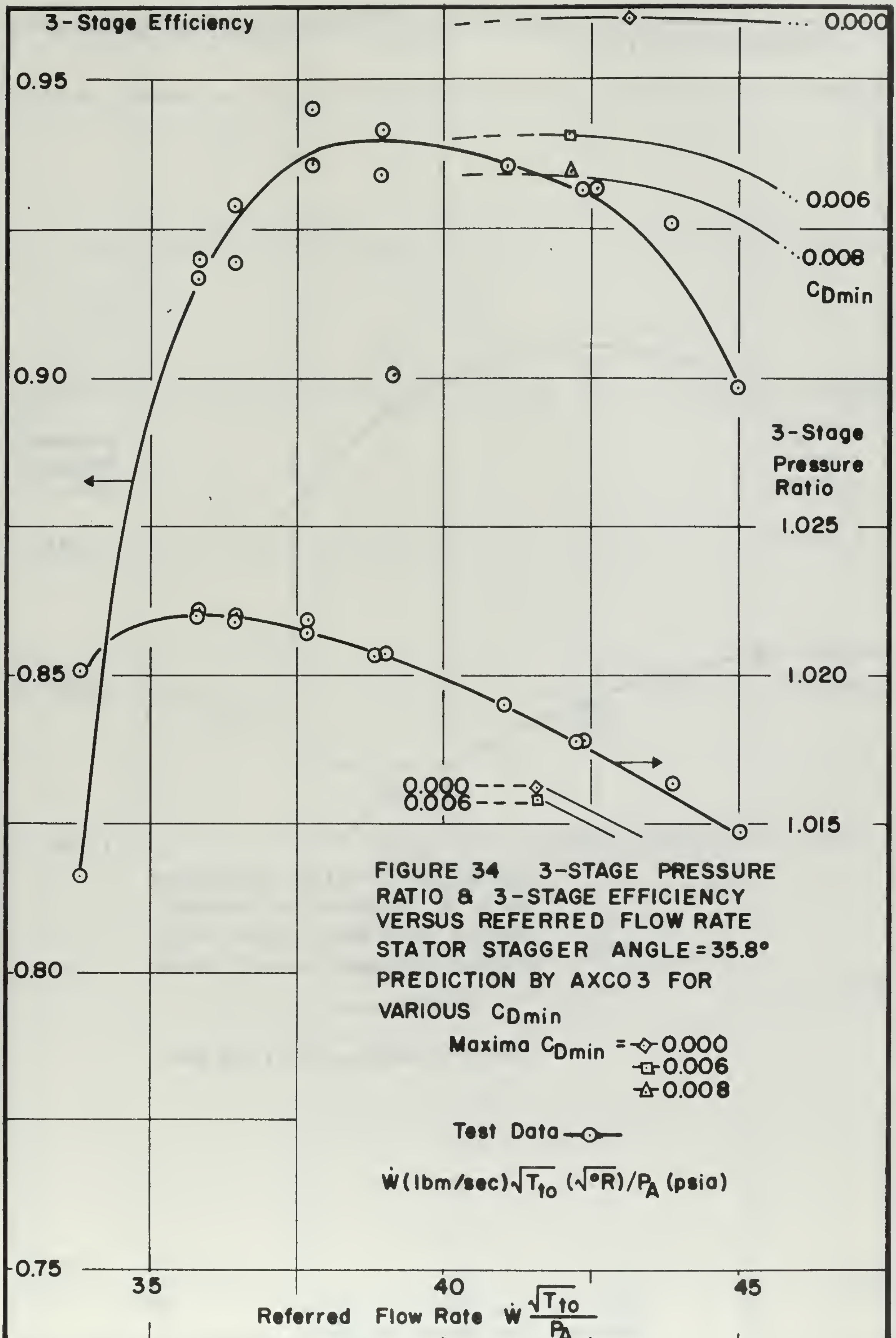

3-Stage Efficiency
0.95
0.90
0.85
0.80
0.75
35
40
45
Referred Flow Rate $\dot{W}\frac{\sqrt{T_{to}}}{P_A}$
0.000
0.006
0.008
C_{Dmin}
3-Stage Pressure Ratio
1.025
1.020
1.015
0.000
0.006
FIGURE 34 3-STAGE PRESSURE RATIO & 3-STAGE EFFICIENCY VERSUS REFERRED FLOW RATE
STATOR STAGGER ANGLE = 35.8°
PREDICTION BY AXCO3 FOR VARIOUS C_{Dmin}
Maxima C_{Dmin} = 0.000
0.006
0.008
Test Data
$\dot{W}$(lbm/sec)$\sqrt{T_{to}}$ ($\sqrt{°R}$)/P_A (psia)

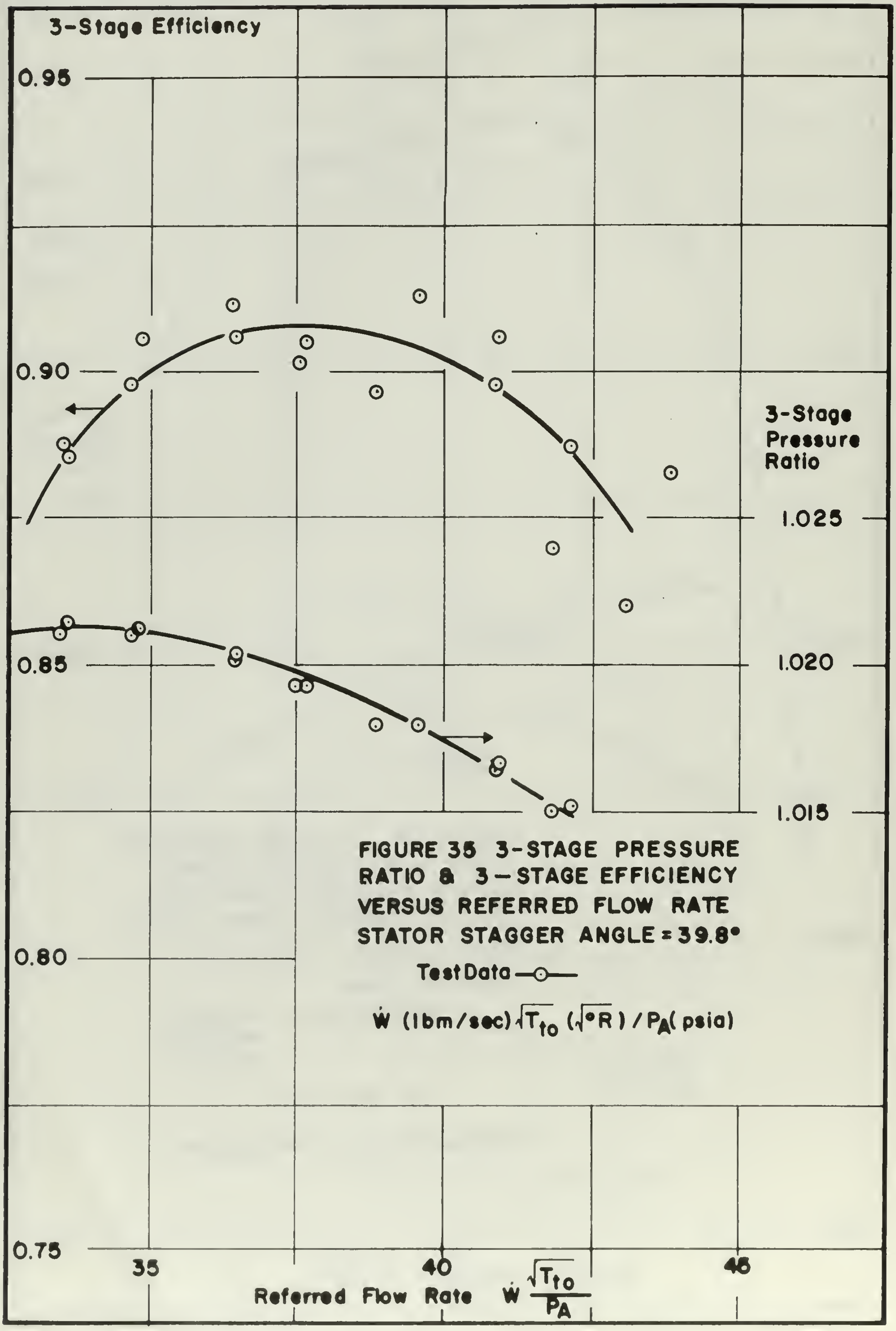

FIGURE 35 3-STAGE PRESSURE RATIO & 3-STAGE EFFICIENCY VERSUS REFERRED FLOW RATE STATOR STAGGER ANGLE = 39.8°

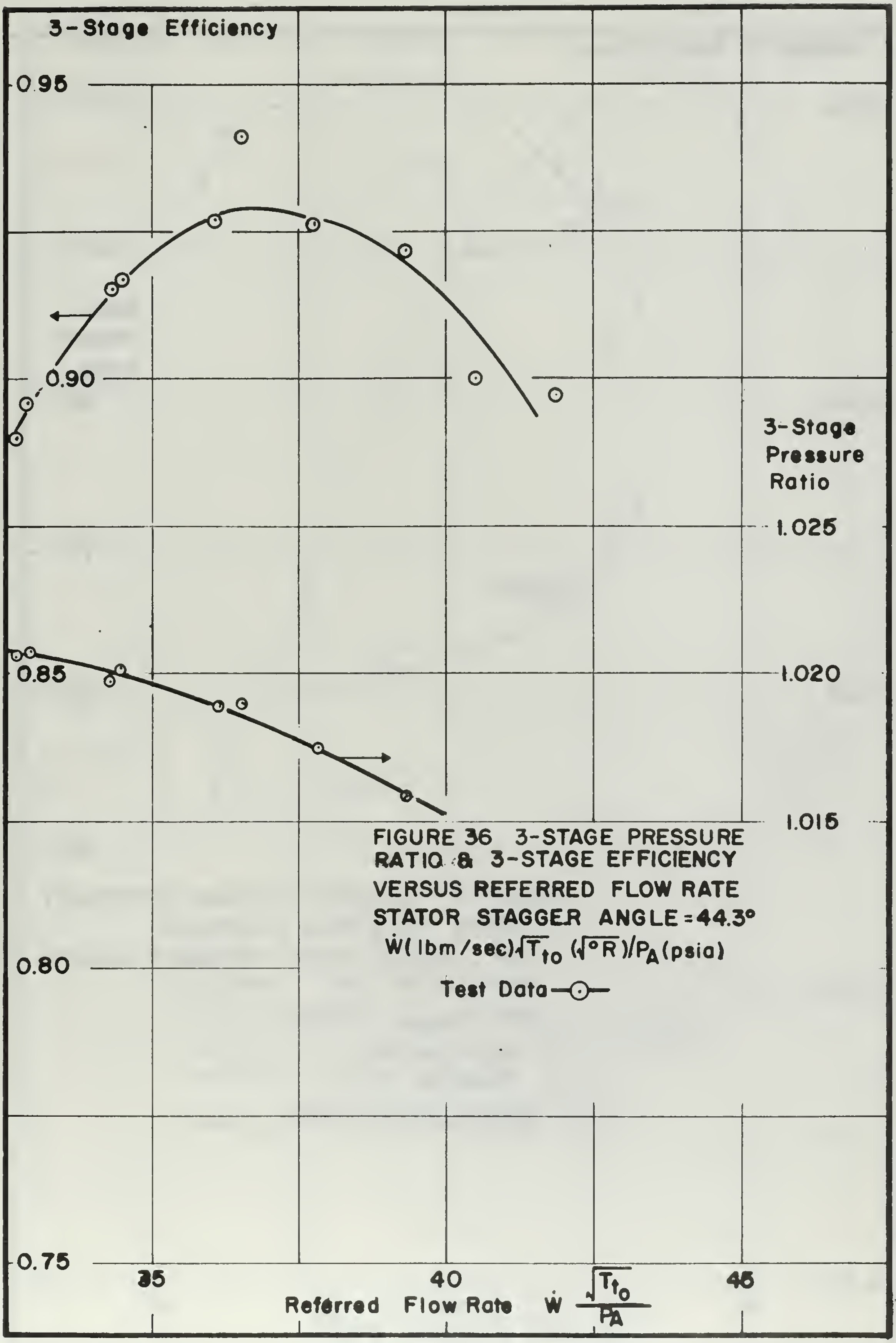

FIGURE 36 3-STAGE PRESSURE RATIO & 3-STAGE EFFICIENCY VERSUS REFERRED FLOW RATE STATOR STAGGER ANGLE = 44.3°

$\dot{W}$(lbm/sec)$\sqrt{T_{t0}}$ ($\sqrt{°R}$)/P_A(psia)

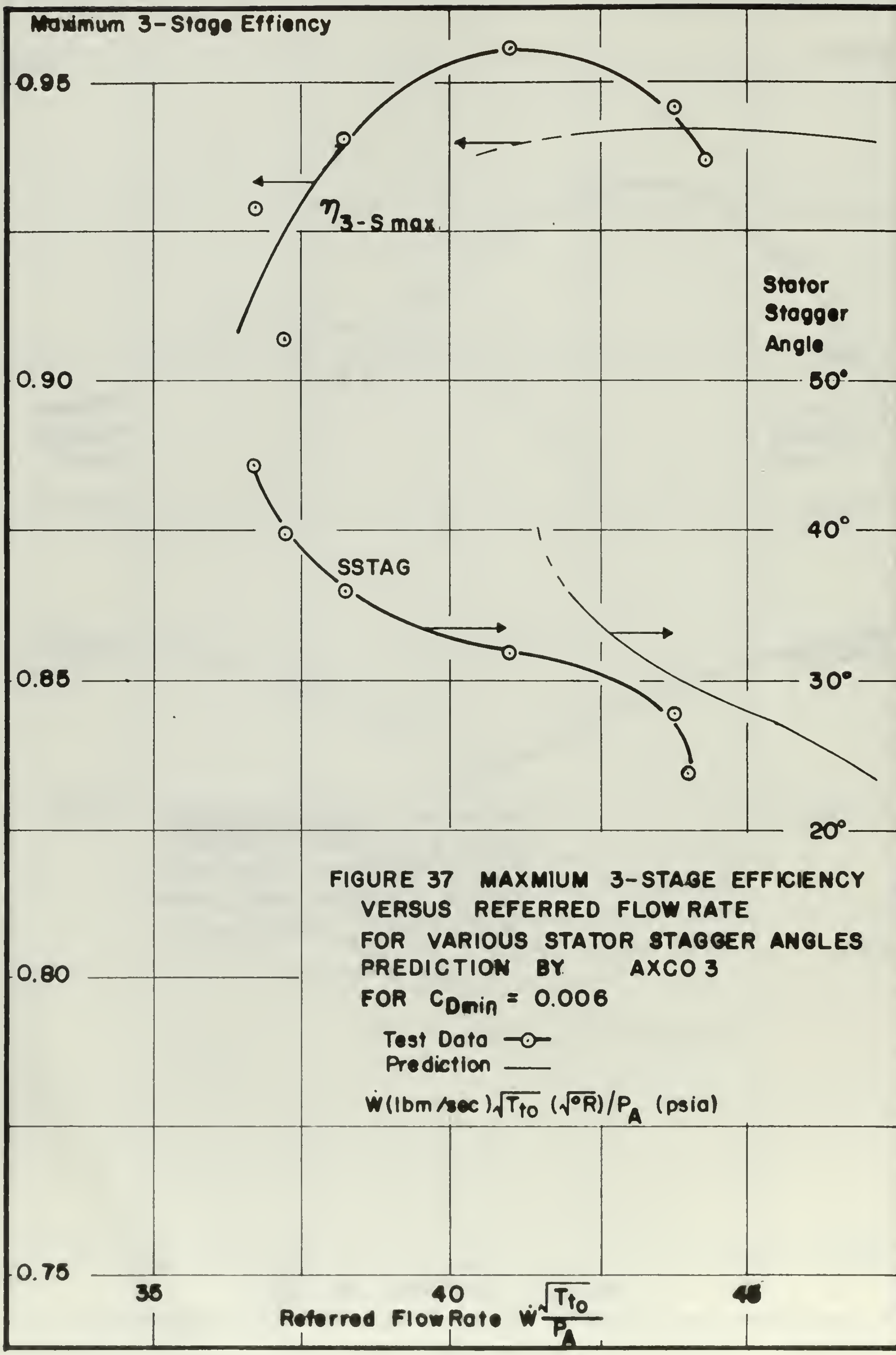

FIGURE 37 MAXMIUM 3-STAGE EFFICIENCY VERSUS REFERRED FLOW RATE FOR VARIOUS STATOR STAGGER ANGLES PREDICTION BY AXCO 3 FOR $C_{Dmin} = 0.006$

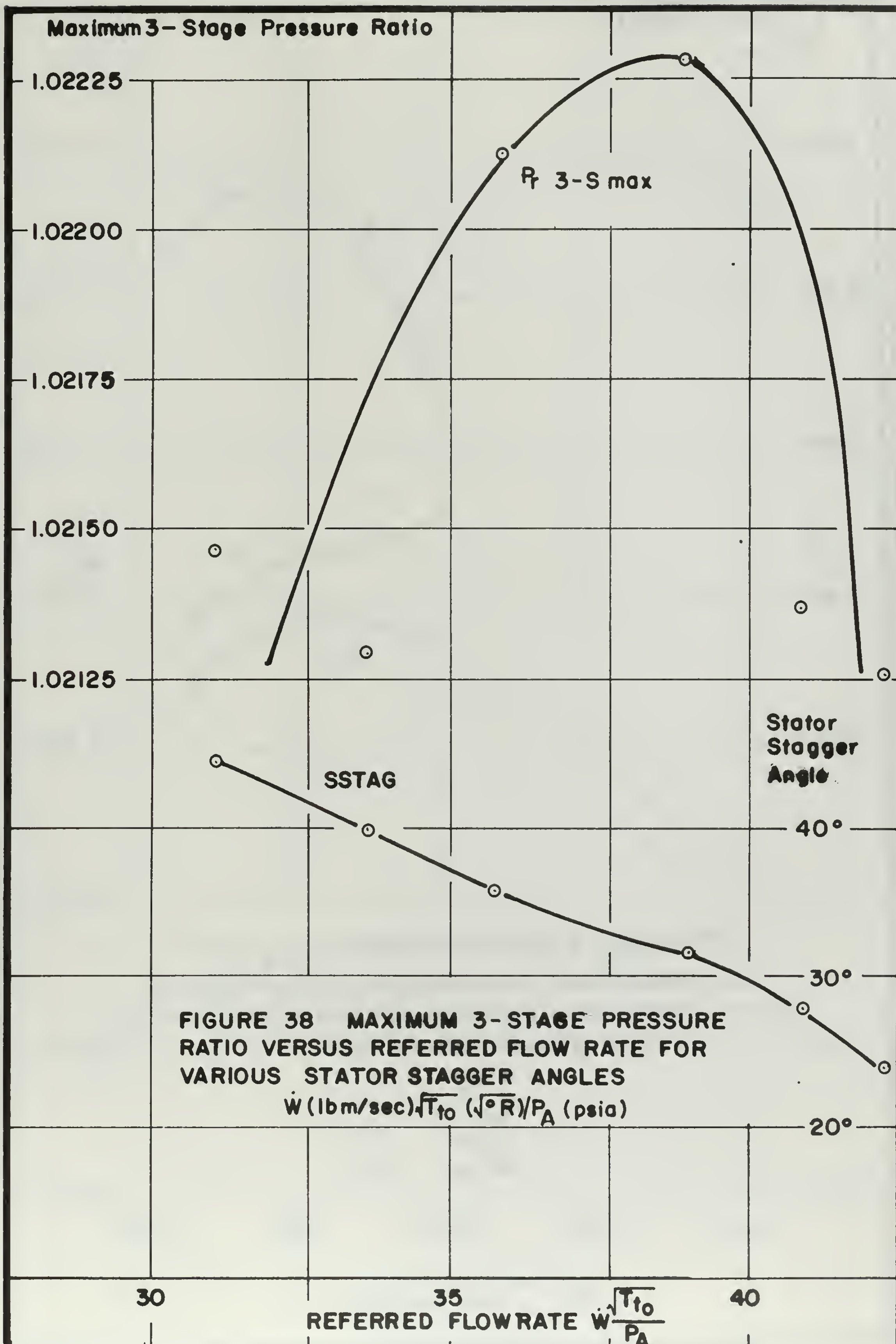

FIGURE 38 MAXIMUM 3-STAGE PRESSURE RATIO VERSUS REFERRED FLOW RATE FOR VARIOUS STATOR STAGGER ANGLES
$\dot{W}$ (lbm/sec)$\sqrt{T_{t0}}$ ($\sqrt{°R}$)/P_A (psia)

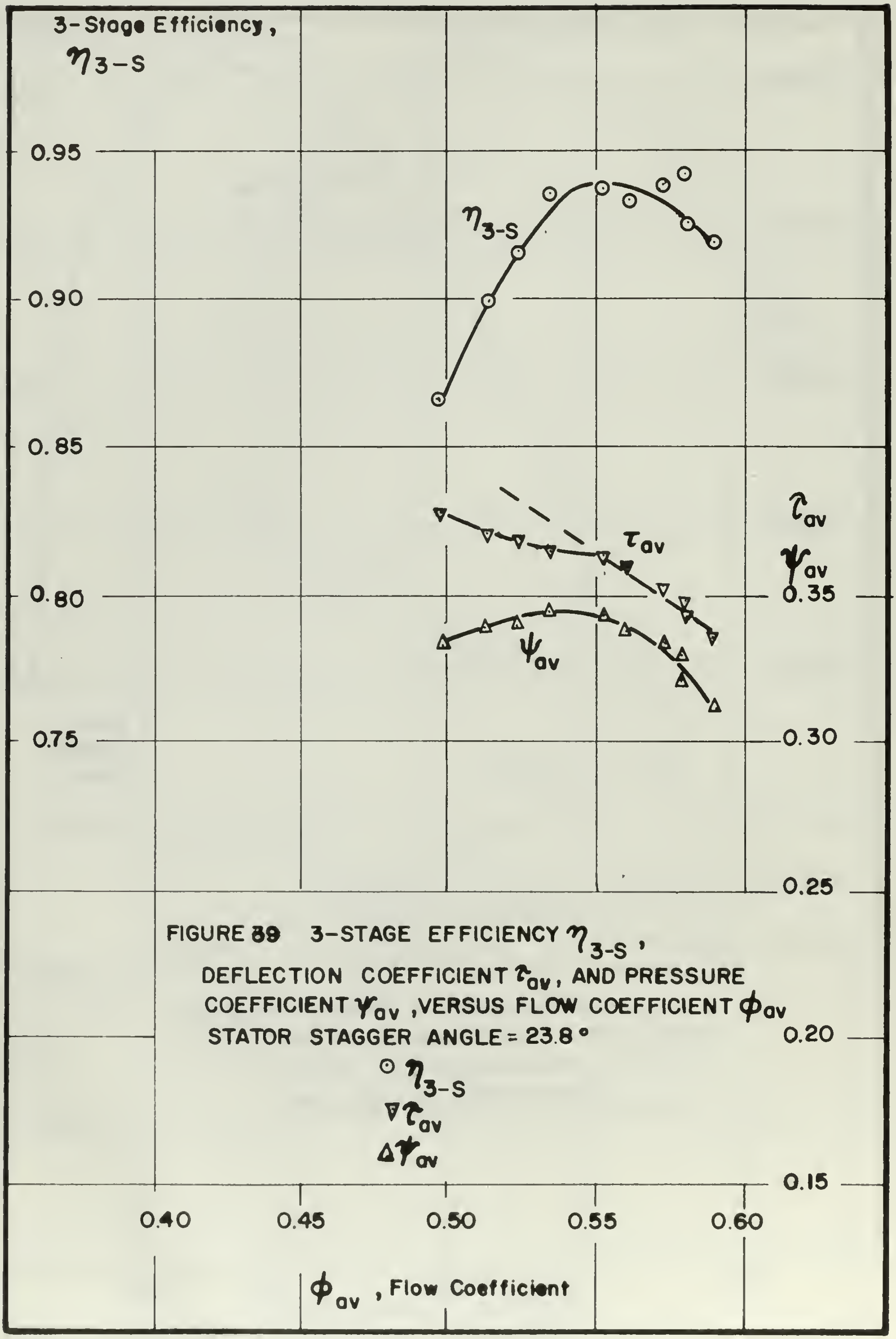

FIGURE 39 3-STAGE EFFICIENCY η_{3-S}, DEFLECTION COEFFICIENT τ_{av}, AND PRESSURE COEFFICIENT ψ_{av}, VERSUS FLOW COEFFICIENT ϕ_{av} STATOR STAGGER ANGLE = 23.8°

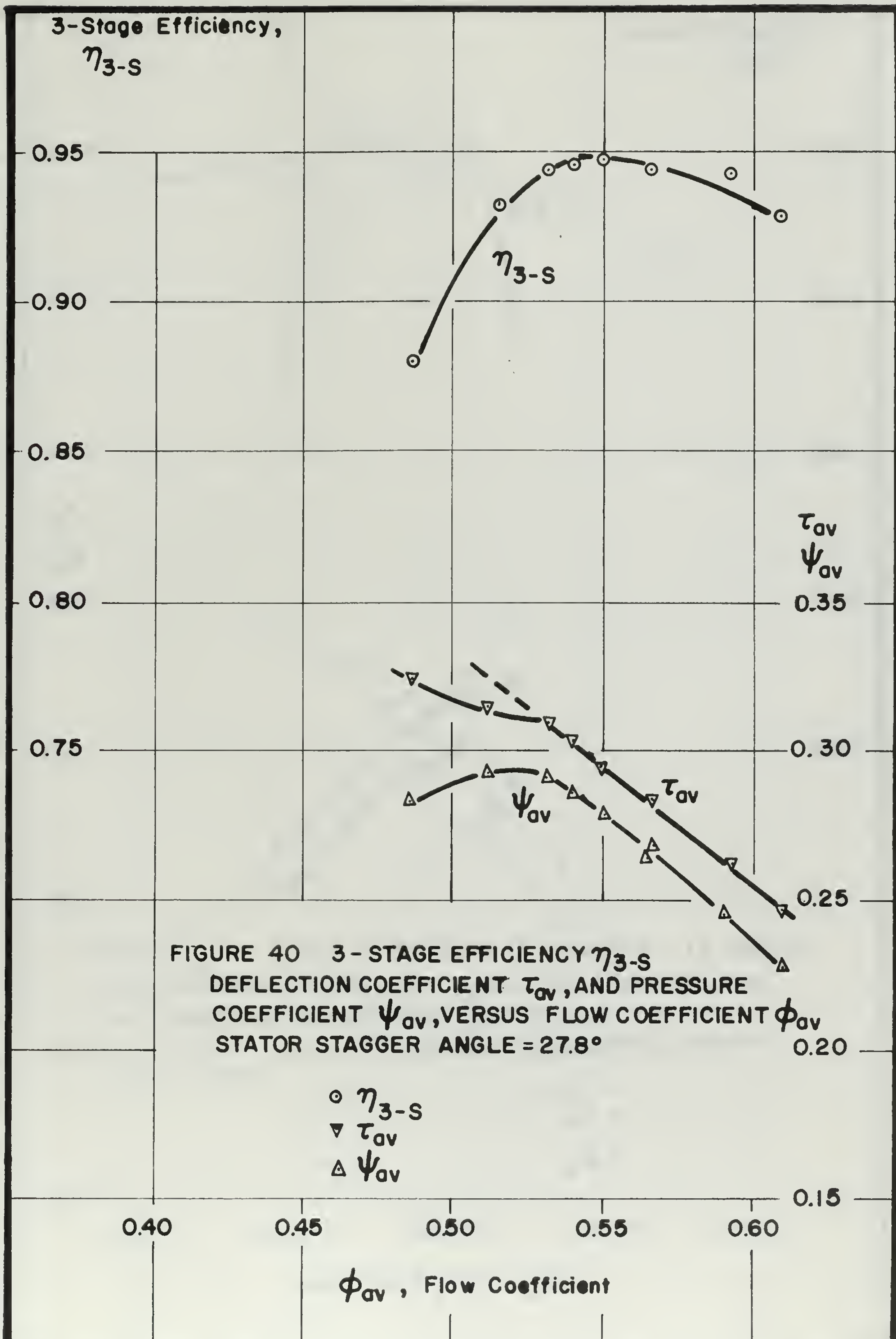

FIGURE 40 3-STAGE EFFICIENCY η_{3-S} DEFLECTION COEFFICIENT τ_{av}, AND PRESSURE COEFFICIENT ψ_{av}, VERSUS FLOW COEFFICIENT ϕ_{av} STATOR STAGGER ANGLE = 27.8°

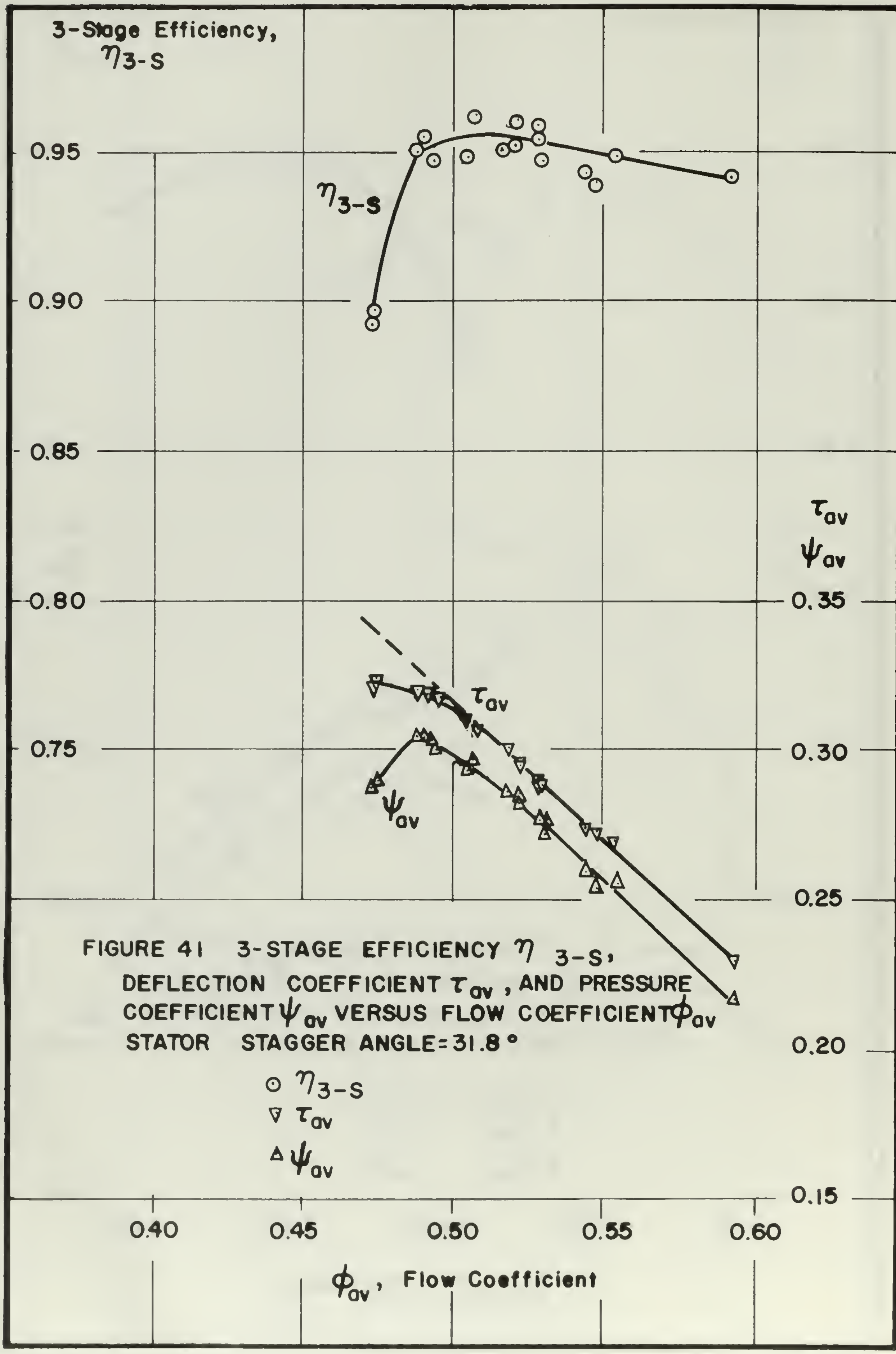

FIGURE 41 3-STAGE EFFICIENCY η_{3-S}, DEFLECTION COEFFICIENT τ_{av}, AND PRESSURE COEFFICIENT ψ_{av} VERSUS FLOW COEFFICIENT ϕ_{av} STATOR STAGGER ANGLE = 31.8°

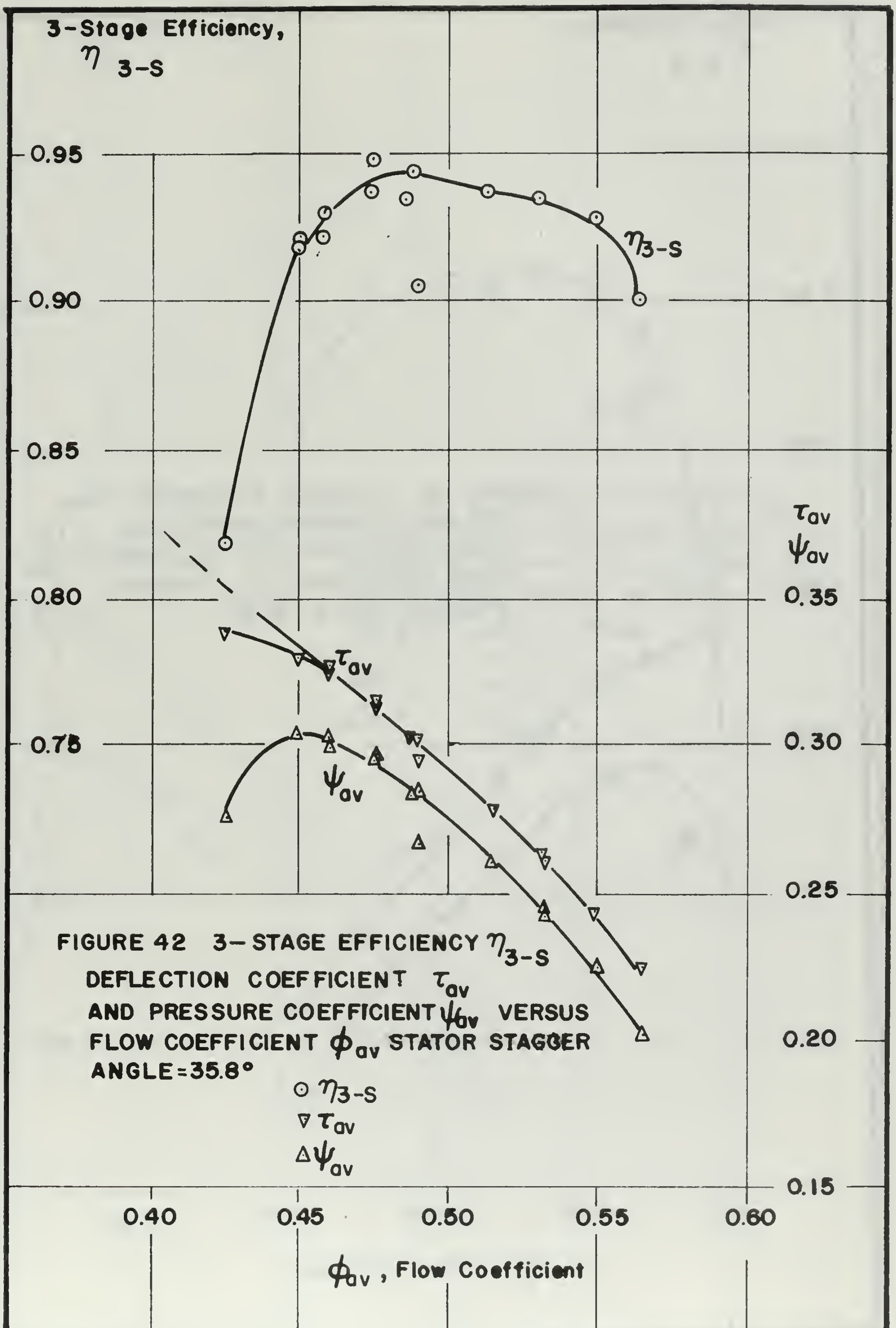

FIGURE 42 3-STAGE EFFICIENCY η_{3-S} DEFLECTION COEFFICIENT τ_{av} AND PRESSURE COEFFICIENT ψ_{av} VERSUS FLOW COEFFICIENT ϕ_{av} STATOR STAGGER ANGLE=35.8°

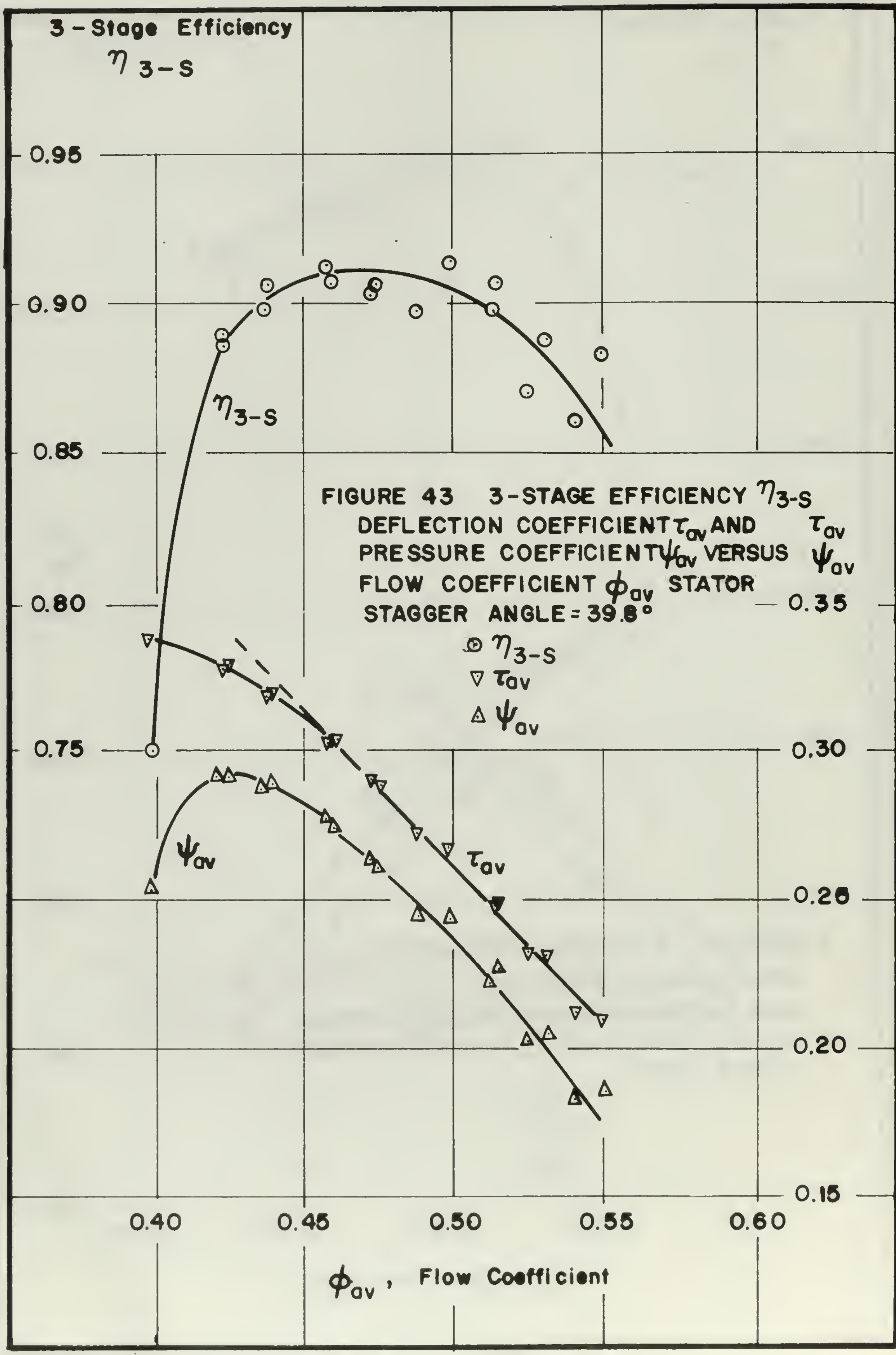

3 - Stage Efficiency
η_{3-S}
0.95
0.90
0.85
0.80
0.75
η_{3-S}
ψ_{av}
τ_{av}
FIGURE 43 3-STAGE EFFICIENCY η_{3-S} DEFLECTION COEFFICIENT τ_{av} AND PRESSURE COEFFICIENT ψ_{av} VERSUS FLOW COEFFICIENT ϕ_{av} STATOR STAGGER ANGLE = 39.8°
$\odot$ η_{3-S}
$\triangledown$ τ_{av}
$\triangle$ ψ_{av}
τ_{av}
ψ_{av}
0.35
0.30
0.25
0.20
0.15
0.40
0.45
0.50
0.55
0.60
ϕ_{av}, Flow Coefficient

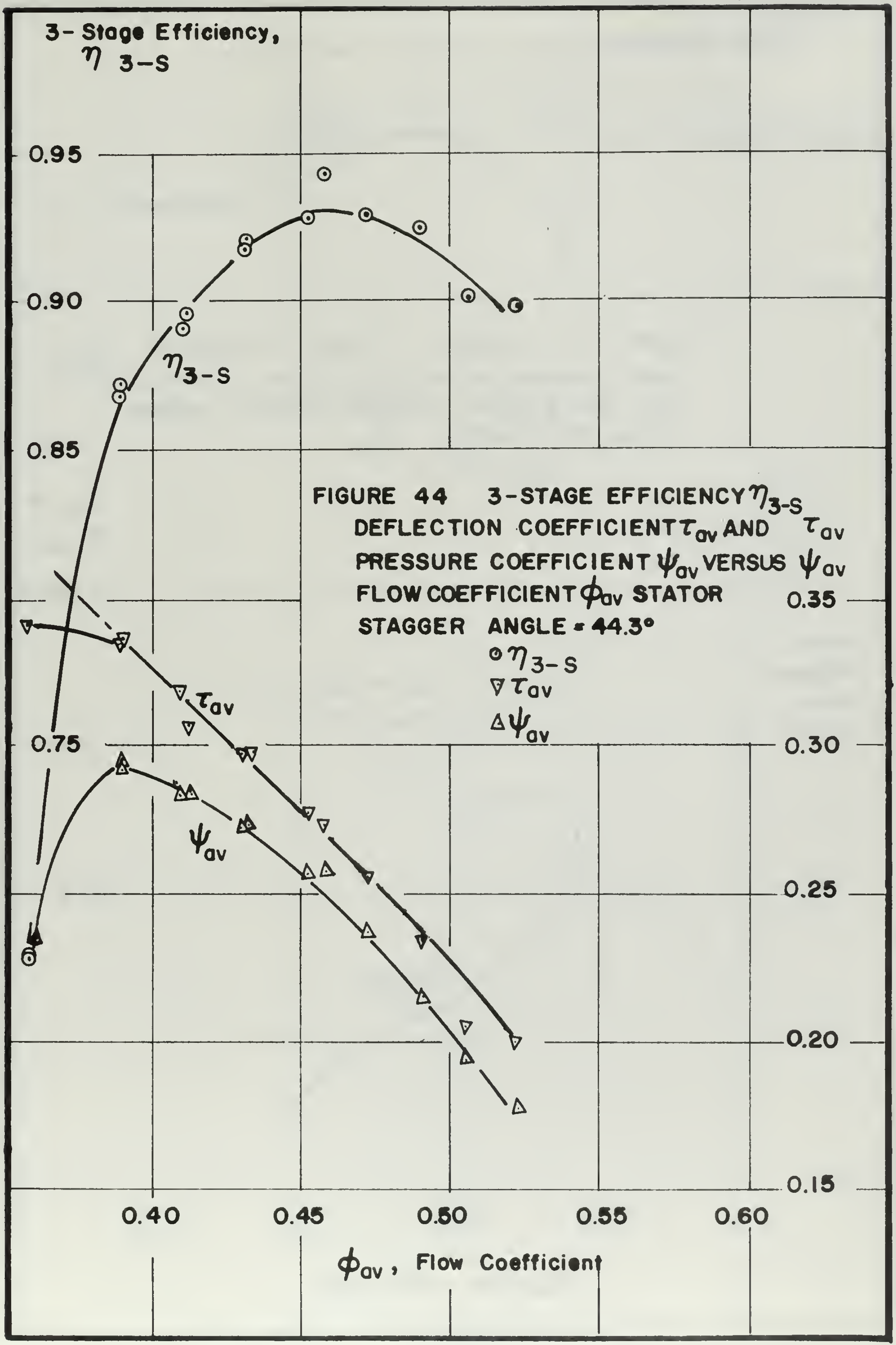

FIGURE 44 3-STAGE EFFICIENCY η_{3-S} DEFLECTION COEFFICIENT τ_{av} AND PRESSURE COEFFICIENT ψ_{av} VERSUS FLOW COEFFICIENT ϕ_{av} STATOR STAGGER ANGLE = 44.3°

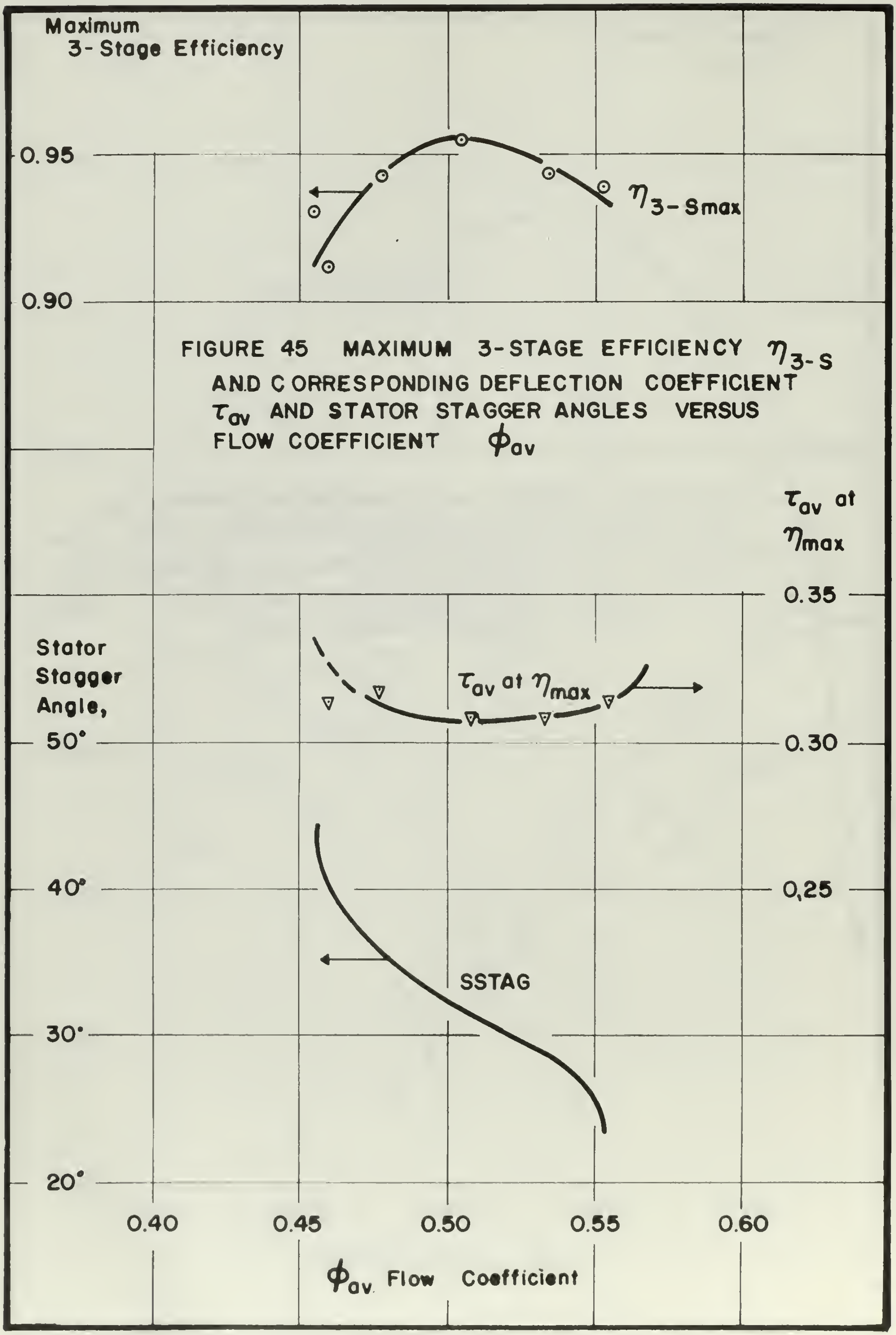

Maximum 3-Stage Efficiency
0.95
0.90
η_{3-Smax}
FIGURE 45 MAXIMUM 3-STAGE EFFICIENCY η_{3-S} AND CORRESPONDING DEFLECTION COEFFICIENT τ_{av} AND STATOR STAGGER ANGLES VERSUS FLOW COEFFICIENT ϕ_{av}
τ_{av} at η_{max}
0.35
0.30
0.25
Stator Stagger Angle,
50°
40°
30°
20°
τ_{av} at η_{max}
SSTAG
0.40
0.45
0.50
0.55
0.60
ϕ_{av} Flow Coefficient

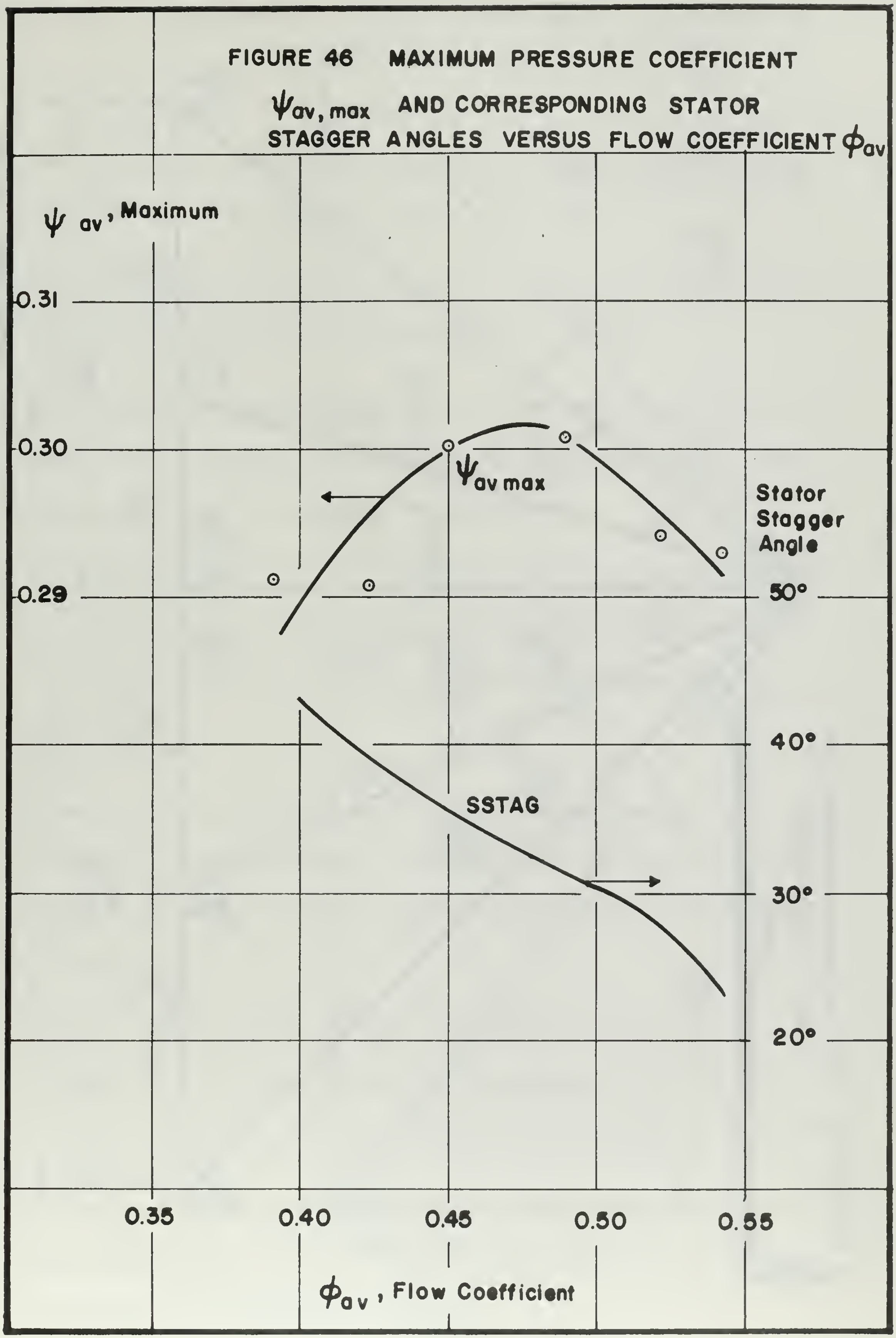
FIGURE 46 MAXIMUM PRESSURE COEFFICIENT
$\psi_{av,max}$ AND CORRESPONDING STATOR
STAGGER ANGLES VERSUS FLOW COEFFICIENT ϕ_{av}
ψ_{av}, Maximum
0.31
0.30
0.29
$\psi_{av\,max}$
Stator
Stagger
Angle
50°
40°
30°
20°
SSTAG
0.35
0.40
0.45
0.50
0.55
ϕ_{av}, Flow Coefficient

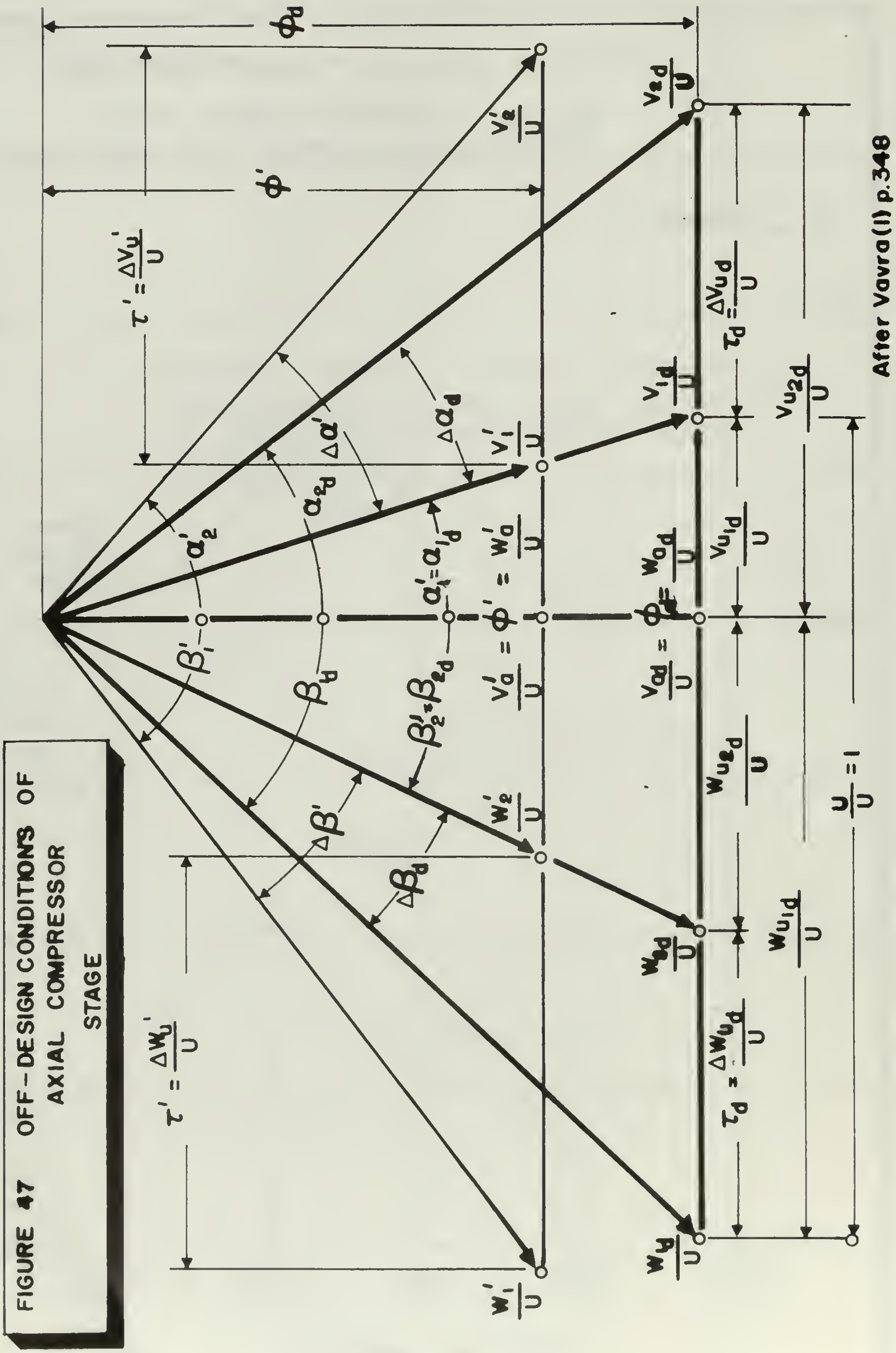

FIGURE 47 OFF-DESIGN CONDITIONS OF AXIAL COMPRESSOR STAGE

SECTION 9

REFERENCES

1. Vavra, M. H., "Aero-Thermodynamics and Flow in Turbomachines," John Wiley & Sons, Inc., New York, N. Y., 1960.

2. Lieblein, Seymour, "Experimental Flow in Two-Dimensional Cascades," Chapter VI of NASA SP-36, Washington, D. C., 1965.

3. Vavra, M. H., "Analysis of Performance of Clark CSN-2 Axial-Flow Compressor for ML-1", Report AGN-VA #26, Aerojet-General Nucleonics, San Ramon, California, November 1963.

4. Gibbons, Thomas and Bartels, Harlan B., "An Analytical Investigation of Off-Design Performance in Multi-Stage Axial Flow Compressors" Unpublished Masters Thesis, Naval Postgraduate School, May 1966.

5. Bowen, John T., Sabersky, Rolf H. and Rannie, Duncan W., "Theoretical and Experimental Investigations of Axial Flow Compressors (Summary Report)," California Institute of Technology, January 1949.

6. Bowen, John T., Sabersky, Rolf H. and Rannie, Duncan W., "Theoretical and Experimental Investigations of Axial Flow Compressors, Part 2," California Institute of Technology, July 1949.

7. Alsworth, Charles C. and Iura, Toru, "Theoretical and Experimental Investigations of Axial Flow Compressors, Part 3," California Institute of Technology, July 1951.

8. Iura, Toru, and Rannie, Duncan W., "Observations of Propagating Stall in Axial Flow Compressors," California Institute of Technology, April 1953.

9. Howell, A. R., "Axial Compressor Design," Rpt. E3946, Royal Aircraft Establishment, Farnborough, England, June 1942.

10. National Research Council, "International Critical Tables, Vol. III," McGraw-Hill, 1928.

11. Waitman, B. A., Reneau, L. R. and Kline, S. J., "Effects of Inlet Conditions on Performance of Two Dimensional Subsonic Diffusers," Journal of Basic Engineering, Transactions of the A. S. M. E., Sept. 1961, pp. 349-360.

APPENDIX A

CALIBRATION OF INSTRUMENTS

The measuring devices were calibrated to determine their accuracy and precision.

The Berkeley digital counter is located near a Hewlett-Packard digital counter in the control room. At a given flow rate, there was no difference between the two instruments. The Hewlett-Packard device was recently calibrated with a cesium wave length frequency standard in the Standards Laboratory of the Electrical Engineering Department of the Naval Postgraduate School. The speed measured is considered accurate to 0.5 rpm.

The Baldwin-Lima-Hamilton torque meter was calibrated statically as illustrated in Fig. 24. A bar was attached to the drive end of the shaft and was clamped to the stand. A symmetrical lever bar was attached to the rotor end of the shaft. The lever arm is 20.0 in. Two weight pans were adjusted to 1.44 lb. each with lead shot in a plastic bag. The weights themselves were checked on the Toledo Precision Scales of the Cascade Laboratory. On the first run, different readings were obtained while loading and unloading the pans. This problem was overcome in subsequent runs by tapping the stand with a mallet prior to recording the reading. This simulated the vibration of dynamic operation which eliminated any frictional effects. Good agreement was obtained during tests where the loading was increased and decreased. The possibility of temperature effects on the strain gauges was explored in a third test. The torque meter cannot be calibrated while the motor is running, but it was calibrated immediately after shutdown. The shaft was only slightly warmer to the touch than ambient temperature.

The data of the three calibration runs are shown in Table A-1. The results are plotted in Fig. A-1. Run A-3 revealed no temperature effect. A fourth run was made later for checking purposes and did not reveal any discrepancies. The calibration tests established a constant for the torque meter of 4.1565 foot-pounds of torque per pound reading of the meter. The maximum relative error among the runs is 0.6 per cent. The meter may be read to within 0.03 pounds, or 1 per cent of the meter reading.

The newly acquired low range bourdon tube was calibrated also. Run B-1 was made by using the mercury manometer board in the control room of the Compressor Laboratory. The transsonic turbine test rig was used to provide the pressure difference for the higher pressure range. The present compressor tests required pressure measurements down to 0.6 in. of water. Runs B-3 and B-5 were made at low pressure difference with a Merriam water micro-manometer. Pressure was supplied from a static source.

The data of the three calibration runs are shown in Table A-2. The results are plotted in Fig. A-2. The calculation of velocities was set up using pressure difference in lb/ft^2. Measured pressures are therefore very small numbers. An inverse calibration constant was used. The bourdon tube has a constant of 240.423 counts per lb/ft^2. The maximum relative error among the calibration runs was 0.12 per cent. The meter may be read to within 5 counts. The meter's servo system tends to overcorrect. In the manual null mode the meter needle tends to wander a similar amount. The five count reading error amounts to 1 per cent of the velocity head reading in the inlet duct during flow rate calibration. The error is 0.5 per cent of the velocity head reading at the permanent Pitot tube. The error is only 0.05 per cent of the measured pressure difference across the three stages.

The Pitot-static tube used to traverse the inlet duct during flow rate calibration is a modified Prandtl-type tube. Another Pitot-static tube was attached to the traverse shaft and the tubes compared. Sufficient difference existed between the two to justify further tests. The low speed calibration tunnel in the Cascade Laboratory was modified to receive the Pitot-static tube from the inlet duct.

The data of the calibration runs are shown in Table A-3. The results are plotted in Fig. A-3. Each point represents the average of four readings. Run C-3 indicated that the velocity head of the Pitot-static tube from the inlet duct was at most 1.1 per cent less than that of the calibration tunnel. Run C-4 indicated that the static pressure below atmospheric was at most 1.8 per cent less than that of the calibration tunnel. These maximum errors occurred at the lower pressure differences. It is probable that the effect recorded is in part the reading error due to bourdon tube oscillation.

TABLE A-1

CALIBRATION OF BLH TORQUE METER

RUN A-2

APPLIED TORQUE FT-LB	METER READING LB
4.167	0.995
8.333	2.005
12.500	3.000
16.667	3.985
20.833	4.995
25.000	5.985
29.167	6.980
33.333	7.960
37.500	8.940
41.667	9.970
45.833	10.925
50.000	11.950
54.167	12.915
58.333	13.930
62.500	14.905
66.667	15.925
70.833	16.935
75.000	17.945
79.167	18.910
83.333	19.970

RUN A-3

APPLIED TORQUE FT-LB	METER READING LB
19.792	4.745
39.583	9.620
59.375	14.540
77.708	18.445
92.708	22.400
109.375	26.345
126.042	30.285

RUN A-4

APPLIED TORQUE FT-LB	METER READING LB
19.792	4.77
38.958	9.610
59.792	14.545
76.458	18.510
93.125	22.435
109.792	26.405
126.458	30.370
130.675	31.340

FIGURE A-1 TORQUE METER CALIBRATION

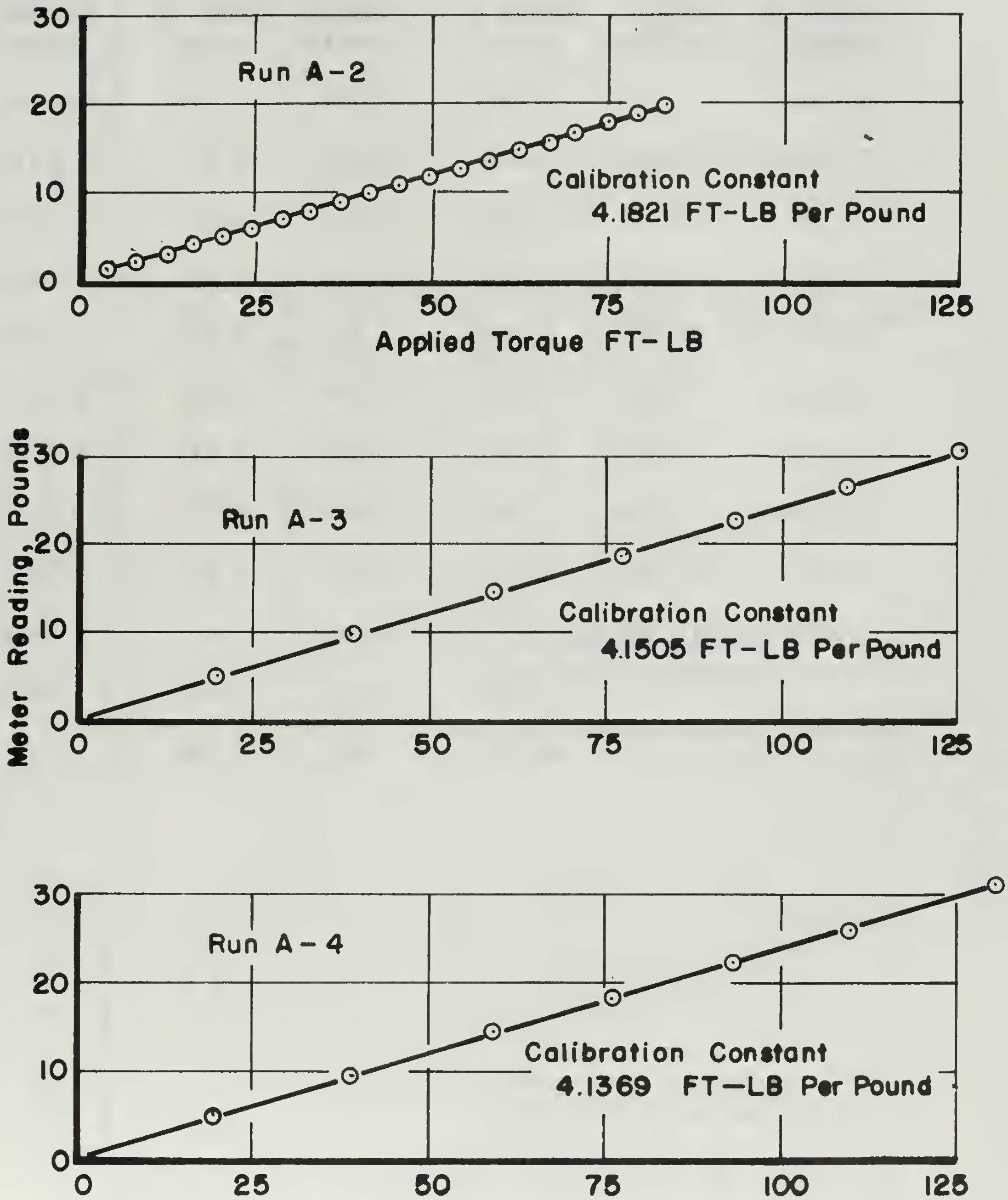

Average Calibration Constant 4.1565 FT-LB Per Pound

TABLE A-2

CALIBRATION OF 0-12 in. Hg BOURDON TUBE

RUN B-1		RUN B-3		RUN B-5	
PRESSURE INCHES OF MERCURY	METER READING COUNTS	PRESSURE INCHES OF WATER	METER READING COUNTS	PRESSURE INCHES OF WATER	METER READING COUNTS
10.260	174,300	13.978	17.409	14.519	18,218
8.290	139,450	12.459	15,518	12.914	16,119
7.445	125,750	11.062	13,784	11.397	14,222
6.065	102,900	9.853	12,276	9.913	12,368
5.235	88,200	6.993	8,737	8.471	10,560
4.440	74,800	6.198	7,738	6.989	8,715
4.035	67,950	4.992	6,230	5.471	6.826
3.320	57,100	3.996	4,993	4.493	5,613
2.415	40,900	3.036	3,794	3.470	4,398
1.000	16,300	2.195	2,741	2.401	2,994
		1.602	1,997	1.512	1,885
		0.785	982	0.620	762

FIGURE A-2 BOURDON TUBE CALIBRATION

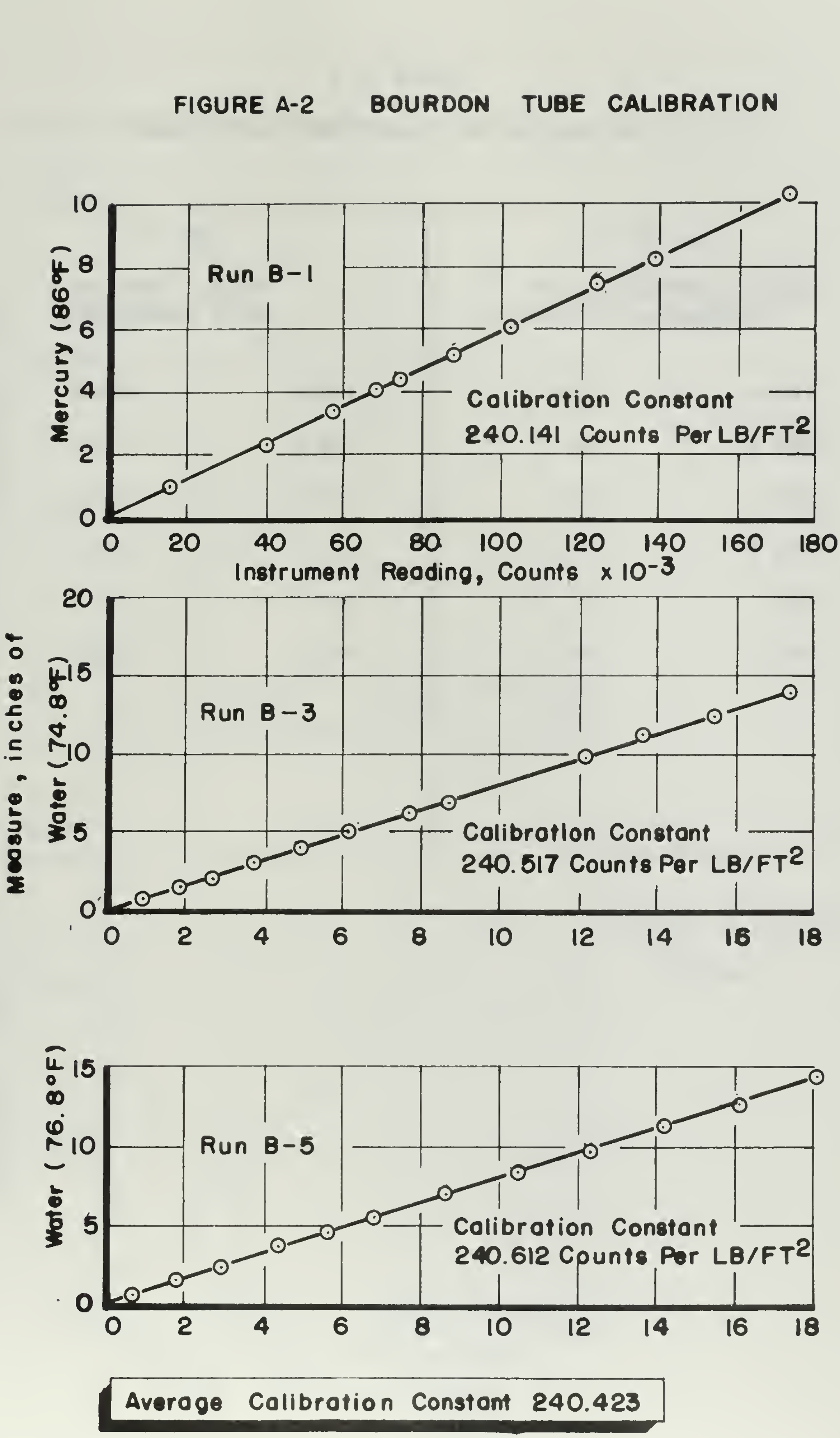

TABLE A-3

CALIBRATION OF INLET PITOT-STATIC TUBE

RUN C-3 TOTAL PRESSURE MINUS STATIC PRESSURE		RUN C-4 STATIC PRESSURE BELOW ATMOSPHERIC	
PROBE	TUNNEL	PROBE	TUNNEL
2486.25	2508.75	2450.0	2455.0
2157.5	2182.5	2190.0	2190.0
1413.75	1421.25	1422.5	1425.0
1002.5	1011.25	1087.5	1012.5
793.75	797.5	795.0	810.0

FIGURE A-3 INLET TRAVERSE PITOT-STATIC CALIBRATION

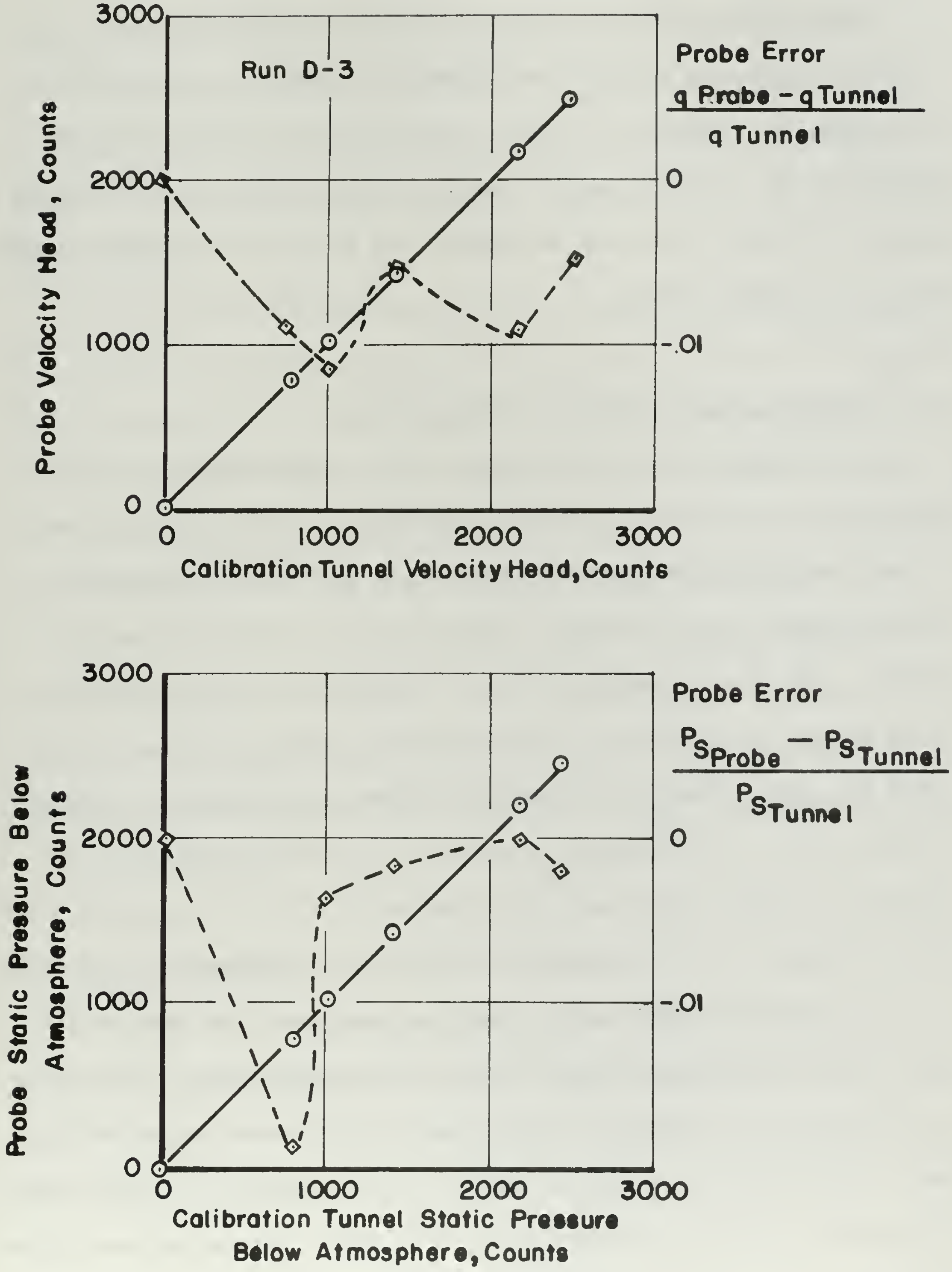

APPENDIX B

FLOW RATE CALIBRATION DETAILS

Particulars of the flow rate calibration scheme which may be of special interest to a restricted number of readers are included in this Appendix. Section B-1 gives details of the construction and testing of the variable length capillary damping devices. Section B-2 gives a listing of the program ONRFLO, and Section B-3 presents sample output of program ONRFLO.

B-1 Variable Length Capillary Damping Devices

The problem of oscillating pressures at the traversing Pitot-static tube in the inlet has been described. Pressure oscillations in the tubing were damped with alternating sections of smaller and larger diameter flow passages. Figure B-1 is a picture of such a device. The device consists of three lengths of needle stainless steel tubing, of 0.020 in. inside diameter, which are 4 in., 6 in., and 8 in. long. They are connected as shown to polyethylene tubing by brass "T's." By clamping the tubing at various positions it is possible to obtain total capillary lengths of 4 in., 6 in., 8 in., or 18 in. Figure B-2 is a schematic showing the operation of the device.

Two variable length damping devices were used, one each in the total and static pressure lines from the traversing Pitot-static tube in the inlet. Two effects of these devices were observed on velocity head, the difference between total and static pressure. As the length of capillary tube was increased, the fluctuation of the pressure gauge was decreased. But as the length of capillary tubing was increased, the time to come to a steady reading was also increased. Table B-1 presents the results of tests of various lengths of capillary tubing.

Immediately before taking the velocity head reading the traverse probe was placed at a new radial position. This task took about 20 sec. to perform. The best precision for a time to damp of 20 sec or less was used. The combination of a total pressure capillary length of 18 in. and a static pressure length of 8 in. satisfied this requirement.

Later in the investigation, when the simplified pressure selection system was used, it became possible to use both 18 in. lengths of tubing and have a time to damp to a steady reading of less than 20 sec. It appears that the 12-channel pressure scanners increased the time required for the system to stabilize. This was probably due to admittance of air from other channels during sequencing of the scanner. However as the survey progressed, flow rate measurements were made at lower flow rates. As the machine was operated nearer to the stalled condition, greater pressure oscillations were observed. The meter precision was no better than $\pm$ 15 counts, and sometimes as much as $\pm$ 50 counts.

B-2 <u>Program ONRFLO</u>

The flow rate calculations described in Section 3 were accomplished by program ONRFLO which is included as Table B-2. Since the calculations are straightforward and have been described earlier, they will not be repeated here.

The input format is as follows:

Card 1:	NCASE	run number (arbitrary)
(I7,3F7.2)	PBAR	reading of barometer (in.)
	TBAR	temperature at barometer ($^{\circ}$F)
	TO	temperature at inlet screen ($^{\circ}$F)
Cards 2, 3, and 4:	R	the 23 radii at which data were
(8F10.2)		taken (17.75, 17.50, ...4.00, 0.00,
		4.00...17.50,17.75) (in.)
Cards 5 through 50:	QI	velocity head in inlet duct (counts)
(4F7.0)	PSI	static pressure with reference to
		atmospheric in inlet duct (counts)
	QO	velocity head at permanent Pitot-
		static tube (counts)
	PSO	static pressure with reference to
		atmospheric at permanent Pitot-
		static tube (counts)

The radii of cards 2, 3 and 4 are repeated internally to account for the cross traverse. Cards 5 through 27 introduce measurements made at the data points for one traverse, and data for the cross traverse are introduced on cards 28 through 50.

B-3 Output of ONRFLO

Table B-3 is a sample of the output of ONRFLO. It is for the final calibration, run 14. The first data block is a list of input data. For each point on the two traverses, QI, PSI, QO, and PSO are listed. The second data block is a list of computed velocities VI, VO, and VIAD. The third block shows how the "no boundary layer" flow rate, VFT, is computed by summing the product of VA and A. The fourth block shows how the flow rate deficiency, VFD, is computed. It lists the inputs to and outputs from SUBROUTINE QTFE, which performs the integration by the trapezoidal rule. The final statements list the final computed flow rate VFC and the final calibration constant CCC.

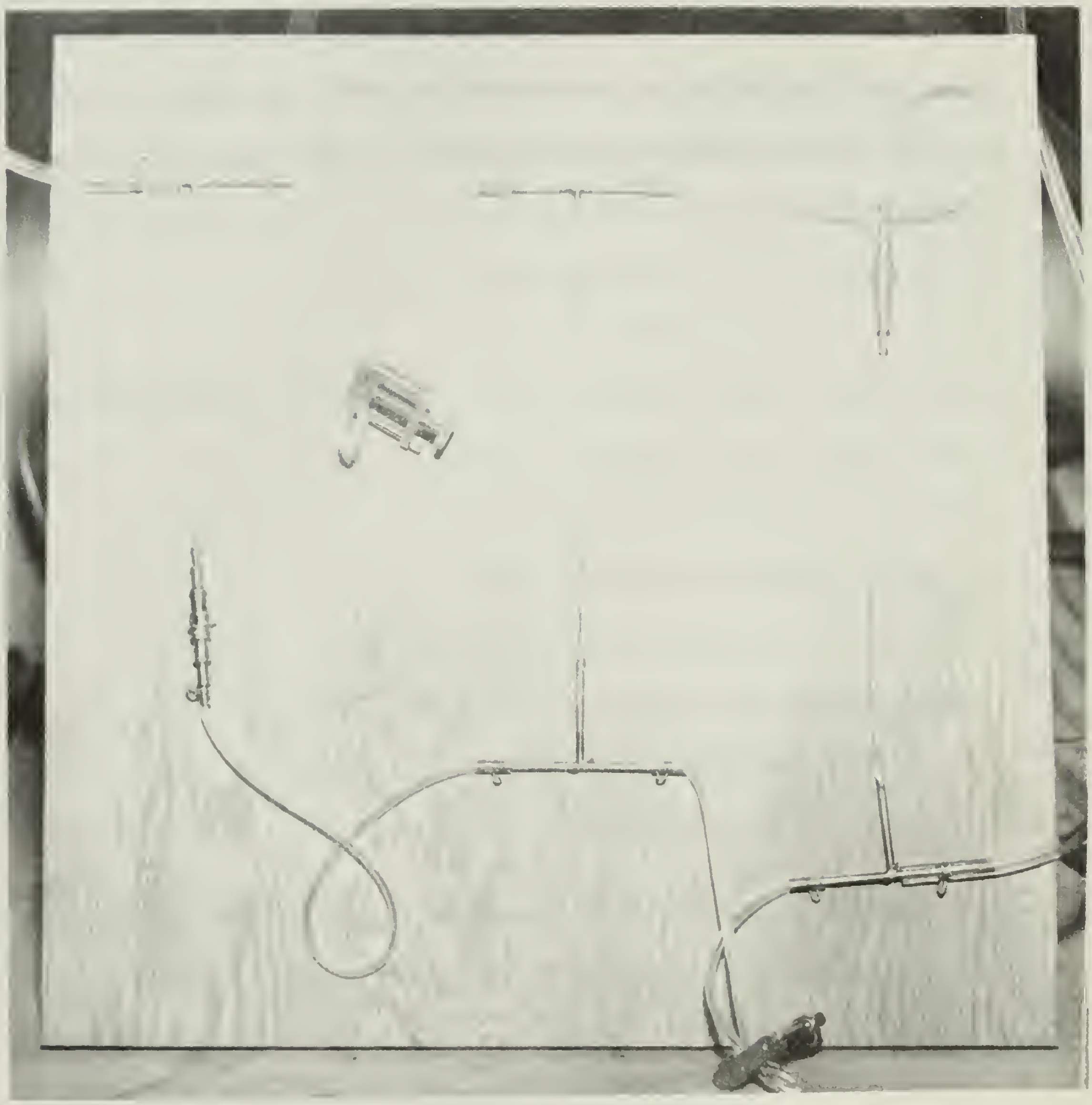

FIGURE B-1 VARIABLE LENGTH CAPILLARY DAMPING DEVICE

VARIABLE LENGTH CAPILLARY
DAMPING DEVICE
OPERATION

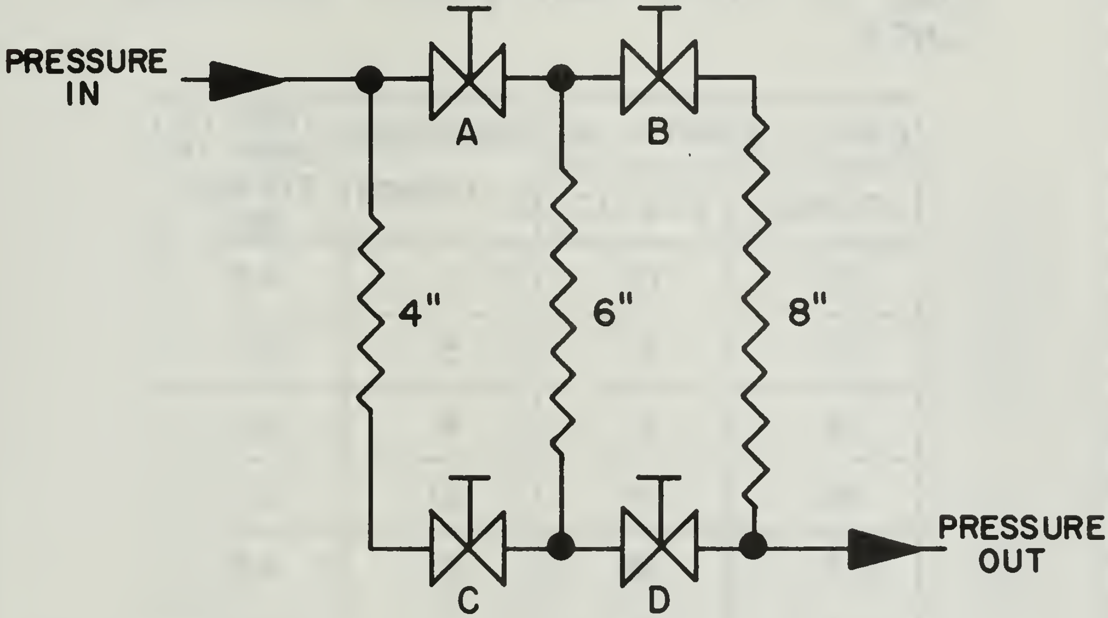

MATERIALS

CAPILLARY: NEEDLE STAINLESS TUBE 0.020" I.D.
VALVE: POLYETHYLENE TUBE & LAB CLAMPS.

CAP. LENGTH DESIRED	VALVES			
	A	B	C	D
4"	CLOSED	CLOSED	OPEN	OPEN
6"	OPEN	CLOSED	CLOSED	OPEN
8"	OPEN	OPEN	CLOSED	CLOSED
18"	CLOSED	OPEN	OPEN	CLOSED

FIG. B-2

PRECISION & TIME TO DAMP FOR VARIOUS LENGTHS OF CAPILLARY TUBE IN TOTAL AND STATIC PRESSURE LINES.

CAP. LENGTH IN.		PRECISION, ± COUNTS	TIME TO DAMP TO STEADY, SEC.
TOTAL	STATIC		
18	18	1	45
18	8	5	20
18	6	8	10
18	4	10	5
8	18	5	45
8	8	5	35
8	6	10	20
8	4	10	5
6	18	5	30
6	8	10	15
6	6	10	10
6	4	20	10
4	18	15	30
4	8	25	15
4	6	30	10
4	4	40	8

TABLE BI

```
      DIMENSION QI(50),PSI(50),QO(50),PSO(50),VI(50),VO(50),VIAD(50),A(5
     1),VA(5),VF(5),R(50),V3(10),VD(10),VR(10),VFD(10)
   11 READ(5,700,END=999)(NCASE,PBAR,TBAR,TO)
      WRITE(6,749)
      WRITE(6,750)
      WRITE(6,751) NCASE
      READ(5,701)(R(N),N=1,23)
      DO 1 N=24,46
      K=N-23
    1 R(N)=R(K)
      DO 2 N=1,46
      READ(5,702)(QI(N),PSI(N),QO(N),PSO(N))
    2 WRITE(6,752)(R(N),QI(N),PSI(N),QO(N),PSO(N))
      C1=.49280 + TBAR*.5/10000
      PA=PBAR*C1*144.
      TTO=TO + 459.7
      C2=SQRT((2.*2115.36)/(.002378*518.7))
      C3=240.329
      DO 3 N=1,46
      PI=PA-PSI(N)/C3
      QI1 = QI(N)/C3
      VI(N)=C2*SQRT(TTO)* SQRT(QI1/PI)
      PO=PA-PSO(N)/C3
      QO1 = QO(N)/C3
    3 VO(N)=C2 * SQRT(TTO)* SQRT(QO1/PO)
      VOT=0.
      DO 4 N=1,46
    4 VOT=VOT+VO(N)
      VOAV = VOT/46.
      DO 5 N=1,46
    5 VIAD(N)=VI(N) * VOAV  /VO(N)
      WRITE(6,753)
      DO 6 N=1,23
    6 WRITE(6,754)(R(N),VI(N),VO(N),VIAD(N))
      WRITE(6,755)
      DO 7 N=24,46
    7 WRITE(6,754)(R(N),VI(N),VO(N),VIAD(N))
      A(1)=3.14159 *2.*2./144.
      A(2)=2.*3.14159*4.0*4./144.
      A(3)=2.*3.14159*8.0*4./144.
      A(4)=2.*3.14159*12.*4./144.
      A(5)=2.*3.14159*16.*4./144.
      VA(1) = (VIAD(12) + VIAD(35))/2.
      VA(2) = (VIAD(11) + VIAD(13) + VIAD(34) + VIAD(36))/4.
      VA(3) = (VIAD(10) + VIAD(14) + VIAD(33) + VIAD(37))/4.
      VA(4) = (VIAD( 9) + VIAD(15) + VIAD(32) + VIAD(38))/4.
      VA(5) = (VIAD( 8) + VIAD(16) + VIAD(31) + VIAD(39))/4.
      WRITE(6,749)
```

Table B-2. Listing of Program ONRFLO

```
0048             WRITE(6,756)
0049             VFT=0.
0050             DO 8 N=1,5
0051             VF(N)=A(N)*VA(N)
0052             VFT=VFT+VF(N)
0053           8 WRITE(6,757)(N,VA(N),A(N),VF(N),VFT)
0054             CC=VFT/VOAV
0055             WRITE(6,758)(VFT,VOAV,CC)
0056             VB(1)=VA(5)
0057             VB(2) = (VIAD( 7) + VIAD(17) + VIAD(30) + VIAD(40))/4.
0058             VB(3) = (VIAD( 6) + VIAD(18) + VIAD(29) + VIAD(41))/4.
0059             VB(4) = (VIAD( 5) + VIAD(19) + VIAD(28) + VIAD(42))/4.
0060             VB(5) = (VIAD( 4) + VIAD(20) + VIAD(27) + VIAD(43))/4.
0061             VB(6) = (VIAD( 3) + VIAD(21) + VIAD(26) + VIAD(44))/4.
0062             VB(7) = (VIAD( 2) + VIAD(22) + VIAD(25) + VIAD(45))/4.
0063             VB(8) = (VIAD( 1) + VIAD(23) + VIAD(24) + VIAD(46))/4.
0064             VB(9)=0.
0065             DO 9 N=1,9
0066           9 VD(N)=VA(5)-VB(N)
0067             DO 10 N=1,8
0068             K=15+N
0069          10 VR(N)=VD(N)*R(K)*2.*3.14159/12.
0070             VR(9)=VD(9)*18.*2.*3.14159/12.
0071             H=.25/12.
0072             NDIM=9
0073             CALL QTFE(H,VR,VFD,NDIM)
0074             WRITE(6,755)
0075             WRITE(6,760)
0076             DO 12 N=1,8
0077             K=15+N
0078          12 WRITE(6,761)(R(K),VD(N),VR(N),VFD(N))
0079             VFF = VFD(9)
0080             VFC=VFT-VFF
0081             CCC=VFC/VOAV
0082             WRITE(6,759)(VFF,VFC,CCC)
0083         700 FORMAT(I7,3F7.2)
0084         701 FORMAT(8F10.2)
0085         702 FORMAT(4F7.0)
0086         749 FORMAT(1H1)
0087         750 FORMAT(23X,52HNAVAL POSTGRADUATE SCHOOL TURBOPROPULSION LABORATORY
                1///23X53HO.N.R. 3-STAGE AXIAL COMPRESSOR FLOW RATE CALIBRATION//)
0088         751 FORMAT(13X,18HINPUT DATA FOR RUNI3,27X,15HN = 1200 R.P.M.//5X,11HR
                1ADIUS FROM,7X,14HINLET VELOCITY,7X,12HINLET STATIC,7X,14HPROBE VEL
                2OCITY,7X,12HPROBE STATIC/1X,18HCENTERLINE, INCHES,5X,12HHEAD, COUN
                3TS,6X,16HPRESSURE, COUNTS,6X,12HHEAD, COUNTS,6X,16HPRESSURE, COUNT
                4S)
0089         752 FORMAT(F13.2,4F20.0)
0090         753 FORMAT(1H1,21X,38HCALCULATED VELOCITIES, FEET PER SECOND//5X,11HRA
```

Table B-2. Listing of Program ONRFLO (cont.)

```
              1DIUS FROM,12X,5HINLET,14X,5HPROBE,11X,14HADJUSTED INLET/1X,18HCENT
              2ERLINE, INCHES,7X,8HVELOCITY,12X,8HVELOCITY,12X,8HVELOCITY/)
0091     754 FORMAT(F13.2,3F20.3)
0092     755 FORMAT(//)
0093     756 FORMAT(//4X,74HCALCULATION OF VOLUME FLOW RATE ASSUMING NO BOUNDAR
              1Y LAYER EXISTS IN INLET//3X,6HSECTOR,4X16HAVERAGE VELOCITY,8X,5H A
              2REA,4X,16HSECTOR FLOW RATE,5X,15HTOTAL FLOW RATE/)
0094     757 FORMAT(I6,4F18.3)
0095     758 FORMAT(//1X,19HVOLUME FLOW RATE = ,F10.3,5X,25HAVERAGE PROBE VELOC
              1ITY = ,F8.3//1X,48HTHE "NO BOUNDARY LAYER" CALIBRATION CONSTANT IS
              2 ,F8.4,2X,39HCUBIC FEET PER SECOND / FOOT PER SECOND)
0096     759 FORMAT(//1X,25HVOLUME FLOW DEFICIENCY = ,F8.3,5X,25HFINAL VOLUME F
              1LOW RATE = ,F10.3//1X,34HTHE FINAL CALIBARTION CONSTANT IS ,F8.4,2
              2X,39HCUBIC FEET PER SECOND / FOOT PER SECOND)
0097     760 FORMAT(9X,55HCALCULATION OF VOLUME FLOW DEFICIENCY IN BOUNDARY LAY
              1ER//5X,11HRADIUS FROM,10X,8HVELOCITY,12X,8HVALUE OF,12X,9HFLOW RAT
              2E/1X,18HCENTERLINE,INCHES,6X,11HDEFICIENCY ,10X,9HINTEGRAND,11X,10
              3HDEFICIENCY//)
0098     761 FORMAT(F13.2,3F20.3)
0099         GO TO 11
0100     999 RETURN
0101         END
```



```
0001         SUBROUTINE QTFE(H,Y,Z,NDIM)
0002         DIMENSION Y(9),Z(9)
0003         SUM2=0.
0004         IF(NDIM-1)4,3,1
0005       1 HH=.5*H
0006         DO 2 N=2,NDIM
0007         I=N
0008         SUM1=SUM2
0009         SUM2=SUM2+HH*(Y(I)+Y(I-1))
0010       2 Z(I-1)=SUM1
0011       3 Z(NDIM)=SUM2
0012       4 RETURN
0013         END
```

Table B-2. Listing of Program ONRFLO (cont.)

NAVAL POSTGRADUATE SCHOOL TURBOPROPULSION LABORATORY

C.N.R. 3-STAGE AXIAL COMPRESSOR FLOW RATE CALIBRATION

INPUT DATA FOR RUN 14 N = 1200 R.P.M.

RADIUS FROM CENTERLINE, INCHES	INLET VELOCITY HEAD, COUNTS	INLET STATIC PRESSURE, COUNTS	PROBE VELOCITY HEAD, COUNTS	PROBE STATIC PRESSURE, COUNTS
17.75	545.	825.	1785.	2465.
17.50	605.	865.	1795.	2490.
17.25	665.	860.	1775.	2480.
17.00	685.	870.	1755.	2495.
16.75	705.	845.	1780.	2485.
16.50	700.	845.	1800.	2475.
16.25	700.	835.	1790.	2515.
16.00	695.	830.	1775.	2475.
12.00	720.	875.	1785.	2490.
8.00	725.	895.	1780.	2495.
4.00	715.	915.	1775.	2505.
0.0	750.	905.	1780.	2480.
4.00	740.	935.	1800.	2450.
8.00	710.	970.	1770.	2495.
12.00	750.	880.	1760.	2470.
16.00	725.	860.	1795.	2455.
16.25	700.	855.	1775.	2470.
16.50	695.	835.	1780.	2480.
16.75	700.	830.	1795.	2460.
17.00	670.	840.	1845.	2485.
17.25	635.	830.	1780.	2455.
17.50	585.	845.	1775.	2505.
17.75	525.	815.	1760.	2480.
17.75	515.	785.	1785.	2480.
17.50	655.	835.	1790.	2465.
17.25	685.	800.	1795.	2470.
17.00	705.	815.	1785.	2480.
16.75	705.	840.	1780.	2450.
16.50	705.	850.	1775.	2470.
16.25	710.	860.	1780.	2465.
16.00	720.	825.	1810.	2450.
12.00	735.	870.	1830.	2465.
8.00	735.	880.	1790.	2475.
4.00	760.	935.	1765.	2485.
0.0	730.	875.	1800.	2465.
4.00	730.	820.	1645.	2450.
8.00	730.	930.	1665.	2465.
12.00	710.	835.	1735.	2440.
16.00	685.	860.	1780.	3475.
16.25	680.	835.	1775.	2440.
16.50	700.	835.	1790.	2455.
16.75	695.	845.	1780.	2465.
17.00	670.	815.	1805.	2465.
17.25	645.	845.	1810.	2465.
17.50	625.	855.	1800.	2445.
17.75	545.	885.	1795.	2475.

Table B-3. Sample Output of Program ONRFLO-Input for Run 14

CALCULATED VELOCITIES, FEET PER SECOND

RADIUS FROM CENTERLINE, INCHES	INLET VELOCITY	PROBE VELOCITY	ADJUSTED INLET VELOCITY
17.75	44.116	79.968	44.052
17.50	46.483	80.193	46.285
17.25	48.733	79.745	48.799
17.00	49.461	79.295	49.809
16.75	50.177	79.857	50.174
16.50	49.999	80.304	49.717
16.25	49.998	80.084	49.854
16.00	49.819	79.744	49.886
12.00	50.709	79.970	50.635
8.00	50.886	79.858	50.882
4.00	50.535	79.746	50.602
0.0	51.757	79.857	51.753
4.00	51.412	80.302	51.124
8.00	50.361	79.633	50.499
12.00	51.755	79.406	52.046
16.00	50.884	80.191	50.669
16.25	49.999	79.744	50.067
16.50	49.819	79.857	49.816
16.75	49.998	80.191	49.786
17.00	48.915	81.302	48.043
17.25	47.620	79.855	47.618
17.50	45.707	79.746	45.768
17.75	43.299	79.407	43.541
17.75	42.883	79.969	42.820
17.50	48.364	80.080	48.227
17.25	49.458	80.192	49.248
17.00	50.175	79.969	50.102
16.75	50.177	79.854	50.175
16.50	50.177	79.744	50.245
16.25	50.355	79.856	50.353
16.00	50.707	80.525	50.283
12.00	51.235	80.969	50.527
8.00	51.235	80.080	51.089
4.00	52.102	79.520	52.319
0.0	51.060	80.303	50.773
4.00	51.058	76.767	53.110
8.00	51.063	77.233	52.795
12.00	50.354	78.838	51.002
16.00	49.461	79.935	49.410
16.25	49.279	79.741	49.347
16.50	49.998	80.079	49.856
16.75	49.820	79.856	49.817
17.00	48.914	80.414	48.572
17.25	47.994	80.526	47.593
17.50	47.245	80.301	46.980
17.75	44.119	80.192	43.932

Table B-4. Sample Output of Program ONRFLO-Velocities for Run 14

CALCULATION OF VOLUME FLOW RATE ASSUMING NO BOUNDARY LAYER EXISTS IN INLET

SECTOR	AVERAGE VELOCITY	AREA	SECTOR FLOW RATE	TOTAL FLOW RATE
1	51.263	0.087	4.474	4.474
2	51.789	0.698	36.155	40.629
3	51.316	1.396	71.651	112.280
4	51.052	2.094	106.924	219.203
5	50.062	2.793	139.800	359.003

VOLUME FLOW RATE = 359.003 AVERAGE PROBE VELOCITY = 79.852

THE "NO BOUNDARY LAYER" CALIBRATION CONSTANT IS 4.4959 CUBIC FEET PER SECOND / FOOT PER SECOND

CALCULATION OF VOLUME FLOW DEFICIENCY IN BOUNDARY LAYER

RADIUS FROM CENTERLINE, INCHES,	VELOCITY DEFICIENCY	VALUE OF INTEGRAND	FLOW RATE DEFICIENCY
16.00	0.0	0.0	0.0
16.25	0.157	1.337	0.014
16.50	0.153	1.325	0.042
16.75	0.074	0.649	0.062
17.00	0.931	8.286	0.155
17.25	1.743	15.785	0.406
17.50	3.247	29.753	0.880
17.75	6.476	60.184	1.817

VOLUME FLOW DEFICIENCY = 7.359 FINAL VOLUME FLOW RATE = 351.644

THE FINAL CALIBARTION CONSTANT IS 4.4037 CUBIC FEET PER SECOND / FOOT PER SECOND

Table B-5. Sample Output of Program ONRFLO-Calibration Constant for Run 14

APPENDIX C

PERFORMANCE MEASUREMENTS

It was decided to take flow measurements at the mean streamline, using the radial survey holes. The assumption was made that measurements made at this point accurately represented the flow in the entire flow annulus. The truth of the assumption is verified in Section C-1. Section C-2 presents details concerning the data reduction program ONRETA.

C-1 Verification of Assumptions

The assumption that measurements made at the mean streamline using the radial survey holes accurately represent the flow in the entire flow annulus was verified in three ways. The total pressure measured at the mean radius was shown to be nearly equal to the integrated average of total pressure at each radius. It was demonstrated that the total pressure measured at the peripheral location of a radial survey hole was nearly equal to the integrated average of total pressure at each peripheral location in a blade channel. The flow was shown to be nearly axisymmetric.

Concerning the radial variation of total pressure, the existence of a boundary layer at the outer radius in the inlet has already been shown. It was further shown that a boundary layer existed ahead of the first stage and behind the last stage. With the stator stagger angle at 27.8° and the flow rate at about 400 ft^3/sec., a radial traverse was made at the radial survey hole labeled 37°27'30" in survey plane 8 of Fig. 7. Data points were established each 0.3 in.

from a radius of 11.1 in. to 18.0 in. After recording the barometric pressure P_{Bar} and ambient temperature T_o the following measurements were taken:

P_{td} - total pressure with reference to atmospheric after third stator (counts)

P_{sd} - static pressure with reference to atmospheric after third stator (counts)

q_d - velocity head after the third stator (counts)

The total pressure at the inner radius could not be measured but was assumed to be the static pressure at 11.1 in. With the relations listed on p. 35 these measuring data establish the following quantities:

$$P_A = P_{Bar} \ (71.467) \qquad \text{(psfa)} \qquad (1)$$

$$T_{to} = T_o + 459.7 \qquad (^oR) \qquad (2)$$

$$P_{tda} = P_A + \frac{P_{td}}{240.423} \qquad \text{(psfa)} \qquad (3)$$

$$P_{sda} = P_A + \frac{P_{sd}}{240.423} \qquad \text{(psfa)} \qquad (3)$$

With the assumption that the total temperature after the third stator T_{td} is nearly equal to the inlet total temperature T_{to}

$$\rho_d = \frac{0.002378 \ P_{sda}}{(14.696)(144)} \frac{518.7}{T_{to}} = \frac{P_{sda}}{T_{to}}\left(5.82\times10^{-4}\right) (\text{lb sec}^2/\text{ft}^4) \qquad (4)$$

$$q_{d1} = \frac{q_d}{240.423} \qquad \text{(psf)} \qquad (5)$$

$$V_d = \sqrt{\frac{2\, q_{d1}}{\rho_d}} \qquad \text{(ft/sec)} \qquad (6)$$

The average total pressure was calculated from the integral expression

$$\overline{P_{tda}} = \frac{\int_{10.8}^{18.0} 2\pi\, V_d\, \frac{r}{12}\, P_{tda}\, \frac{dr}{12}}{\int_{10.8}^{18.0} 2\pi\, V_d\, \frac{r}{12}\, \frac{dr}{12}}$$

Both integrations were performed by the trapezoidal rule. Figure C-1 is a graphical representation of the integration. The integrated average total pressure $\overline{P_{tda}}$ was 2184.20 lb/ft^2 while the total pressure measured at the mean streamline was 2184.34 lb/ft^2. The relative error between the two pressures is 0.006 per cent. A second radial survey was made at the radial survey hole labeled 149°57'30" in the plane called S. P. 8 on Fig. 7. The integrated average pressure for this survey was 2183.92 lb/ft^2. The total pressure measured at the mean radial position was 2184.32 lb/ft^2. The relative error between the two pressures was 0.018 per cent. Since the pressure measured at the mean radius was nearly equal to the integrated average of pressure at each radial location, mean streamline values were used to measure compressor performance.

The traverse carriage was used for peripheral surveys. Since it would be necessary to remove the first stage rotor to survey in the axial plane ahead of the first stage, the investigation was confined to the plane behind the third stage stator where measurements could be made simply. The locations of the radial survey holes with reference to the indicated meridional angle of the carriage are shown in Fig. 23.

There are 32 stator blades. Each blade channel is 11.25^{o} in peripheral direction. With the stator stagger angle at 27.8^{o} a peripheral survey was made at the mean radius, 14.4 in. The average reading over the entire 15^{o} of carriage travel was 9256 counts. The reading taken at the radial survey hole marked $37^{o}27'30''$ on Fig. 7 was 9246 counts, a relative error of 0.11 per cent. The average over the first 11.25^{o} of carriage travel, representing one blade channel, was 9218 counts, a relative error of 0.30 per cent. Figure C-2 illustrates the results of this mean radius survey. A second survey was conducted near the hub at a radius of 11.2 in. The average pressure reading of the traverse was 9532.47 counts. The pressure measurement at the radial survey hole was 9569.23 counts. A relative error of 0.36 per cent existed between the two pressures. On the basis of the surveys made behind the third stage stator the measurements taken at the radial survey taps were accepted as accurately representing the flow in the entire blade channel.

An investigation of the axisymmetry of the flow was conducted. The results are tabulated in Table C-1. The total pressure behind the inlet guide vanes, P_{tig}, was measured at eight different radial survey holes in plane S. P. 2 of Fig. 7. The average reading of P_{tig} was 578.1 counts. The nearest reading to the average was 573.9 counts, taken at the hole labeled $33^{o}45'$. This hole was used for all readings of P_{tig}. The relative error was 0.73 per cent. The average of readings taken behind the third stage stator P_{td} was 10, 821.5 counts. The nearest reading to the average was 10, 810 counts, taken at the hole marked $37^{o}27'30''$ on Fig. 7. This hole was used for all readings of P_{td}. The relative error was 0.10 per cent. Within the measurement capability of the instrument, the flow was considered axisymmetric and the most representative readings have been used.

C-2 Program ONRETA

The data reduction described in Section 4 was accomplished by Program ONRETA (Table C-2). Since the calculations are straightforward and have been described in the body of the thesis, they will not be repeated here.

The input format is as follows:

Card 1:	NCASE	run number (arbitrary)
(2I8,4F8.2)	NRUN	number of data points per run
	PBAR	reading of barometer (in. of Hg)
	TBAR	temperature of barometer (^{o}F)
	RSTAG	rotor stagger angle (43.8^{o})
	SSTAG	stator stagger angle (various ^{o})
Card 2:	TO	temperature at inlet screen (^{o}F)
(F8.1,4F8.0 F8.1,F8.2)	QO	velocity head at permanent Pitot-static tube (counts)
	PSO	static pressure with reference to atmospheric at permanent Pitot-static tube (counts)
	PTIG	total pressure with reference to atmospheric ahead of first rotor (counts)
	DELP	pressure rise across the 3 stages (counts)
	TACH	reading of the speed counter (rpm)
	TRAW	reading of the torque meter (lb)

Cards 3 through (NRUN - 1): repeat of Card 2 for remaining data points

The first five entries on cards 2 through (NRUN - 1) are the arithmetic average of four readings taken two minutes apart. The last two entries are the average of two readings taken five minutes apart.

The first section of program output is a printout of the input data. The second section is the calculated data for the run. The third section is the calculated nondimensional coefficients.

Tables C-3 through C-13 present the results of runs 1 through 11.

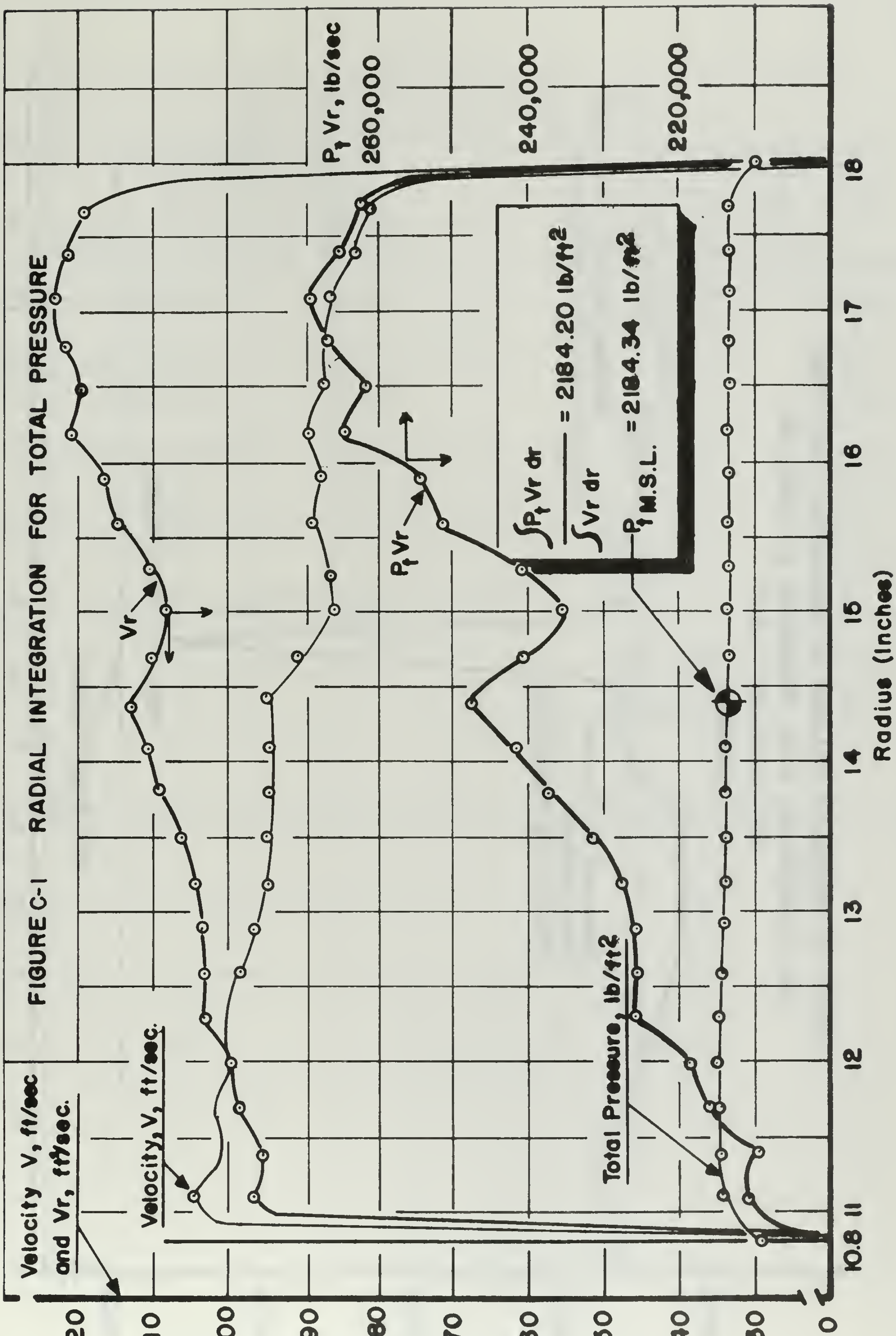

FIGURE C-1 RADIAL INTEGRATION FOR TOTAL PRESSURE

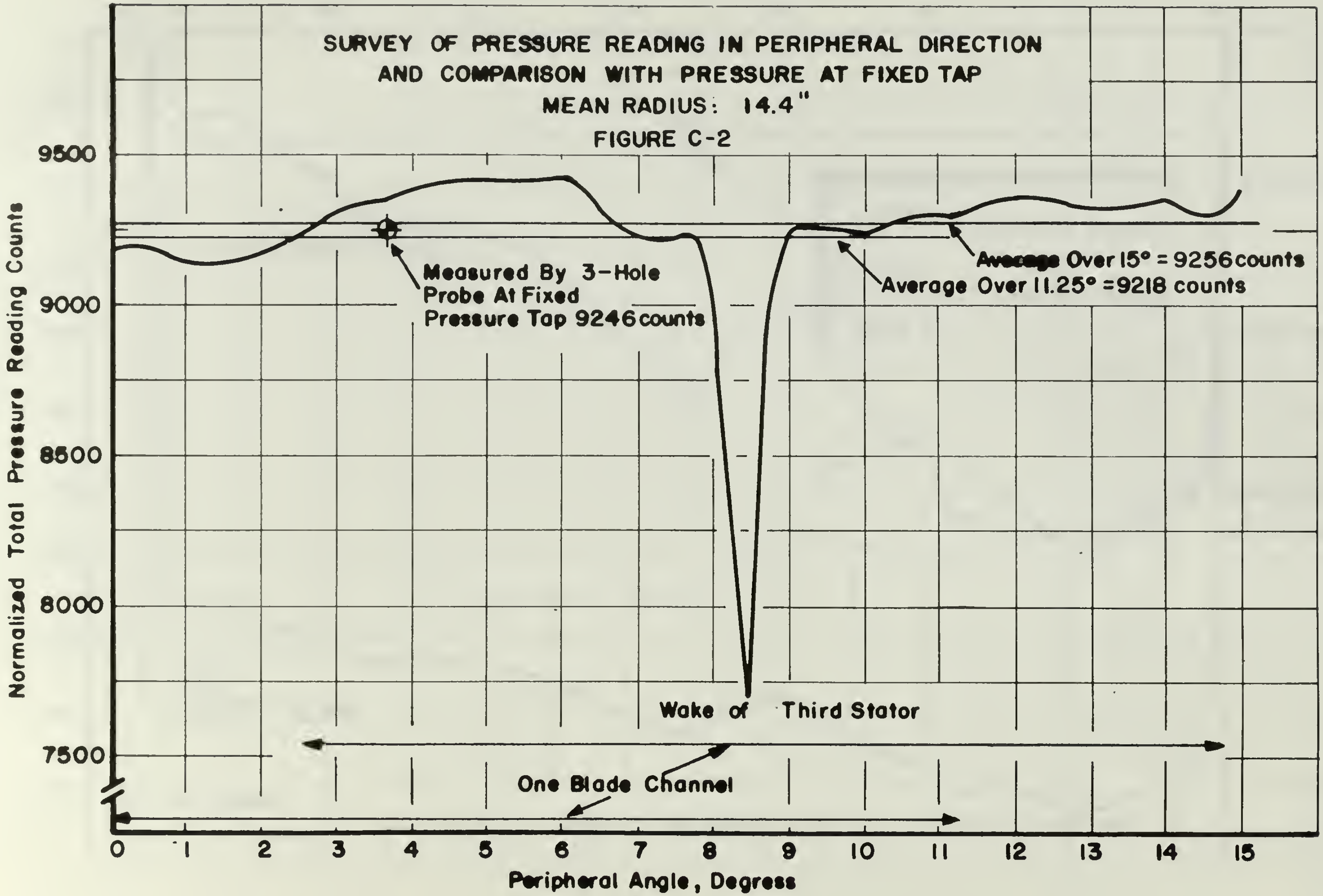

SURVEY OF PRESSURE READING IN PERIPHERAL DIRECTION
AND COMPARISON WITH PRESSURE AT FIXED TAP
MEAN RADIUS: 14.4"
FIGURE C-2
Measured By 3-Hole Probe At Fixed Pressure Tap 9246 counts
Average Over 15° = 9256 counts
Average Over 11.25° = 9218 counts
Wake of Third Stator
One Blade Channel
Normalized Total Pressure Reading Counts
9500
9000
8500
8000
7500
0 1 2 3 4 5 6 7 8 9 10 11 12 13 14 15
Peripheral Angle, Degress

TABLE C-1

INVESTIGATION OF AXISYMMETRY OF FLOW

TOTAL PRESSURE BEHIND INLET GUIDE VANES

RADIAL SURVEY HOLE	READING
26°12'30"	10,860
* 37°27'30"	10,810
93°42'30"	10,810
149°57'30"	10,805
AVERAGE	10,821

* READING CLOSEST TO AVERAGE

TOTAL PRESSURE BEHIND THIRD STAGE STATOR

RADIAL SURVEY HOLE	READING
11°15'	564.2
22°30'	587.2
* 33°45'	573.9
45°	601.5
56°15'	557.3
67°30'	565.9
76°45'	611.6
88°7'30"	563.2
AVERAGE	578.1

```
0001         DIMENSION TO(20),QO(20),PSO(20),PTIG(20),DELP(20),TACH(20),TRAW(20
            1),VFC(20),WREM(20),DELTAP(20),PRATS3(20),TRQ(20),OMEG(20),ETAST3(2
            20),PSIAV(30),PHIAV(30),TAUAV(30),PO(30),TTO(30)
0002      11 READ(5,700,END=9999)(NCASE,NRUN,PBAR,TBAR,RSTAG,SSTAG)
0003         WRITE(6,750)(NCASE,PBAR,TBAR,RSTAG,SSTAG)
0004         WRITE(6,1750)
0005         DO 12 N=1,NRUN
0006         READ(5,701)(TO(N),QO(N),PSO(N),PTIG(N),DELP(N),TACH(N),TRAW(N))
0007      12 WRITE(6,751)(TO(N),QO(N),PSO(N),PTIG(N),DELP(N),TACH(N),TRAW(N))
0008         WRITE(6,752)(NCASE)
0009         C1=.49280 + TBAR*.5/10000
0010         C2=SQRT((2.*14.696*144.)/(.002378*518.7))
0011         C3=240.423
0012         C4=4.1565
0013         CCC = 4.4050
0014         CP = .24
0015         GAM = 1.4
0016         EXP2 = (GAM-1.) / GAM
0017         AANUL=651.4/144.
0018         RAV=28.8/(2.*12.)
0019         PA=PBAR*C1*144.
0020         DO 13 N=1,NRUN
0021         TTO(N)=TO(N)+459.7
0022         PO(N)=PA-PSO(N)/C3
0023         QO1=QO(N)/C3
0024         VO=C2*SQRT(TTO(N)*QO1/PO(N))
0025         VFC(N)= CCC * VO
0026         WDOT = VFC(N)*32.174*.002378*518.7*PA/(TTO(N)*14.696*144.)
0027         WREM(N) = WDOT * SQRT(TTO(N)) * 144. / PA
0028         DELTAP(N) = DELP(N)/C3
0029         PTIGA = PA - PTIG(N)/C3
0030         PRATS3(N) =( PTIGA    + DELTAP(N))/ PTIGA
0031         TRQ(N) = TRAW(N)*C4
0032         OMEG(N) = TACH(N)*2.*3.14159/60.
0033         A = EXP2 *ALOG(PRATS3(N))
0034         B = EXP(A) - 1.
0035         ETAST3(N) =WDOT*CP*TTO(N)*B*778.3/ (TRQ(N) * OMEG(N))
0036      13 WRITE(6,753)(WREM(N),VFC(N),DELTAP(N),PRATS3(N),TRQ(N),OMEG(N),ETA
            1ST3(N))
0037         WRITE(6,754)(NCASE)
0038         DO 14 N=1,NRUN
0039         UAV=RAV*OMEG(N)
0040         PHIAV(N)=VFC(N)/(AANUL*UAV)
0041         RHOI=.002378*PO(N)*518.7/(TTO(N)*14.696*144.)
0042         PSIAV(N)=DELTAP(N)/(3*RHOI*(UAV**2.))
0043         TAUAV(N)=PSIAV(N)/ETAST3(N)
0044      14 WRITE(6,755)(PHIAV(N),ETAST3(N),TAUAV(N),PSIAV(N))
0045     700 FORMAT(2I8,4F8.2)
```

Table C-2. Listing of Program ONRETA

```
0046          701 FORMAT(F8.1,4F8.0,F8.1,F8.2)
0047          750 FORMAT(1H1,23X,52HNAVAL POSTGRADUATE SCHOOL TURBOPROPULSION LABORA
                 1TORY///23X,51HO.N.R. 3-STAGE AXIAL COMPRESSOR, 3-STAGE EFFICIENCY/
                 2/6X,18HINPUT DATA FOR RUNI3,9X,19HBAROMETRIC PRESSUREF7.2,4X,2HATF
                 36.1,2X,10HDEGREES,F.//6X,19HROTOR STAGGER ANGLEF5.1,15X,20HSTATOR
                 4STAGGER ANGLEF5.1)
0048         1750 FORMAT(//5X,5HTEMP,,7X,8HVELOCITY,6X,8HPSTATIC,,8X,5HPTIG,,9X,5HDE
                 1LP,,6X,10HTACHOMETER,4X,11HTORQUEMETER/4X,7HDEG. F.,4X,12HHEAD, CO
                 2UNTS,5X,6HCOUNTS,8X,6HCOUNTS,8X,6HCOUNTS,8X,6HR.P.M.,8X,6HPOUNDS/)
0049          751 FORMAT(F9.1,4F14.0,F14.1,F14.2)
0050          752 FORMAT(///,6X,19HOUTPUT DATA FOR RUNI3,//3X,8HREFERRED,5X,10HVOLFL
                 1ORATE,5X,8HPTD-PTIG,6X,8HPRESSURE,7X,6HTORQUE,9X,5HOMEGA,7X,7H3-ST
                 2AGE/3X,9HFLOW RATE,4X,11HCU.FT./SEC.3X,10HLB./SQ.FT.,6X,5HRATIO,9
                 3X,7HFT.-LB.,6X,9HRAD./SEC.4X,10HEFFICIENCY/)
0051          753 FORMAT(F10.3,F15.3,F13.3,F14.5,2F14.3,F14.5)
0052          754 FORMAT(///,6X,37HNON-DIMENSIONAL COEFFICIENTS FOR RUN I3,//5X,16HF
                 1LOW COEFFICIENT,7X,18H3-STAGE EFFICIENCY,5X,22HDEFLECTION COEFFICI
                 2ENT,4X,20HPRESSURE COEFFICIENT/)
0053          755 FORMAT(F16.4,3F25.4)
0054              GO TO 11
0055         9999 RETURN
0056              END
```

Table C-2. Listing of Program ONRETA (cont.)

NAVAL POSTGRADUATE SCHOOL TURBOPROPULSION LABORATORY

O.N.R. 3-STAGE AXIAL COMPRESSOR, 3-STAGE EFFICIENCY

INPUT DATA FOR RUN 1 BAROMETRIC PRESSURE 30.02 AT 76.7 DEGREES,F.

ROTOR STAGGER ANGLE 42.8 STATOR STAGGER ANGLE 27.8

TEMP, DEG. F.	VELOCITY HEAD, COUNTS	PSTATIC, COUNTS	PTIG, COUNTS	DELP, COUNTS	TACHOMETER R.P.M.	TORQUEMETER POUNDS
72.3	2470.	3240.	835.	8595.	1190.5	30.62
71.0	2340.	3045.	815.	9265.	1190.0	31.60
71.4	2135.	2825.	750.	10110.	1189.5	32.87

OUTPUT DATA FOR RUN 1

REFERRED FLOW RATE	VOLFLORATE CU.FT./SEC.	PTO-PTIG LB./SQ.FT.	PRESSURE RATIO	TORQUE FT.-LB.	OMEGA RAD./SEC.	3-STAGE EFFICIENCY
48.354	413.005	35.749	1.01668	127.272	124.669	0.92725
47.055	401.422	38.536	1.01798	131.345	124.616	0.94138
44.937	383.498	42.051	1.01962	136.624	124.564	0.94319

NON-DIMENSIONAL COEFFICIENTS FOR RUN 1

FLOW COEFFICIENT	3-STAGE EFFICIENCY	DEFLECTION COEFFICIENT	PRESSURE COEFFICIENT
0.6103	0.9273	0.2457	0.2278
0.5934	0.9414	0.2603	0.2451
0.5672	0.9432	0.2339	0.2677

Table C-3. Output of Program ONRETA, Run 1, Stator Stagger Angle = 27.8°

NAVAL POSTGRADUATE SCHOOL TURBOPROPULSION LABORATORY

O.N.R. 3-STAGE AXIAL COMPRESSOR, 3-STAGE EFFICIENCY

INPUT DATA FOR RUN 2 BAROMETRIC PRESSURE 30.04 AT 74.2 DEGREES,F.

ROTOR STAGGER ANGLE 42.8 STATOR STAGGER ANGLE 27.8

TEMP, DEG. F.	VELOCITY HEAD, COUNTS	PSTATIC, COUNTS	PTIG, COUNTS	DELP, COUNTS	TACHOMETER R.P.M.	TORQUEMETER POUNDS
70.5	2130.	2870.	727.	10087.	1189.8	32.78
69.5	2030.	2757.	705.	10545.	1189.4	33.20
71.0	1948.	2657.	655.	10785.	1188.9	33.40
70.3	1890.	2553.	565.	11015.	1189.0	33.62

OUTPUT DATA FOR RUN 2

REFERRED FLOW RATE	VOLFLORATE CU.FT./SEC.	PTD-PTIG LB./SQ.FT.	PRESSURE RATIO	TORQUE FT.-LB.	OMEGA RAD./SEC.	3-STAGE EFFICIENCY
44.877	382.660	41.955	1.01956	136.250	124.595	0.94128
43.806	373.177	43.860	1.02045	137.996	124.554	0.94745
42.908	366.044	44.858	1.02091	138.827	124.501	0.94499
42.260	360.279	45.815	1.02135	139.742	124.512	0.94325

NON-DIMENSIONAL COEFFICIENTS FOR RUN 2

FLOW COEFFICIENT	3-STAGE EFFICIENCY	DEFLECTION COEFFICIENT	PRESSURE COEFFICIENT
0.5658	0.9413	0.2831	0.2664
0.5519	0.9475	0.2936	0.2781
0.5416	0.9450	0.3021	0.2855
0.5330	0.9433	0.3086	0.2911

Table C-4. Output of Program ONRETA, Run 2, Stator Stagger Angle = 27.8°

NAVAL POSTGRADUATE SCHOOL TURBOPROPULSION LABORATORY

C.N.R. 3-STAGE AXIAL COMPRESSOR, 3-STAGE EFFICIENCY

INPUT DATA FOR RUN 3 BAROMETRIC PRESSURE 30.05 AT 74.9 DEGREES,F.

ROTOR STAGGER ANGLE 42.8 STATOR STAGGER ANGLE 27.8

TEMP, DEG. F.	VELOCITY HEAD, COUNTS	PSTATIC, COUNTS	PTIG, COUNTS	DELP, COUNTS	TACHOMETER R.P.M.	TORQUEMETER POUNDS
72.0	1765.	2347.	607.	11027.	1189.0	32.93
72.3	1570.	2075.	550.	10750.	1189.0	32.13

OUTPUT DATA FOR RUN 3

REFERRED FLOW RATE	VOLFLORATE CU.FT./SEC.	PTD-PTIG LB./SQ.FT.	PRESSURE RATIO	TORQUE FT.-LB.	OMEGA RAD./SEC.	3-STAGE EFFICIENCY
40.823	348.579	45.865	1.02137	136.874	124.512	0.93285
38.491	328.765	44.713	1.02083	133.548	124.512	0.87917

NON-DIMENSIONAL COEFFICIENTS FOR RUN 3

FLOW COEFFICIENT	3-STAGE EFFICIENCY	DEFLECTION COEFFICIENT	PRESSURE COEFFICIENT
0.5157	0.9329	0.3131	0.2921
0.4864	0.8792	0.3239	0.2847

Table C-5. Output of Program ONRETA, Run 3, Stator Stagger Angle = 27.8°

NAVAL POSTGRADUATE SCHOOL TURBOPROPULSION LABORATORY

O.N.R. 3-STAGE AXIAL COMPRESSOR, 3-STAGE EFFICIENCY

INPUT DATA FOR RUN 4 BAROMETRIC PRESSURE 29.92 AT 75.6 DEGREES,F.

ROTOR STAGGER ANGLE 42.8 STATOR STAGGER ANGLE 23.8

TEMP, DEG. F.	VELOCITY HEAD, COUNTS	PSTATIC, COUNTS	PTIG, COUNTS	DELP, COUNTS	TACHOMETER R.P.M.	TORQUEMETER POUNDS
74.0	2292.	3140.	780.	9730.	1189.4	33.88
76.4	2207.	2920.	757.	10350.	1189.1	34.55
75.2	2073.	2783.	707.	10683.	1188.9	34.85
75.4	1880.	2520.	657.	10919.	1189.0	33.80
74.3	1740.	2360.	593.	10743.	1189.5	33.23

OUTPUT DATA FOR RUN 4

REFERRED FLOW RATE	VOLFLORATE CU.FT./SEC.	PTD-PTIG LB./SQ.FT.	PRESSURE RATIO	TORQUE FT.-LB.	OMEGA RAD./SEC.	3-STAGE EFFICIENCY
46.655	399.133	40.470	1.01894	140.822	124.554	0.91681
45.772	392.458	43.049	1.02015	143.607	124.522	0.94022
44.355	379.880	44.434	1.02080	144.854	124.501	0.93116
42.229	361.739	45.416	1.02125	140.490	124.512	0.93412
40.620	347.597	44.684	1.02091	138.120	124.564	0.89788

NON-DIMENSIONAL COEFFICIENTS FOR RUN 4

FLOW COEFFICIENT	3-STAGE EFFICIENCY	DEFLECTION COEFFICIENT	PRESSURE COEFFICIENT
0.5903	0.9168	0.2836	0.2600
0.5806	0.9402	0.2955	0.2779
0.5621	0.9312	0.3073	0.2862
0.5352	0.9341	0.3130	0.2924
0.5141	0.8979	0.3194	0.2868

Table C-6. Output of Program ONRETA, Run 4, Stator Stagger Angle = 23.8°

NAVAL POSTGRADUATE SCHOOL TURBOPROPULSION LABORATORY

O.N.R. 3-STAGE AXIAL COMPRESSOR, 3-STAGE EFFICIENCY

INPUT DATA FOR RUN 5 BAROMETRIC PRESSURE 30.06 AT 75.6 DEGREES,F.

ROTOR STAGGER ANGLE 42.8 STATOR STAGGER ANGLE 23.8

TEMP, DEG. F.	VELOCITY HEAD, COUNTS	PSTATIC, COUNTS	PTIG, COUNTS	DELP, COUNTS	TACHOMETER R.P.M.	TORQUEMETER POUNDS
73.0	2240.	3075.	750.	10137.	1189.3	34.50
74.1	2169.	2903.	737.	10587.	1189.0	35.00
74.5	2021.	2703.	680.	10910.	1188.8	34.85
75.3	1815.	2460.	655.	10865.	1189.1	33.70
76.2	1635.	2102.	563.	10550.	1189.5	32.83

OUTPUT DATA FOR RUN 5

REFERRED FLOW RATE	VOLFLORATE CU.FT./SEC.	PTD-PTIG LB./SQ.FT.	PRESSURE RATIO	TORQUE FT.-LB.	OMEGA RAD./SEC.	3-STAGE EFFICIENCY
46.012	393.260	42.163	1.01964	143.399	124.543	0.92405
45.269	387.312	44.035	1.02051	145.477	124.512	0.93676
43.689	373.932	45.378	1.02114	144.854	124.491	0.93599
41.393	354.544	45.191	1.02105	140.074	124.522	0.91371
39.273	336.670	43.881	1.02044	136.458	124.564	0.86446

NON-DIMENSIONAL COEFFICIENTS FOR RUN 5

FLOW COEFFICIENT	3-STAGE EFFICIENCY	DEFLECTION COEFFICIENT	PRESSURE COEFFICIENT
0.5817	0.9240	0.2913	0.2691
0.5730	0.9368	0.3007	0.2817
0.5533	0.9360	0.3104	0.2905
0.5245	0.9137	0.3168	0.2895
0.4979	0.8645	0.3252	0.2812

Table C-7. Output of Program ONRETA, Run 5, Stator Stagger Angle = 23.8°

NAVAL POSTGRADUATE SCHOOL TURBOPROPULSION LABORATORY

O.N.R. 3-STAGE AXIAL COMPRESSOR, 3-STAGE EFFICIENCY

INPUT DATA FOR RUN 6 BAROMETRIC PRESSURE 30.04 AT 76.2 DEGREES,F.

ROTOR STAGGER ANGLE 42.8 STATOR STAGGER ANGLE 31.8

TEMP, DEG. F.	VELOCITY HEAD, COUNTS	PSTATIC, COUNTS	PTIG, COUNTS	DELP, COUNTS	TACHOMETER R.P.M.	TORQUEMETER POUNDS
71.8	1978.	2703.	758.	9772.	1191.0	30.55
73.5	1866.	2515.	633.	10313.	1190.3	31.23
74.6	1810.	2400.	617.	10627.	1190.6	31.50
74.9	1675.	2270.	598.	11138.	1190.0	31.90
74.0	1618.	2190.	570.	11340.	1190.0	31.93
73.6	1485.	2028.	563.	10913.	1190.3	31.18

OUTPUT DATA FOR RUN 6

REFERRED FLOW RATE	VOLFLORATE CU.FT./SEC.	PTD-PTIG LB./SQ.FT.	PRESSURE RATIO	TORQUE FT.-LB.	OMEGA RAD./SEC.	3-STAGE EFFICIENCY
43.235	369.109	40.645	1.01895	126.981	124.721	0.94316
41.985	359.014	42.895	1.01999	129.807	124.648	0.94696
41.346	353.910	44.201	1.02060	130.930	124.679	0.95327
39.769	340.509	46.327	1.02159	132.592	124.616	0.94931
39.084	334.357	47.167	1.02198	132.717	124.616	0.94797
37.437	320.150	45.391	1.02115	129.600	124.648	0.89459

NON-DIMENSIONAL COEFFICIENTS FOR RUN 6

FLOW COEFFICIENT	3-STAGE EFFICIENCY	DEFLECTION COEFFICIENT	PRESSURE COEFFICIENT
0.5452	0.9432	0.2737	0.2581
0.5306	0.9470	0.2888	0.2735
0.5229	0.9533	0.2960	0.2822
0.5034	0.9493	0.3120	0.2961
0.4943	0.9480	0.3175	0.3010
0.4732	0.8946	0.3232	0.2892

Table C-8. Output of Program ONRETA, Run 6, Stator Stagger Angle = 31.8°

NAVAL POSTGRADUATE SCHOOL TURBOPROPULSION LABORATORY

O.N.R. 3-STAGE AXIAL COMPRESSOR, 3-STAGE EFFICIENCY

INPUT DATA FOR RUN 7 BAROMETRIC PRESSURE 29.88 AT 74.0 DEGREES,F.

ROTOR STAGGER ANGLE 42.8 STATOR STAGGER ANGLE 31.8

TEMP, DEG. F.	VELOCITY HEAD, COUNTS	PSTATIC, COUNTS	PTIG, COUNTS	DELP, COUNTS	TACHOMETER R.P.M.	TORQUEMETER POUNDS
70.0	2331.	3145.	760.	8139.	1191.0	27.73
71.4	2023.	2755.	734.	9614.	1190.0	30.31
72.6	1850.	2568.	639.	10431.	1189.9	31.10
72.0	1764.	2464.	630.	10735.	1189.8	31.55
71.3	1705.	2393.	626.	11135.	1189.6	31.73
72.0	1581.	2260.	630.	11419.	1190.2	31.73
71.9	1484.	2108.	626.	10903.	1190.5	31.11
71.4	1594.	2276.	630.	11432.	1190.0	31.83
71.6	1689.	2400.	626.	11071.	1190.0	31.85
72.0	1806.	2524.	630.	10708.	1191.0	31.48
71.6	1851.	2610.	639.	10391.	1190.5	31.12
71.5	1994.	2801.	734.	9588.	1191.0	30.32

OUTPUT DATA FOR RUN 7

REFERRED FLOW RATE	VOLFLORATE CU.FT./SEC.	PTD-PTIG LB./SQ.FT.	PRESSURE RATIO	TORQUE FT.-LB.	OMEGA RAD./SEC.	3-STAGE EFFICIENCY
47.087	401.308	33.853	1.01587	115.260	124.721	0.94195
43.849	374.207	39.988	1.01874	125.983	124.616	0.94901
41.924	358.187	43.386	1.02033	129.267	124.606	0.95981
40.934	349.531	44.650	1.02093	131.138	124.595	0.95005
40.241	343.385	46.314	1.02171	131.886	124.574	0.96252
38.745	330.838	47.495	1.02226	131.886	124.637	0.95043
37.532	320.450	45.349	1.02125	129.309	124.669	0.89657
38.904	332.013	47.550	1.02228	132.301	124.616	0.95198
40.052	341.869	46.048	1.02158	132.384	124.616	0.94886
41.421	353.688	44.538	1.02087	130.847	124.721	0.96004
41.937	357.962	43.220	1.02026	129.350	124.669	0.95447
43.535	371.567	39.880	1.01869	126.025	124.721	0.93868

NON-DIMENSIONAL COEFFICIENTS FOR RUN 7

FLOW COEFFICIENT	3-STAGE EFFICIENCY	DEFLECTION COEFFICIENT	PRESSURE COEFFICIENT
0.5928	0.9420	0.2289	0.2156
0.5532	0.9490	0.2693	0.2556
0.5295	0.9598	0.2895	0.2779
0.5168	0.9501	0.3007	0.2857
0.5078	0.9625	0.3075	0.2960
0.4890	0.9504	0.3194	0.3035
0.4735	0.8966	0.3229	0.2895
0.4908	0.9520	0.3190	0.3037
0.5054	0.9489	0.3101	0.2943
0.5224	0.9600	0.2962	0.2844
0.5289	0.9545	0.2892	0.2761
0.5488	0.9387	0.2712	0.2546

Table C-9. Output of Program ONRETA, Run 7, Stator Stagger Angle = 31.8°

NAVAL POSTGRADUATE SCHOOL TURBOPROPULSION LABORATORY

O.N.R. 3-STAGE AXIAL COMPRESSOR, 3-STAGE EFFICIENCY

INPUT DATA FOR RUN 8 BAROMETRIC PRESSURE 30.01 AT 77.2 DEGREES,F.

ROTOR STAGGER ANGLE 42.8 STATOR STAGGER ANGLE 35.8

TEMP, DEG. F.	VELOCITY HEAD, COUNTS	PSTATIC, COUNTS	PTIG, COUNTS	DELP, COUNTS	TACHOMETER R.P.M.	TORQUEMETER POUNDS
74.9	2124.	2915.	795.	7550.	1192.0	25.80
75.1	2016.	2723.	710.	8384.	1192.0	27.06
76.0	1882.	2550.	665.	9122.	1191.5	28.27

OUTPUT DATA FOR RUN 8

REFERRED FLOW RATE	VOLFLORATE CU.FT./SEC.	PTO-PTIG LB./SQ.FT.	PRESSURE RATIO	TORQUE FT.-LB.	OMEGA RAD./SEC.	3-STAGE EFFICIENCY
44.832	383.855	31.403	1.01465	107.238	124.826	0.89788
43.669	373.969	34.872	1.01627	112.475	124.826	0.92550
42.186	361.569	37.941	1.01770	117.504	124.773	0.93184

NON-DIMENSIONAL COEFFICIENTS FOR RUN 8

FLOW COEFFICIENT	3-STAGE EFFICIENCY	DEFLECTION COEFFICIENT	PRESSURE COEFFICIENT
0.5665	0.8979	0.2233	0.2005
0.5519	0.9255	0.2406	0.2226
0.5338	0.9318	0.2605	0.2428

Table C-10. Output of Program ONRETA, Run 8, Stator Stagger Angle = 35.8°

NAVAL POSTGRADUATE SCHOOL TURBOPROPULSION LABORATORY

O.N.R. 3-STAGE AXIAL COMPRESSOR, 3-STAGE EFFICIENCY

INPUT DATA FOR RUN 9 BAROMETRIC PRESSURE 29.99 AT 76.2 DEGREES,F.

ROTOR STAGGER ANGLE 42.8 STATOR STAGGER ANGLE 35.8

TEMP, DEG. F.	VELOCITY HEAD, COUNTS	PSTATIC, COUNTS	PTIG, COUNTS	DELP, COUNTS	TACHOMETER R.P.M.	TORQUEMETER POUNDS
71.3	1611.	2359.	645.	10028.	1191.0	29.54
73.4	1599.	2156.	654.	10665.	1191.0	30.06
74.8	1503.	2044.	689.	11141.	1191.0	30.33
75.0	1405.	1928.	629.	11290.	1191.0	30.24
72.8	1357.	1861.	581.	11405.	1191.0	30.28
71.9	1211.	1665.	520.	10406.	1191.0	29.37
74.2	1356.	1866.	516.	11340.	1191.0	30.22
75.0	1405.	1933.	524.	11200.	1191.0	30.32
73.9	1505.	2056.	543.	11019.	1191.0	30.30
72.5	1589.	2191.	576.	10619.	1191.0	30.06
72.7	1775.	2416.	628.	9774.	1191.5	29.21
72.8	1891.	2564.	671.	9128.	1191.0	28.29

OUTPUT DATA FOR RUN 9

REFERRED FLOW RATE	VOLFLORATE CU.FT./SEC.	PTD-PTIG LB./SQ.FT.	PRESSURE RATIO	TORQUE FT.-LB.	OMEGA RAD./SEC.	3-STAGE EFFICIENCY
39.038	333.122	41.710	1.01947	122.783	124.721	0.90300
38.885	332.469	44.359	1.02071	124.944	124.721	0.94143
37.695	322.721	46.339	1.02164	126.067	124.721	0.94584
36.442	312.046	46.959	1.02192	125.693	124.721	0.92940
35.811	306.018	47.437	1.02214	125.859	124.721	0.91932
33.824	288.788	43.282	1.02020	122.076	124.721	0.81657
35.758	306.308	47.167	1.02201	125.609	124.721	0.91669
36.442	312.047	46.585	1.02174	126.025	124.721	0.91941
37.721	322.668	45.832	1.02139	125.942	124.721	0.93602
38.764	331.158	44.168	1.02062	124.944	124.721	0.93361
40.979	350.147	40.653	1.01898	121.411	124.773	0.93529
42.303	361.493	37.966	1.01773	117.587	124.721	0.93190

NON-DIMENSIONAL COEFFICIENTS FOR RUN 9

FLOW COEFFICIENT	3-STAGE EFFICIENCY	DEFLECTION COEFFICIENT	PRESSURE COEFFICIENT
0.4920	0.9030	0.2933	0.2649
0.4911	0.9414	0.3003	0.2827
0.4767	0.9458	0.3130	0.2960
0.4609	0.9294	0.3228	0.3000
0.4520	0.9193	0.3283	0.3018
0.4266	0.8166	0.3365	0.2748
0.4524	0.9167	0.3282	0.3009
0.4609	0.9194	0.3237	0.2976
0.4766	0.9360	0.3123	0.2923
0.4891	0.9336	0.3010	0.2810
0.5170	0.9353	0.2766	0.2587
0.5339	0.9319	0.2596	0.2419

Table C-11. Output of Program ONRETA, Run 9, Stator Stagger Angle = 35.8°

NAVAL POSTGRADUATE SCHOOL TURBOPROPULSION LABORATORY

O.N.R. 3-STAGE AXIAL COMPRESSOR, 3-STAGE EFFICIENCY

INPUT DATA FOR RUN 10 BAROMETRIC PRESSURE 29.88 AT 74.0 DEGREES,F.

ROTOR STAGGER ANGLE 42.8 STATOR STAGGER ANGLE 39.8

TEMP, DEG. F.	VELOCITY HEAD, COUNTS	PSTATIC, COUNTS	PTIG, COUNTS	DELP, COUNTS	TACHOMETER R.P.M.	TORQUEMETER POUNDS
72.0	2015.	2675.	430.	6986.	1193.0	23.62
73.0	1836.	2514.	361.	7579.	1193.0	24.82
71.9	1766.	2343.	370.	8483.	1191.0	26.17
72.9	1653.	2198.	324.	9138.	1191.0	27.06
72.5	1500.	2040.	296.	9794.	1191.0	27.84
72.5	1403.	1899.	298.	10304.	1191.0	28.28
73.2	1280.	1733.	258.	10858.	1190.5	28.50
73.5	1191.	1618.	250.	10931.	1190.0	28.32
73.7	1059.	1436.	228.	9504.	1191.0	27.48
73.4	1184.	1589.	243.	10914.	1190.5	28.12
73.2	1271.	1701.	256.	10756.	1191.5	28.35
72.6	1398.	1889.	279.	10408.	1191.5	28.32
73.5	1486.	2025.	314.	9814.	1191.5	27.89
71.9	1584.	2221.	341.	9203.	1192.0	27.13
72.3	1759.	2384.	376.	8380.	1192.0	26.00
72.6	1876.	2500.	383.	7708.	1192.5	25.02
72.0	1951.	2683.	401.	6860.	1193.0	23.42

OUTPUT DATA FOR RUN 10

REFERRED FLOW RATE	VOLFLOWRATE CU.FT./SEC.	PTO-PTIG LB./SQ.FT.	PRESSURE RATIO	TORQUE FT.-LB.	OMEGA RAD./SEC.	3-STAGE EFFICIENCY
43.759	373.648	29.057	1.01361	98.176	124.930	0.88247
41.763	356.945	31.524	1.01477	103.164	124.930	0.86985
40.952	349.654	35.304	1.01654	108.776	124.721	0.90605
39.615	338.553	38.008	1.01780	112.475	124.721	0.91285
37.731	322.333	40.737	1.01908	115.717	124.721	0.90485
36.486	311.694	42.858	1.02007	117.546	124.721	0.90598
34.844	297.865	45.162	1.02115	118.460	124.669	0.90524
33.607	287.372	45.466	1.02129	117.712	124.616	0.88514
31.685	270.982	39.530	1.01851	114.221	124.721	0.74800
33.507	286.491	45.395	1.02126	116.881	124.669	0.88693
34.720	296.807	44.738	1.02095	117.837	124.773	0.89753
36.420	311.165	43.290	1.02028	117.712	124.773	0.91186
37.554	321.242	40.820	1.01912	115.925	124.773	0.90170
38.760	331.108	38.278	1.01793	112.766	124.826	0.89593
40.873	349.106	34.855	1.01633	108.069	124.826	0.89815
42.215	360.672	32.060	1.01502	103.996	124.878	0.88694
43.058	367.669	28.533	1.01337	97.345	124.930	0.85979

NON-DIMENSIONAL COEFFICIENTS FOR RUN 10

FLOW COEFFICIENT	3-STAGE EFFICIENCY	DEFLECTION COEFFICIENT	PRESSURE COEFFICIENT
0.5510	0.8825	0.2096	0.1850
0.5263	0.8699	0.2311	0.2010
0.5165	0.9061	0.2487	0.2253
0.5001	0.9128	0.2662	0.2430
0.4761	0.9049	0.2875	0.2601
0.4604	0.9060	0.3020	0.2736
0.4401	0.9052	0.3191	0.2888
0.4248	0.8851	0.3289	0.2911
0.4003	0.7480	0.3378	0.2527
0.4233	0.8869	0.3274	0.2904
0.4382	0.8975	0.3182	0.2856
0.4594	0.9119	0.3029	0.2762
0.4743	0.9017	0.2896	0.2611
0.4887	0.8959	0.2722	0.2438
0.5152	0.8981	0.2475	0.2223
0.5321	0.8869	0.2305	0.2044
0.5422	0.8598	0.2113	0.1817

Table C-12. Output of Program ONRETA, Run 10, Stator Stagger Angle = 39.8°

NAVAL POSTGRADUATE SCHOOL TURBOPROPULSION LABORATORY

O.N.R. 3-STAGE AXIAL COMPRESSOR, 3-STAGE EFFICIENCY

INPUT DATA FOR RUN 11   BAROMETRIC PRESSURE 29.91 AT 74.1 DEGREES,F.

ROTOR STAGGER ANGLE 42.8   STATOR STAGGER ANGLE 44.3

TEMP, DEG. F.	VELOCITY HEAD, COUNTS	PSTATIC, COUNTS	PTIG, COUNTS	DELP, COUNTS	TACHOMETER R.P.M.	TORQUEMETER POUNDS
68.0	1841.	2469.	455.	6736.	1194.0	21.31
68.1	1730.	2331.	360.	7356.	1194.0	22.47
68.4	1628.	2200.	345.	8155.	1193.5	23.59
69.0	1504.	2023.	308.	8948.	1193.0	24.76
69.3	1373.	1871.	290.	9691.	1192.5	25.62
68.5	1256.	1708.	281.	10325.	1192.5	26.34
69.0	1144.	1548.	245.	10700.	1192.0	26.67
69.7	1020.	1380.	219.	11010.	1192.5	26.80
70.4	864.	1163.	210.	8725.	1192.0	25.08
72.2	1021.	1351.	201.	11015.	1192.0	26.59
71.4	1128.	1545.	250.	10665.	1192.5	26.64
71.6	1245.	1696.	253.	10246.	1192.5	26.15
68.4	1409.	1849.	288.	9728.	1192.0	25.62

OUTPUT DATA FOR RUN 11

REFERRED FLOW RATE	VOLFLORATE CU.FT./SEC.	PTC-PTIG LB./SQ.FT.	PRESSURE RATIO	TORQUE FT.-LB.	OMEGA RAD./SEC.	3-STAGE EFFICIENCY
41.797	355.552	28.017	1.01311	88.575	125.035	0.89674
40.512	344.653	30.596	1.01432	93.396	125.035	0.89965
39.294	334.391	33.919	1.01587	98.052	124.983	0.92163
37.762	321.531	37.218	1.01741	102.915	124.930	0.92631
36.074	307.250	40.308	1.01886	106.490	124.878	0.92629
34.498	293.595	42.945	1.02009	109.482	124.878	0.91694
32.918	280.292	44.505	1.02082	110.854	124.826	0.89602
31.078	264.797	45.794	1.02142	111.394	124.878	0.86624
28.597	243.818	36.290	1.01698	104.245	124.826	0.67664
31.092	265.544	45.815	1.02143	110.937	124.826	0.87290
32.687	278.955	44.359	1.02075	110.729	124.878	0.88949
34.346	293.163	42.617	1.01994	108.692	124.878	0.91513
36.543	310.981	40.462	1.01893	106.490	124.826	0.94161

NON-DIMENSIONAL COEFFICIENTS FOR RUN 11

FLOW COEFFICIENT	3-STAGE EFFICIENCY	DEFLECTION COEFFICIENT	PRESSURE COEFFICIENT
0.5238	0.8967	0.1968	0.1765
0.5078	0.8996	0.2142	0.1927
0.4929	0.9216	0.2321	0.2139
0.4741	0.9263	0.2538	0.2351
0.4533	0.9263	0.2751	0.2549
0.4331	0.9169	0.2956	0.2710
0.4137	0.8960	0.3139	0.2813
0.3906	0.8662	0.3342	0.2895
0.3598	0.6766	0.3396	0.2298
0.3919	0.8729	0.3336	0.2912
0.4115	0.8895	0.3164	0.2814
0.4325	0.9151	0.2956	0.2705
0.4569	0.9416	0.2715	0.2556

Table C-13. Output of Program ONRETA, Run 11, Stator Stagger Angle = 44.3°

APPENDIX D

DETAILS OF PREDICTION PROGRAM

This Appendix contains details concerning AXC03 which may be of interest to a limited number of readers. Table D-1 is a listing of the main program and the seven subroutines. Section D-1 is a description of the method of inserting data. Table D-2 is a sample of program output. The rewrite of input data, a sample of interstage data,and a sample summary of one case are included. Tables D-3 through D-16 are the summary printouts of the cases which were compared to measured performance of the machine. Table D-17 is a printout of program CHECK which verified the errors in the polynomials of subroutines THEORY and CASCAD.

D-1 Input Data

There is no limit to the number of cases which may be considered, since data are read in prior to execution for each case, and output printed prior to considering the next case. The executive routine reads input data and prints it before computation begins. The input data consists of thirteen cards per case.

Card 1:	NUM	case number (arbitrary)
(I7,	GAM	ratio of specific heats
4F7.3)	RN	referred speed (rpm/$\sqrt{^{o}R}$)
	WREM	initial referred flow rate (lbm$\sqrt{^{o}R}$/sec psia)
	DW	referred flow rate increment (lbm$\sqrt{^{o}R}$/sec psia)

Card 2:	LMAX	number of stages (3)
(I7,	ZETAI	loss coefficient of inlet duct
5F7.3)		(assumed 0.0)
	ZIGV	loss coefficient of inlet guide vanes
		(assumed 0.05)
	EGV	efficiency of exit guide vanes (assumed 0.85)
	ETD	efficiency of diffuser (assumed 1.0)
	EEX	efficiency of exit (assumed 1.0)
Card 3:	DIN	inlet pipe diameter, in.
(3F7.3,	DAV	average blade diameter, in.
4F7.1,	DOU	outlet pipe diameter, in.
3F7.3)	AEA	annulus area ahead of IGV, $in.^2$
	AIGV	annulus area after IGV, $in.^2$
	AGV	annulus area after EGV, $in.^2$
	ADI	diffuser exit area, $in.^2$
	ALE	inlet guide vane exit angle, degrees
	SMAX	maximum limit, $(i-i_{10})/\epsilon_{10}$, set by Fig. 29
	SMI	minimum limit, $(i-i_{10})/\epsilon_{10}$, set by Fig. 29
Card 4:	AAA	an array of annulus areas after rotor one,
(10F7.3)		stator one,....stator LMAX, $in.^2$
Card 5:	BH	an array of blade heights of rotor one....
(10F7.3)		stator LMAX, in.
Card 6:	BLOCK	an array of blockage factors for rotor one....
(10F7.3)		stator LMAX (assumed 1.0)
Card 7:	WDO	an array of work done factors for stage one....
(10F7.3)		stage LMAX (assumed 1.0)

Card 8:	BLDR	number of blades in the row
(Rotor	CAMR	camber angle, degrees
data)	STAGR	stagger angle, degrees
(9F7.3)	SHR	shape correction factor, (1.0)
	THR	thickness to chord ratio
	CHR	blade chord length, in.
	DIAR	mean blade diameter, in.
	DER	tip clearance, in
	CDR	minimum profile drag coefficient (assumed various)
Card 9:	BLDS	number of blades in the row
(Stator	CAMS	camber angle, degrees
data)	STAGS	stagger angle, degrees
(9F7.3)	SHS	shape correction factor (1.0)
	THS	thickness to chord ratio
	CHS	blade chord length, in.
	DIAS	blade mean diameter, in.
	DES	tip clearance, in.
	CDS	minimum profile drag coefficient (assumed various)

Cards 10 and 12 are duplicates of 8

Cards 11 and 13 are duplicates of 9

```
FORTRAN IV G LEVEL 0, MOD 0                MAIN              DATE = 67224           00/08/30                 PAGE 000

0001          DIMENSION AAA(2,15),BH(2,15),BLOCK(2,15),WDO(15),BLDR(15),BLDS(15)00000005
             1,CAMR(15),CAMS(15),STAGR(15),STAGS(15),SHR(15),SHS(15),THR(15),THS00000006
             2(15),CHR(15),CHS(15),DIAR(15),DIAS(15),DER(15),DES(15),CDR(15),CDS00000007
             3(15),FLOW(30),RATIO(30),DETA(30),POCO(30),BLETA(30),ITITLE(12),LAB00000008
             4EL(5),X(30),Y(30),XY(30),STAPR(30),STAETA(30)                     10000008
        C       USES ORIGINAL DATA OF HOWELL BETWEEN CD=0.02 AND 0.04          10000001
        C CALCULATES PERFORMANCE MAP OF AXIAL COMPRESSORS AT SPECIFIED REFERRED 00000002
        C SPEEDS BASED ON CASCADE DATA CALCULATED FROM BLADING GEOMETRY  - USES 00000003
        C NACA DATA (NACA SP-36 CHAP 6) AND DATA FROM HOWELL                   00000004
0002     3002 READ(5,700,END=3001)(NUM,GAM,RN,WREM,DW)                           0    11
0003          READ(5,701)(LMAX,ZETAI,ZIGV,EGV,ETD,EEX)                          00000012
0004          READ(5,713)(DIN,DAV,DOU,AEA,AIGV,AGV,ADI,ALE,SMAX,SMI)            00000013
0005          READ(5,703)((AAA(J,I),J=1,2),I=1,LMAX)                            00000014
0006          READ(5,703)((BH(J,I),J=1,2),I=1,LMAX)                             00000015
0007          READ(5,703)((BLOCK(J,I),J=1,2),I=1,LMAX)                          00000016
0008          READ(5,703)(WDO(I),I=1,LMAX)                                      00000017
0009          DO 1 K=1,LMAX                                                     00000018
0010          READ(5,702)(BLDR(K),CAMR(K),STAGR(K),SHR(K),THR(K),CHR(K),DIAR(K),00000019
             1DER(K),CDR(K))                                                    00000020
0011          READ(5,702)(BLDS(K),CAMS(K),STAGS(K),SHS(K),THS(K),CHS(K),DIAS(K),00000021
             1DES(K),CDS(K))                                                    00000022
0012        1 CONTINUE                                                          00000023
0013          WRITE(6,750)(NUM)                                                 00000024
0014          WRITE(6,751)(NUM,GAM,RN,WREM,DW)                                  00000025
0015          WRITE(6,752)(LMAX,ZETAI,ZIGV,EGV,ETD,EEX)                         00000026
0016          WRITE(6,753)(DIN,DAV,DOU,AEA,AIGV,AGV,ADI,ALE,SMAX,SMI)           00000027
0017          WRITE(6,754)                                                      00000028
0018          WRITE(6,714)((AAA(J,I),J=1,2),I=1,LMAX)                           00000029
0019          WRITE(6,755)                                                      00000030
0020          WRITE(6,703)((BH(J,I),J=1,2),I=1,LMAX)                            00000031
0021          WRITE(6,756)                                                      00000032
0022          WRITE(6,703)((BLOCK(J,I),J=1,2),I=1,LMAX)                         00000033
0023          WRITE(6,757)                                                      00000034
0024          WRITE(6,703)(WDO(I),I=1,LMAX)                                     00000035
0025          DO 20 K=1,LMAX                                                    00000036
0026          IF(1-K) 22,23,23                                                  00000037
0027       22 KL=KL+1                                                           00000038
0028          WRITE(6,758)(KL,K)                                                00000043
0029          GO TO 28                                                          00000044
0030       23 KL=K+7                                                            00000046
0031          WRITE(6,761)(KL,K)                                                00000047
0032       28 WRITE(6,702)(BLDR(K),CAMR(K),STAGR(K),SHR(K),THR(K),CHR(K),DIAR(K)00000048
             1,DER(K),CDR(K))                                                   00000049
0033          KL=KL+1                                                           00000050
0034          WRITE(6,759)(KL,K)                                                00000051
0035          WRITE(6,702)(BLDS(K),CAMS(K),STAGS(K),SHS(K),THS(K),CHS(K),DIAS(K)00000052
             1,DES(K),CDS(K))                                                   00000053
0036       20 CONTINUE                                                          00000054
```

Table D-1. Listing of Program AXC03

```
      AGV=AGV*BLOCK(2,LMAX)                                             00000055
      EXP1=GAM/(GAM-1.)                                                 00000056
      EXP2=(GAM-1.)/GAM                                                 00000057
      C=2.*32.174*53.346*EXP1                                           00000058
      B=1./C                                                            00000059
      RAG=SQRT (53.346/32.174)                                          00000060
      UAV=RN*DAV*3.14159/720.                                           00000061
      MMM=1                                                             10000061
      WRE=WREM                                                          00000062
    3 WRITE(6,704)(NUM,RN,GAM,UAV)                                      00000063
      AA=3.14159*DIN*DIN/4.                                             00000064
      CALL PREX(WRE,1.,1.,0.,AA,GAM,RAG,C,XXX,PIN,XXY,XXZ)              00000065
      CALL PREX(WRE,1.,PIN,ZETAI,AEA,GAM,RAG,C,YXX,YXY,PTE,YXZ)         00000066
      A=AIGV*COS (ALE/57.29578)                                         00000067
      CALL PREX(WRE,1.,PTE,ZIGV,A,GAM,RAG,C,TSIG,PSIG,PTIG,VE)          00000068
      AL3=ALE/57.29578                                                  00000069
      VA1=VE*COS (AL3)                                                  00000070
      WRITE(6,763)(YXX,YXY,VA1,VE)                                      00000071
      TS1=TSIG                                                          00000072
      TT1=1.                                                            00000073
      PS1=PSIG                                                          00000074
      PT1=PTIG                                                          00000075
      L=1                                                               00000076
    4 I=1                                                               00000077
      BLOK=BLOCK(I,L)                                                   00000078
      A2=AAA(I,L)                                                       00000079
      HR=BH(I,L)                                                        00000080
      WODO=WDO(L)                                                       00000081
      DD=DIAR(L)                                                        00000082
      BLD=BLDR(L)                                                       00000083
      CAM=CAMR(L)                                                       00000084
      STAG=STAGR(L)                                                     00000085
      RSTAG=STAG                                                        10000085
      SH=SHR(L)                                                         00000086
      TH=THR(L)                                                         00000087
      CH=CHR(L)                                                         00000088
      DE=DER(L)                                                         00000089
      CD=CDR(L)                                                         00000090
      CALL ROTOR(WRE,DD,BLOK,A2,HR,WODO,BLD,CAM,STAG,SH,TH,CH,DE,VA1,AL300000091
     1,TS1,TT1,PS1,PT1,CD,B,EXP1,RN,L,SMAX,SMI,BE2,VA2,TS2,TT2,PS2,M,NCA00000092
     2SF)                                                               10000092
      WRITE(6,764)(TT2,PT1)                                             00000093
      GO TO (5,8,10),M                                                  00000094
    5 I=2                                                               00000095
      BLOK=BLOCK(I,L)                                                   00000096
      A3=AAA(I,L)                                                       00000097
      HS=BH(I,L)                                                        00000098
      DD=DIAS(L)                                                        00000099
```

Table D-1. Listing of Program AXC03 (cont.)

```
0083             BLD=BLDS(L)                                                    00000100
0084             CAM=CAMS(L)                                                    00000101
0085             STAG=STAGS(L)                                                  00000102
0086             SSTAG=STAG                                                     10000102
0087             SH=SHS(L)                                                      00000103
0088             TH=THS(L)                                                      00000104
0089             CH=CHS(L)                                                      00000105
0090             DE=DES(L)                                                      00000106
0091             CD=CDS(L)                                                      00000107
0092             CALL STATOR(WRE,DD,BLOK,A3,HS,WODO,BLD,CAM,STAG,SH,TH,CH,DE,VA2,BE00000108
                12,TS2,PS2,CD,B,EXP1,RN,L,SMAX,SMI,AL3,VA3,TS3,PS3,PT3,K,NCASE) 00000109
0093             WRITE(6,764)(TT2,PT3)                                          00000110
0094             GO TO (6,9,11),K                                               00000111
0095           6 L=L+1                                                          00000112
0096             IF(L-LMAX) 7,7,12                                              00000113
0097           7 VA1=VA3                                                        00000114
0098             TS1=TS3                                                        00000115
0099             TT1=TT2                                                        00000116
0100             PS1=PS3                                                        00000117
0101             PT1=PT3                                                        00000118
0102             GO TO 4                                                        00000119
0103           8 WRITE(6,711)                                                   00000120
0104             WRITE(6,705)(WRE,L)                                            00000121
0105             WRE=WRE+DW                                                     00000122
0106             GO TO 3                                                        00000123
0107           9 WRITE(6,711)                                                   00000124
0108             WRITE(6,706)(WRE,L)                                            00000125
0109             WRE=WRE+DW                                                     00000126
0110             GO TO 3                                                        00000127
0111          10 WRITE(6,711)                                                   00000128
0112             WRITE(6,707)(WRE,L)                                            00000129
0113             GO TO 2000                                                     00000130
0114          11 WRITE(6,711)                                                   00000131
0115             WRITE(6,707)(WRE,L)                                            00000132
0116             GO TO 2000                                                     00000133
0117          12 ACU=3.14159*DOU*DOU/4.                                         00000134
0118             ZEX=1.-EEX                                                     00000135
0119             CALL PRCO(WRE,TT2,TS3,PS3,EGV,AGV,GAM,RAG,C,PSEG,XXX,PTEG,TSEG) 00000136
0120             WRITE(6,709)(TSEG,PSEG)                                        00000137
0121             WRITE(6,764)(TT2,PTEG)                                         00000138
0122             CALL PRCO(WRE,TT2,TSEG,PSEG,ETD,ADI,GAM,RAG,C,PSEX,XXX,PTEX,TSEX) 00000139
0123             WRITE(6,712)(TSEX,PSEX)                                        10000139
0124             WRITE(6,764)(TT2,PTEX)                                         20000139
0125             PRATS3=PT3/PTIG                                                30000139
0126             ETAST3=(PRATS3**EXP2-1.)/(TT2-1.)                              40000139
0127             ETAB=((PTEG/PTE)**EXP2 - 1.)/(TT2-1.)                          00000140
0128             ETT=(PTEX**EXP2 -1.)/(TT2-1.)                                  00000141
0129             AM=WRE*53.346*(TT2-1.)*1.055*GAM/((GAM-1.)*778.16)             00000142
```

Table D-1. Listing of Program AXC03 (cont.)

```
0130          WRITE(6,711)                                                      00000143
0131          WRITE(6,710)(WRE,PTEX,ETT,AM,ETAB,PRATS3,ETAST3)                  00000144
0132          FLOW(MMM)=WRE                                                     10000144
0133          RATIO(MMM)=PTEX                                                   20000144
0134          OETA(MMM)=ETT                                                     30000144
0135          POCO(MMM)=AM                                                      40000144
0136          BLETA(MMM)=ETAB                                                   50000144
0137          STAPR(MMM)=PRATS3                                                 51000144
0138          STAETA(MMM)=ETAST3                                                52000144
0139          MMM=MMM+1                                                         60000144
0140          WRE=WRE+DW                                                        00000145
0141          GO TO 3                                                           00000146
0142      700 FORMAT(I7,4F7.3)                                                  00000147
0143      701 FORMAT(I7,5F7.3)                                                  00000148
0144      702 FORMAT(9F7.3)                                                     00000149
0145      703 FORMAT(10F7.3)                                                    00000150
0146      713 FORMAT(3F7.3,4F7.1,3F7.3)                                         10000150
0147      704 FORMAT(1H1,38X,39HCALCULATED AXIAL COMPRESSOR PERFORMANCE//40X,   00000151
         1//8H RUN NO.I4,9X,16HREFERRED SPEED =F7.4,9X,7HGAMMA =F6.3,9X,35HA00000152
         2VERAGE PERIPHERAL VELOCITY RATIO =F7.4//51X,15HINTERSTAGE DATA//1100000153
         35H BLADE  INLET INLET AXIAL INLET  OUT  ROTOR BLADE INLET  OUT   C00000154
         4DP   CDP  REFERENCE REFERENCE    ACTUAL    STALLING/116H  ROW   TE00000155
         5MP. PRES. VELOC VELOC VELOC VELOC EFFIC ANGLE ANGLE  MIN  RATIO IN00000156
         6CIDENCE DEFLECTION DEFLECTION DEFLECTION//)                       00000157
0148      705 FORMAT(F8.3,5X,18HSURGE IN ROTOR NO.I3)                           00000158
0149      706 FORMAT(F8.3,5X,19HSURGE IN STATOR NO.I3)                          00000159
0150      707 FORMAT(F8.3,5X,26HMIN. PRESSURE IN ROTOR NO.I3)                   00000160
0151      708 FORMAT(F8.3,5X,27HMIN. PRESSURE IN STATOR NO.I3)                  00000161
0152      709 FORMAT(6H  EGV ,2F6.2)                                            00000162
0153      710 FORMAT(F8.3,F13.5,F10.4,F15.5,F12.4,F13.5,F13.4)                  00000163
0154      711 FORMAT(2X,///86H REFERRED    PRESSURE    OVERALL        POWER     00000164
         1  BLADING       3-STAGE       3-STAGE/88H FLOW RATE    RATIO     EF00000165
         2FICIENCY   COEFFICIENT  EFFICIENCY  PRESSURE RATIO  EFFICIENCY//) 00000166
0155      712 FORMAT(6H  DIFF,2F6.2)                                            00000167
0156      714 FORMAT(10F7.2)                                                    2     167
0157      750 FORMAT(1H1,14X,39HCALCULATED AXIAL COMPRESSOR PERFORMANCE/26X,21HI00000168
         1NPUT DATA OF RUN NO.I4//)                                         00000169
0158      751 FORMAT(2X,6HCARD 1//I7,4F7.3//)                                   00000170
0159      752 FORMAT(2X,6HCARD 2//I7,5F7.3//)                                   00000171
0160      753 FORMAT(2X,6HCARD 3//3F7.3,4F7.1,3F7.3//)                          00000172
0161      754 FORMAT(2X,22HCARD 4   ANNULUS AREAS//)                            00000173
0162      755 FORMAT(2X,//2X,22HCARD 5   BLADE HEIGHTS//)                       00000174
0163      756 FORMAT(2X,//2X,25HCARD 6   BLOCKAGE FACTORS//)                    00000175
0164      757 FORMAT(2X,//2X,26HCARD 7   WORK-DONE FACTORS//)                   00000176
0165      758 FORMAT(2X,//2X, 4HCARD,I3,3X,18HROTOR DATA   STAGE,I3//)          00000177
0166      759 FORMAT(2X,//2X,4HCARD,I3,3X,19HSTATOR DATA   STAGE,I3//)          00000178
0167      761 FORMAT(1H1,//2X,4HCARD,I3,3X,18HROTOR DATA   STAGE,I3//)          00000179
0168      762 FORMAT(I7)                                                        00000180
```

Table D-1. Listing of Program AXC03 (cont.)

```
0169          763 FORMAT(6H  IGV ,2F6.2,F7.2,6X,F6.2)                             00000181
0170          764 FORMAT(6X2F6.2,2X,25H(TOTAL OUTLET CONDITIONS))                 00000182
0171          765 FORMAT(1H1,34X,53HCALCULATED AXIAL COMPRESSOR PERFORMANCE, OVERALL10000182
                 1 DATA//8H RUN NO.I4,9X,16HREFERRED SPEED =F7.4,9X,7HGAMMA =F6.3,9X20000182
                 2,35HAVERAGE PERIPHERAL VELOCITY RATIO =F7.4//)                  30000182
0172          7660FORMAT(20X,22HROTOR STAGGER ANGLE = ,F5.2,15X,23HSTATOR STAGGER AN31000182
                 1GLE = ,F5.2//)                                                  32000182
0173         2000 WRITE(6,765)(NUM,RN,GAM,UAV)                                    40000182
0174              WRITE(6,766)(RSTAG,SSTAG)                                       41000182
0175              WRITE(6,711)                                                    51000182
0176              NNN=MMM-1                                                       60000182
0177              DO 911 I=1,NNN                                                  70000182
0178              X(I)= FLOW(I)                                                   80000182
0179              Y(I)= RATIC(I)                                                  90000182
0180              XY(I)=OETA(I)                                                   11000182
0181          911 WRITE(6,710)(FLOW(I),RATIO(I),OETA(I),POCO(I),BLETA(I),STAPR(I),ST12000182
                 1AETA(I))                                                        13000182
0182         3000 GO TO 3002                                                      00000183
0183         3001 RETURN                                                          00000184
0184              END                                                             00000184
```

Table D-1. Listing of Program AXC03 (cont.)

```
0001             SUBROUTINE RCTOR(W,DD,BLOK,A2,HR,WO,BL,CA,ST,SH,TH,CH,DE,VA1,AL3, 00000185
                1TS1,TT1,PS1,PT1,CD,B,EXP1,RN,L,SMA,SMI,BE2,VA2,TS2,TT2,PS2,M,NCASE00000186
                2)                                                                 10000186
           C CALCULATES CONDITICNS AT ROTOR DISCHARGE                              00000187
0002             U=RN*DD*3.14159/720.                                              00000188
0003             WU1=U-VA1*TAN(AL3)                                                00000189
0004             BE1=ATAN(WU1/VA1)                                                 00000190
0005             ANG=BE1*57.29578                                                  00000191
0006             SO=CH*BL/(3.14159*DD)                                             00000192
0007             CALL THEORY(TH,SH,CA,ST,SO,STARI,STARD,BETA,ASTAR,DFSTAR)         00000193
0008             CALL CASCAD(STARI,STARD,DFSTAR,BETA,CA,ASTAR,ANG,SO,SMA,SMI,ALG,R,00000194
                1DFACT,DFMAX,N,NCASE)                                              00000195
0009             GO TO (400,405,405),N                                             00000196
0010         400 XX=VA1                                                            00000197
0011             BE2=ALG/57.29578                                                  00000198
0012             BE2=ATAN((1.-WO)*TAN(BE1)+WO*TAN(BE2))                            00000199
0013             ALG=BE2*57.29578                                                  00000200
0014             KK=1                                                              00000201
0015         401 CALL ETACAL(CD,R,BE1,BE2,VA1,XX,SO,HR,DE,CH,ETAR)                 00000202
0016             W1=VA1/COS(BE1)                                                   00000203
0017             W2=XX/COS(BE2)                                                    00000204
0018             D=B*(W1*W1-W2*W2)                                                 00000205
0019             TS2=TS1+D                                                         00000206
0020             TT2=TT1+2.*B*U*(WU1-XX*TAN(BE2))                                  00000207
0021             PS2=PS1*(1.+ETAR*D/TS1)**EXP1                                     00000208
0022             RA=53.346                                                         00000209
0023             VA2=W*TS2*RA/(A2*BLOK*PS2)                                        00000210
0024             XX=VA2                                                            00000211
0025             GO TO (450,450,450,450,450,403),KK                                00000212
0026         450 KK=KK+1                                                           00000213
0027             GO TO 401                                                         00000214
0028         403 WRITE(6,404)(L,TS2,PS2,VA2,W1,W2,U,ETAR,ANG,ALG,CD,R,STARI,DFSTAR,00000215
                1DFACT,DFMAX)                                                      00000216
0029         404 FORMAT(3H  R,I3,2F6.2,F7.2,3F6.2,F6.3,2F6.2,2F6.3,F8.3,2F11.3,F10.00000217
                13)                                                                00000218
0030         405 M=N                                                               00000219
0031             RETURN                                                            00000220
0032             END                                                               00000221
```

Table D-1. Listing of Program AXCO3 (cont.)

```
FORTRAN IV G LEVEL 0, MOD 0              STATOR              DATE = 67224          00/08/30                PAGE 0001

0001              SUBROUTINE STATOR(W,DD,BLOK,A3,HS,WO,BL,CA,ST,SH,TH,CH,DE,VA2,BE2,
                 1TS2,PS2,CD,B,EXP1,RN,L,SMA,SMI,AL3,VA3,TS3,PS3,PT3,K,NCASE)
            C CALCULATES CONDITIONS AT STATOR DISCHARGE
0002              U=RN*DD*3.14159/720.
0003              VU2=U-VA2*TAN(BE2)
0004              AL2=ATAN(VU2/VA2)
0005              AMG=AL2*57.29578
0006              SO=CH*BL/(3.14159*DD)
0007              CALL THEORY(TH,SH,CA,ST,SO,STARI,STARD,BETA,ASTAR,DFSTAR)
0008              CALL CASCAD(STARI,STARD,DFSTAR,BETA,CA,ASTAR,AMG,SO,SMA,SMI,AKG,R,
                 1DFACT,DFMAX,N,NCASE)
0009              GO TO (600,605,605),N
0010          600 XX=VA2
0011              AL3=AKG/57.29578
0012              AL3=ATAN((1.-WO)*TAN(AL2)+WO*TAN(AL3))
0013              AKG=AL3*57.29578
0014              KK=1
0015          601 CALL ETACAL(CD,R,AL2,AL3,VA2,XX,SO,HS,DE,CH,ETAS)
0016              V2=VA2/COS(AL2)
0017              V3=XX/COS(AL3)
0018              D=B*(V2*V2-V3*V3)
0019              PS3=PS2*(1.+ETAS*D/TS2)**EXP1
0020              TS3=TS2+D
0021              PT3=PS3*(1.+B*V3*V3/TS3)**EXP1
0022              RA=53.346
0023              VA3=W*TS3*RA/(A3*BLOK*PS3)
0024              XX=VA3
0025              GO TO (650,650,650,650,650,603),KK
0026          650 KK=KK+1
0027              GO TO 601
0028          603 WRITE(6,604)(L,TS3,PS3,VA3,V2,V3,U,ETAS,AMG,AKG,CD,R,STARI,DFSTAR,
                 1DFACT,DFMAX)
0029          604 FORMAT(3H  S,I3,2F6.2,F7.2,3F6.2,F6.3,2F6.2,2F6.3,F8.3,2F11.3,F10.
                 13)
0030          605 K=N
0031              RETURN
0032              END
```

Table D-1. Listing of Program AXCO3 (cont.)

```
0001            SUBROUTINE THEORY(TH,SH,CA,ST,SO,SI,SD,BET,AS,DFS)                     00000259
          C                                                                             00000260
          C CALCULATES MINIMUM LOSS CONDITIONS OF COMPRESSOR CASCADES USING THE        00000261
          C METHOD OF LIEBLEIN  -  NACA SP-36  CHAP.  VI                                00000262
          C                                                                             00000263
          C                                                                             00000264
          C ZERO-CAMBER INCIDENCE VS SOLIDITY AND ALPHA 1  FIG 137                      00000265
          C                                                                             00000266
0002            FIGAF(A,S)=0.96195E-02- 0.21961E-01*S+0.10963E-01*S*S-0.42930E-02*00000267
               1A+0.85403E-01*A*S-0.34503E-02*A*S*S+0.27923E-04*A*A-0.64301E-04*A*00000268
               2A*S+0.32138E-04*A*A*S*S                                                 00000269
          C                                                                             00000270
          C THICKNESS CORRECTION FACTOR (INCIDENCE) VS THICKNESS-CHORD RATIO F 14200000271
          C                                                                             00000272
0003            FIGBF(TH)=0.03472777+17.891945*TH-118.09901*TH*TH+429.53472*TH**3-00000273
               1685.43011*TH**4                                                        00000274
          C                                                                             00000275
          C SLOPE FACTOR N (INCIDENCE) VS SOLIDITY AND ALPHA 1   FIG 138                00000276
          C                                                                             00000277
0004            FIGCF(A,S)=-0.11890+0.21192*S-0.17854*S*S+0.57160E-01*S*S*S-0.368700000278
               13E-02*A-0.76207E-04*A*S+0.18208E-02*A*S*S-0.55334E-03*A*S*S*S-0.360000000279
               2825E-04*A*A+0.66620E-04*A*A*S+0.16243E-04*A*A*S*S-0.22671E-04*A*A*00000280
               3S*S*S-0.72311E-07*A*A*A-0.54986E-06*A*A*A*S-0.49472E-06*A*A*A*S*S+00000281
               40.37471E-06*A*A*A*S*S*S                                                 00000282
          C                                                                             00000283
          C ZERO-CAMBER DEVIATION VS SOLIDITY AND ALPHA 1   FIG 161                     00000284
          C                                                                             00000285
0005            FIGDF(A,S)=-0.017896+0.10058*S-0.14687*S*S+0.58557E-01*S*S*S-0.11900000286
               187E-01*A+0.65167E-01*A*S-0.44822E-01*A*S*S+0.11478E-01*A*S*S*S-0.200000287
               24947E-03*A*A+0.66468E-03*A*A*S-0.94528E-03*A*A*S*S+0.28823E-03*A*A00000288
               3*S*S*S+0.67269E-05*A*A*A-0.17987E-04*A*A*A*S+0.25862E-04*A*A*A*S*S00000289
               4-0.77546E-05*A*A*A*S*S*S                                                00000290
          C                                                                             00000291
          C THICKNESS CORRECTION FACTOR (DEVIATION) VS THICKNESS-CHORD RATIO F 17200000292
          C                                                                             00000293
0006            FIGEF(TH)=0.1169385+2.6167113*TH+70.722724*TH*TH-85.664637*TH**3   00000294
          C                                                                             00000295
          C SLOPE FACTOR M (DEVIATION) VS SOLIDITY AND ALPHA 1   FIG 168                00000296
          C                                                                             00000297
0007            FIGGF(A,S)=1.06850-1.68830*S+1.15690*S*S-0.28879*S*S*S+0.36581E-0300000298
               1*A-0.19185E-02*A*S+0.36235E-02*A*S*S-0.13993E-02*A*S*S*S-0.57353E-00000299
               205*A*A+0.11329E-03*A*A*S-0.19416E-03*A*A*S*S+0.74911E-04*A*A*S*S*S00000300
               3-0.16187E-06*A*A*A-0.79239E-06*A*A*A*S+0.22558E-05*A*A*A*S*S-0.99200000301
               418E-06*A*A*A*S*S*S                                                      00000302
          C                                                                             00000303
0008            BET=ST + 0.5*CA                                                         00000304
0009            CTHK=FIGBF(TH)                                                          10000304
0010            SIP=2.0                                                                 20000304
```

Table D-1. Listing of Program AXC03 (cont.)

```
0011          201 A=BET+SIP                                                    00000305
0012              DENCE=FIGAF(A,SO)                                            00000306
0013              SLOPN=FIGCF(A,SO)                                            00000307
            C     CALCULATE SI AND COMPARE TO SIP UNTIL WITHIN 0.02 DEGREE     00000308
0014              SI=DENCE*SH*CTHK + SLOPN*CA                                  00000309
0015              CHEC=ABS (SI-SIP)                                            10000309
0016              IF(CHEC-0.02)2C3,203,202                                     20000309
0017          202 SIP=SI                                                       30000309
0018              GO TO 201                                                    40000309
0019          203 CEVAT=FIGDF(A,SO)                                            00000310
0020              DTHK=FIGEF(TH)                                               00000311
0021              SLOPM=FIGGF(A,SO)                                            00000312
0022              SD=DEVAT*SH*DTHK + SLOPM*CA                                  00000313
0023              AS = A                                                       00000314
0024              DFS=CA+SI-SD                                                 00000315
0025              RETURN                                                       00000316
0026              END                                                          00000317
```

Table D-1. Listing of Program AXCO3 (cont.)

```
      SUBROUTINE CASCAD(SI,SD,DFS,BET,CA,AS,A,SO,SMA,SMI,AA,R,DFF,DFMAX,
     1N,NCASE)
C
C CALCULATES CASCADE PERFORMANCE DATA FOR COMPRESSOR BLADING USING
C THE METHOD OF LIEBLEIN (NACA SP-36  CHAP 6
C
C SLOPE FACTOR (DI/DD)* VS SOLIDITY AND ALPHA 1   FIG 177
C
C   CAUTION  THIS POLYNOMIAL GENERATED FOR SOLIDITIES FROM 0.6 TO 1.4
C
     OFIGHF(A,S)=.81324E+00-.17818E+01*S+.13558E+01*S*S-.35174E+00*S*S*S
     1-.40846E-02*A+.18322E-01*A*S-.21692E-01*A*S*S+.76075E-02*A*S*S*S+.
     218174E-03*A*A-.83518E-03*A*A*S+.10421E-02*A*A*S*S-.38235E-03*A*A*S
     3*S*S-.94842E-06*A*A*A+.86041E-05*A*A*A*S-.12163E-04*A*A*A*S*S+.467
     421E-05*A*A*A*S*S*S
C
      SLOPD=FIGHF(AS,SO)
      DI=A-BET
      DEV=SD+(DI-SI)*SLOPD
      DF=CA+DI-DEV
      Z=DF/DFS
      X=(DI-SI)/DFS
      DFMAX=DFS/0.80
      IF(X) 300,300,301
  300 IF(X-SMI) 302,303,303
  302 N=3
      RETURN
  301 IF(X-SMA) 303,303,304
  304 N=2
      RETURN
  303 IF(X-0.10) 305,306,306
  305 DELZ=0.
      GO TO 307
  306 DELZ=0.0250-0.3250*X+1.750*X**2
  307 Y=Z-DELZ
      DFF=Y*DFS
      AA=A-DFF
      R = 1.0034396+0.01430105*X+2.8807456*X**2-0.19234646*X**3+4.422982
     10*X**4+22.349047*X**5+21.533222*X**6
      N=1
      RETURN
      END
```

Table D-1. Listing of Program AXCO3 (cont.)

```
FORTRAN IV G LEVEL 0, MOD C          ETACAL          DATE = 67224          00/08/30          PAGE 0001

0001          SUBROUTINE ETACAL(CD,R,ALI,ALE,VI,VE,SO,H,DE,CH,ETA)
           C CALCULATES EFFICIENCY OF ROTOR OR STATOR
0002          AI=VI*TAN(ALI)
0003          AE =VE*TAN(ALE)
0004          D=AI-AE
0005          VU= SQRT(((AI+AE)/2.)**2+((VI+VE)/2.)**2)
0006          CL=2.*D/(SO*VU)
0007          E=CD*R/CL+.04*CL*CH/H+.25*CL*DE/(H* COS(ALE))+ .018 * CH/(CL*H)
0008          T=(AI+AE)/(VI+VE)
0009          ETA=(1.-E/T)/(1.+E*T)
0010          RETURN
0011          END
```

Table D-1. Listing of Program AXC03 (cont.)

```
FORTRAN IV G LEVEL 0, MOD 0          PREX          DATE = 67224          00/08/30          PAGE 0001

      SUBROUTINE PREX(W,TTI,PTI,Z,A,GAM,RAG,C,TSE,PSE,PTE,VE)
C CALCULATES PRESSURE DROP IN CHANNEL FOR FLOW WITH FRICTION
      EN=GAM/(1.+Z*(GAM-1.) )
      EX1=2./EN
      EX2=(EN+1.)/EN
      EX3=(EN-1.)/EN
      PHI=W*SQRT (TTI)*RAG/(PTI*A)
      PRA=1.
      KM=1
  100 PH2=SQRT ((2.*GAM/(GAM-1.))* (PRA**EX1-PRA**EX2))
      GO TO (101,104),KM
  101 IF(PH2-PHI)102,106,103
  102 PRA=PRA-.001
      GO TO 100
  103 KM=2
  104 IF(PH2 -PHI)106,106,105
  105 PRA=PRA+.0001
      GO TO 100
  106 TSE=TTI*PRA**EX3
      VE=SQRT (C*(TTI-TSE))
      PSE=PRA*PTI
      PTE=PSE/(PRA**(1.-Z))
      RETURN
      END
```

Table D-1. Listing of Program AXC03 (cont.)

```
      SUBROUTINE PRC0(W,TTI,TSI,PSI,E,A,GAM,RAG,C,PSE,VE,PTE,TSE)
C CALCULATES PRESSURE RISE IN DIFFUSOR FOR FLOW WITH FRICTION
      EN=GAM*E/(1.-GAM*(1.-E))
      EX1=2./EN
      EX2=(EN+1.)/EN
      PHI=W*SQRT (TSI)*RAG/(PSI*A)
      PRA=1.
      KM=1
  500 PH2=SQRT ((2.*GAM/(GAM-1.))*((TTI/TSI)*PRA**EX1-PRA**EX2))
      GO TO (501,504),KM
  501 IF(PHI-PH2)502,506,503
  502 PRA=PRA+.001
      GO TO 500
  503 KM=2
  504 IF(PHI-PH2)506,506,505
  505 PRA=PRA-.00005
      GO TO 500
  506 PSE=PRA*PSI
      TSE=TSI*PRA**((EN-1.)/EN)
      VE=SQRT (C*(TTI-TSE))
      PRE=(TTI/TSE)**(GAM/(GAM-1.))
      PTE=PRE*PSE
      RETURN
      END
```

Table D-1. Listing of Program AXC03 (cont.)

```
                 CALCULATED AXIAL CCMPRESSOR PERFORMANCE
                       INPUT DATA OF RUN NO.    1

 CARD 1
     1  1.400 52.474 4C.000  0.500

 CARD 2
     3  0.0     0.050  C.850  1.00C  1.000

 CARD 3
36.000 28.800 36.000  651.0  651.C  651.0 1017.0 19.500  0.400 -0.510

 CARD 4   ANNULUS AREAS

651.0C 651.00 651.00 651.00 651.0C 651.00

 CARD 5   BLADE HEIGHTS

 7.20C  7.200  7.20C  7.200  7.20C  7.200

 CARD 6   BLOCKAGE FACTORS

 1.00C  1.000  1.000  1.000  1.00C  1.000

 CARD 7   WORK-DONE FACTCRS

 1.00C  1.000  1.000
```

Table D-2. Sample Output of Program AXC03

```
 CARD  8   ROTOR DATA   STAGE  1

30.000 20.320 42.800  1.000  0.1CC  2.600 28.800  0.037  0.020

 CARC  9   STATOR DATA   STAGE  1

32.000 29.980 27.800  1.000  0.10C  2.600 28.800  0.020  0.020

 CARC 1C   ROTOR CATA   STAGE  2

30.000 20.320 42.800  1.00C  0.10C  2.600 28.800  0.037  0.020

 CARD 11   STATOR DATA   STAGE  2

32.000 29.980 27.800  1.000  0.10C  2.600 28.800  0.020  0.020

 CARD 12   ROTOR DATA   STAGE  3

30.000 20.320 42.800  1.000  0.10C  2.60C 28.800  0.037  0.020

 CARD 13   STATOR DATA   STAGE  3

32.000 29.980 27.800  1.00C  0.100  2.60C 28.800  0.020  0.020
```

Table D-2. Sample Output of Program AXCO3 (cont.)

CALCULATED AXIAL CCMPRESSOR PERFORMANCE

RUN NO. 1 REFERRED SPEEC =52.4740 GAMMA = 1.400 AVERAGE PERIPHERAL VELOCITY RATIO = 6.5941

INTERSTAGE DATA

BLADE ROW	INLET TEMP.	INLET PRES.	AXIAL VELOC	INLET VELOC	CUT VELOC	ROTOR VELOC	BLADE EFFIC	INLET ANGLE	OUT ANGLE	CDP MIN	CDP RATIO	REFERENCE INCIDENCE	REFERENCE DEFLECTION	ACTUAL DEFLECTION	STALLING DFFLECTION
IGV	1.CC	C.99	3.77		4.CC										
R 1	1.00	1.00	3.78	6.47	5.02	6.59	0.904	54.35	41.21	0.020	1.153	-1.017	11.412	13.141	14.265
	1.00	1.00	(TOTAL OUTLET CCNDITIONS)												
S 1	1.0C	1.00	3.77	5.01	4.08	6.59	0.905	41.02	22.57	0.020	1.003	-1.673	18.542	18.450	23.177
	1.00	1.00	(TOTAL OUTLET CONDITIONS)												
R 2	1.00	1.00	3.76	6.28	4.97	6.59	0.907	53.11	40.79	0.020	1.036	-1.017	11.412	12.329	14.265
	1.00	1.00	(TOTAL OUTLET CONDITIONS)												
S 2	1.00	1.01	3.76	5.04	4.07	6.59	0.907	41.67	22.62	0.020	1.006	-1.673	18.542	19.054	23.177
	1.00	1.01	(TOTAL OUTLET CONDITIONS)												
R 3	1.00	1.01	3.75	6.28	4.95	6.59	0.907	53.25	40.81	0.020	1.044	-1.017	11.412	12.438	14.265
	1.01	1.01	(TOTAL OUTLET CONDITIONS)												
S 3	1.00	1.01	3.74	5.03	4.05	6.59	0.907	41.89	22.64	0.020	1.009	-1.673	18.542	19.253	23.177
	1.01	1.02	(TOTAL OUTLET CONDITIONS)												
EGV	1.0C	1.01													
	1.01	1.02	(TOTAL OUTLET CCNDITICNS)												
DIFF	1.01	1.02													
	1.01	1.02	(TCTAL CUTLET CCNDITICNS)												

REFERREC FLCW RATE	PRESSURE RATIC	OVERALL EFFICIENCY	POWER COEFFICIENT	BLADING EFFICIENCY	3-STAGE PRESSURE RATIO	3-STAGE EFFICIENCY
46.000	1.01737	0.8136	0.C7060	0.8894	1.01936	0.9058

Table D-2. Sample Output of Program AXC03 (cont.)

CALCULATED AXIAL COMPRESSOR PERFORMANCE, OVERALL DATA

RUN NO. 1 REFERRED SPEED =52.4740 GAMMA = 1.400 AVERAGE PERIPHERAL VELOCITY RATIO = 6.5941

ROTOR STAGGER ANGLE = 42.80 STATOR STAGGER ANGLE = 27.80

REFERRED FLOW RATE	PRESSURE RATIO	OVERALL EFFICIENCY	POWER COEFFICIENT	BLADING EFFICIENCY	3-STAGE PRESSURE RATIO	3-STAGE EFFICIENCY
43.500	1.01871	0.8191	0.07140	0.8854	1.02056	0.8992
44.000	1.01860	0.8211	0.07162	0.8882	1.02045	0.9021
44.500	1.01842	0.8220	0.07165	0.8897	1.02027	0.9040
45.000	1.01809	0.8171	0.07158	0.8901	1.02005	0.9050
45.500	1.01776	0.8155	0.07121	0.8899	1.01974	0.9058
46.000	1.01737	0.8136	0.07060	0.8894	1.01936	0.9058
46.500	1.01694	0.8070	0.07016	0.8891	1.01902	0.9058
47.000	1.01648	0.8035	0.06929	0.8873	1.01856	0.9047
47.500	1.01589	0.7944	0.06833	0.8852	1.01808	0.9033
48.000	1.01543	0.7898	0.06746	0.8830	1.01764	0.9019
48.500	1.01486	0.7827	0.06627	0.8784	1.01708	0.8988
49.000	1.01425	0.7712	0.06513	0.8750	1.01657	0.8961
49.500	1.01372	0.7639	0.06397	0.8707	1.01604	0.8926
50.000	1.01308	0.7500	0.06277	0.8656	1.01551	0.8888
50.500	1.01253	0.7405	0.06154	0.8595	1.01498	0.8841
51.000	1.01198	0.7300	0.06028	0.8529	1.01443	0.8787
51.500	1.01128	0.7109	0.05887	0.8441	1.01384	0.8714
52.000	1.01073	0.6986	0.05756	0.8364	1.01329	0.8646
52.500	1.01006	0.6773	0.05617	0.8265	1.01274	0.8572
53.000	1.00950	0.6623	0.05479	0.8164	1.01218	0.8487
53.500	1.00888	0.6432	0.05325	0.8040	1.01157	0.8375
54.000	1.00820	0.6171	0.05178	0.7913	1.01100	0.8265
54.500	1.00763	0.5961	0.05030	0.7771	1.01044	0.8153

Table D-2. Sample Output of Program AXC03 (cont.)

CALCULATED AXIAL COMPRESSOR PERFORMANCE, OVERALL DATA

RUN NO. 11 REFERRED SPEED =51.6500 GAMMA = 1.400 AVERAGE PERIPHERAL VELOCITY RATIO = 6.4905

ROTOR STAGGER ANGLE = 43.80 STATOR STAGGER ANGLE = 23.80

REFERRED FLOW RATE	PRESSURE RATIO	OVERALL EFFICIENCY	POWER COEFFICIENT	BLADING EFFICIENCY	3-STAGE PRESSURE RATIO	3-STAGE EFFICIENCY
41.500	1.02015	0.8857	0.06782	0.9434	1.02175	0.9552
42.000	1.02001	0.8807	0.06852	0.9433	1.02172	0.9553
42.500	1.01994	0.8805	0.06911	0.9430	1.02164	0.9552
43.000	1.01982	0.8802	0.06956	0.9430	1.02153	0.9555
43.500	1.01958	0.8750	0.06990	0.9429	1.02139	0.9555
44.000	1.01938	0.8739	0.07007	0.9424	1.02120	0.9554
44.500	1.01913	0.8726	0.07009	0.9419	1.02096	0.9555
45.000	1.01874	0.8667	0.06992	0.9417	1.02068	0.9554
45.500	1.01840	0.8651	0.06952	0.9414	1.02034	0.9559
46.000	1.01803	0.8632	0.06906	0.9407	1.01997	0.9555
46.500	1.01766	0.8572	0.06886	0.9405	1.01971	0.9558
47.000	1.01717	0.8545	0.06791	0.9400	1.01923	0.9559
47.500	1.01658	0.8463	0.06691	0.9392	1.01875	0.9561
48.000	1.01611	0.8435	0.06591	0.9388	1.01827	0.9560
48.500	1.01558	0.8396	0.06475	0.9376	1.01776	0.9559
49.000	1.01499	0.8301	0.06365	0.9364	1.01727	0.9560
49.500	1.01452	0.8266	0.06256	0.9360	1.01680	0.9557
50.000	1.01392	0.8162	0.06139	0.9343	1.01632	0.9556
50.500	1.01344	0.8112	0.06024	0.9330	1.01584	0.9553
51.000	1.01296	0.8063	0.05904	0.9318	1.01537	0.9554
51.500	1.01234	0.7933	0.05767	0.9295	1.01486	0.9546
52.000	1.01186	0.7877	0.05640	0.9281	1.01439	0.9546
52.500	1.01128	0.7743	0.05509	0.9266	1.01391	0.9540
53.000	1.01080	0.7673	0.05376	0.9246	1.01344	0.9538
53.500	1.01029	0.7585	0.05229	0.9222	1.01294	0.9528
54.000	1.00970	0.7415	0.05089	0.9188	1.01246	0.9518
54.500	1.00923	0.7330	0.04947	0.9168	1.01199	0.9511
55.000	1.00864	0.7142	0.04800	0.9137	1.01151	0.9502

Table D-3. Output of Program AXC03, Case 11, C_{Dmin} = 0.000

CALCULATED AXIAL COMPRESSOR PERFORMANCE, OVERALL DATA

RUN NO. 12 REFERRED SPEED =51.650 GAMMA = 1.400 AVERAGE PERIPHERAL VELOCITY RATIO = 6.4905

ROTOR STAGGER ANGLE = 43.80 STATOR STAGGER ANGLE = 23.80

REFERRED FLOW RATE	PRESSURE RATIO	OVERALL EFFICIENCY	POWER COEFFICIENT	BLADING EFFICIENCY	3-STAGE PRESSURE RATIO	3-STAGE EFFICIENCY
41.500	1.01967	0.8645	0.06782	0.9226	1.02126	0.9340
42.000	1.01956	0.8613	0.06851	0.9238	1.02126	0.9356
42.500	1.01952	0.8623	0.06909	0.9250	1.02122	0.9372
43.000	1.01942	0.8624	0.06956	0.9254	1.02114	0.9379
43.500	1.01919	0.8581	0.06988	0.9259	1.02100	0.9387
44.000	1.01900	0.8573	0.07006	0.9259	1.02082	0.9388
44.500	1.01877	0.8565	0.07006	0.9259	1.02060	0.9396
45.000	1.01840	0.8511	0.06990	0.9260	1.02033	0.9397
45.500	1.01806	0.8496	0.06951	0.9257	1.01999	0.9399
46.000	1.01770	0.8478	0.06904	0.9252	1.01964	0.9398
46.500	1.01732	0.8412	0.06883	0.9245	1.01937	0.9400
47.000	1.01684	0.8383	0.06787	0.9239	1.01890	0.9402
47.500	1.01625	0.8299	0.06689	0.9229	1.01841	0.9395
48.000	1.01576	0.8260	0.06586	0.9214	1.01793	0.9391
48.500	1.01523	0.8211	0.06472	0.9191	1.01741	0.9376
49.000	1.01465	0.8115	0.06363	0.9178	1.01693	0.9373
49.500	1.01415	0.8062	0.06252	0.9153	1.01644	0.9358
50.000	1.01357	0.7957	0.06138	0.9137	1.01596	0.9349
50.500	1.01306	0.7889	0.06019	0.9109	1.01547	0.9336
51.000	1.01256	0.7821	0.05899	0.9077	1.01497	0.9313
51.500	1.01193	0.7675	0.05764	0.9038	1.01444	0.9282
52.000	1.01143	0.7599	0.05636	0.9004	1.01396	0.9265
52.500	1.01083	0.7440	0.05504	0.8962	1.01346	0.9240
53.000	1.01034	0.7349	0.05372	0.8924	1.01297	0.9212
53.500	1.00977	0.7214	0.05224	0.8853	1.01243	0.9167
54.000	1.00917	0.7025	0.05083	0.8802	1.01193	0.9131
54.500	1.00868	0.6905	0.04940	0.8748	1.01144	0.9092
55.000	1.00807	0.6679	0.04793	0.8679	1.01094	0.9042

Table D-4. Output of Program AXCO3, Case 12, $C_{Dmin} = 0.006$

CALCULATED AXIAL COMPRESSOR PERFORMANCE, OVERALL DATA

RUN NO. 13 REFERRED SPEED =51.6500 GAMMA = 1.400 AVERAGE PERIPHERAL VELOCITY RATIO = 6.4905

ROTOR STAGGER ANGLE = 43.80 STATOR STAGGER ANGLE = 23.80

REFERRED FLOW RATE	PRESSURE RATIO	OVERALL EFFICIENCY	POWER COEFFICIENT	BLADING EFFICIENCY	3-STAGE PRESSURE RATIO	3-STAGE EFFICIENCY
41.000	1.01952	0.8579	0.06781	0.9158	1.02110	0.9273
42.000	1.01941	0.8547	0.06851	0.9171	1.02111	0.9290
42.500	1.01938	0.8561	0.06909	0.9188	1.02108	0.9309
43.000	1.01928	0.8563	0.06956	0.9193	1.02100	0.9318
43.500	1.01906	0.8523	0.06988	0.9202	1.02087	0.9328
44.000	1.01888	0.8519	0.07005	0.9202	1.02070	0.9334
44.500	1.01866	0.8514	0.07006	0.9207	1.02048	0.9341
45.000	1.01827	0.8454	0.06990	0.9204	1.02021	0.9343
45.500	1.01794	0.8440	0.06951	0.9202	1.01988	0.9346
46.000	1.01759	0.8427	0.06903	0.9202	1.01953	0.9348
46.500	1.01722	0.8361	0.06883	0.9194	1.01926	0.9346
47.000	1.01672	0.8327	0.06787	0.9181	1.01878	0.9343
47.500	1.01615	0.8246	0.06689	0.9174	1.01830	0.9338
48.000	1.01565	0.8204	0.06586	0.9159	1.01782	0.9335
48.500	1.01512	0.8152	0.06470	0.9135	1.01730	0.9320
49.000	1.01452	0.8049	0.06362	0.9113	1.01681	0.9308
49.500	1.01403	0.7998	0.06251	0.9092	1.01632	0.9293
50.000	1.01344	0.7885	0.06135	0.9067	1.01583	0.9280
50.500	1.01294	0.7818	0.06018	0.9038	1.01534	0.9259
51.000	1.01244	0.7746	0.05899	0.9002	1.01485	0.9238
51.500	1.01179	0.7590	0.05761	0.8953	1.01431	0.9204
52.000	1.01129	0.7505	0.05635	0.8911	1.01381	0.9171
52.500	1.01069	0.7347	0.05504	0.8869	1.01331	0.9139
53.000	1.01018	0.7239	0.05370	0.8813	1.01281	0.9104
53.500	1.00962	0.7162	0.05223	0.8741	1.01227	0.9053
54.000	1.00901	0.6901	0.05081	0.8676	1.01176	0.9005
54.500	1.00850	0.6764	0.04940	0.8607	1.01126	0.8945
55.000	1.00789	0.6531	0.04792	0.8529	1.01075	0.8894

Table D-5. Output of Program AXC03, Case 13, $C_{Dmin} = 0.008$

CALCULATED AXIAL COMPRESSOR PERFORMANCE, OVERALL DATA

RUN NO. 21 REFERRED SPEED =51.6500 GAMMA = 1.400 AVERAGE PERIPHERAL VELOCITY RATIO = 6.4905

ROTOR STAGGER ANGLE = 43.80 STATOR STAGGER ANGLE = 27.80

REFERRED FLOW RATE	PRESSURE RATIO	OVERALL EFFICIENCY	POWER COEFFICIENT	BLADING EFFICIENCY	3-STAGE PRESSURE RATIO	3-STAGE EFFICIENCY
41.500	1.01961	0.8841	0.06612	0.9435	1.02122	0.9562
42.000	1.01935	0.8789	0.06642	0.9434	1.02107	0.9565
42.500	1.01917	0.8781	0.06664	0.9430	1.02089	0.9564
43.000	1.01889	0.8771	0.06655	0.9428	1.02063	0.9569
43.500	1.01849	0.8707	0.06636	0.9422	1.02033	0.9570
44.000	1.01809	0.8688	0.06585	0.9416	1.01994	0.9568
44.500	1.01774	0.8673	0.06542	0.9417	1.01960	0.9573
45.000	1.01716	0.8599	0.06457	0.9409	1.01912	0.9574
45.500	1.01668	0.8574	0.06364	0.9406	1.01865	0.9577
46.000	1.01621	0.8541	0.06279	0.9393	1.01819	0.9579
46.500	1.01561	0.8458	0.06173	0.9387	1.01769	0.9578
47.000	1.01511	0.8425	0.06065	0.9381	1.01719	0.9579
47.500	1.01450	0.8329	0.05951	0.9372	1.01669	0.9578
48.000	1.01399	0.8284	0.05836	0.9359	1.01619	0.9577
48.500	1.01344	0.8223	0.05707	0.9335	1.01566	0.9571
49.000	1.01284	0.8112	0.05582	0.9324	1.01516	0.9574
49.500	1.01233	0.8054	0.05459	0.9304	1.01466	0.9567
50.000	1.01173	0.7925	0.05329	0.9287	1.01416	0.9563
50.500	1.01123	0.7861	0.05197	0.9275	1.01367	0.9561
51.000	1.01073	0.7785	0.05063	0.9251	1.01318	0.9557
51.500	1.01009	0.7621	0.04912	0.9223	1.01265	0.9547
52.000	1.00959	0.7537	0.04770	0.9195	1.01216	0.9542
52.500	1.00900	0.7364	0.04625	0.9172	1.01166	0.9531

Table D-6. Output of Program AXC03, Case 21, $C_{Dmin} = 0.000$

CALCULATED AXIAL COMPRESSOR PERFORMANCE, OVERALL DATA

RUN NO. 22   REFERRED SPEED =51.6500   GAMMA = 1.400   AVERAGE PERIPHERAL VELOCITY RATIO = 6.4905

ROTOR STAGGER ANGLE = 43.80   STATOR STAGGER ANGLE = 27.80

REFERRED FLOW RATE	PRESSURE RATIO	OVERALL EFFICIENCY	POWER COEFFICIENT	BLADING EFFICIENCY	3-STAGE PRESSURE RATIO	3-STAGE EFFICIENCY
41.500	1.01921	0.8662	0.06611	0.9254	1.02082	0.9382
42.000	1.01897	0.8618	0.06640	0.9262	1.02069	0.9395
42.500	1.01881	0.8619	0.06663	0.9269	1.02053	0.9403
43.000	1.01855	0.8612	0.06654	0.9270	1.02027	0.9407
43.500	1.01815	0.8555	0.06634	0.9270	1.01999	0.9414
44.000	1.01776	0.8533	0.06582	0.9261	1.01961	0.9413
44.500	1.01742	0.8517	0.06540	0.9259	1.01927	0.9417
45.000	1.01684	0.8441	0.06454	0.9253	1.01880	0.9418
45.500	1.01635	0.8408	0.06362	0.9240	1.01831	0.9411
46.000	1.01589	0.8376	0.06278	0.9229	1.01787	0.9409
46.500	1.01528	0.8283	0.06171	0.9212	1.01736	0.9403
47.000	1.01477	0.8238	0.06061	0.9197	1.01685	0.9395
47.500	1.01415	0.8130	0.05948	0.9173	1.01634	0.9385
48.000	1.01364	0.8077	0.05832	0.9154	1.01584	0.9374
48.500	1.01307	0.8002	0.05702	0.9115	1.01529	0.9353
49.000	1.01245	0.7874	0.05580	0.9084	1.01477	0.9334
49.500	1.01193	0.7795	0.05456	0.9047	1.01426	0.9308
50.000	1.01131	0.7650	0.05325	0.9012	1.01375	0.9291
50.500	1.01078	0.7556	0.05192	0.8969	1.01322	0.9258
51.000	1.01026	0.7459	0.05058	0.8924	1.01272	0.9233
51.500	1.00959	0.7251	0.04907	0.8855	1.01215	0.9184
52.000	1.00908	0.7139	0.04765	0.8799	1.01164	0.9146
52.500	1.00845	0.6926	0.04618	0.8738	1.01112	0.9103

Table D-7. Output of Program AXC03, Case 22, C_{Dmin} = 0.006

CALCULATED AXIAL COMPRESSOR PERFORMANCE, OVERALL DATA

RUN NO. 23 REFERRED SPEED =51.650 GAMMA = 1.400 AVERAGE PERIPHERAL VELOCITY RATIO = 6.4905

ROTOR STAGGER ANGLE = 4[illegible].80 STATOR STAGGER ANGLE = 27.80

REFERRED FLOW RATE	PRESSURE RATIO	OVERALL EFFICIENCY	POWER COEFFICIENT	BLADING EFFICIENCY	3-STAGE PRESSURE RATIO	3-STAGE EFFICIENCY
41.500	1.01937	0.86[illegible]1	0.06610	0.9195	1.02069	0.9326
42.000	1.01885	0.8565	0.06640	0.9209	1.02057	0.9339
42.500	1.01869	0.8565	0.06662	0.9215	1.02041	0.9352
43.000	1.01843	0.8561	0.06653	0.9218	1.02016	0.9359
43.500	1.01804	0.8501	0.06633	0.9215	1.01988	0.9362
44.000	1.01765	0.8483	0.06581	0.9212	1.01950	0.9364
44.500	1.01730	0.8464	0.06539	0.9207	1.01916	0.9366
45.000	1.01673	0.8387	0.06454	0.9199	1.01869	0.9362
45.500	1.01624	0.8356	0.06361	0.9187	1.01821	0.9361
46.000	1.01578	0.8317	0.06275	0.9170	1.01776	0.9356
46.500	1.01517	0.8224	0.06170	0.9152	1.01725	0.9345
47.000	1.01466	0.8180	0.06061	0.9139	1.01675	0.9335
47.500	1.01404	0.8070	0.05948	0.9113	1.01623	0.9319
48.000	1.01351	0.8007	0.05831	0.9084	1.01571	0.9304
48.500	1.01295	0.7928	0.05702	0.9041	1.01517	0.9279
49.000	1.01232	0.7795	0.05579	0.9008	1.01465	0.9256
49.500	1.01179	0.7710	0.05453	0.8961	1.01412	0.9224
50.000	1.01117	0.7558	0.05324	0.8921	1.01361	0.9195
50.500	1.01064	0.7459	0.05192	0.8873	1.01308	0.9162
51.000	1.01011	0.7349	0.05058	0.8817	1.01256	0.9119
51.500	1.00943	0.7136	0.04906	0.8738	1.01199	0.9065
52.000	1.00891	0.7009	0.04764	0.8669	1.01147	0.9017
52.500	1.00827	0.6780	0.04617	0.8592	1.01093	0.8957

Table D-8. Output of Program AXC03, Case 23, C_{Dmin} = 0.008

CALCULATED AXIAL COMPRESSOR PERFORMANCE, OVERALL DATA

RUN NO. 31 REFERRED SPEED =51.6[illegible] GAMMA = 1.400 AVERAGE PERIPHERAL VELOCITY RATIO = 6.4905

ROTOR STAGGER ANGLE = 43.80 STATOR STAGGER ANGLE = 31.80

REFERRED FLOW RATE	PRESSURE RATIO	OVERALL EFFICIENCY	POWER COEFFICIENT	BLADING EFFICIENCY	3-STAGE PRESSURE RATIO	3-STAGE EFFICIENCY
41.500	1.01832	0.879[illegible]	0.0621[illegible]	0.9429	1.01996	0.9579
42.000	1.01787	0.873[illegible]	0.06179	0.9421	1.01963	0.9582
42.500	1.01756	0.8715	0.06155	0.9418	1.01932	0.9583
43.000	1.01713	0.8695	0.06091	0.9414	1.01891	0.9589
43.500	1.01659	0.8623	0.06018	0.9410	1.01847	0.9592
44.000	1.01612	0.8589	0.05939	0.9397	1.01801	0.9592
44.500	1.01564	0.8558	0.05849	0.9388	1.01754	0.9589
45.000	1.01505	0.8473	0.05750	0.9382	1.01705	0.9592
45.500	1.01454	0.8434	0.05645	0.9371	1.01655	0.9589
46.000	1.01405	0.8390	0.05545	0.9355	1.01608	0.9593
46.500	1.01343	0.8287	0.05425	0.9344	1.01555	0.9588
47.000	1.01290	0.8235	0.05302	0.9328	1.01504	0.9589
47.500	1.01226	0.8105	0.05175	0.9306	1.01451	0.9583
48.000	1.01174	0.8046	0.05046	0.9290	1.01400	0.9580
48.500	1.01119	0.7977	0.04902	0.9269	1.01345	0.9575
49.000	1.01055	0.7819	0.04762	0.9240	1.01292	0.9573

Table D-9. Output of Program AXC03, Case 31, C_{Dmin} = 0.000

CALCULATED AXIAL COMPRESSOR PERFORMANCE, OVERALL DATA

RUN NO. 32 REFERRED SPEED =51.6500 GAMMA = 1.400 AVERAGE PERIPHERAL VELOCITY RATIO = 6.4905

ROTOR STAGGER ANGLE = 43.80 STATOR STAGGER ANGLE = 31.80

REFERRED FLOW RATE	PRESSURE RATIO	OVERALL EFFICIENCY	POWER COEFFICIENT	BLADING EFFICIENCY	3-STAGE PRESSURE RATIO	3-STAGE EFFICIENCY
41.500	1.01795	0.8627	0.06207	0.9258	1.01960	0.9411
42.000	1.01752	0.8565	0.06177	0.9256	1.01928	0.9416
42.500	1.01722	0.8551	0.06152	0.9253	1.01899	0.9423
43.000	1.01680	0.8529	0.06089	0.9248	1.01857	0.9424
43.500	1.01626	0.8453	0.06016	0.9241	1.01814	0.9422
44.000	1.01579	0.8418	0.05937	0.9225	1.01768	0.9417
44.500	1.01530	0.8378	0.05847	0.9208	1.01720	0.9412
45.000	1.01470	0.8282	0.05748	0.9191	1.01671	0.9403
45.500	1.01418	0.8232	0.05641	0.9171	1.01619	0.9393
46.000	1.01370	0.8185	0.05542	0.9150	1.01572	0.9385
46.500	1.01305	0.8058	0.05422	0.9116	1.01518	0.9362
47.000	1.01252	0.7994	0.05299	0.9088	1.01465	0.9349
47.500	1.01186	0.7849	0.05172	0.9051	1.01411	0.9326
48.000	1.01132	0.7761	0.05042	0.9009	1.01357	0.9301
48.500	1.01074	0.7660	0.04898	0.8953	1.01299	0.9261
49.000	1.01008	0.7479	0.04759	0.8901	1.01245	0.9234

Table D-10. Output of Program AXC03, Case 32, C_{Dmin} = 0.006

CALCULATED AXIAL COMPRESSOR PERFORMANCE, OVERALL DATA

RUN NO. 33 REFERRED SPEED =51.6500 GAMMA = 1.400 AVERAGE PERIPHERAL VELOCITY RATIO = 6.4905

ROTOR STAGGER ANGLE = 43.80 STATOR STAGGER ANGLE = 31.80

REFERRED FLOW RATE	PRESSURE RATIO	OVERALL EFFICIENCY	POWER COEFFICIENT	BLADING EFFICIENCY	3-STAGE PRESSURE RATIO	3-STAGE EFFICIENCY
41.500	1.01783	0.8568	0.06207	0.9199	1.01948	0.9353
42.000	1.01741	0.8511	0.06176	0.9204	1.01916	0.9361
42.500	1.01711	0.8499	0.06152	0.9201	1.01888	0.9370
43.000	1.01669	0.8474	0.06088	0.9194	1.01846	0.9369
43.500	1.01614	0.8394	0.06015	0.9181	1.01802	0.9366
44.000	1.01568	0.8359	0.05936	0.9168	1.01757	0.9361
44.500	1.01520	0.8324	0.05846	0.9155	1.01710	0.9357
45.000	1.01459	0.8220	0.05748	0.9131	1.01660	0.9342
45.500	1.01407	0.8168	0.05641	0.9106	1.01608	0.9326
46.000	1.01358	0.8111	0.05542	0.9076	1.01560	0.9311
46.500	1.01294	0.7988	0.05422	0.9046	1.01505	0.9288
47.000	1.01239	0.7914	0.05298	0.9008	1.01452	0.9268
47.500	1.01172	0.7756	0.05170	0.8958	1.01397	0.9233
48.000	1.01117	0.7666	0.05039	0.8915	1.01343	0.9204
48.500	1.01059	0.7556	0.04896	0.8850	1.01285	0.9161
49.000	1.00992	0.7365	0.04759	0.8784	1.01229	0.9115

Table D-11. Output of Program AXC03, Case 33, C_{Dmin} 0.008

CALCULATED AXIAL COMPRESSOR PERFORMANCE, OVERALL DATA

RUN NO. 41 REFERRED SPEED =51.6500 GAMMA = 1.400 AVERAGE PERIPHERAL VELOCITY RATIO = 6.4905

ROTOR STAGGER ANGLE = 43.80 STATOR STAGGER ANGLE = 35.80

REFERRED FLOW RATE	PRESSURE RATIO	OVERALL EFFICIENCY	POWER COEFFICIENT	BLADING EFFICIENCY	3-STAGE PRESSURE RATIO	3-STAGE EFFICIENCY
41.500	1.01634	0.8700	0.05604	0.9401	1.01804	0.9600
42.000	1.01582	0.8621	0.05544	0.9391	1.01763	0.9599
42.500	1.01538	0.8587	0.05476	0.9376	1.01720	0.9599
43.000	1.01495	0.8566	0.05399	0.9375	1.01677	0.9604
43.500	1.01437	0.8466	0.05313	0.9356	1.01630	0.9599
44.000	1.01389	0.8430	0.05218	0.9346	1.01583	0.9599
44.500	1.01339	0.8385	0.05115	0.9334	1.01535	0.9603
45.000	1.01277	0.8271	0.05002	0.9316	1.01483	0.9598
45.500	1.01223	0.8215	0.04880	0.9298	1.01430	0.9597

Table D-12. Output of Program AXC03, Case 41, C_{Dmin} 0.000

CALCULATED AXIAL COMPRESSOR PERFORMANCE, OVERALL DATA

RUN NO. 42 REFERRED SPEED =51.6500 GAMMA = 1.400 AVERAGE PERIPHERAL VELOCITY RATIO = 6.4905

ROTOR STAGGER ANGLE = 43.80 STATOR STAGGER ANGLE = 35.80

REFERRED FLOW RATE	PRESSURE RATIO	OVERALL EFFICIENCY	POWER COEFFICIENT	BLADING EFFICIENCY	3-STAGE PRESSURE RATIO	3-STAGE EFFICIENCY
41.500	1.01597	0.8508	0.05601	0.9208	1.01767	0.9408
42.000	1.01547	0.8432	0.05542	0.9202	1.01727	0.9409
42.500	1.01504	0.8399	0.05474	0.9188	1.01685	0.9406
43.000	1.01459	0.8361	0.05397	0.9169	1.01640	0.9398
43.500	1.01400	0.8252	0.05311	0.9142	1.01593	0.9383
44.000	1.01351	0.8204	0.05215	0.9122	1.01545	0.9377
44.500	1.01300	0.8144	0.05111	0.9094	1.01495	0.9361
45.000	1.01236	0.8011	0.04998	0.9057	1.01442	0.9339
45.500	1.01182	0.7940	0.04878	0.9023	1.01388	0.9318

Table D-13. Output of Program AXC03, Case 42, C_{Dmin} 0.006

CALCULATED AXIAL COMPRESSOR PERFORMANCE, OVERALL DATA

RUN NO. 43 REFERRED SPEED =51.6500 GAMMA = 1.400 AVERAGE PERIPHERAL VELOCITY RATIO = 6.4905

ROTOR STAGGER ANGLE = 43.80 STATOR STAGGER ANGLE = 35.80

REFERRED FLOW RATE	PRESSURE RATIO	OVERALL EFFICIENCY	POWER COEFFICIENT	BLADING EFFICIENCY	3-STAGE PRESSURE RATIO	3-STAGE EFFICIENCY
41.500	1.01585	0.8444	0.05601	0.9143	1.01754	0.9342
42.000	1.01534	0.8364	0.05540	0.9134	1.01714	0.9343
42.500	1.01491	0.8331	0.05473	0.9121	1.01673	0.9342
43.000	1.01447	0.8295	0.05396	0.9104	1.01628	0.9332
43.500	1.01388	0.8184	0.05308	0.9076	1.01581	0.9319
44.000	1.01338	0.8126	0.05214	0.9045	1.01532	0.9299
44.500	1.01286	0.8062	0.05111	0.9010	1.01482	0.9279
45.000	1.01222	0.7924	0.04998	0.8972	1.01428	0.9252
45.500	1.01168	0.7847	0.04877	0.8930	1.01374	0.9227

Table D-14. Output of Program AXC03, Case 43, C_{Dmin} = 0.008

CALCULATED AXIAL COMPRESSOR PERFORMANCE, OVERALL DATA

RUN NO. 51 REFERRED SPEED =51.6500 GAMMA = 1.400 AVERAGE PERIPHERAL VELOCITY RATIO = 6.4905

ROTOR STAGGER ANGLE = 43.80 STATOR STAGGER ANGLE = 39.80

REFERRED FLOW RATE	PRESSURE RATIO	OVERALL EFFICIENCY	POWER COEFFICIENT	BLADING EFFICIENCY	3-STAGE PRESSURE RATIO	3-STAGE EFFICIENCY
41.500	1.01515	0.8081	0.05595	0.8781	1.01683	0.8976

Table D-15. Output of Program AXC03, Cases 51, 52, and 53, All C_{Dmin}

CALCULATED AXIAL COMPRESSOR PERFORMANCE, OVERALL DATA

RUN NO. 61   REFERRED SPEED =51.6500   GAMMA = 1.400   AVERAGE PERIPHERAL VELOCITY RATIO = 6.4905

ROTOR STAGGER ANGLE = 43.80   STATOR STAGGER ANGLE = 44.30

REFERRED FLOW RATE	PRESSURE RATIO	OVERALL EFFICIENCY	POWER COEFFICIENT	BLADING EFFICIENCY	3-STAGE PRESSURE RATIO	3-STAGE EFFICIENCY
41.500	1.01515	0.8081	0.05595	0.8781	1.01683	0.8976

Table D-16. Output of Program AXC03, Cases 61, 62, and 63, All C_{Dmin}

```
0001          0DIMENSION BETA(15),ADENCE(15),CDENCE(15),DDENCE(15),ASLOPN(15),CSL      2
              1OPN(15),DSLOPN(15),ADEVAT(15),CDEVAT(15),DDEVAT(15),ASLOPM(15),CSL      3
              2OPM(15),DSLOPM(15),ASLOPD(15),CSLOPD(15),DSLOPD(15),PDENCE(15),PSL      4
              3OPN(15),PDEVAT(15),PSLOPM(15),PSLOPD(15)                              1       4
        C  THIS PROGRAM CHECKS THE ACCURACY WITH WHICH THE POLYNOMIALS IN AXCOM4
        C  REPRESENT THE FIGURES IN NACA SP-36
        C                                                                      00000264
        C ZERO-CAMBER INCIDENCE VS SOLIDITY AND ALPHA 1  FIG 137               00000265
        C                                                                      00000266
0002           FIGAF(A,S)=0.96195E-02- 0.21961E-01*S+0.10963E-01*S*S-0.42930E-02*00000267
              1A+0.85403E-01*A*S-0.34503E-02*A*S*S+0.27923E-04*A*A-0.64301E-04*A*00000268
              2A*S+0.32138E-04*A*A*S*S                                         00000269
        C                                                                      00000275
        C SLOPE FACTOR N (INCIDENCE) VS SOLIDITY AND ALPHA 1   FIG 138         00000276
        C                                                                      00000277
0003           FIGCF(A,S)=-0.11890+0.21192*S-0.17854*S*S+0.57160E-01*S*S*S-0.368700000278
              13E-02*A-0.76207E-04*A*S+0.18208E-02*A*S*S-0.55334E-03*A*S*S*S-0.3600000279
              2825E-04*A*A+0.66620E-04*A*A*S+0.16243E-04*A*A*S*S-0.22671E-04*A*A*00000280
              3S*S*S-0.72311E-07*A*A*A-0.54986E-06*A*A*A*S-0.49472E-06*A*A*A*S*S+00000281
              40.37471E-06*A*A*A*S*S*S                                         00000282
        C                                                                      00000283
        C ZERO-CAMBER DEVIATION VS SOLIDITY AND ALPHA 1   FIG 161              00000284
        C                                                                      00000285
0004           FIGDF(A,S)=-0.017896+0.10058*S-0.14687*S*S+0.58557E-01*S*S*S-0.11900000286
              187E-01*A+0.65167E-01*A*S-0.44822E-01*A*S*S+0.11478E-01*A*S*S*S-0.200000287
              24947E-03*A*A+0.66468E-03*A*A*S-0.94528E-03*A*A*S*S+0.28823E-03*A*A00000288
              3*S*S*S+0.67269E-05*A*A*A-0.17987E-04*A*A*A*S+0.25862E-04*A*A*A*S*S00000289
              4-0.77546E-05*A*A*A*S*S*S                                        00000290
        C                                                                      00000295
        C SLOPE FACTOR M (DEVIATION) VS SOLIDITY AND ALPHA 1   FIG 168         00000296
        C                                                                      00000297
0005           FIGGF(A,S)=1.06850-1.68830*S+1.15690*S*S-0.28879*S*S*S+0.36581E-0300000298
              1*A-0.19185E-02*A*S+0.36235E-02*A*S*S-0.13993E-02*A*S*S*S-0.57353E-00000299
              205*A*A+0.11329E-03*A*A*S-0.19416E-03*A*A*S*S+0.74911E-04*A*A*S*S*S00000300
              3-0.16187E-06*A*A*A-0.79239E-06*A*A*A*S+0.22558E-05*A*A*A*S*S-0.99200000301
              418E-06*A*A*A*S*S*S                                              00000302
        C                                                                      00000323
        C SLOPE FACTOR (DI/DD)* VS SOLIDITY AND ALPHA 1   FIG 177              00000324
        C                                                                      00000325
        C   CAUTION  THIS POLYNOMIAL GENERATED FOR SOLIDITIES FROM 0.6 TO 1.4  10000325
        C                                                                      20000325
0006          0FIGHF(A,S)=.81324E+00-.17818E+01*S+.13558E+01*S*S-.35174E+00*S*S*S00000326
              1-.40846E-02*A+.18322E-01*A*S-.21692E-01*A*S*S+.76075E-02*A*S*S*S+.00000327
              218174E-03*A*A-.83518E-03*A*A*S+.10421E-02*A*A*S*S-.38235E-03*A*A*S00000328
              3*S*S-.94842E-06*A*A*A+.86041E-05*A*A*A*S-.12163E-04*A*A*A*S*S+.46710000328
              421E-05*A*A*A*S*S*S                                              20000328
0007           READ(5,700)(BETA(I),I=1,15)                                           5
0008           READ(5,700)(ADENCE(I),I=1,15)                                         6
```

Table D-17. Program CHECK, Listing and Output

```
FORTRAN IV G LEVEL 0, MOD 0              MAIN              DATE = 67160          16/30/48              PAGE 0002

0009                READ(5,700)(ASLOPN(I),I=1,15)                                          7
0010                READ(5,700)(ADEVAT(I),I=1,15)                                          8
0011                READ(5,700)(ASLOPM(I),I=1,15)                                          9
0012                READ(5,700)(ASLOPD(I),I=1,15)                                         10
0013                S=0.8                                                                 11
0014                A=0.0                                                                 12
0015                I=1                                                                   13
0016              1 DENCE=FIGAF(A,S)                                                     101
0017                CDENCE(I)=DENCE                                                      102
0018                AE=ADENCE(I)                                                         103
0019                DE=AE-DENCE                                                          104
0020                DDENCE(I)=DE                                                         105
0021                PE=100.*DE/AE                                                   1    105
0022                PDENCE(I)=PE                                                    2    105
0023                SLOPN=FIGCF(A,S)                                                     106
0024                CSLOPN(I)=SLOPN                                                      107
0025                AN=ASLOPN(I)                                                         108
0026                DN=AN-SLOPN                                                          109
0027                DSLOPN(I)=DN                                                         110
0028                PN=100.*DN/AN                                                    1000110
0029                PSLOPN(I)=PN                                                     2000110
0030                DEVAT=FIGDF(A,S)                                                     111
0031                CDEVAT(I)=DEVAT                                                      112
0032                AT=ADEVAT(I)                                                         113
0033                DT=AT-DEVAT                                                          114
0034                DDEVAT(I)=DT                                                         115
0035                PT=100.*DT/AT                                                   1    115
0036                PDEVAT(I)=PT                                                    2    115
0037                SLOPM=FIGGF(A,S)                                                     116
0038                CSLOPM(I)=SLOPM                                                      117
0039                AM=ASLOPM(I)                                                         118
0040                DM=AM-SLOPM                                                          119
0041                DSLOPM(I)=DM                                                         120
0042                PM=100.*DM/AM                                                   1    120
0043                PSLOPM(I)=PM                                                    2    120
0044                SLOPD=FIGHF(A,S)                                                     121
0045                CSLOPD(I)=SLOPD                                                      122
0046                AD=ASLOPD(I)                                                         123
0047                DD=AD-SLOPD                                                          124
0048                DSLOPD(I)=DD                                                         125
0049                PD=100.*DD/AD                                                   1    125
0050                PSLOPD(I)=PD                                                    2    125
0051                IF(I-15)2,3,3                                                        126
0052              2 I=I+1                                                                127
0053                A=A+5.                                                               128
0054                GO TO 1                                                              129
0055              3 WRITE(6,750)S                                                        130
0056                WRITE(6,751)                                                         131
```

Table D-17. Program CHECK, Listing and Output (cont.)

```
0057          DO 4 I=1,15
0058        4 WRITE(6,757)BETA(I),ADENCE(I),CDENCE(I),DDENCE(I),PDENCE(I)
0059          WRITE(6,752)
0060          WRITE(6,753)
0061          DO 5 I=1,15
0062        5 WRITE(6,757)BETA(I),ASLOPN(I),CSLOPN(I),DSLOPN(I),PSLOPN(I)
0063          WRITE(6,754)
0064          DO 6 I=1,15
0065        6 WRITE(6,757)BETA(I),ADEVAT(I),CDEVAT(I),DDEVAT(I),PDEVAT(I)
0066          WRITE(6,755)
0067          WRITE(6,753)
0068          DO 7 I=1,15
0069        7 WRITE(6,757)BETA(I),ASLOPM(I),CSLOPM(I),DSLOPM(I),PSLOPM(I)
0070          WRITE(6,756)
0071          WRITE(6,753)
0072          DO 8 I=1,15
0073        8 WRITE(6,757)BETA(I),ASLOPD(I),CSLOPD(I),DSLOPD(I),PSLOPD(I)
0074      700 FORMAT(8F8.3)
0075      7500FORMAT(1H1,9X,74HCOMPARISON OF ACTUAL VALUES IN NASA SP-36 WITH VA
             1LUES CALCULATED BY AXCOM2//43X,11HSOLIDITY = ,F3.1//)
0076      7510FORMAT(//33X,34HZERO CAMBER INCIDENCE VERSUS ANGLE/3X,14HANGLE, DE
             1GREES,5X,16HACTUAL INCIDENCE,2X,20HCALCULATED INCIDENCE,2X,19HACTU
             2AL - CALCULATED,5X,13HPERCENT ERROR/)
0077      752 FORMAT(//36X,27HSLOPE FACTOR N VERSUS ANGLE/)
0078      7530FORMAT(3X,14HANGLE, DEGREES,6X,13HACTUAL FACTOR,5X,17HCALCULATED F
             1ACTOR,3X,19HACTUAL - CALCULATED,6X,13HPERCENT ERROR/)
0079      7540FORMAT(//39X,22HDEVIATION VERSUS ANGLE//3X,14HANGLE, DEGREES,5X,16
             1HACTUAL DEVIATION,2X,20HCALCULATED DEVIATION,2X,19HACTUAL - DEVIAT
             2ION,5X,13HPERCENT ERROR/)
0080      755 FORMAT(1H1,36X,27HSLOPE FACTOR M VERSUS ANGLE/)
0081      756 FORMAT(//39X,32HSLOPE FACTOR DI/DD VERSUS ANGLE/)
0082      757 FORMAT(5F20.10)  .
0083          END
```

Table D-17. Program CHECK, Listing and Output (cont.)

COMPARISON OF ACTUAL VALUES IN NASA SP-36 WITH VALUES CALCULATED BY AXCOM2

SOLIDITY = 0.8

ZERO CAMBER INCIDENCE VERSUS ANGLE

ANGLE, DEGREES	ACTUAL INCIDENCE	CALCULATED INCIDENCE	ACTUAL - CALCULATED	PERCENT ERROR
0.0	0.0	-0.0009329878	0.0009329878	0.0932987332
5.0000000000	0.3299999833	0.3080989718	0.0219010115	6.6366682053
10.0000000000	0.6799999475	0.6169836521	0.0630162954	9.2671022415
15.0000000000	0.9899999499	0.9257200956	0.0642798543	6.4929141998
20.0000000000	1.3099994659	1.2343072891	0.0756921768	5.7780303955
25.0000000000	1.6199998856	1.5427494049	0.0772504807	4.7685480118
30.0000000000	1.9299993515	1.8510446548	0.0789546967	4.0909175873
35.0000000000	2.2299995422	2.1591939926	0.0708055496	3.1751365662
40.0000000000	2.5499992371	2.4671907425	0.0828084946	3.2473926544
45.0000000000	2.8299999237	2.7750444412	0.0549554825	1.9418897629
50.0000000000	3.1199998856	3.0827503204	0.0372495651	1.1938962936
55.0000000000	3.3899993896	3.3903064728	-0.0003070831	-0.0090584978
60.0000000000	3.6199996856	3.6977157593	-0.0777158737	-2.1468467712
65.0000000000	3.8299999237	4.0049800873	-0.1749801636	-4.5686721802
70.0000000000	4.0099992752	4.3120946884	-0.3020954132	-7.5335502625

SLOPE FACTOR N VERSUS ANGLE

ANGLE, DEGREES	ACTUAL FACTOR	CALCULATED FACTOR	ACTUAL - CALCULATED	PERCENT ERROR
0.0	-0.0389999971	-0.0343636572	-0.0046363398	11.8880500793
5.0000000000	-0.0499999970	-0.0483931080	-0.0016068891	3.2137775421
10.0000000000	-0.0609999970	-0.0621372499	0.0011372529	-1.8643474579
15.0000000000	-0.0739999413	-0.0760737062	0.0020737648	-2.8023862839
20.0000000000	-0.0879999995	-0.0906807184	0.0026807189	-3.0462713242
25.0000000000	-0.1039999723	-0.1064355373	0.0024355650	-2.3418893814
30.0000000000	-0.1209999919	-0.1238162518	0.0028162599	-2.3274869919
35.0000000000	-0.1409999728	-0.1433003545	0.0023003817	-1.6314764023
40.0000000000	-0.1619999409	-0.1653655767	0.0033656359	-2.0775537491
45.0000000000	-0.1859999895	-0.1904897094	0.0044897199	-2.4138278961
50.0000000000	-0.2119999528	-0.2191501260	0.0071501732	-3.3727235794
55.0000000000	-0.2409999967	-0.2518250346	0.0108250380	-4.4917144775
60.0000000000	-0.2769999504	-0.2889920473	0.0119920969	-4.3292751312
65.0000000000	-0.3209999800	-0.3311289549	0.0101289749	-3.1554431915
70.0000000000	-0.3759999871	-0.3787130713	0.0027130842	-0.7215649486

DEVIATION VERSUS ANGLE

ANGLE, DEGREES	ACTUAL DEVIATION	CALCULATED DEVIATION	ACTUAL - DEVIATION,	PERCENT ERROR
0.0	0.0	-0.0014475845	0.0014475845	0.1447584033
5.0000000000	0.0599999987	0.0814747810	-0.0214747824	-35.7912902832
10.0000000000	0.1299999952	0.1593298316	-0.0293298364	-22.5614013672
15.0000000000	0.2099999785	0.2358062267	-0.0258062482	-12.2886896133
20.0000000000	0.2999999523	0.3145923018	-0.0145923495	-4.8641147614
25.0000000000	0.3999999762	0.3993784785	0.0006214976	0.1553744078
30.0000000000	0.5099999905	0.4938524365	0.0161475539	3.1661853790
35.0000000000	0.6299999952	0.6017042994	0.0282956958	4.4913787842
40.0000000000	0.7599999905	0.7266232967	0.0333766937	4.3916702271
45.0000000000	0.8999999762	0.8722926378	0.0277073383	3.0785923004
50.0000000000	1.0599994659	1.0424118042	0.0175876617	1.6592140198
55.0000000000	1.2500000000	1.2406597137	0.0093402863	0.7472229004
60.0000000000	1.4799995422	1.4707336426	0.0092658997	0.6260744929
65.0000000000	1.7500000000	1.7363204956	0.0136795044	0.7816859484
70.0000000000	2.0699996948	2.0411033630	0.0288963318	1.3959579468

Table D- 17. Program CHECK,Listing and Output (cont.)

SLOPE FACTOR M VERSUS ANGLE

ANGLE, DEGREES	ACTUAL FACTOR	CALCULATED FACTOR	ACTUAL - CALCULATED	PERCENT ERROR
0.0	0.3099999428	0.3104162812	-0.0004163384	-0.1343027353
5.0000000000	0.3119999766	0.3125761747	-0.0005761981	-0.1846788526
10.0000000000	0.3149999976	0.3147908449	0.0002091527	0.0663976669
15.0000000000	0.3169999719	0.3171648979	-0.0001649261	-0.0520271473
20.0000000000	0.3209999800	0.3198031187	0.0011968613	0.3728539944
25.0000000000	0.3239999413	0.3228106499	0.0011892915	0.3670653105
30.0000000000	0.3279999495	0.3262923956	0.0017075539	0.5205957294
35.0000000000	0.3329999447	0.3303530812	0.0026468635	0.7948539853
40.0000000000	0.3379999995	0.3350979686	0.0029020309	0.8585889935
45.0000000000	0.3439999819	0.3406320214	0.0033679605	0.9790582657
50.0000000000	0.3499999642	0.3470600843	0.0029398799	0.8399657607
55.0000000000	0.3569999933	0.3544869423	0.0025130510	0.7039358616
60.0000000000	0.3649999499	0.3630179167	0.0019820333	0.5430228710
65.0000000000	0.3750000000	0.3727575541	0.0022424459	0.5979855657
70.0000000000	0.3879999518	0.3838108182	0.0041891336	1.0796728134

SLOPE FACTOR DI/DO VERSUS ANGLE/

ANGLE, DEGREES	ACTUAL FACTOR	CALCULATED FACTOR	ACTUAL - CALCULATED	PERCENT ERROR
0.0	0.0769999623	0.0754218698	0.0015780926	2.0494718552
5.0000000000	0.0789999962	0.0780347586	0.0009652376	1.2218189240
10.0000000000	0.0809999704	0.0802936554	0.0007063150	0.8719941378
15.0000000000	0.0829999447	0.0826053023	0.0003946424	0.4754729667
20.0000000000	0.0859999657	0.0853770375	0.0006229281	0.7243353128
25.0000000000	0.0899999738	0.0890154839	0.0009844899	1.0938777924
30.0000000000	0.0939999819	0.0939274430	0.0000725389	0.0771690011
35.0000000000	0.1019999981	0.1005203128	0.0014796853	1.4506711960
40.0000000000	0.1109999418	0.1092003584	0.0017995834	1.6212463379
45.0000000000	0.1209999919	0.1203768849	0.0006231070	0.5149644613
50.0000000000	0.1319999695	0.1344547272	-0.0024547577	-1.8596649170
55.0000000000	0.1499999762	0.1518397331	-0.0018397570	-1.2265043259
60.0000000000	0.1719999909	0.1729413271	-0.0009413362	-0.5472884774
65.0000000000	0.1979999542	0.1981655955	-0.0001656413	-0.0836572051
70.0000000000	0.2269999981	0.2279177904	-0.0009177923	-0.4043137431

Table D-17. Program CHECK,Listing and Output (cont.)

APPENDIX E

PROPOSED DESIGN OF AN IMPROVED INLET DUCT

The present inlet duct is deficient because of the shape of its bellmouth, because of the small velocities that occur in it during operation which make accurate determination of volume flow rates impossible, and because it has no provision to eliminate effects of atmospheric gusts or winds.

The entrance bellmouth should have more gradual changes in wall curvature to eliminate local separations at the entrance to the cylindrical duct. It was stated earlier that the velocity head in this duct with 36 in. diameter is about 0.6 in. of water, a value too small for accurate measurements. To avoid large fluctuations of the read-out of the Texas Instruments pressure gauge, for small variation in flow rate, the velocity head should be increased to about 6 in. of water or 33 lb/ft^2, at a volume flow rate of 360 ft^3/sec, giving a response at the instrument of about 8000 counts. For an assumed incompressible flow with a mass density ρ_i of 0.002378 lb sec^2/ft^4, and a velocity head q_{i1} of 33 lb/ft^2, the velocity V_i in the measuring plane of the inlet duct would have to be

$$V_i = \sqrt{\frac{2\, q_{i1}}{\rho_i}} \quad \text{(ft/sec)} \qquad (6)$$

Hence the required flow area is 360/166 = 2.16 ft^2, corresponding to a circular area with 19.9 in. diameter. Because of the small pressure rise of the compressor it is necessary to convert the velocity head at the measuring plane into static pressure rise by arranging an optimum diffuser between this section and the inlet pipe to the compressor that has a diameter of 36 in. Test data of Reference 11 show that the included diffuser angle should be 8° for the present application. Larger diffuser angles produce separation with associated flow instabilities, and smaller angles require ducts with increased lengths where the boundary layer growth is excessive and reduces pressure recovery. For a diffuser angle of 8° the length L of the diffuser is

$$L = \frac{36 - 19.9}{2 \tan 4^\circ} = 116 \text{ in.}$$

Figure E-1 shows the design of the proposed inlet duct. A well designed bellmouth from a diameter of 48 in. to the throat of 19.9 in. requires an axial length of about 26 in., giving a total length of the duct of 116 + 26 = 142 in. Ahead of the bellmouth inlet a structure will be attached to support several layers of fine mesh screen to eliminate flow disturbances by gusts in the surrounding atmosphere. The whole duct is mounted on a trolley which can be rolled onto the apron outside the test cell to permit simple attachment to and removal from the presently installed cylindrical inlet duct. It is recommended also that an additional honeycomb flow straightener be installed at the entrance of this duct.

The bellmouth and the diffuser could be molded out of plastics, reinforced by fiberglass, by using a wooden template which is split at the smallest diameter.

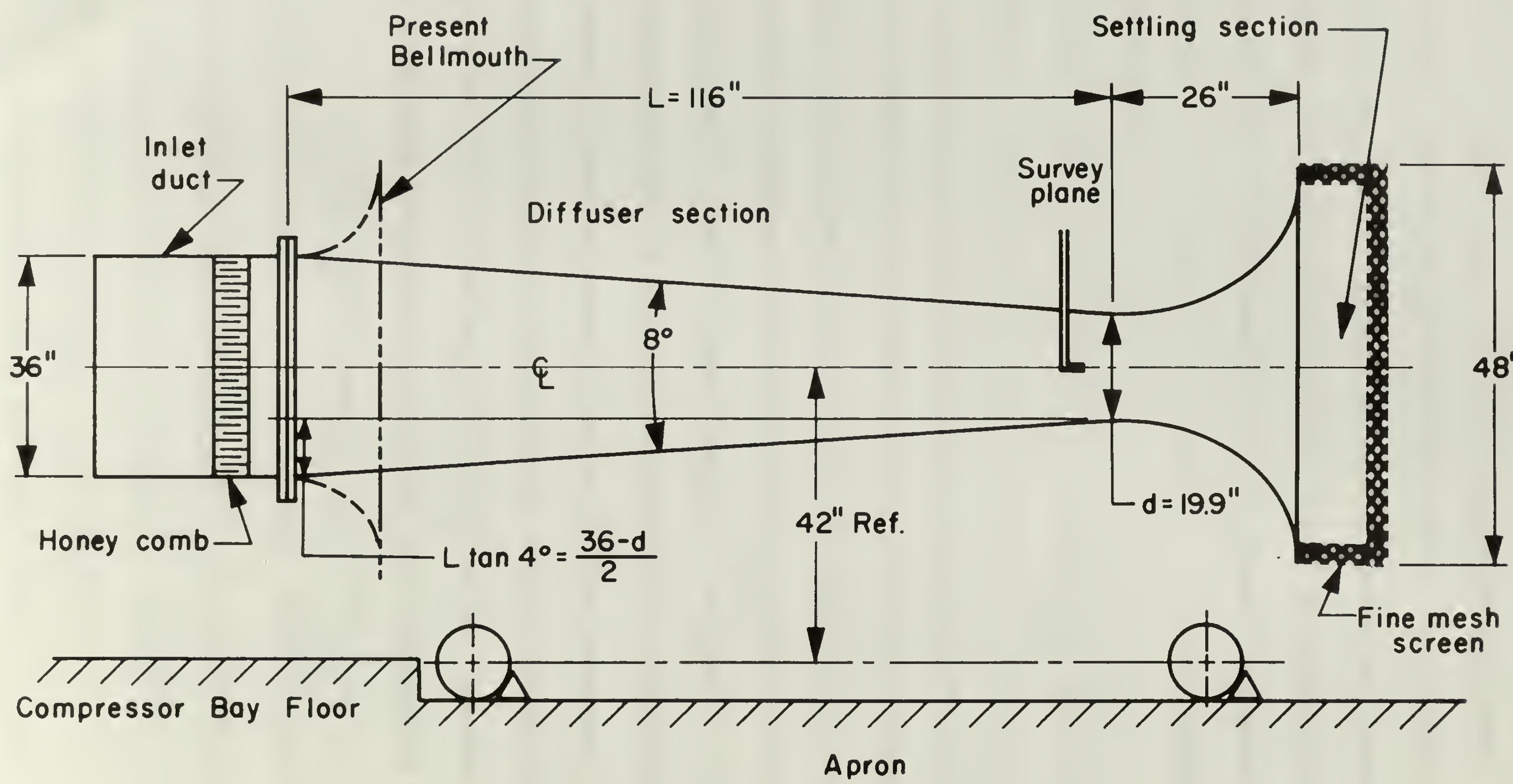

FIG. E-1 PROPOSED IMPROVED INLET DUCT

INITIAL DISTRIBUTION LIST

		Copies
1.	Defense Documentation Center Cameron Station Alexandria, Virginia 22314	20
2.	Library Naval Postgraduate School Monterey, California 93940	2
3.	Commander, Naval Air Systems Command Navy Department Washington, D. C. 20360	1
4.	Commander, Naval Ship Systems Command Navy Department Washington, D. C. 20360	1
5.	Dr. O. H. Johnson Naval Air Systems Command (Code 330 B) Navy Department Washington, D. C. 20360	1
6.	Capt. A. Bodnaruk, USN Naval Ship Systems Command (Code 6140) Navy Department Washington, D. C. 20360	1
7.	Office of Naval Research (Power Branch) Attn: Mr. J. K. Patton, Jr. Navy Department Washington, D. C. 20360	1
8.	Chairman, Department of Aeronautics Naval Postgraduate School Monterey, California 93940	3
9.	Professor M. H. Vavra Department of Aeronautics Naval Postgraduate School Monterey, California 93940	3
10.	Lt. B. C. Marshall Air Antisubmarine Squadron 35 Fleet Post Office San Francisco, California 96601	4

UNCLASSIFIED

Security Classification

DOCUMENT CONTROL DATA - R&D

(Security classification of title, body of abstract and indexing annotation must be entered when the overall report is classified)

1. ORIGINATING ACTIVITY *(Corporate author)*

Naval Postgraduate School
Monterey, California 93940

2a. REPORT SECURITY CLASSIFICATION

UNCLASSIFIED

2b. GROUP

-

3. REPORT TITLE

EFFECT OF STATOR BLADE ORIENTATION ON THE PERFORMANCE OF AN AXIAL FLOW COMPRESSOR

4. DESCRIPTIVE NOTES *(Type of report and inclusive dates)*

Thesis

5. AUTHOR(S) *(Last name, first name, initial)*

Marshall, Bruce C., Lieutenant, U. S. Navy

6. REPORT DATE	7a. TOTAL NO. OF PAGES	7b. NO. OF REFS
September 1967	199	11

8a. CONTRACT OR GRANT NO.

b. PROJECT NO.

c.

d. Unlimited dist

9a. ORIGINATOR'S REPORT NUMBER(S)

9b. OTHER REPORT NO(S) *(Any other numbers that may be assigned this report)*

10. AVAILABILITY/LIMITATION NOTICES

This document is subject to special export controls and each transmittal to foreign nationals may be made only with prior approval of the Naval Postgraduate School.

11. SUPPLEMENTARY NOTES

-

12. SPONSORING MILITARY ACTIVITY

Commander, Naval Air Systems Command
Department of the Navy
Washington, D. C. 20360

13. ABSTRACT

A mean streamline analysis of the effect of stator blade orientation on the performance of an axial flow compressor was performed by means of a computer program. Measurements were made on a 3-stage axial flow compressor at the Naval Postgraduate School at six stator stagger angles between 23.8^{o} and 44.3^{o} for a fixed orientation of the rotor blades. Maximum efficiency and pressure ratio were measured at a stator stagger angle of 31.8^{o}. Results at other blade settings showed that by varying stator stagger angle with flow rate optimum efficiencies and pressure ratios can be achieved over a wide range of operating conditions.

The results of the analysis were compared with the measured results. Suggestions are made for improving the manner of adapting cascade test data to performance predictions.

By applying a non-dimensional deflection coefficient it could be shown that minimum work input corresponded to maximum efficiency.

The test compressor has a tip diameter of 36 in. and a hub/tip ratio of 0.6. The blading tested is of the free-vortex type with a design degree of reaction of 0.5. Tip speed was about 185 ft/sec.

DD FORM 1 JAN 64 1473

UNCLASSIFIED

Security Classification

14. KEY WORDS	LINK A		LINK B		LINK C	
	ROLE	WT	ROLE	WT	ROLE	WT
compressor						
compressor performance						
axial flow						
variable stator						
stator blade orientation						